U.S.NRC

United States Nuclear Regulatory Commission

Protecting People and the Environment

NUREG/CR-7025

Radionuclide Release from Slag and Concrete Waste Materials

Part 1: Conceptual Models of Leaching from Complex Materials and Laboratory Test Methods

Office of Nuclear Regulatory Research

AVAILABILITY OF REFERENCE MATERIALS IN NRC PUBLICATIONS

NRC Reference Material

As of November 1999, you may electronically access NUREG-series publications and other NRC records at NRC's Public Electronic Reading Room at http://www.nrc.gov/reading-rm.html Publicly released records include, to name a few, NUREG-series publications; *Federal Register* notices; applicant, licensee, and vendor documents and correspondence; NRC correspondence and internal memoranda; bulletins and information notices; inspection and investigative reports; licensee event reports; and Commission papers and their attachments.

NRC publications in the NUREG series, NRC regulations, and *Title 10, Energy*, in the Code of *Federal Regulations* may also be purchased from one of these two sources.

1. The Superintendent of Documents
   U.S. Government Printing Office
   Mail Stop SSOP
   Washington, DC 20402–0001
   Internet: bookstore.gpo.gov
   Telephone: 202-512-1800
   Fax: 202-512-2250
2. The National Technical Information Service
   Springfield, VA 22161–0002
   www.ntis.gov
   1–800–553–6847 or, locally, 703–605–6000

A single copy of each NRC draft report for comment is available free, to the extent of supply, upon written request as follows:

Address: U.S. Nuclear Regulatory Commission
Office of Administration
Publications Branch
Washington, DC 20555-0001
E-mail: DISTRIBUTION.RESOURCE@NRC.GOV
Facsimile: 301–415–2289

Some publications in the NUREG series that are posted at NRC's Web site address http://www.nrc.gov/reading-rm/doc-collections/nuregs are updated periodically and may differ from the last printed version. Although references to material found on a Web site bear the date the material was accessed, the material available on the date cited may subsequently be removed from the site.

Non-NRC Reference Material

Documents available from public and special technical libraries include all open literature items, such as books, journal articles, and transactions, *Federal Register* notices, Federal and State legislation, and congressional reports. Such documents as theses, dissertations, foreign reports and translations, and non-NRC conference proceedings may be purchased from their sponsoring organization.

Copies of industry codes and standards used in a substantive manner in the NRC regulatory process are maintained at—

The NRC Technical Library
Two White Flint North
11545 Rockville Pike
Rockville, MD 20852–2738

These standards are available in the library for reference use by the public. Codes and standards are usually copyrighted and may be purchased from the originating organization or, if they are American National Standards, from—

American National Standards Institute
11 West 42nd Street
New York, NY 10036–8002
www.ansi.org
212–642–4900

Legally binding regulatory requirements are stated only in laws; NRC regulations; licenses, including technical specifications; or orders, not in NUREG-series publications. The views expressed in contractor-prepared publications in this series are not necessarily those of the NRC.

The NUREG series comprises (1) technical and administrative reports and books prepared by the staff (NUREG–XXXX) or agency contractors (NUREG/CR–XXXX), (2) proceedings of conferences (NUREG/CP–XXXX), (3) reports resulting from international agreements (NUREG/IA–XXXX), (4) brochures (NUREG/BR–XXXX), and (5) compilations of legal decisions and orders of the Commission and Atomic and Safety Licensing Boards and of Directors' decisions under Section 2.206 of NRC's regulations (NUREG–0750).

DISCLAIMER: This report was prepared as an account of work sponsored by an agency of the U.S. Government. Neither the U.S. Government nor any agency thereof, nor any employee, makes any warranty, expressed or implied, or assumes any legal liability or responsibility for any third party's use, or the results of such use, of any information, apparatus, product, or process disclosed in this publication, or represents that its use by such third party would not infringe privately owned rights.

U.S.NRC

United States Nuclear Regulatory Commission

Protecting People and the Environment

NUREG/CR-7025

Radionuclide Release from Slag and Concrete Waste Materials

Part 1: Conceptual Models of Leaching from Complex Materials and Laboratory Test Methods

Manuscript Completed: March 2010
Date Published: December 2010

Prepared by
W.L. Ebert

Argonne National Laboratory
9700 South Cass Avenue
Argonne, IL 60439

M. Fuhrmann, NRC Project Manager

NRC Job Code N6669

Office of Nuclear Regulatory Research

Abstract

The technical literature was surveyed to evaluate test methods and modeling approaches used to characterize the release of contaminants during the weathering of portland cement-based materials and slag wastes from metal processing and recycling operations. Data sets were selected to represent various approaches used to study contaminant leaching, mineral dissolution, and waste material corrosion, and both the testing methods and data interpretations were evaluated. Models were evaluated with regard to both interpreting the test results and predicting long-term behavior. This study concludes that test results can be misinterpreted if testing artifacts are not taken into account, such as the interval used in solution replacement tests, the flow rate used in dynamic tests, and failure to reach steady-state, or if an inappropriate process is modeled. Contaminant release may be controlled by a diffusion process (mass transport) or by the chemical reaction affinity, and oxidation reactions can affect the releases of multivalent contaminants, such as Tc. The mechanism controlling the release might not be identifiable by a single test method. While well-established models for each of these processes and standardized test methods are available, the challenge is to identify which process controls contaminant release under the conditions of interest and how the laboratory test results relate to the model and long-term material behavior.

Table of Contents

Abstract iii

Table of Contents v

List of Figures ix

List of Tables xiii

Executive Summary xv

Acknowledgements xix

Acronyms and Abbreviations xxi

1 Introduction 1.1

1.1 Technical Approach 1.2

1.2 Introduction to Conceptual Models of Leaching from Complex Materials and Laboratory Test Methods 1.4

1.3 Theoretical Overview 1.5

2 Radionuclide Release Modes and Models 2.1

2.1 Empirical Rate Expressions 2.4

2.2 Electrochemistry-Based Models 2.8

2.3 Reaction Affinity Model 2.9

3 Applying the Reaction Affinity Model 3.1

3.1 Solution Feed-Back Effects 3.1

3.2 Using Test Results to Parameterize Models 3.3

3.3 Static Laboratory Test Methods 3.4

3.3.1 ASTM C1220 ..... 3.5

3.3.2 ASTM C1285 ..... 3.5

3.3.3 Partial Removal and Partial Replacement Tests 3.6

3.3.4 Example: ASTM C1220 Tests with LRM Glass 3.6

3.3.5 Example: ASTM C1285 Tests with Glass-Bonded Sodalite 3.8

4 Mass Transport Equations 4.1

4.1 Simple Diffusion-Controlled Release 4.1

4.2 Semi-Static Laboratory Test Methods 4.4

4.2.1 ANS 16.1 ..... 4.4

4.2.2 ASTM C1308 ..... 4.5

4.2.3 Solution Feed-back Effects in Semi-Static Tests 4.7

4.2.4 Example: Release of Cs from a Cement-Sludge Waste Form 4.8

4.2.5 Partition Model 4.12

4.3 Diffusion-Controlled Release with Concentration-Dependent Reactions 4.13
4.3.1 Example: Release of Cs from a Cement-Sludge Waste Form 4.17
4.3.2 Linking Reaction and Diffusion 4.18
4.3.3 Solution Exchange Tests for Affinity-Controlled Release 4.19
5 Static and Semi-Static Laboratory Test Results 5.1
5.1 Tests with Grouted Wastes 5.1
5.1.1 Christensen 5.2
5.1.2 Habayeb 5.4
5.1.3 Crawford et al. 5.6
5.1.4 Neilson et al. 5.8
5.1.5 Mattigod et al. 5.12
5.1.6 Rorif et al. 5.16
5.1.7 Côté et al. 5.18
5.2 Tests with Contaminated Slags 5.23
5.2.1 Pickett et al. 5.23
5.2.2 Fuhrmann and Schoonen 5.27
5.2.3 Sampling Interval 5.32
6 Dynamic Test Methods 6.1
6.1 Column Reactors 6.2
6.1.1 White and Brantley 6.3
6.1.2 Fuhrmann and Schoonen 6.5
6.1.3 Steady State in Column Reactors 6.9
6.2 Dynamic Tests and Affinity-Controlled Dissolution 6.14
6.2.1 Determining Dissolution Rate from Experimental Results 6.15
6.2.2 Significance of the Measured Rate 6.18
6.3 Single-Pass Flow-Through Test Method 6.20
6.3.1 Forward Dissolution Rates 6.21
6.3.2 Surface Area of Crushed Material 6.24
6.3.3 Model Parameter Values 6.26
6.3.4 Dependence on Chemical Affinity 6.27
6.4 Fluidized Bed Recirculating Reactor 6.29
6.5 Pressurized Unsaturated Flow Reactor 6.30
6.6 Forced-Through Reactor 6.33
6.6.1 Butcher et al. 6.33

6.6.2 Poon et al. 6.34
6.7 Soxhlet Reactor 6.35
6.7.1 Delage and Dussossoy 6.36
6.7.2 Atkinson et al. 6.37
7 Discussion 7.1
7.1 Modeling Waste Site Releases 7.1
7.2 Relating Models and Laboratory Tests to Waste Sites 7.2
7.3 Testing Objectives and Test Method Selection 7.3
7.4 Interpreting Test Results 7.5
7.4.1 Affinity vs. Diffusion 7.6
7.4.2 Comparing Responses from Static and Semi-Static Tests 7.7
7.4.3 Effect of Sampling Interval 7.8
7.4.4 Effect of Solution Exchange on Affinity-Controlled Release 7.9
7.4.5 Effect of Flow on Diffusion-Controlled Release 7.10
7.5 Conclusions and Comments 7.12
7.5.1 Contaminant Source Term Models 7.12
7.5.2 Testing 7.13
7.5.3 Laboratory Test Methods 7.14
7.5.4 Laboratory Test Interpretations 7.16
7.5.5 Recommended Test Methods 7.17
7.5.6 Concluding Remarks 7.19
8 References 8.1
APPENDIX A Affinity-Controlled Dissolution A.1
APPENDIX B Method Used to Reproduce Data Plots from Literature B.1
APPENDIX C Diffusion-Controlled Release with Concentration-Dependent Reactions C.1
APPENDIX D Diffusive Release from a Finite Cylinder D.1
APPENDIX E Summary of Laboratory Test Methods E.1
E.1 ANS 16.1 Leach Test (ANS 2009) E.5
E.2 ASTM C1220 Monolith Immersion Test (ASTM 2009a) E.5
E.3 ASTM C1285 Product Consistency Test (ASTM 2009a) E.6
E.4 ASTM C1308 Accelerated Leach Test (ASTM 2009a) E.7
E.5 ASTM C1662 Single-Pass Flow-Through Test (ASTM 2009a) E.7
E.6 Pressurized Unsaturated Flow Test (McGrail et al. 1997a) E.8
E.7 ISO 16797 Soxhlet-Mode Chemical Durability Test (ISO 1982) E.9

E.8 Solution Replacement Tests (Johnson et al. 2002) E.9
E.9 Lysimeter Tests E.10
E.10 EPA Methods E.10
E.11 Other Test Methods E.12

List of Figures

Figure 2.1. Schematic drawing of some possible radionuclide release modes: (1) wash-off, (2) dissolution of host phase, (3) diffusion-limited release, (4) diffusion-limited release coupled with chemical reaction, (5) diffusion-limited release coupled with dissolution of encapsulated host phase, and (6) solubility-limited release. 2.2

Figure 2.2. Data from Lasaga and Luttge (2001): comparison of dissolution theory with experimental data for (a) albite at pH 8.8 and 80°C and (b) labradorite at pH 3 and 25°C. 2.12

Figure 2.3. Data from Hellman and Tisserand (2006): Dissolution rate of albite at 80°C and pH 3 as a function of ΔG_r. 2.13

Figure 3.1. Results from Ebert (2006): Regression of pooled C1220 test results. 3.7

Figure 3.2. Results from Ebert (2006): ASTM C1285 Method B tests with sodalite, binder glass, PC CWF, and HIP CWF materials. 3.9

Figure 4.1. Schematic plot of testing increment. 4.2

Figure 4.2 Results in ANS 16.1 test procedure: (a) Example 1 and (b) from Example 2 for cumulative fractional release (CFR, filled circles) and leachability index (L, open circles). 4.6

Figure 4.3 Results from Spence and Cox (1990): Impact of assuming zero surface concentration on cumulative release for four diffusion coefficients and two specimen V_{wf}/S ratios. 4.7

Figure 4.4. Data from Godbee and Joy (1974): (a) Cumulative release × (V/S) vs. time and (b) cumulative fraction leached vs. root time with analytical fits. Filled symbols represent exchange intervals ≤3 days and open symbols represent exchange frequencies ≥7 days. 4.10

Figure 4.5. Data from Godbee and Joy (1974): Incremental leach rate vs. mean root time with regression fit. 4.11

Figure 4.6. Data from Godbee and Joy (1974): Plot of incremental release values vs. duration of increment. 4.12

Figure 4.7. Results from Fuhrmann et al. (1990): (a) Regressed to diffusion model and power law fit and expected partition model fit, and (b) $t \leq 1$ day regressed to diffusion model and $t \geq$ 2 days regressed to power-law fit. 4.14

Figure 4.8. Plots of Equation 4.15 with $D_e = 1 \times 10^{-7}$ cm^2 d^{-1} and various values of k_f. 4.16

Figure 4.9. Data from Godbee and Joy (1974): Plot of cumulative release vs. cumulative time for cement-sludge material. Dashed line shows fit with the simple diffusion equation given in Equation 4.8 and solid line shows fit with the coupled diffusion-reaction equation Equation 4.18 . ..... 4.17

Figure 4.10. Results from Ebert (2005a): Solution exchange tests with HIP CWF and PC CWF in 110 mg L^{-1} H_4SiO_4 leachant solution. Open symbols represent 10 or 11-day exchange intervals and filled symbols represent 21-day exchange intervals. 4.20

Figure 4.11. Results from Ebert (2005a): SEM photomicrograph of (a) HIPCWF and (b) PC CWF materials reacted with 110 mg L^{-1} H_4SiO_4 at 90°C. 4.21

Figure 5.1. Results from Christensen (1982): ANS 16.1-like tests with BWR bead resins immobilized in cement (a) cumulative release vs. cumulative time, and (b) cumulative release vs. root cumulative time. 5.4

Figure 5.2. Results from Christensen (1982): ANS 16.1-like tests with BWR bead resins immobilized in cement fit (a) by shifting diffusion equation to fit the long-term results, and (b) with regressed diffusion equation and diffusion + reaction equation. 5.5

Figure 5.3. Results from Habayeb (1985): ANS16.1-type tests with portland cement (a) cumulative ^{134}Cs release vs. cumulative time and (b) cumulative ^{134}Cs release vs. root time. 5.6

Figure 5.4. Results of tests from Crawford et al. (1984): (a) Cumulative release vs. time and (b) cumulative release vs. root time of ^{134}Cs from 28-day grout, and (c) cumulative releases from materials cured for three different durations vs. root time. 5.7

Figure 5.5. Results from Neilson et al. (1982): Full-scale ANS16.1 tests with PWR evaporator concentrate waste in masonry cement (a) cumulative fraction release vs. cumulative time and (b) cumulative fraction release vs. root-time. 5.10

Figure 5.6. Results from Neilson et al. (1982): Full-scale ANS16.1 tests with BWR evaporator concentrate waste in portland Type III cement (a) cumulative fraction release vs. cumulative time and (b) cumulative fraction release vs. root-time. 5.11

Figure 5.7. Results of tests by Mattigod et al. (2001): Cumulative fractions released from cement without added steel vs. time for (a) ^{99}Tc and (b) ^{125}I. 5.13

Figure 5.8. Results of tests by Mattigod et al. (2001): Cumulative fractions released from cement with added steel vs. time for (a) ^{99}Tc and (b) ^{125}I. 5.14

Figure 5.9. Results of tests by Mattigod et al. (2001): Cumulative fraction released from cement without added steel: vs. root time for (a) ^{99}Tc and (b) ^{125}I 5.15

Figure 5.10. Results from Rorif et al. (2005): Solution exchange tests conducted following the ANS 16.1, ISO 6961, and OND sampling schedules (a) CFL vs. cumulative time, (b) CFL vs. root time for ANS 16.1 and ISO 6961 tests with identified sampling intervals, and (c) linear fits to OND test results for different sampling intervals. 5.17

Figure 5.11. Results from Côté et al. (1987): Cumulative amounts of (a) Cd, (b) Cr, and (c) Pb leached from soluble silicate-cement, fly ash-cement, and fly-ash-lime waste forms. 5.19

Figure 5.12. Results from Côté et al. (1987): Cumulative amounts of Cd, Cr, and Pb leached from (a) fly ash-lime, (b) fly-ash-cement, (c) clay-cement, and (d) soluble silicates-cement waste forms. 5.20

Figure 5.13. Results from Côté et al. (1987): Releases of Cr from fly ash-cement and fly ash-lime waste forms. 5.22

Figure 5.14. Results from Pickett et al. (1998): ANS 16.1 tests with Whittaker-Greenville site slag plotted as (a) cumulative release vs. cumulative time, and (b) cumulative release vs. cumulative root-time. 5.25

Figure 5.15. Results from Pickett et al. (1998): ANS 16.1 tests with Molycorp-Washington site slag plotted against (a) and (b) cumulative time and (c) cumulative root-time. 5.26

Figure 5.16. Results from Pickett et al. (1998): ANS 16.1 tests with Cabot-Reading site slag plotted against (a) cumulative time and (b) cumulative root-time, and (c) release of Ca. 5.28

Figure 5.17. Results from Fuhrmann and Schoonen (1997): ALT at 60 °C with slag E-1 plotted against (a) cumulative time, (b) cumulative root-time, and (c) cumulative time with linear fits. 5.30

Figure 5.18. Results from Fuhrmann and Schoonen (1997): ALT at 60 °C with slag AS-3 plotted against (a) cumulative time, (b) cumulative root-time, and (c) cumulative time with regression fits. 5.31

Figure 6.1. Results from White and Brantley (2003): Measured dissolution rate of (a) fresh plagioclase and (b) weathered plagioclase based on release of Na. 6.4

Figure 6.2. Results from Fuhrmann and Schoonen (1997): Column tests with slags (a) E-1, (b) Q-BOPA, and (c) AS-3. ..... 6.6

Figure 6.3. Results from Fuhrmann and Schoonen (1997): Solution concentrations in column tests with slag (a) E1, (b) Q-BOP, and (c) AS-3. ..... 6.8

Figure 6.4. Results from Mogollon et al. (1996): Measured Al concentrations vs. *L/v* for tests conducted with leachant having four different pH values. 6.11

Figure 6.5. Results from Taylor et al. (2000a): Measured flow rate, Si, and Sr concentrations vs. *L/v* for 5.0 cm column tests with plagioclase 6.12

Figure 6.6. Results from Taylor et al. (2000a): Measured Si concentrations vs. *L/v* for tests conducted with $L = 3.5$ cm and $L = 5.0$ cm columns. The diagonal line is fit to the low *L/v* data to show the far-from-equilibrium limit where the steady-state concentration is linear with the inverse flow rate (at very high flow rates) and the dissolution rate is constant 6.13

Figure 6.7. Schematic plot of dissolution rate dependence on flow rate and limiting values. 6.19

Figure 6.8. Results from Ebert (2005b): SPFT tests with LRM-1 glass (a) test 5(8) conducted at an intermediate flow rate ($F/S = 1.75 \times 10^{-8}$ m s^{-1}) and (b) test 9(45) conducted at a very high flow rate ($F/S = 2.38 \times 10^{-5}$ m s^{-1}). 6.22

Figure 6.9. Results from Ebert (2005b): SPFT tests with LRM glass (a) combined results from all participants and (b) subset of results with rates <2.3 g m^{-2}d^{-1} and steady-state Si concentrations <10 mg L^{-1} 6.23

Figure 6.10. Results from Ebert (2005b): SPFT tests showing (a) leachant flow rate normalized to specimen surface area *F/S* (circles) and Si concentration (squares) for each sampling and (b) cumulative release vs. cumulative reaction time. 6.25

Figure 6.11. Results from McGrail et al. (1997): SPFT tests with LD6-5412 glass at various temperatures and pH values. 6.27

Figure 6.12. Results from Yang and Steefel (2008): SPFT tests with kaolinite at 22°C and pH 4. . 6.28

Figure 6.13. Schematic diagram of recirculating flow-through reactor. 6.29

Figure 6.14. Results from Chou and Wollast (1984): Dissolution of albite at pH 5.1 and pH 3.5. .. 6.30

Figure 6.15. Results from Pierce et al. (2006): PUF tests of glass LAWAN102 in demineralized water at 90°C. 6.32

Figure 6.16. Results from Butcher et al. (1996): Force-through tests with ordinary portland cement and acetic acid 6.33

Figure 6.17. Results from Poon et al. (2001): Force-through test with portland cement and water . 6.34

Figure 6.18. Schematic diagram of a Soxhlet reactor. 6.36

Figure 6.19. Results from Delage and Dussossoy (1991): Soxhlet tests with R7T7 glass. 6.37

Figure 6.20. Results from Atkinson et al. (1984): Soxhlet tests with cement (a) depletion depth vs. time and (b) depletion depth vs. root time. 6.38

Figure 7.1. Results from Bourcier et al. (1991): Static tests fit to diffusion and affinity models. 7.6

Figure 7.2 Schematic illustration of effect of sampling interval on incremental rate. 7.9

Figure 7.3. Schematic illustrations of (a) the effect of leachant exchange frequency on measured release rate and (b) the expected responses for diffusion-controlled and affinity-controlled release mechanisms. 7.10

Figure 7.4. Schematic illustration of depleted surface region of diffusion-controlled release (a) before and (b) after increase in solution concentration of contaminant due to an external source. 7.11

List of Tables

Table 2.1. Coefficients used in model commercial spent nuclear fuel 2.7

Table 4.1. Data from ANS 16.1 Table A.2 for Example 1, expressed in hours 4.5

Table 4.2. Test data from Godbee and Joy (1974) 4.9

Table 5.1. Estimated data for tests by Christensen (1982) 5.3

Table 5.2. Results from tests by Crawford et al. (1984) 5.8

Table 5.3. Waste form and testing data for Neilson et al. (1982) 5.9

Table 5.4. Data read from plots for release of ^{137}Cs 5.9

Table 5.5. Sampling intervals used in ANS 16.1, ISO 6961, and OND test methods 5.16

Table 5.6. Coefficients regressed with power law fits 5.20

Table 5.7. Coefficients from the regression analyses by Côté et al. (1987) 5.21

Table 5.8. Chemical compositions of Molycorp-Washington, Whittaker-Greenville, and Cabot-Reading site slags 5.24

Table 6.1. Initial concentrations in slags, as elemental mass% 6.7

Table C.1. Boundary conditions in Danckwerts (1950) and in Godbee and Joy (1974) C.2

Table D.1. Values of the Parameters β_m for m=1 to 20 ..... D.3

Table E.1. Summary of test methods E.3

Table E.2. Regulatory levels for RCRA-regulated inorganic elements E.11

Executive Summary

This is the first of four reports to be written documenting the critical analyses of the testing and modeling methods that are available to predict the long-term performance of disposal sites containing radioactive cement and slag wastes. These reports will discuss laboratory and field tests conducted to measure contaminant release rates and behavior, mathematical models based on the degradation mechanism used to predict the release behavior, and the possible use of those models as source term submodels in the performance models used for contaminant migration and dose assessments. For this first report, the technical literature has been surveyed to characterize and evaluate the test methods that have been used to study contaminant leaching and matrix degradation behaviors of portland cement-based materials and slag wastes generated by metal processing and recycling operations. The intent is not to provide a thorough literature review addressing the results of tests conducted with cement-based materials and slags. Rather, the purpose is to critically evaluate the test methods and modeling approaches that have been and are being used to predict the release of contaminants from these materials as they are weathered with regard to supporting and informing assessments of the long-term behavior of waste sites. Therefore, data sets were selected to demonstrate common experimental approaches and interpretation of results for a range of test methods as a part of the evaluation, with the primary focus on the consistency and relevance between the test data and the process model.

The two predominant processes that were evaluated are diffusion-controlled release and affinity-controlled dissolution. Diffusion-controlled release usually dominates the behavior of cements and affinity-controlled dissolution usually dominates the behavior of the mineral, oxide, and glass phases that comprise slag wastes, although both processes are often operative during the weathering of waste materials. The mathematics is well developed for modeling both diffusion-controlled and affinity-controlled processes, and aspects of various models relative to test methods are discussed in detail. The development of models for both diffusion and dissolution processes are reproduced in this report because they are important for assessing the usefulness of particular test methods, interpreting test results on the basis of the models, and, in some cases, guiding recommended modifications of a test method and test conditions to improve consistency with model. These modifications include models coupling diffusion and reaction, accounting for the effects of flow in laboratory tests, and approaches taken to model mass transport through unsaturated media. Aspects of transport models were considered in detail because many of the models that have been developed to represent the transport of contaminants through the environment are also useful for modeling contaminant transport through the waste itself. Most of that discussion will occur in a later report focused on transport through the geosphere. Some discussion of the combined oxidative-dissolution process is included because it will be relevant to the degradation of metallic and semi-conducting phases present in some slags that will be evaluated at a later stage of this project. The development of tests and models for oxidation reactions relevant to waste material weathering is less mature than those for dissolution-controlled and diffusion-controlled processes.

The ultimate objective of laboratory testing is to identify the process (or processes) that will control the release of contaminants over long time periods, measure parameters for a model that quantifies the release by that process, and then integrate the parameterized model into a contaminant transport model that can be used to provide a source term for dose assessment calculations. The analyses in this report are primarily focused on using laboratory tests to measure model parameter values and evaluating the consistency of the test results with regard to the basis of the model. An initial analysis of several dose assessment codes was also performed with regard

to how source term models are (or could be) incorporated into those codes. The contaminant source term is incorporated into the reactive-transport models used to simulate the release and transport of contaminants in geologic environments for performance and dose assessment calculations as a separate time-dependent term in a conservation of mass expression that includes other terms to account for advection, diffusion, sorption, radionuclide decay, and other processes that will affect the amount of the contaminant of interest. Essentially the same governing equations are used for modeling reactive transport in all simulation codes except for small modifications related to the identities and distributions of the contaminants and phases that are present. Additional terms may be required to model the release and transport of redox-sensitive components in slags and concrete waste. The codes and how laboratory test data can be incorporated will be evaluated in greater detail at a later stage of this project.

Commonly used and standardized test methods are summarized and evaluated for use in characterizing and modeling the behavior of cement and slag waste materials. This is done by critically analyzing test data available in the literature with regard to the mathematical descriptions of the process models. Test methods are categorized as static, semi-static (wherein all or part of the test solution is exchanged during the test), or dynamic (wherein solution is continuously flowed). The effects of differences in specific methodologies are interpreted based on the process models for diffusion, dissolution, and transport. The primary conclusion reached from these analyses is that many test results have been misinterpreted due to the inappropriate application of a process model to the data set. Key conclusions regarding the test methods are summarized below:

The ANS 16.1 leaching method is a solution exchange test that was developed to characterize diffusion-controlled release. The method does not purport to characterize long-term behavior, and careful scrutiny indicates that it does not quantify the short-term kinetics very well either. This is because the test response is sensitive to the different sampling intervals that are used to measure the extent of component releases. Release rates and model parameters determined from consecutive exchange intervals that differ by only a few days agree within experimental uncertainties, but the rates determined from intervals that differ by more than about 7 days usually do not agree. This is because the linear rate that is determined for the sampling interval (which provides one data point) is used to represent a process in which the rate depends on the square root of the reaction time. The discrepancies between the data and the model increase with the solution exchange interval. While useful as a screening test for various waste materials, it is not recommended for modeling waste degradation behavior for long-term predictions. The ASTM C1308 ALT uses the same methodology, but is preferred to the ANS 16.1 method because it includes ten consecutive 1-day exchange intervals and because the test results are assessed to confirm that diffusion is the controlling mechanism for contaminant release or to assess the possibility of affinity-controlled release. The first three exchange intervals that are called in the ASTM C1308 method (after 2-, 5-, and 17-hour intervals) provide no added insight for determining or quantifying the mechanism and should be replaced by a single 1-day interval. Application of the ASTM C1308 method to a material that dissolves provides information regarding the dissolution rate. Using two series of constant exchange intervals is expected to allow the test results to better distinguish between diffusion-controlled and affinity-controlled dissolution mechanisms for contaminant release. For example, replacing the final five 1-day exchange intervals with five 7-day intervals would increase the usefulness of the test.

Column tests are used to simulate the percolation of water through soils and rock and to characterize the dissolution of materials that are contacted. The dissolution of most minerals, oxides, and glasses occurs by an affinity-controlled mechanism, wherein the dissolved components (e.g., silica) moderate the intrinsic dissolution rate of the material. Insight into dynamic dissolution tests (i.e., tests with flowing solution) is drawn from a variety of test methods and

consideration of the underlying theory and modeling. Although a dissolution rate can readily be determined by passing solution through a cell containing the mineral, the measured dissolution rate will depend on the flow rate of the solution and the reactive surface area that is contacted. Mineral dissolution rates in dynamic tests will only be independent of the flow rate when the mineral dissolves at the highest possible rate at the particular temperature and pH used (or attained) in the test. Neglecting erosion, the effect of flow is through the solution chemistry and the feedback effects of dissolved components. The dependence of the dissolution rate on the flow rate can only be quantified when the system is at steady state; that is, when the rate at which a component is released from the dissolving material into the reaction cell is equal to the rate at which the dissolved component is removed from the reaction cell by solution flow. In a column dominated by solids (e.g., a packed column), the solution chemistry and materials dissolution rate will vary with distance through the column: the solution near the entrance will remain the most dilute and the solution near the exit will remain the concentrated in dissolved components, even when the system reaches steady state. At steady state, these concentrations do not change with time. The eluted solution that is analyzed represents the solution at very end of the column.

In a column that is dominated by solution (e.g., a fluidized bed), the solution within the column (or reaction cell containing the solid) is assumed to be well mixed with a uniform composition. The eluted solution that is analyzed represents the solution within the column or reaction cell. In most cases, concentrations that are high enough to be measured are high enough to impact the dissolution rate of the dissolving solid. The intrinsic dissolution rate (the rate with no solute feedback effects) can only be inferred as an asymptotic limit of the rates measured in increasingly dilute solutions. Whereas one can be confident that all particles experience the same solution flow rate in a fluidized bed reactor, it is likely that a range of flows occurs in a column reactor due to preferred flow paths, variances in the porosity, etc. Column tests can be used to represent a natural system, but the system may be too complicated to measure model parameter values and, in some cases, to identify which process controls contaminant release. The value of column tests (and of related tests with lysimeters in natural environments) with regard to waste degradation modeling is to confirm that the appropriate performance models are used to quantify the processes controlling contaminant release and transport and to calibrate the model for the system of interest (e.g., scaling the model to the effective porosity).

In summary, process models are available to describe the release of contaminants from slags, contaminated concretes, and other waste materials in laboratory tests and natural environments. Various static, semi-static, and dynamic laboratory test methods have been applied to waste materials and the results interpreted based on the process models. In many cases, details of the test methodology have not been consistent with how the models were applied. Key shortcomings identified in this report are the variable sampling intervals used in solution exchange tests including ANS 16.1 and ASTM C1308 tests and the effect of the solution flow rate in column tests. The use of these relatively simple laboratory methods to inform performance assessments can be improved by simple modifications to the test methodologies and more selective applications of particular test methods based on an understanding of the process controlling contaminant releases and the effects of testing parameters on experimental results and how they should be modeled. The first objective of a laboratory test should be to identify the process controlling release of the contaminant of interest. This could be diffusion, dissolution, or reaction (e.g., oxidation). Subsequent tests are conducted to provide the model parameters. In most cases, separate series of laboratory tests will be needed to characterize the properties of the waste material (e.g., diffusion coefficients, dissolution rate, and solubility) and the effects of the natural environment (e.g., porosity, groundwater composition, and flow) on the weathering of the material. These issues will be discussed further in subsequent reports.

Acknowledgements

This report was prepared to document work performed by Argonne National Laboratory (contractor) for the Nuclear Regulatory Commission (NRC) under Contract No. 60-09-270 (job number N6669). The analyses reported here were performed on behalf of the NRC Office of Nuclear Regulatory Research, Division of Risk Analysis (Environmental Transport Branch). The NRC project manager is Mark Fuhrmann. This report is an independent product of Argonne National Laboratory and does not necessarily reflect the views or regulatory position of the NRC.

Quality of Data and Analyses

Only data from the literature sources cited in the report were used in these analyses. In many cases, the data presented in this report were generated by reading values from plotted data in the literature publications. These were used to analyze trends in the data to evaluate reaction behavior and analyze the effects of testing parameters, and not to extract results for other uses.

The spreadsheet program Microsoft EXCEL 2003 and the plotting program KaleidaGraph version 3.6 (Synergy software) were used to plot data, perform regression fits, and compute modeled values. These are commercial software packages.

Acronyms and Abbreviations

ALT	Accelerated Leach Test
ANL	Argonne National Laboratory
ANS	American Nuclear Society
ASTM	ASTM-International
BWR	Boiling Water Reactor
CFL	Cumulative Fraction Leached
CSH	Calcium Silicate Hydroxide
CWF	Ceramic Waste Form
DOE	U.S. Department of Energy
DUST	Disposal Unit Source Term (computer code)
EP	Extraction Procedure (test method)
EPA	U.S. Environmental Protection Agency
HIP	Hot Isostatic Press
HIP-CWF	CWF made by Hot Isostatic Pressing
IAEA	International Atomic Energy Agency
NRC	U.S. Nuclear Regulatory Commission
PC-CWF	CWF made by Pressureless Consolidation
PCT	Product Consistency Test
PUF	Pressurized Unsaturated Flow (test reactor)
PWR	Pressurized Water Reactor
RESRAD	Residual Radioactivity (computer code)
SEM	Scanning Electron Microscopy
SPFT	Single-Pass Flow-Through (test)
SPLP	Synthetic Precipitation Leaching Procedure
TCLP	Toxicity Characteristic Leaching Procedure
TSPA	Total System Performance Assessment
USGS	U.S. Geological Survey
WET	Wet Extraction Test
WIPP	Waste Isolation Pilot Plant

1 Introduction

The U.S. Nuclear Regulatory Commission (NRC) issues licenses for the possession of nuclear materials and regulates the disposition of radioactive wastes in the United States. License termination requires a determination of whether a waste material is likely to remain sufficiently durable to retain radionuclides while being weathered or if the waste must be further stabilized. This decision is typically made by considering the predicted long-term impact of waste degradation and contaminant release on the groundwater composition based on short-term measurements of the corrosion behavior of the waste material and limited characterization of the site. The calculations currently used to assess long-term waste material behavior utilize fairly simple models for radionuclide source terms, which may or may not be consistent with the degradation mechanisms of the wastes being evaluated. The ability to identify mechanistic bases for the laboratory tests and source term models used in assessment calculations will add credence to site assessments and the evaluation of site remediation plans.

Argonne National Laboratory (ANL) has initiated an NRC-sponsored activity to identify the laboratory and field tests used to characterize waste form degradation. It also measures the release of radionuclides and how they interface with the models used to predict radiation doses in risk assessment calculations. The terms "waste material" and "waste form" are used in this report to represent the source material from which the radionuclide is being released and the stabilized material, respectively. The current use of test methods to parameterize degradation and transport models is being evaluated so they can better represent the mechanisms of radionuclide release in site assessments. The expected product of this activity is a protocol that can be used by the NRC to integrate the results of short-term laboratory tests and field measurements that address waste material (or waste form) degradation and leaching into the model calculations that are used to assess the stability of wastes at NRC-regulated sites prior to decommissioning. The approach will be to (1) develop a mechanistic understanding of the weathering processes of the particular waste material, (2) identify the appropriate degradation model(s) to describe the release of radionuclides, and (3) follow an appropriate testing protocol to measure values of the model parameters to be used in performance assessment calculations. Guidance will also be developed for utilizing leach test data in source term models.

Two groups of waste materials that are currently of interest to the NRC are (1) slags produced during ore processing and metal recycling, and (2) contaminated concrete and metal debris from decommissioning activities. Slags are typically heterogeneous mixtures of glassy and crystalline phases, and can be hard, dense, and glassy, soft and porous, or rock-like. Since slags are formed as molten material solidifies, hazardous elements can become incorporated into the structures of both the glassy and crystalline phases by substituting into structural lattice sites, as interstitial defects, forming separate phases, etc. Degradation by weathering is expected to occur by the dissolution of each component phase at a rate that depends both on the intrinsic properties of the phase and the environment. The distributions of hazardous components in contaminated concrete are usually restricted by the accessibility of groundwater to pores where interactions with other phases in the concrete structure and pore water can occur. Degradation of contaminated concrete by weathering is expected to occur by advection or diffusion of water through the pore structure coupled with the dissolution of both the occluded and structural phases of the concrete. The presence of other materials, such as rebar, may affect the weathering behavior by sorption, generation of colloids, affecting the pore water chemistry, redox, etc. It is expected that different models and testing protocols will be required to determine source term values for the releases of hazardous components from slags and concretes due to differences in the release mechanisms.

1.1 Technical Approach

The work described in this and the three subsequent reports includes literature reviews to identify materials of interest and existing information regarding corrosion behavior and test results, descriptions of degradation mechanisms, key interactions, and approaches for developing long-term predictions. Based on these reviews, source term modeling approaches will be recommended for slag and concrete waste materials and suites of test methods to provide data for use in the models will be identified. These activities are being conducted as four mostly sequential activities that are summarized below. Separate reports will be produced that focus on each part of the evaluation, although all aspects will be discussed in each report to some extent. It is anticipated that the evaluation of any particular aspect of the project will continue to be developed and will evolve over the course of the project as additional insights are gained. For example, aspects of field testing, leaching data for slags and concretes, and basic approaches in dose calculation models are discussed in this report from the perspective of conceptual models and laboratory test methods to better understand what information is needed and how that information will be used. Subsequent reports that are focused on field testing, specific data bases, and modeling approaches will probably include discussions that further elaborate the roles of various laboratory test methods. The primary technical issues to be addressed in the four parts of this work are summarized below.

Part I: Conceptual Model of Leaching from Complex Materials and Laboratory Test Methods

This report provides a summary of the initial review and analysis of existing literature regarding the weathering of various slag and concrete waste materials and waste forms, including experimental results, field measurements, and modeling approaches. The mechanistic basis of existing conceptual models and the current use of laboratory and field data are evaluated. The inherent uncertainties associated with current modeling approaches (both in concept and quantization) are discussed and the need to develop models that better represent the release mechanisms of matrix and hazardous components is assessed. Various test methods currently used to study waste form weathering are summarized and evaluated with regard to the information provided, limitations of the test method, and the role of the test data in assessing the degradation mechanism and the long-term release behavior. The applications of specific test methods to slag and concrete wastes are discussed and test protocols recommended for parameterizing the source term models deemed to be appropriate for various waste types, including slag and concrete wastes. This report is focused on the results for Part I.

Part II: Relationship between Laboratory Tests and Field Leaching

The relationships between the behavior measured in laboratory tests and field measurements will be evaluated and methods used to relate laboratory-measured values to field measurements will be discussed. Insights from previous analyses of minerals and natural materials used as analogs for waste glass (e.g., basalts, obsidians, and tektites) in laboratory and field tests will be brought to bear on the systems of interest in this project. Weathering rates determined from field measurements are typically and systematically 100 to 1000 times lower than rates determined from laboratory tests, and several reasons for this have been postulated. By design, most laboratory tests maintain constant environmental conditions to accurately measure the effect of a specific variable on the degradation rate, such as the effect of temperature or pH, whereas weathering in the field is affected by continuous changes in many conditions that are not fully known and not represented explicitly (or perhaps not accurately) in laboratory tests. In general, the replication of reaction conditions in the field lead to weathering rates that are too low to measure directly in

laboratory tests. Rates measured in specific laboratory tests should not be directly compared with values measured in the field with the intent or expectation of quantitative agreement. Instead, values measured in laboratory tests should be interpreted based on a mechanistic understanding to take into account the range and combination of effects experienced in the field. For example, transport may be a limiting factor in the rates determined from field observation but have an insignificant effect on laboratory results. From this perspective, field measurements can help "calibrate" laboratory measurements to better represent the combined effects of environmental conditions and perhaps identify other processes that should be taken into account in testing and/or modeling activities. It is anticipated that field leaching results would be better compared with model results that take several processes into account rather than directly with the results of a specific laboratory test that is dominated by one process. Laboratory tests specifically designed to represent the ranges of environmental conditions and interactions that affect in-field behavior are useful for confirming model results, but are not likely to provide the mechanistic data needed to select or parameterize the appropriate degradation model. What we expect to provide in this Task is a technically based recommendation for addressing this difference in decommissioning analyses.

Part III: Application of Models to Leaching Data from Slags and Concrete

Existing source term models that may be useful for calculating weathering behaviors of slags and concretes will be identified, summarized, and evaluated. The consistency of these models with data available for the release of components from slags and concretes will be evaluated with several examples. How well current models represent the measured release behavior will be assessed with regard to the uncertainty in long-term predictions due to uncertainties in the measured model parameters and uncertainty in how well the model represents the degradation behavior. Alternative models or modeling approaches will be recommended as appropriate.

Part IV: Application of Leaching Model to Dose Assessment Codes

The source term models for radioactive and hazardous contaminants must be interfaced with a dose assessment code to evaluate the performance of a waste site. In most cases, mechanistic models must be simplified (abstracted) for use in performance assessment codes to meet constraints in performing the calculations or due to the limitations of aleatory (random chance) or epistemic (absence of knowledge) uncertainties. The abstraction may include the combining of several model parameters into a single parameter that can be tracked in the performance assessment, replacing a variable with a bounding constant value, etc. Abstraction is usually a consequence of changing from the atomic scale of the mechanistic model (nm) to the intermediate scale of laboratory tests (cm) and then to the large scale of waste sites (km). Guidance will be developed regarding the appropriate use (or the need for integration) of laboratory data and field test information in dose assessment codes such as the Disposal Unit Source Term (DUST) and Residual Radioactivity (RESRAD) codes. The approach will be to combine insights gained with experience and insights from other site assessments done for other disposal systems at the Waste Isolation Pilot Plant (WIPP), Hanford, and Yucca Mountain to describe the use of test data and source models in dose assessment calculations. This will include propagating uncertainties in the mechanistic and abstracted source term models and in the coefficient values to estimate confidence levels. It is important that the abstracted models capture the environmental and temporal effects on material degradation and the release of hazardous components that are important to performance assessment.

1.2 Introduction to Conceptual Models of Leaching from Complex Materials and Laboratory Test Methods

One objective of this report is to evaluate the mechanistic basis of test methods and modeling approaches that have been used to assess the weathering of slag and concrete waste materials. The inherent uncertainties in the concept and quantization of these modeling approaches are discussed with the goal of better integrating mechanistic models for the release of hazardous and radioactive components from waste materials and waste forms in performance assessments. The "garbage in/garbage out" axiom for computer modeling holds, and an important component of this study is evaluating the laboratory and field tests that are currently used to provide parameter values for the assessment calculations, verifying the calculated results, and confirming that the model adequately represents the system being assessed.

The modeling approach commonly used to evaluate radionuclide transport in the environment is considered first to determine how the waste form source term is incorporated into the assessment code. The computer models used to calculate radionuclide release over extended periods are commonly comprised of separate model components that represent water flow, waste form degradation, and radionuclide transport. They may also include a model component for container breaching. Breaching containers, waste form degradation, and radionuclide transport all depend on the groundwater flow rate, but the groundwater flow rate is independent of these processes. The groundwater flow rate is an explicit parameter in transport models (and in some degradation models) and an implicit factor in the selection of a model to represent waste form degradation in the system. The goal of the initial effort discussed in this report is to evaluate the submodels used to describe specific processes in order to evaluate how waste material degradation test results are incorporated.

Computer codes used to assess contamination transport, such as the DUST (e.g., Sullivan 1993) and RESRAD (e.g., Yu et al. 2001) codes, provide deterministic reactive-transport calculations based on the same groundwater transport models and waste form degradation models. Deterministic models presume that a system operates according to governing equations that give certain input-response relationships. The computer code developed for the Hanford low-activity waste disposal system uses the same governing equations for contaminant transport coupled with waste degradation rate equations in a deterministic approach (Bacon et al. 2004). The computer model developed for the Yucca Mountain repository Total System Performance Assessment (TSPA) also utilizes the same degradation and transport equations, but uses a stochastic approach (DOE 2008). Stochastic models quantify uncertainties in models and parameters to calculate the probabilities of possible outcomes from input-response relationships. Aspects of the approaches used in DUST, RESRAD, and the Hanford and Yucca Mountain performance assessments will be considered in the evaluation of assessment models that could be utilized for NRC-regulated waste sites.

Various waste form degradation models account for the release modes of simple wash-off, solubility-limited release due to waste form dissolution, and diffusion-controlled release. In practice, the amount of material that is released will depend on the surface area (or the volume of a porous waste form) that is in contact with water. Laboratory tests provide an area-specific release rate that must be multiplied by the area of the waste form that is contacted by water in the disposal or waste site to calculate the amounts of radionuclides that are released. It is usually convenient to express the amount released as the fraction of the total that is initially present in the waste form (i.e., as a fractional release rate). The waste materials of interest can range in size from powders to boulder-sized chunks and cover large areas of various terrains and soil types. A crucial aspect of

the assessment is scaling the values measured in well-controlled laboratory tests with small specimens to the large scale of materials in the disposal system.

The accuracy of performance assessment codes depends in large part on user-input information regarding the waste material source term. A thorough understanding of the reaction mechanism and the effects of environmental variables is beneficial for identifying the appropriate laboratory test method to represent waste material behavior in the field. For example, it is often difficult to determine the release mechanism based on the initial degradation behaviors of many materials within the short durations of most laboratory tests, but the long-term behaviors of materials that degrade by solution affinity control will differ from the long-term behaviors of materials that degrade by diffusion-control. Several test methods may be required to determine the mechanism by which radionuclides or hazardous components are released from a particular waste material in order to reliably predict the long-term behavior that is of primary interest in assessment calculations.

Property values measured in laboratory tests may not represent field behavior well because the reaction conditions can be very different. Field studies using lysimeters to subject a waste form to natural conditions have a low success rate (sometimes due to physical failure of the lysimeter system, but often due to termination of the program prior to long test durations that are usually necessary to obtain useful results) and conclusions that have been drawn from test results often conflict with those based on laboratory tests. In many cases, this is because the details of the waste form degradation mechanism measured with laboratory tests are masked by transport behavior that dominates the field test results. That is, the affinity- or solubility-controlled release of a radionuclide from a waste form can be masked by diffusion-controlled transport limitations in the field. Many years may be required to attain steady-state behavior in a field environment; the measured release may not be sensitive to the waste material degradation kinetics until the transport rate is constant.

1.3 Theoretical Overview

The starting point for evaluating the spread of contamination is an expression of the mass balance equation at any location in the system domain, which can be generalized as

$$\frac{\partial M_i}{\partial t} = -\nabla \bullet \vec{J}_i + \sum_n Q_{n,i} + r_i \tag{1.1}$$

where M_i is the mass concentration of a radionuclide species i that is dissolved (mass per volume), $\vec{J}_i$ is the mass flux vector for species i in the mobile water phase (mass per area per time), $Q_{n,,i}$ is the net rate of the nth mass transfer process (mass per volume per time), and r_i accounts for reactions affecting the concentration of i (mass per volume per time). The first term on the right-hand side takes into account the three dimensional advection and hydrodynamic dispersion of the dissolved species i through the disposal system. The del operator is defined as $\nabla \equiv \frac{\partial}{\partial x} + \frac{\partial}{\partial y} + \frac{\partial}{\partial z}$.

The negative sign indicates a decrease in mass as species move out of that location in the system. In the mass balance expression, processes that contribute i to the system are added and processes that remove i are subtracted. The second term takes into account the "n" mass transfer processes including dissolution of the waste materials, precipitation of phases containing i, sorption (both

reversible and irreversible), various colloid-facilitated transport processes, etc. The reaction term r_i includes the ingrowth and annihilation of i through radioactive decay.

Implementation of the mass balance equation in performance assessment calculations requires identification of the important processes and parameterization of the appropriate process models for the disposal system, waste form(s), and radionuclides of interest. These calculations can span a wide range of scale: by necessity, phenomenological rate expressions are used to calculate mass transport by advection and diffusion on a gross macroscopic scale that ignores the details of pore structure in the geosphere. Although radionuclide release from the waste material or waste form may be calculated using either atomistic or macroscopic models, the transport properties that generally control the release rates of most radionuclides from the disposal system can mask the detailed kinetics of release from the waste form. The mechanistic and phenomenological bases of the transport and waste form degradation models that are used in coupled reactive-transport models will be discussed in the next report which will focus on field studies.

Of particular interest in this report is the release of radionuclides during waste form degradation. This provides the source term $Q_{dissolution}$ for the radionuclide in the summation term of Equation 1.1. A generalized rate law for the dissolution of i due to waste form degradation can be written as

$$Q_{dissolution} = A \times k_0 \times e^{-E_a/RT} \sum_j fn(a_j) \times fn(\Delta G_r) \tag{1.2}$$

where A is the reactive surface area, k_0 is the intrinsic reaction rate, in this case the dissolution rate, E_a is the activation energy for Arrhenius form of the temperature dependence, $fn(a_j)$ is a function describing the effects of solute component j, including H^+, on the reaction rate, and $fn(\Delta G_r)$ is the dependence of the reaction on the Gibbs free energy change. This last term can be thought of as the effect of the saturation state of the system on the dissolution rate. The functional form of the free energy dependence depends on the reaction mechanism (see Lasaga 1995). For example, the functional relationship commonly used in transition state theory models is

$$fn(\Delta G_r) = 1 - \exp\left(\frac{\Delta G_r}{RT}\right). \tag{1.3}$$

The functional forms for other mechanisms can be quite different, but the values of $fn(\Delta G_r)$ are fixed when the system is at equilibrium at $fn(0) = 0$ and when the system is far from equilibrium at $fn(-\infty) = 0$. Values for the terms preceding $fn(\Delta G_r)$ in Equation 1.2 are usually measured under test conditions far from equilibrium where the rate is essentially independent of ΔG_r. The units of $Q_{dissolution}$ are mass volume^{-1} time^{-1}. Note that the formulation in Equation 1.2 uses a separation of terms with no cross terms between variables. Various dissolution models that can be used to describe the release of radionuclides are discussed in Section 2. These include chemical affinity models, coupled oxidation and reaction models, and empirical models. The chemical affinity model is further discussed in Section 3 in terms of using the chemical affinity to model dissolution processes and using laboratory tests to parameterize affinity-controlled processes.

Instead of being released at the same rate at which the waste material degrades, the releases of some radionuclides may be controlled by mass transport of reactants (e.g., water) or products (e.g., the radionuclides) through the waste form. In a disposal site, the relative importance of reaction (equilibrium) and mass transport often depends on the percolation rate of groundwater and the

porosity of the waste: mass transport will control release when percolation occurs through fractures and is fast relative to diffusion, reaction/equilibrium will control release when percolation occurs slowly through granular and porous materials. Mass transport models and diffusion-controlled contaminant release are discussed in Section 4. Although they have the same theoretical basis, diffusion models for release from the waste form and transport through the disposal system are discussed separately because of different application and boundary conditions. Coupled diffusion and reaction processes are addressed briefly in Section 4.

Literature results of laboratory tests applied to various cement-based and slag waste forms are evaluated with regard to the utility of various test methods and modeling approaches in Sections 5 and 6. Section 5 is focused on results from static and semi-static test methods and Section 6 is focused on results from dynamic test methods. Although comments regarding the testing and modeling of contaminant release are provided throughout most sections, several important issues based on the evaluation of literature results and consideration of the testing methods are discussed further in Section 7 to support technical recommendations. Several conclusions based on evaluation of the literature are included in Section 7. They relate to the suitability of available contaminant source term models and laboratory test methods for the project goal of supporting waste site performance assessments.

2 Radionuclide Release Modes and Models

The specific release rate measured in laboratory tests, *rate*, with units of mass unit area^{-1} time^{-1}, can be related to the overall release rate from a finite solid, R, with units of mass volume^{-1} time^{-1}, as

$$R = rate \bullet \frac{A_w}{V_s}\left(\frac{m}{M}\right)^n = Q_{dissolution} \tag{2.1}$$

where A_w is the reactive surface area of the waste material and V_s is the volume of solution contacting the waste material in the disposal system. The parenthetical term takes into account the loss of surface area as the solid dissolves, where m is the mass of solid at the particular time of interest, M is the mass of solid present initially, and the value of n depends on the geometry of the waste form. For uniformly dissolving (shrinking) spherical and cubic forms, $n = 2/3$ (see discussion of spherical particles in Section 6.2.1). Note that the mole ratio could be used instead of the mass ratio. Equation 2.1 expresses the link between the overall dissolution rate that is needed for site assessments ($Q_{dissolution}$) and the specific release rate (*rate*) that is measured with laboratory tests. The functionality of the specific rate can be modeled according to the mechanism for radionuclide release and then scaled to the system being modeled by using Equation 2.1.

The importance of the areal dependence of the laboratory rate cannot be overemphasized when scaling a value measured with a few square centimeters of specimen surface area to behavior over many hectares of waste material based on the surface term A_w and its evolution as the waste material degrades. Implicit in Equation 2.1 is that the *reactive* surface area available in laboratory tests scales with the *reactive* surface area in the field. Most laboratory tests provide a reaction rate that is the weighted average of reactions at a large number of sites on a heterogeneous surface. This average may or may not represent reactive material sites in the field. For example, many laboratory tests are conducted with crushed material to provide large surface areas within small sample volumes. The abundance of highly reactive fracture surfaces (points and edges) generated by crushing the material can yield a rate that is biased high relative to the dissolution behavior of that material in the field, where the surfaces have been smoothed by prior reaction. While this aspect will be discussed in greater detail in the report for Part II addressing the relationship between laboratory tests and field measurements, such differences in the samples of the material of interest should be borne in mind when evaluating the atomistic-scale models for laboratory test results and the laboratory test methods. This report addresses determination of the laboratory-measured rate and its functionality.

The analytical models used to calculate radionuclide release rates are based on what is referred to herein as the radionuclide release mode. This is the process (or combination of processes) by which a radionuclide is released from the waste material as the transportable species quantified by the release model. Possible release modes are summarized below and illustrated in Figure 2.1.

(1) Wash-off

Fractions of some radionuclide inventories may be only weakly bound to the surface of the waste form by physical or chemical sorption or electrostatic attraction, or may be present in soluble residual salts trapped in voids, at grain boundaries, etc. These radionuclides may dissolve as soon as they are contacted by groundwater or leachate without degradation of the underlying phases,

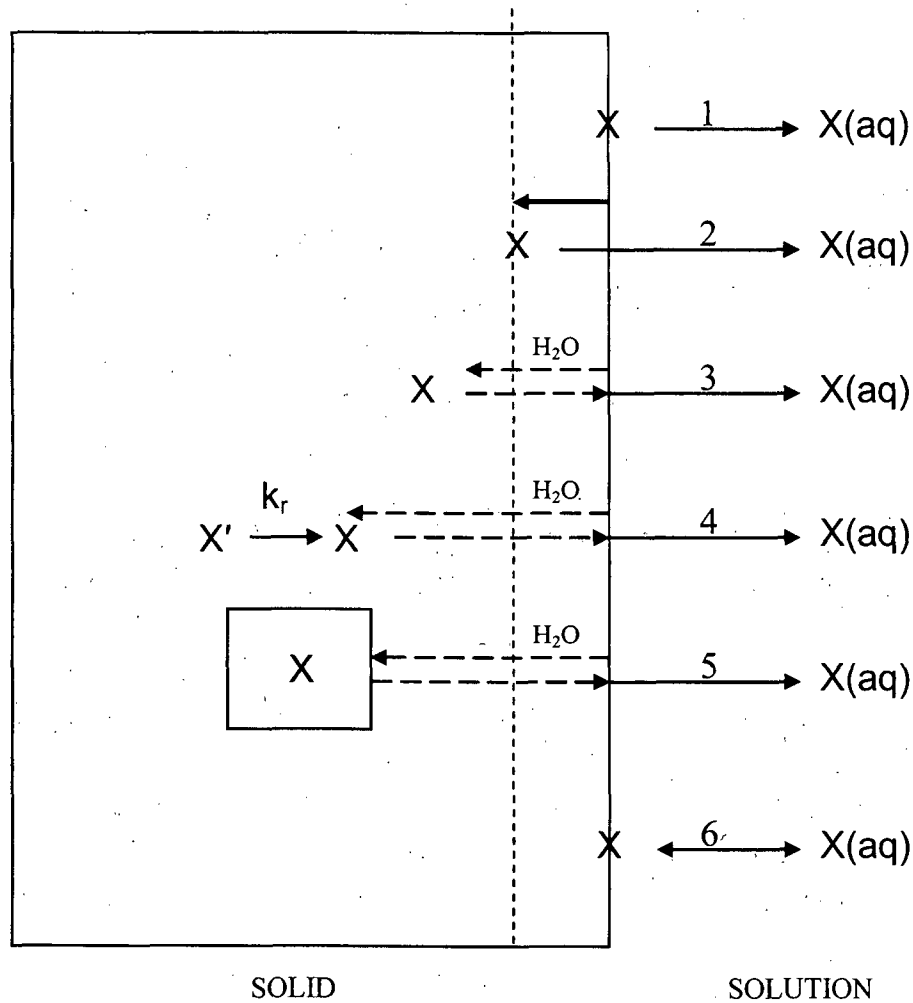

Figure 2.1. Schematic drawing of some possible radionuclide release modes: (1) wash-off; (2) dissolution of host phase; (3) diffusion-limited release; (4) diffusion-limited release coupled with chemical reaction; (5) diffusion-limited release coupled with dissolution of encapsulated host phase; and (6) solubility-limited release.

although the amount dissolved may be limited by the solubility of the phase. Including a term to take for surface wash-off into account in a degradation model provides the flexibility to account for release from the surface separately from release from the bulk, which may be controlled by a different mechanism. In laboratory tests, the chemical and physical properties of the near-surface region of a test specimen often differ from the underlying material due to preparation artifacts. These may include leaching of contaminants during polishing, the generation of highly reactive sites due to fracturing or polishing scratches, contraction or densification of material in the near-surface region, oxidation of the near-surface region by exposure to air or water, etc. The different behavior of the near-surface region could be modeled with Equation 2.1 by using different functions for the *rate* and different values for V_s, m, M, and n for radionuclides at the surface and for radionuclides in the underlying bulk.

(2) Dissolution of the host phase

The release of radionuclides that are incorporated into the structure of a phase require chemical reactions to degrade the immobilizing phase enough to expose the radionuclide to the leachant and reactions to break the bonds that immobilize it. The release of a radionuclide depends on the degradation rate of the host phase and the solubility limit of the radionuclide, which is governed by the solubility-controlling phase. The solubility-controlling phase can be the dissolving phase, a secondary phase that forms as the host phase dissolves, or a separate phase present in the system (e.g., a mineral in the host geology). For example, PuO_2 could form to establish the Pu concentration limit as a Pu-bearing glassy phase present in a slag waste material dissolves. The reaction to release a radionuclide from the host phase can itself be complex. Hydrolysis of a single bond may result in release, or an additional reaction may be required to generate a soluble species suitable for release and transport. For example, dissolution of UO_2 requires the oxidation of U(IV) to U(VI) prior to release.

(3) Diffusion-limited release

The release of a radionuclide from a waste material or waste form may be controlled by the diffusion of water through the host phase or diffusion of the radionuclide out of the host phase. Although mass transport (diffusion) at the reacting surface is a component in most degradation processes at the atomic scale, diffusion-limited release addresses diffusion control on the larger scale of the bulk material. The waste material is treated as an inert matrix through which the contaminant migrates at a rate characterized by a representative diffusion coefficient.

(4) Diffusion-limited release coupled with chemical reaction

The release of a radionuclide from an encapsulating phase may require dissolution of a host phase or other chemical reaction to occur prior to diffusion of the radionuclide out of the host phase. For example, oxidation of an encapsulated metallic waste or dissolution of an encapsulated oxide waste may be required to mobilize radionuclides prior to diffusion through the waste matrix.

(5) Diffusion-limited release coupled with dissolution of host phase

The release of radionuclides bound in a phase that is itself encapsulated in another phase requires water to penetrate through the encapsulating phase (either by diffusion or dissolution of the encapsulating phase) before contacting and then degrading the phase that contains the radionuclide. The release of a radionuclide depends on the degradation rates of both the encapsulating phase and host phases, and also on the solubility limit of the radionuclide. The solubility limit is determined by the solubility-controlling phase, which might be the dissolving phase or a secondary phase; different phases can control the solubility limit during the course of waste form degradation. For example, analcime that forms as a secondary phase during borosilicate glass dissolution can replace glass as the controlling phase for dissolved silica and establish a lower solubility limit that results in an increase in the glass dissolution rate (Ebert and Bates 1993). The increased glass dissolution rate could increase the release rates of radionuclides that are dissolved in the glass or sequestered within inclusion phases due to both physical effects (exposure of more surface to water) and chemical effects of the solution chemistry (higher pH, precipitation of radionuclide-bearing silicates, etc.). The degradation rate of a radiounuclide-bearing phase encapsulated in another phase can be different than that of the separate material.

(6) Solubility-limited release

Solubility limits may restrict the amounts of some radionuclides that can accumulate in solution after they have been released from the matrix by one of the modes listed above. Radionuclides in excess of the solubility limit are expected to precipitate as the solubility-limiting phase. Solubility limits are a component of all release mechanisms and are often modeled as a separate constraint on the dissolved concentrations of radionuclides released from the waste form.

These release modes are shown schematically in Figure 2.1. Wash-off (mode 1): This occurs at the surface of the waste form with negligible diffusion of water into the waste form. Dissolution of the host phase (mode 2): The phase containing the radionuclide must dissolve and the surface retreat until the radionuclide is exposed to the solution. Diffusion-limited release (mode 3): Water must diffuse through the host phase to contact the radionuclide, which then diffuses out of the encapsulating phase. Diffusion-limited release coupled with chemical reaction (mode 4): Water must diffuse through the host phase to react with the radionuclide, which then diffuses out of the host phase. Diffusive release coupled with dissolution of host phase (mode 5): Water must diffuse through the encapsulating phase to dissolve the host phase and release the radionuclide, which then diffuses out of the encapsulating phase. Modes 3, 4, and 5 differ only in the mechanism by which the radionuclide is released from the immobilizing matrix. In mode 3 diffusive release, the radionuclide is only weakly bonded to the host phase and the reaction to release it is taken into account by the diffusion coefficient. In mode 4, the reaction to release the radionuclide from the host phase modeled using a separate constant rate term. In mode 5, the radionuclide is immobilized in a separate host phase within the encapsulating phase and that host phase must dissolve before the radionuclide can be released to solution. The dissolution rate is sensitive to the solution composition. Adsorption (mode 6): This represents the adsorption of the radionuclide onto the surface of the waste form, another solid, or a colloid due to a solubility limitation. Mode 6 can affect the release rates for all modes. Various mathematical expressions can be used to calculate the release rates of radionuclides from waste forms based on the dissolution rate of the waste form. Several rate expressions that could be appropriate for modeling radionuclide release from a particular waste material are discussed below.

2.1 Empirical Rate Expressions

For the general chemical reaction

$$v_1 \mathrm{A} + v_2 \mathrm{B} = v_3 \mathrm{C} + v_4 \mathrm{D} \tag{2.2}$$

where A and B are reactants and C and D are products with stoichiometric coefficient v_i (positive for products and negative for reactants), the extent of reaction ξ can be written in terms of the number of moles n_i of either a reactant or product as $n_i = n_{i0} + v_i\xi_i$ where n_{i0} is the number of moles initially and n_i is the number of moles at some later time. The reaction rate can be written in terms of any reactant or product (where v_1 and v_2 are negative, and v_3 and v_4 are positive):

$$\frac{d\xi}{dt} = \frac{1}{v_i}\frac{dn_i}{dt} = \frac{1}{v_1}\frac{dA}{dt} = \frac{1}{v_2}\frac{dB}{dt} = \frac{1}{v_3}\frac{dC}{dt} = \frac{1}{v_4}\frac{dD}{dt}. \tag{2.3}$$

The dependence of the rate on the concentrations of reactants and products (and the concentrations of catalysts and inhibitors) is expressed as a rate law. The rates of many reactions are proportional to integer powers of reactant concentrations where the proportionality factor is referred to as the

rate constant. The rates of complex reactions may also depend on the concentrations of products, catalysts, and inhibitors. The general rate law is written as

$$\frac{1}{\nu_1}\frac{dA}{dt} = k' A^a B^b C^c D^d \,, \tag{2.4}$$

where k' is the rate constant. Note that the values of the exponents in Equation 2.4 are not necessarily the same as the stoichiometric coefficients in Equation 2.2. The temperature dependence of the rate constants for most thermally activated processes can be represented using the Arrhenius expression

$$k = \alpha\, e^{-E_a/RT} \,, \tag{2.5}$$

where α is the pre-exponential factor and E_a is the activation energy. The concentration and temperature dependencies of an elementary reaction rate (and the rates of many complex reactions) are commonly written in the general form (e.g., Lasaga 1981; Lasaga 1984)

$$\frac{-dA}{dt} = \nu_1 k' A^a B^b C^c D^d \,\alpha \exp\left(\frac{-E_a}{RT}\right) = k A^a B^b C^c D^d \exp\left(\frac{-E_a}{RT}\right), \tag{2.6}$$

where the reaction rate is expressed by the consumption of species A over time, k is the rate constant incorporating ν_1 and α, A is the activity of species A with a reaction order a, B is the activity of species B with a reaction order b, etc. and the last term is the temperature dependence expressed in the Arrhenius form. Note that the pre-exponential factor of the Arrhenius expression has the same units as the rate constant and has been absorbed into k. The rate is written as negative in terms of the time dependence of reactant A to indicate the consumption of A as the reaction proceeds and the value of ν_1 has been absorbed into k. Surface terms must be included for heterogeneous reactions and solution concentrations replaced with mole fractions sorbed onto the surface, but this does not change the general form of the rate expression. For example, A_2 could represent the surface area of the reacting solid and A_3 the mole fraction of species A_3 that is sorbed. Taking the natural logarithm of Equation 2.6 gives

$$\ln\frac{-dA}{dt} = \ln k + a\ln A + b\ln B + c\ln C + d\ln D - \frac{E_a}{RT}\,. \tag{2.7}$$

By measuring the change in A with different initial amounts of A, B, C, and D and different temperatures, the reaction orders, activation energy, and rate constant can be determined. These parameter values are usually determined based on the initial rates measured far from equilibrium. An empirical rate law can be parameterized and used without understanding the underlying mechanism that controls the process.

Empirical rates laws can also be used when the mechanism is known but be cannot be expressed analytically due to a lack of data. An important example is the empirical models used to calculate the release of radionuclides due to degradation of commercial spent oxide nuclear fuel in the Yucca Mountain TSPA (BSC 2004). The fuel consists of stacked pellets of UO_2 with air gaps between neighboring pellets and between the pellets and the cladding hull. Each pellet is formed as an aggregate of sintered and pressed UO_2 particles and has a complex network of grain

boundaries. Fission products produced within the UO_2 particles during reaction migrate to grain boundaries and surfaces of the particles by solid-state diffusion. The distribution of radionuclides in the used fuel will depend on the diffusion properties of the nuclides and the reaction conditions. The release behaviors of the radionuclides in the disposal system will be affected by their distributions in the fuel and their solubilities in the contacting groundwater. The entire gap and grain boundary inventories of ^{90}Sr, ^{99}Tc, ^{129}I, and ^{137}C are modeled to be released instantaneously and without solubility limits when the fuel is contacted by water in the disposal system. (This is an example of the wash-off model via mode 2.) The release of radionuclides from the matrix occurs stoichiometrically at what is referred to as the matrix degradation rate. The corrosion processes affecting oxide fuels have been reviewed by Shoesmith (2000). Dissolution of the UO_2 matrix occurs through an oxidative dissolution mechanism in which sparingly soluble UO_2 is first oxidized to UO_3 by reaction with oxygen and then UO_3 dissolves by reaction with water. The oxidation step itself occurs through two steps: slowly to form a stable intermediate with mixed valence referred to as $UO_{2.33}$ (e.g., U_3O_7) and then to a U(VI)-bearing phase (e.g., hydrated schoepite $UO_3 \bullet xH_2O$), depending on the solution composition. Dissolution is observed to occur faster under acidic conditions and in the presence of complexants, such as carbonate/bicarbonate. Dissolution can be inhibited by the precipitation of calcium and silicon from groundwater to form a surface layer on the surface of the fuel grain.

The dissolution rate of UO_2 can be controlled by either the transport of oxygen through the oxidized surface layers, the rate of oxidation to $UO_{2.33}$, the rate of oxidation to UO_3, or the dissolution rate of UO_3 under different conditions. In reducing environments, the availability of oxygen may limit the release of radionuclides, whereas the dissolution of UO_3 may control the release under oxidizing conditions. Overall, the reaction with dissolved oxygen

$$UO_2 + O_2 + 2\,H^+ \rightarrow UO_3 + H_2O \tag{2.8}$$

involves an anodic reaction:

$$UO_2 + 0.5\,O_2 \rightarrow UO_3 + 2e^-, \tag{2.9a}$$

and a cathodic reaction

$$0.5\,O_2 + 2\,H^+ + 2e^- \rightarrow H_2O, \tag{2.9b}$$

either of which can control the overall rate. In general, the anodic reaction to oxidize UO_2 will proceed only when the equilibrium half-cell potential is less than the half-cell potential of one of several possible a cathodic reactions so that current will flow. The rate could instead be controlled by the dissolution reaction, for example, to form a uranyl silicate (e.g., boltwoodite) upon dissolution in a groundwater,

$$2\,UO_3 + 2\,K^+ + 2\,H_3SiO_4^- + H_2O \leftrightarrows K_2(UO_2)_2(SiO_3)_2(OH)_2 \bullet 3H_2O. \tag{2.10}$$

The separate oxidation and dissolution reactions were not modeled mechanistically for Yucca Mountain TSPA calculations due to incomplete knowledge of the possible cathodic reactions. Therefore, separate empirical models were used to calculate the extent of dissolution in acidic and alkaline solutions based on the results of short-term immersion tests to measure the gap inventory and single-pass flow-through (SPFT) tests to measure the effects of temperature, pH, O_2, and total CO_3. The point emphasized here is that for even a relatively simple waste material with perhaps unparalleled worldwide importance as used commercial oxide fuel, the degradation/dissolution rate cannot be quantified with a mechanistic model. This indicates the likely importance of

empirical models for assessing the behaviors of slag and concrete wastes. For TSPA calculations with UO_2 fuel, the experimental results from tests conducted to quantify the effects of particular variables were assessed using the general expression given in Equation 2.7. The test results for acidic and alkaline solutions were modeled separately. For solutions with pH ≥ 6.8:

$$\log(F) = \log(S) + a_0 + \frac{a_1}{T} + a_2 \times p(\mathrm{CO_3}) + a_3 \times p(\mathrm{O_2}) \tag{2.11}$$

and for solutions with pH < 6.8:

$$\log(F) = \log(S) + a_4 + \frac{a_5}{T} + a_6 \times p(\mathrm{O_2}) + a_7 \times \mathrm{pH} \tag{2.12}$$

where $\log(F)$ = base 10 logarithm of the fractional dissolution rate (d^{-1})
$\log(S)$ = base 10 logarithm of specific surface area ($m^2\ mg^{-1}$)
T = absolute temperature (K)
$p(CO_3)$ = negative base 10 logarithm of carbonate concentration ($HCO_3^- + CO_3^{2-}$, molar)
$p(O_2)$ = negative base 10 logarithm of oxygen pressure (atmospheres)
pH = negative base 10 logarithm of hydrogen ion concentration (molar)

The variables included in the model were selected based on previous experimental findings (by multivariate regression). The surface area of UO_2, oxygen partial pressure, and pH terms arise based on the chemical reactions: a temperature term is included because all of the reactions are thermal processes and a carbonate term is included because it is known to be a strong complexant of uranyl ions and to affect the dissolution rate. Coefficient values determined from SPFT experiments are summarized in Table 2.1. Note that the dissolution rates increase with increasing temperature (a_1 and a_5 are negative for the inverse temperature dependence) and increase with increasing P_{O_2} and P_{CO_3} (a_2, a_3, and a_6 are negative and the variables are expressed as negative logarithms) in both acidic and alkaline solutions. Dissolution in alkaline solutions is independent of the pH (there is no pH term in Equation 2.11) whereas dissolution in acidic solution decreases with increasing pH (a_7 has a negative value). Dissolution in alkaline solutions also has an explicit carbonate dependence, but dissolution in acidic solutions does not.

The model for commercial spent nuclear fuel represents dissolution far from equilibrium where the rate is essentially independent of the free energy of reaction. This is reasonable for this waste because the overall rate is controlled by the initial oxidation of UO_2 and the formation of alteration phases that are more stable than U_3O_7. The formation of alteration phases will maintain a dissolved uranyl concentration well below the solubility limit of U_3O_7 and maintain a relatively high affinity for the dissolution of U_3O_7.

Table 2.1. Coefficients used in model commercial spent nuclear fuel (BSC 2004).

Alkaline Conditions		Acidic Conditions	
$\log(S)$	-6.7	$\log(S)$	-6.7
a_0	4.705	a_4	6.60
a_1	-1094	a_5	-1094
a_2	-0.102	a_6	-0.338
a_3	-0.338	a_7	-0.340

2.2 Electrochemistry-Based Models

Modeling the rates of individual oxidation and reduction reactions provides an electrochemical approach to waste material dissolution that could be applicable to phases in slag wastes that are metallic or semi-conducting. Although they are not expected to provide quantitative radionuclide release models needed for performance assessments, electrochemistry-based models do provide a mechanistic basis for empirical models and the parameters that are included. The key variable in the electrochemical model is the environment corrosion potential ($E_{corrosion}$), which is determined by the concentrations of oxidizing agents *at the surface of the dissolving material*, including dissolved oxygen and radiolysis products such as hydrogen peroxide. Oxidation can occur if the equilibrium potential for the oxidative dissolution of the material lies below the corrosion potential that is established at the surface of the material by the environmental conditions (E_{corr}). The dissolution kinetics will be affected by charge transfers to form oxidized species at the surface (which can then dissolve) and alterations that must occur at the surface to form the oxidized species. The refreshment of oxidants can also control the dissolution rate. The corrosion potential of the solution will decrease as oxidants are consumed and dissolution in a closed system will eventually cease. Other solutes in the groundwater can inhibit corrosion by blocking surface reaction sites.

At $E_{corrosion}$, the currents from the anodic and cathodic reactions will be equal but opposite in sign, and the anodic current will be equal to the corrosion current $I_{corrosion}$. The cathodic current will be the sum of currents for all cathodic reactions supporting corrosion of the material being oxidized. The anodic dissolution current that flows as the material is oxidized can be related to the mass of material reacted, W, by using Faraday's law as (Shoesmith 2000; Shoesmith and Sunder 1992)

$$W = \frac{I A_w t}{nF} \tag{2.13}$$

where t is time, I is the corrosion current density, A_w is the molecular weight of the reacting material, n is the stoichiometric number of electrons (equivalents) exchanged, and F is the Faraday constant (96,487 coulombs). The corrosion rate is obtained by dividing the mass reacted by the surface area S and reaction time,

$$rate = \frac{W}{St} = \frac{I_{corrosion} A_w}{nF} \tag{2.14}$$

For alloys, the atomic weight is replaced by an equivalent weight, which is the weighted average of A_w/n for the major alloying elements. Equation 2.14 has been widely used to evaluate the durabilities of metals and alloys, including metallic waste materials, based on uniform corrosion (e.g., McDeavitt et al. 1998).

Analogous to the dissolution rate expression, the corrosion current density for anodic dissolution can be related to the reaction conditions as (Shoesmith and Sunder 1991)

$$I_{corrosion} = k_A X^x Y^y \exp(bE_{corrosion}) \tag{2.15}$$

where k_A is a rate constant for the anodic reaction, X and Y are solute concentrations affecting the rate with reaction orders x and y, and E_{corr} is the potential at the material surface. For UO_2 dissolution, important solutes include bicarbonate and H^+ (pH). The term b is the anodic Tafel slope that gives the dependence of ln $I_{corrosion}$ on the applied potential $E_{corrosion}$. This quantifies the net environmental influence on the corrosion rate. Combining Equation 2.14 and Equation 2.15 gives an expression having a form analogous to Equation 2.6 that is suitable for quantifying corrosion under conditions that are not too near equilibrium.

To model reaction in near-equilibrium conditions, equivalent expressions must be written for the current density due to reaction with each oxidant (O_2, H_2O_2, etc.) and the functionality of the free energy term determined, as was discussed with regard to Equation 1.2. This is challenging and has not been completed for even important materials such as UO_2. A semi-empirical model has been developed for use when expressions for all possible anodic and cathodic current densities have not been fully developed (Shoesmith and Sunder 1991):

1. Determine the Tafel lines for relevant solution compositions by measuring the anodic corrosion current as a function of applied potential.
2. Measure the corrosion potential for relevant groundwater chemistries.
3. Determine the current density by extrapolating the Tafel lines to the corrosion potentials of groundwaters.

This approach incorporates electrochemical aspects of the corrosion process and an underlying mechanistic basis into a simple empirical rate law that can be used in performance calculations. As an example, a simple relationship between the corrosion rate of UO_2 fuel in non-complexing solutions and the steady-state corrosion potential has been determined empirically using this model (Christensen and Sunder 2000):

$$corrosion\ rate = 78\times10^{-4.4+16E_{corr}} \quad . \tag{2.16}$$

The coefficients represent values of material and system variables in the form of Equation 2.15 for the relevant environment.

2.3 Reaction Affinity Model

The reaction affinity model quantifies the intuitive expectation that a system far from equilibrium will react faster to attain equilibrium than when that system is nearer to equilibrium. The reaction rate is expected to be a function of the difference between the free energy of the system in its current state and that of the system at equilibrium. The Gibbs free energy quantifies the energy difference that drives a system towards equilibrium: ΔG_r. Since thermodynamics only requires that the rate be zero when $\Delta G_r = 0$, assumptions regarding the functional dependence of the rate on ΔG_r have lead to various proposed rate laws for different reaction mechanisms. The form that is commonly used in the transition state theory formulations for mineral dissolution in aqueous solutions is (e.g., Lasaga 1995)

$$fn(\Delta G_r) = 1 - \exp\left(\frac{\Delta G_r}{RT}\right). \tag{2.17}$$

As a reacting system approaches equilibrium, the free energy of the system decreases to that of the equilibrium system and ΔG_r approaches 0. As required by thermodynamics, $fn(0) = 0$ and the rate

at equilibrium is 0. The change in the free energy of the system with reaction progress (at constant temperature and pressure) is defined as the chemical affinity A:

$$A = -\left(\frac{\partial G}{\partial \xi}\right)_{T,P}. \tag{2.18}$$

The chemical affinity also represents the change in ΔG_r with reaction progress because the free energy of the system at equilibrium remains constant, so the change in G will be equal to the change in ΔG_r. Therefore, the change in the thermodynamic driving force that is incorporated into the rate expression using the formulation in Equation 2.17 is given by the chemical affinity (Lasaga 1995). Rate expressions for both the forward and reverse reactions (e.g., dissolution and precipitation, respectively) are needed to model the system near equilibrium *regardless of the mechanism.* The net rate of a reaction can be written as

$$rate_{net} = rate_{forward} - rate_{reverse} = rate_{forward} \bullet \left(1 - \frac{rate_{reverse}}{rate_{forward}}\right). \tag{2.19}$$

The ratio in the parenthetic term is related to the chemical affinity as

$$\frac{rate_{reverse}}{rate_{forward}} = \exp\left(\frac{-A}{RT}\right) \tag{2.20}$$

and is referred to as the affinity term. Equation 2.19 can be rewritten as

$$rate_{net} = rate_{forward} \bullet \left[1 - \exp\left(\frac{-A}{RT}\right)\right]. \tag{2.21}$$

The affinity term provides a link between the kinetics of a system in disequilibrium and the thermodynamic expression of that disequilibrium: For a system that is at equilibrium, the value of the chemical affinity is $A = 0$ and the net reaction rate is zero regardless of what the forward rate is. For a system that is not at equilibrium, the forward rate will be modulated by a term having a value between zero and one that represents the degree of disequilibrium.

The reaction affinity A can be expressed in terms of the ion activity product of the solution Q and the equilibrium constant of the dissolving material K (see Appendix A) and Equation 2.21 can be written as

$$rate_{net} = rate_{forward} \bullet \left(1 - \frac{Q}{K}\right) = k_f \bullet \left(1 - \frac{Q}{K}\right), \tag{2.22}$$

where the second equality indicates the common use of k_f to represent $rate_{forward}$ and simplify the equations, as will be done henceforth. The ratio Q/K is referred to as the saturation index and quantifies the deviation from equilibrium; the term in parentheses is the affinity term. The affinity model simply moderates the forward rate using the affinity term to quantify the decrease in the net rate as equilibrium is approached. The affinity term can have values ranging from one at infinite dilution (when $Q = 0$) to zero at saturation (when $Q = K$). When the saturation index has a value of one, the affinity term has a value of zero, the system is at equilibrium, and the net reaction rate is zero. When the saturation index has a value of zero, the affinity term has a value of one, the

system is far from equilibrium (and independent of ΔG_r) and the reaction occurs at the forward rate. At intermediate values of the saturation index and affinity term, the reaction rate lies between zero and the forward rate. The forward rate describes the kinetics of the reaction that leads to dissolution of the material (i.e., the rate limiting step in the reaction mechanism) and, depending on the mechanism, might include terms for the effects of temperature, pressure, pH, solute activities, ionic strength, the mole fractions of species adsorbed onto the surface, etc. on the reaction rate.

It is important to recognize that the relationship given in Equation 2.17 is empirical and that the same functional form for $fn(\Delta G_r)$ may not hold over the full range of disequilibrium in a system (e.g., as the rate-controlling mechanism changes). For example, Lasaga and Luttge (2001) discuss nonlinearities in the dissolution rate of minerals as equilibrium is approached (from undersaturation) and provide as examples the measured dissolution rates of albite, gibbsite, labradorite, and smectite. The results for albite and labradorite are shown in Figure 2.2 with the modeled rates. Note that dissolution is defined to have a negative rate and precipitation to have a positive rate in these plots. For albite, a change in behavior occurs at ΔG_r = -6.5 kcal mol^{-1} between the dependence of the dissolution rate on the Gibbs free energy far from equilibrium (ΔG_r <-6.5 kcal mol^{-1}) and the dependence near equilibrium (ΔG_r >-6.5 kcal mol^{-1}). (Note that the value of ΔG_r is determined by the solution chemistry through the saturation index.) A similar discontinuity occurs at ΔG_r = -7.7 kcal mol^{-1} in tests with labradorite. Lasaga and Luttge refer to the point of discontinuity as $\Delta G_{critical}$ and state that "a substantial reduction in the rate occurs once $\Delta G_r \sim \Delta G_{critical}$, which for many crystals occurs far from equilibrium" (Lasaga and Luttge 2001, p. 2403). The discontinuity represents a change in the rate-determining process and is predicted by the stepwave dissolution theory of etch pits presented by Lasaga and Luttge (2001): the point of unsaturation $\Delta G_{critical}$ corresponds to a change in the rate-controlling mechanism between a localized spiral-growth process near equilibrium and a surface-wide process further from equilibrium. (Stepwave dissolution theory is a corollary to step-wise crystal growth theory.) Note that in Figure 2.2 the rates approach maximum values at very small values of ΔG_r (ΔG_r < 10^{-9} kcal mol^{-1}). Where the rate becomes independent of the free energy is sometimes referred to as the "dissolution plateau region." This corresponds to a chemical affinity term value of one and reaction at the forward dissolution rate in the reaction affinity model. The curved portion of the dependence on ΔG_r (from about ΔG_r = -14 to -6.5) is modeled by the affinity model, but this model is only applicable when $\Delta G_r \leq \Delta G_{critical}$ and will not always pass through the origin, as seen in the results for albite and labradorite (and other materials).

Similar discontinuities could result due to changes in the mechanisms that control the degradation and dissolution of other materials. For example, the behavior seen in Figure 2.2 describes the observed dissolution behavior of borosilicate waste glasses very well. Far from equilibrium, glass dissolves at a maximum rate that depends on the glass composition, temperature, and pH. As silica accumulates in the solution, the dissolution rate is well described by an affinity model based on the hydrolysis of Si-O bonds. The rate decreases to very near zero as the solution approaches an apparent saturation concentration and the chemical affinity (for the hydrolysis reaction) decreases to zero. However, glass dissolution does not cease, but proceeds at a very low rate. It has been hypothesized that reaction continues at a rate determined by water diffusion through an as-yet uncharacterized surface layer (Frugier et al. 2008). The system may remain at disequilibrium as long as a concentration gradient exists to drive water diffusion, ion exchange, or other processes affecting glass corrosion. In other words, glass dissolution occurs as three (or more) simultaneous processes: water diffusion, ion exchange, and hydrolysis. The dissolution behavior observed in laboratory tests is dominated by hydrolysis reactions except under near-

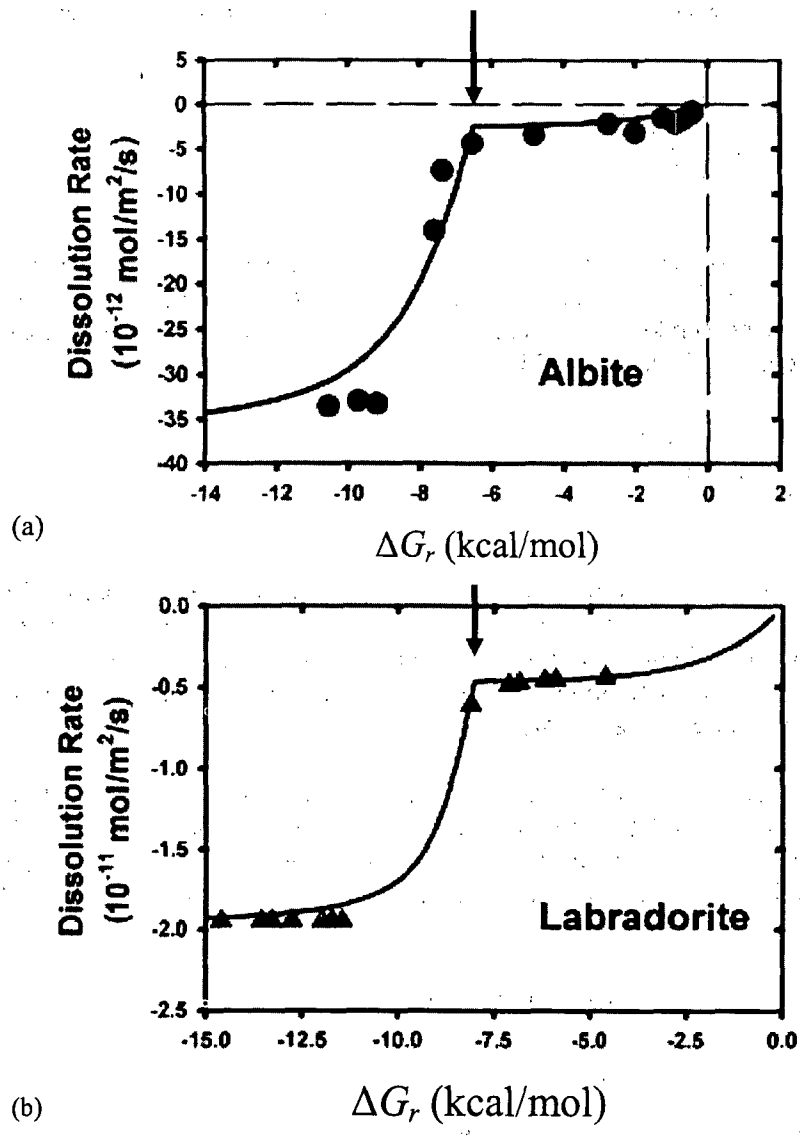

Figure 2.2. Data from Lasaga and Luttge (2001): Comparison of dissolution theory with experimental data for (a) albite at pH 8.8 and 80°C and (b) labradorite at pH 3 and 25°C. The arrows locate $\Delta G_{critical}$ = -6.5 kcal mol^{-1} for albite and $\Delta G_{critical}$ = -7.7 kcal mol^{-1} for labradorite.

equilibrium conditions when the solution contacting the glass is essentially saturated (with respect to the glass). At this point, disequilibrium in the system is determined by the concentration gradient for water diffusing into the glass rather than by the affinity for hydrolysis reactions. Water diffusion can perturb the equilibrium of the hydrolysis reactions and results in continued dissolution, but at a rate controlled by water diffusion rather than the hydrolysis reactions. Understanding and modeling waste glass dissolution under saturated conditions remains an important research objective worldwide.

As a final comment, a more general form of Equation 2.17 can be written for each reaction pathway as

$$f(\Delta G_r) = \left[1 - \exp\left(\frac{\Delta G_r}{\sigma RT} \right)^n \right]^m , \tag{2.23}$$

where n and m are fitting parameters and σ is an empirical coefficient relating the reaction described by ΔG_r to the overall dissolution rate that is measured (see also Appendix A); σ is sometimes referred to as the Temkin coefficient. Using this form of the thermodynamic term, the affinity term in the rate law in Equation 2.22 becomes

$$rate_{net} = k_f \bullet \left[1 - \left(\frac{Q}{K} \right)^{n/\sigma} \right]^m . \tag{2.24}$$

This form of the rate equation is often referred to as having a nonlinear dependence on the deviation from equilibrium, whereas the special case of $n = m = 1$ is referred to as having a linear dependence. The value of the Temkin coefficient must be determined from experiments, and values from 0.1 to 17 have been determined for the dissolution of various materials for the linear dependence model (e.g., Bourcier et al. 1994).

In the case of multiple reaction pathways, the overall rate is calculated as the sum of all parallel pathways. For example, the dissolution rate of albite feldspar has been measured at 80 °C and a pH of 3 over a wide range of ΔG_r by Hellmann and Tisserand (2006): the results are shown in Figure 2.3. (Note that the dissolution rates are given as positive values in contrast to the negative

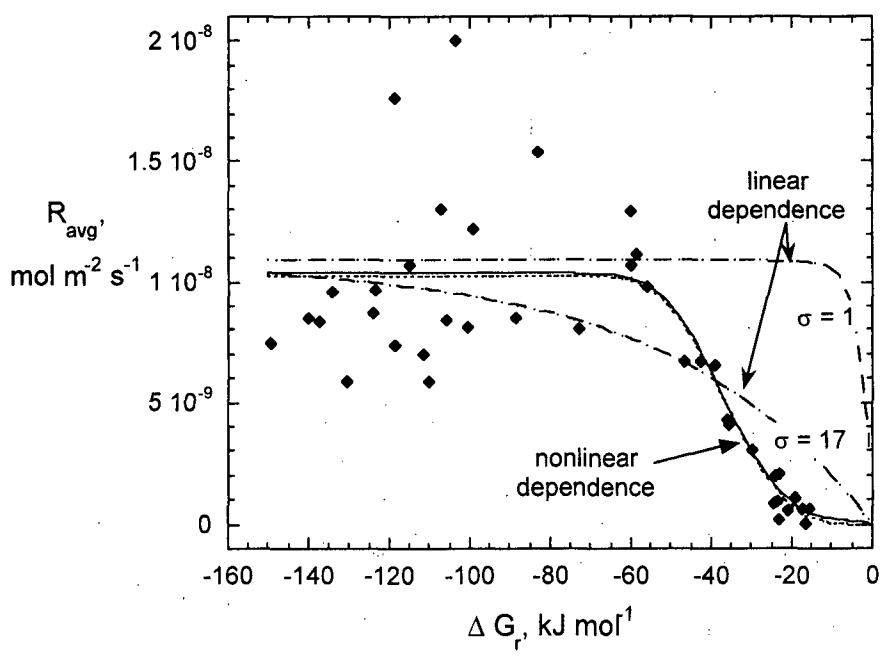

Figure 2.3. Data from Hellman and Tisserand (2006): Dissolution rate of albite at 80°C and pH 3 as a function of ΔG_r.

values used by Lasaga and Luttge and the free energy is in kJ mol^{-1}.) This data base includes an abundance of values in the dissolution plateau (at $\Delta G_r < 60$ kJ mol^{-1}) but with the large uncertainties common for analysis of very dilute test solutions. Hellmann and Tisserand (2006) fitted these results using the two-process model given by Burch et al. (1993)

$$R_{diss} = k_1 \left[1 - \exp\left(-n \frac{|\Delta G_r|^{m1}}{RT} \right) \right] + k_2 \left[1 - \exp\left(-\frac{|\Delta G_r|}{RT} \right) \right]^{m2}, \tag{2.25}$$

where k_1 and k_2 are rate constants and n, $m1$, and m2 are fitting parameters that are regressed to the test data. The Temkin coefficient is included in the value of n or $m1$ in the first term and has a value of 1 in the second term. The first term on the right hand side represents dissolution under near-equilibrium conditions and the second term represents dissolution under far-from-equilibrium conditions. The albite data were fit with $k_1 = 1.02 \times 10^{-8}$ mol $m^{-2}s^{-1}$ and $k_2 = 1.80 \times 10^{-10}$ mol $m^{-2}s^{-1}$, $n = 7.98 \times 10^{-5}$, $m1 = 3.81$ and $m2 = 1.17$ (although the fit shown in Figure 2.3 is with $m1 = 3.57$) by Hellmann and Tisserand (2006). They also fit the data to a simplified rate expression:

$$R_{diss} = k_3 \left[1 - \exp\left(-n \frac{|\Delta G_r|^{m3}}{RT} \right) \right]^{m4} \tag{2.26}$$

with $k_3 = 1.03 \times 10^{-8}$ mol $m^{-2}s^{-1}$, $n = 9.75 \times 10^{-5}$, $m3 = 3.74$, and $m4 = 1$ (although the fit in Figure 2.3 is with $m3 = 3.50$). The fits with both equations are shown in Figure 2.3. The equations fit the data equally well and differ only very near equilibrium, where additional data are needed. For comparison, fits using Equation 2.26 with $k_3 = 1.09 \times 10^{-8}$ mol m^{-2} s^{-1}, $m3 = m4 = 1$, and $n = 1$ or $n = 5.88 \times 10^{-2}$ (corresponding to $\sigma = 1$ or $\sigma = 17$) are included in Figure 2.3 as the dashed lines. These fits are consistent with the uncertainty in the test results under far-from-equilibrium conditions, but both overestimate the dissolution rates as equilibrium is approached. The nonlinear models are consistent with the overall sigmoid shape of the data. The application of a nonlinear model should be supported with other observations suggesting a change in rate-determining mechanism in addition to the better empirical fit to the data, such as the dissolution of pits and terraces by Lasaga and Luttge (2001).

While this level of detail may seem somewhat esoteric with regard to the wastes being considered in this project, the possible change in controlling mechanisms is an important consequence of measuring model parameters under test conditions that are significantly different than the conditions experienced by the waste materials. Many kinetic model parameters are measured under test conditions far from equilibrium to eliminate confounding interactions, whereas equilibrium-related parameters are measured under near-equilibrium conditions. It is possible that different mechanisms control the test responses under such disparate conditions. Therefore, it is important to conduct tests over the full range of conditions to detect obvious changes in the mechanism controlling the material behavior and to understand the influence of the conditions on model predictions. In some cases, several test methods will be required to study material behavior over a wide range of possible reaction conditions. Understanding how the responses of particular test methods relate to the modeled behavior is an important aspect of test selection and data interpretation and is considered in detail in the analyses that follow.

3 Applying the Chemical Reaction Affinity Model

Application of the reaction affinity model using Equation 2.22 requires definition of the species to be included in Q and K, which will depend on the rate-controlling reaction, and the value of K, which will vary with temperature. Application also requires definition of the variables to be included in k_f. The effects of solutes on the rate are taken into account within the forward rate term (independent of their role in the affinity term). For many materials, the dissolution rate depends on the chemistry of the groundwater: the pH is known to be an important parameter for the dissolution of many materials, the Eh and dissolved oxygen concentration are important for redox-sensitive components, other solutes can affect the dissolution rate by forming complexes, etc. Separate rate expressions will probably be needed for each independent reaction comprising a mechanism. For example, the rates of oxidation reactions depend on the redox potential of the groundwater, the concentrations of oxidants such as O_2 and H_2O_2.

3.1 Solution Feed-Back Effects

The effect of the affinity term is often referred to as a solution feedback effect because it is the action of dissolved components promoting the reverse reaction that slows the net dissolution rate. The effect can be quantified by regressing Equation 2.22 to the results of a series of tests in which the concentrations of components released from the waste form (or test specimen) increase with the test duration to increase the value of Q, while maintaining a constant value of k_f (e.g., at constant temperature and pH). From the derivation of Equation 2.22, the values of Q and K represent the dissolution reaction that is being modeled. Depending on the material being studied, the component i that is tracked in experiments may or may not be included in Q and K. For example, the dissolution of borosilicate glass is dominated by the hydrolysis rate of Si-O bonds and only the concentration (activity) of SiO_2(aq) is included in the Q and K terms, but the release of B is often used to measure the dissolution rate. This is because B is not incorporated into alteration phases and the solution concentration of B provides a good measure of the extent of reaction. Implicit in this approach is that the reaction to release B is controlled by the reaction to release Si. Appreciable fractions of Si and other components, including radionuclides, become sequestered in secondary phases.

A very important aspect of Equation 2.22 is that, whereas the value of K is specific to the dissolving material, the value of Q is affected by the presence of other phases that can limit the solution composition to values lower than the composition that would be in equilibrium with the waste form. This is often seen in tests with glass waste forms where the formation of analcime as a secondary phase can cause an increase in the dissolution rate by establishing a lower Si solubility limit and in tests conducted with glass in the presence of clays, which also affect the Si solubility limit. It is also relevant to multiphase waste forms: the dissolution rates of component phases will be linked by the common solution chemistry. In the case of two Si-bearing compounds 1 and 2, the steady-state concentration of dissolved silica $[SiO_2]^{ss}$ can be calculated based on the fact that the dissolution rate of Phase 1 will be equal to the precipitation rate of Phase 2 at steady state (or visa versa), and the precipitation rate of Phase 2 is equal to the negative of the dissolution rate of Phase 2. Application of Equation 2.22 to both phases and including the surface areas yields

$$k_{f1}S_1 \bullet \left(1 - \frac{Q}{K_1}\right) = -k_{f2}S_2 \bullet \left(1 - \frac{Q}{K_2}\right). \tag{3.1}$$

If only SiO_2 (aq) contributes to Q, then the general relationship given by Bethke (1996) is obtained

$$[SiO_2]^{ss} = \frac{1}{\gamma_{SiO_2}} \times \frac{S_1 k_{f1} + S_2 k_{f2}}{\frac{S_1 k_{f1}}{K_1} + \frac{S_2 k_{f2}}{K_2}}, \tag{3.2}$$

where γ_{SiO_2} is the activity coefficient for aqueous SiO_2, S_1 and S_2 are the surface areas, k_{f1} and k_{f2} are the reaction-rate constants, and K_1 and K_2 are the equilibrium constants for Phases 1 and 2. Additional terms can be added for additional phases. It is important to note that this is a steady-state concentration, not an equilibrium concentration. For a system with two Si-bearing phases, the steady-state concentration will be supersaturated with respect to the less soluble phase and under-saturated with respect to the more soluble phase. The deviations from equilibrium concentrations will reflect the differences in the surface areas and rate constants of the two phases. Small amounts of highly reactive phases can significantly affect the fluid chemistry.

The dependence of the forward rate on some test conditions can be modeled directly based on mechanistic or empirical insights. For example, the dependence of dissolution rates of silicate mineral and glasses on pH and temperature is commonly modeled as

$$rate_{forward} = k_f = k_0 \bullet 10^{\eta \bullet pH} \bullet \exp\left(-E_a/RT\right), \tag{3.3}$$

where k_0 is the intrinsic dissolution rate constant of the material, η is the pH dependence, and E_a is the activation energy for the Arrhenius form of the temperature dependence. (Note: in comparing Equation 3.3 with Equation 1.2, the only solute concentration affecting $rate_{forward}$ (k_f) is the H^+ concentration and $rate_{forward}$ (k_f) is expressed on a per-unit-reactive surface area basis.) The pH and temperature are system variables with model coefficients η and E_a, respectively. The term k_0 is an empirical constant that depends on the glass composition, although an analytical expression to calculate that dependence has so far eluded researchers. By conducting separate series of tests with the same glass at constant pH or constant temperature, the effects of pH and temperature on the net dissolution rate expressed as η and E_a can be determined (e.g., McGrail et al. 1997a) and the value for k_0 determined from the set of model coefficients (e.g., Ebert et al. 2000). Additional terms may be needed to model the dissolution of other materials to explicitly quantify the effects of variables such as the oxygen fugacity, chloride concentration, etc., that may have a catalytic or inhibitory effect on the dissolution rate. Effects that are not controlled in the test will be captured in the values of k_0, η, and E_a that are regressed from experimental results and will add to the uncertainty of those coefficients and the modeled reaction rate.

The separation of variables adopted in Equation 3.3 is a convenient form for determining parameter values with test data, but it neglects their possible interdependencies. For example, the activation energy (E_a) could vary with the pH. If that is the case, then the rates measured at constant temperature but different pH values could still be affected by the Arrhenius term and overwhelm the impact of the pH term. This is because the temperature dependence is exponential, whereas the pH dependence is a power law function with typical coefficient values $\eta \approx 0.5$. For this reason, it is prudent to use "sets" of coefficient values to model dissolution behavior when possible so that the potential effects of cross-terms will be captured in the coefficient values and thereby retained in the model calculations.

3.2 Using Test Results to Parameterize Models

Values of model coefficients such as k_0, η, E_a, and K, are usually measured using laboratory tests that are designed for that purpose, and usually based on how the measured dissolution rate is affected by changes in the test variable of interest (i.e., the glass composition, solution pH, temperature, or dissolved silica concentration, respectively) while other variables are held constant (e.g., McGrail et al. 1997; Pierce et al. 2008). Therefore, it is important to understand how the results of a particular laboratory test relate to the model.

The amount of a species released into solution is measured directly in most test methods. A few test methods quantify a change in the test specimen, such as the mass, but this usually does not provide as accurate a measure of the extent of reaction as tracking changes in the solution. The amount of a species of interest that is released into solution can be expressed on a per area basis by simply dividing the released mass by the specimen surface area. While quantifying the available surface area is straightforward in tests conducted with monolith samples having measurable dimensions, many tests are conducted with crushed material to provide enough surface area to generate a measurable response. The surface area of a crushed material can be estimated based on size fractions or measured, for example, by gas adsorption and BET analysis. In some instances, the release of a component other than the component of interest is used as a surrogate to determine the amount of the waste form that has dissolved, which is then used to estimate how much of the species of interest has been released. This approach presumes the material dissolves stoichiometrically and is often utilized for difficult-to-analyze components present in low concentrations or when using non-radioactive specimens as surrogates for highly radioactive materials. For example, the release of B from a borosilicate glass is often used to provide an upper bound to the amounts of radionuclides that are released.

The mass of a test specimen that has dissolved in a laboratory test can be calculated based on the solution concentration of a soluble constituent accumulated in a static test as the normalized mass loss

$$NL(i) = \frac{mass\ i\ dissolved}{specimen\ surface\ area \times mass\ fraction\ i\ in\ specimen}. \tag{3.4}$$

Including the mass fraction of i in the specimen in the denominator of Equation 3.4 gives the mass of the material dissolved based on the amount of component i released during the test normalized to the specimen surface area S. Because this calculation presumes congruent dissolution of the specimen, components that are expected to have high solubility limits, such as B and alkali metals are usually tracked in laboratory tests when possible. The mass of i dissolved includes all species, even though not all species are included in the affinity term. For example, the affinity term for glass dissolution may only include dissolved SiO_2, but all silicon-bearing species would be included if Si was used to track the amount of glass that has dissolved. The speciation of Si as a function of pH could be used to estimate the dissolved SiO_2 concentration. The mass of i released from the specimen can be written in terms of the measured concentrations in the leachate $C(i)$ and in the leachant $C°(i)$, where both concentrations include all species bearing i, and the leachant volume V that was added at the beginning of the test as

$$NL(i) = \frac{[C(i) - C°(i)] \times V}{S \bullet f(i)} = \frac{C(i) - C°(i)}{S/V \bullet f(i)}, \tag{3.5}$$

where $f(i)$ is the mass fraction of i in the solid. The second equality reflects the general characterization of the test conditions used in static tests by the material surface area–to–solution volume ratio (S/V). The S/V ratio itself is simply a convenience for describing the test conditions in calculations and is not a test parameter *per se*. Small amounts of water are sometimes lost during a test due to vessel leakage such that the final volume of leachate is slightly less than the initial volume of leachant added to the test vessel. The final leachate volume is usually calculated by assuming any measured mass loss of the assembled vessel over the test duration is due to leakage of water vapor. In this case, $C(i)$ and $C^{\circ}(i)$ should be multiplied by the leachate and leachant volumes, respectively, to calculate the masses.

The solution concentrations are commonly expressed in units mass i/volume so that $NL(i)$ has units mass glass/specimen surface area. The integrated rate after any time t, referred to as the normalized rate, can be calculated from the amount of component i in solution as

$$NR(i) = \frac{NL(i)}{t} . \tag{3.6}$$

This gives the average rate over the test duration based on the amount of the test specimen that has dissolved (which is based on the amount of i that has accumulated in the solution) over that time period. Values of the forward rate, which is represented hereafter as k_f, and the equilibrium constant K can be determined by equating the expressions in Equations 3.5 and 2.22 to get the relationship between the test results and the dissolution rate model:

$$\frac{NL(i)}{t} = \frac{C(i) - C^{o}(i)}{S/V \bullet f(i) \bullet t} = k_f \bullet \left(1 - \frac{Q}{K}\right) , \tag{3.7}$$

where $C(i)$ is the dissolved concentration of i measured in the test after a reaction time t. Test results for several durations t with the measured concentration of species i can be regressed to determine optimal values of k_f (the forward rate) and K (the equilibrium constant). An example is given in Section 3.3.4.

3.3 Static Laboratory Test Methods

Static test methods are often employed to study the effect of the evolving solution chemistry on the dissolution behavior of a test specimen. These tests are easy to conduct and analyze, but the results can be difficult to interpret due to solution feedback effects, drifting pH, secondary phase formation, etc. A material of known composition and surface area is immersed in a fluid of known composition and volume in a sealed vessel. (Test vessels are usually watertight and airtight, but Teflon vessels are known to be permeable to CO_2). The sealed vessel is left undisturbed at a fixed temperature and not agitated for the desired duration. The vessel is then opened and the solution composition measured. The mass of a soluble component released to solution is used to calculate the mass of the specimen that dissolved by assuming congruent dissolution, or various components can be tracked to characterize non-stoichiometric dissolution. The reacted test specimen can be examined with various analytical methods to help identify alteration products and determine the degradation mechanism.

The impact of solution feed-back can be controlled by adjusting the material S/V ratio used in the test. Two limiting conditions are to immerse a monolithic specimen in a large leachant volume to

provide low *S/V* ratios and to immerse crushed material in a small volume to provide high *S/V* ratios. Solution feedback effects will be negligible initially and increase slowly in the low–*S/V* ratio tests, but will become significant immediately in the high *S/V* ratio tests. These limiting conditions are addressed in two standardized static test methods provided by ASTM-International (ASTM): ASTM C1220 and ASTM C1285.

3.3.1 ASTM C1220

The ASTM C1220 method is a static immersion test in which a monolithic test specimen of known geometric surface area is immersed in a known volume of demineralized water (or other leachant) at a constant temperature for a prescribed duration. At the end of the test, the amounts of soluble glass components in the leachate solution are measured to determine the extent of dissolution. The dissolution rate of the test specimen can be determined by conducting a series of ASTM C1220 tests for different durations under otherwise identical test conditions. Drift in the solution pH can be mitigated by using pH buffers as leachants. The ASTM C1220 method is similar to the Materials Characterization Center test number 1 (MCC-1) that was developed to directly compare the test responses (chemical durabilities) of a wide range of waste form materials, including glass, ceramics, cements, cermets, metals, etc., under specific test conditions. The ASTM C1220 method has been further developed to provide information useful for developing a mechanistic understanding of material behavior and to measure model parameters. For example, the typical test conditions maintain dilute solution conditions to minimize solution feedback effects in short-term tests at low *S/V* ratios, but the test method can be used to quantify the effects of solution feed-back by conducting tests at higher *S/V* ratios and for longer test durations. This test method is useful for measuring the effects of environmental variables on the reaction kinetics while maintaining a high chemical affinity.

3.3.2 ASTM C1285

The product consistency test (ASTM C1285) is a standardized modification of the Materials Characterization Center test number 3 (MCC-3) that was developed to monitor the consistency of borosilicate glass waste forms (ASTM 2009a). The MCC-3 test method was designed to measure the saturation concentrations of a material within short test durations by exposing a relatively large surface area to a relatively small solution volume, e.g., $S/V = 10{,}000\ m^{-1}$. Knowledge of the saturation composition is needed to determine the value of *K* used to calculate affinity term values in long-term degradation models. The dissolution of only a small amount of material is required to generate highly concentrated solutions under these test conditions. In the MCC-3 testing approach, tests were conducted for various durations to demonstrate that a saturated solution was achieved. The ASTM C1285 Method A is a 7-day test that is not intended to generate saturated solutions, but to allow direct comparison of the solution concentrations generated by different waste forms under the specified conditions. It is, in effect, a partial dissolution test that does not measure an intrinsic property of the dissolving material other than the response to these particular test conditions. The test conditions were selected to provide acceptable precision for tests conducted in a hot cell, not to represent any particular service conditions.

The ASTM C1285 Method B allows for variations in all test conditions, including reaction time, temperature, particle size, leachant composition, and *S/V* ratio. Method B tests are useful for understanding reaction mechanisms and parameterizing models. Series of tests can be conducted to determine the saturation conditions to meet the intent of the original MCC-3 test method. The saturation conditions of many materials will depend on test conditions such as temperature and the solution pH. While the temperature can be controlled throughout the test, the pH is often established by dissolution of the test material and evolves during the test. The solution pH is

likely to be influenced by the *S/V* ratio used in the test and will affect the saturated solution composition of many materials. Several series of tests may be needed to determine the sensitivity of the saturation composition to temperature and pH. The Method B tests are useful for characterizing reaction at very low chemical affinities where other processes (e.g., diffusion) may dominate the reaction behavior and test response.

3.3.3 Partial Removal and Partial Replacement Tests

A useful variation of these static tests is to interrupt the test to remove a small aliquant of solution for analysis and then continue the test. (The term *aliquot* refers to one in a series of samplings having the same sample volume, whereas *aliquant* refers to samples that may have different volumes.) If the removed volume is replaced in the test vessel with an equal amount of fresh leachant, the test is referred to as a partial replacement test. If the removed volume is not replaced, the test is referred to as a partial removal test. The so-called "partial removal" test is considered to be a static test because the solution composition is not affected by the removal, although the *S/V* ratio of the test increases and will likely affect the continued reaction. The "partial replacement" test is considered to be a semi-dynamic test because the solution composition is affected by the replacement, but the *S/V* ratio remains constant. The partial replacement test combines aspects of the ASTM C1220 static test and the ASTM C1308 test in which all the leachate is replaced. Both partial removal and partial replacement test methods are convenient and economical to run because the degradation behavior of a single test specimen can be tracked over essentially unlimited test periods. However, the perturbations to the S/V ratio or solution concentrations caused by removing the aliquants or adding fresh leachant complicate the use of the test data in dissolution models. The impacts may be slight for aliquants that are small compared to the solution volume, but the replacements could prevent secondary phase formation, lead to steady-state conditions that are artifacts of the test variables rather than the dissolution behavior, etc.

3.3.4 Example: ASTM C1220 Tests with LRM Glass

Three series of C1220 tests were conducted with a borosilicate glass at 70°C in a pH 11 buffer solution (measured at room temperature) and the Si concentration was measured to track the extent of dissolution (Ebert 2006). Separate test series were conducted using test specimens that had been polished to 600-grit, 800-grit, and 1200-grit surface finishes. The results are plotted in Figure 3.1. These results can be used to determine parameter values for the rate expression in Equation 3.7 as

$$\frac{NL(Si)}{t} = \frac{C(Si) - C^{o}(Si)}{S/V \bullet f(Si) \bullet t} = k_f \bullet \left[1 - \frac{C(Si)}{K}\right] \tag{3.8}$$

where $C(Si)$ is the dissolved silica concentration measured in the test after a reaction time t. This gives the forward rate in units of mass Si per unit surface area per unit time (typically as g m^{-2} d^{-1}). Rearranging Equation 3.8 gives the form used to determine the best-fit values of k_f and K:

$$NL(Si) = k_f \bullet \left(1 - \frac{C(Si)}{K}\right) \bullet t\,. \tag{3.9}$$

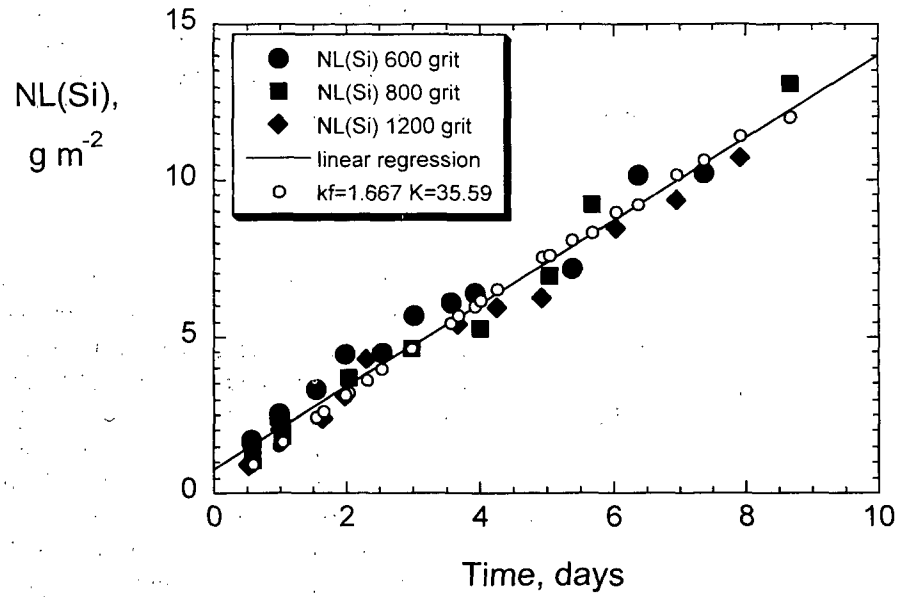

Figure 3.1. Results from Ebert (2006): Regression of pooled C1220 test results. Linear regression is shown by solid line and regression to Equation 3.8 using $k_f = 1.667$ g m^{-2} d^{-1} and $K = 35.59$ mg L^{-1} is shown by small open circles at each test duration.

The test results show no effect of the surface finish, so the pooled test data were used to determine the values of k_f and K that minimize the sum of the squares of the residuals between the calculated and measured values of $NL(Si)$ for all test durations. The results of tests at all durations and with all surface finishes were weighted equally in the regression. Although multi-variant regression analysis routines are available, the regression was done using a Microsoft Excel spreadsheet to demonstrate the easy "brute-force" method. The rate was first approximated by assuming solution feedback was negligible in all tests and assigning the affinity term, which is $\left(1 - \frac{C(Si)}{K}\right)$ in Equation 3.9, a value of 1. The resulting linear fit (which is shown by the solid line) gives a value of $k_f = 1.32$ g m^{-2} d^{-1} with a y-intercept of 0.8 g m^{-2} d^{-1}. The positive y-intercept is due to the slight negative curvature in the data set. That value k_f was then used in Equation 3.9 and the data regressed to find the best value of K. That value of K was then used to find a better value of k_f. This was continued until the best values were found to four significant figures.

The best fit to Equation 3.9 is obtained with $k_f = 1.667$ g m^{-2} d^{-1} and $K = 35.59$ mg L^{-1}. The values of $NL(Si)$ calculated with Equation 3.9 at the test durations using these values of k_f and K are plotted in Figure 3.1 as small circles for comparison with the test results. The calculated values represent the experimental results well and overlie the linear fit to the combined data set. The uncertainty in the values regressed using Equation 3.9 was not determined, but is expected to be within the uncertainty in the linear regression of the same data. The correlation coefficient calculated from the residuals is $R^2 = 0.951$, which is slightly lower than that calculated for the linear fit of the combined data set ($R^2 = 0.969$). The uncertainty in test results is 11% based on the propagated uncertainty in NL(Si). The forward rate of $k_f = 1.667$ g m^{-2} d^{-1} from this analysis is about 26% higher than that determined from linear regression of the test results. This means the affinity term has an average value of 0.74 for this set of tests.

The value $K = 35.59$ mg Si L^{-1} ($K = 10^{-2.897}$ M H_4SiO_4) that was determined by regression of the test results is reasonable; most borosilicate waste glasses are assumed to have a Si saturation concentration of 28 mg Si L^{-1} or higher ($K \geq 10^{-3}$ M H_4SiO_4) (Ebert 1995). (NOTE: Both the saturation concentration of SiO_2(aq) and the value of K are constant with respect to pH, although the total Si concentration increases rapidly above about pH 9.7 due to dissociation. The SiO_2(aq) concentration must be calculated from measured total Si concentration using dissociation constants and the pH.) Since the test results were regressed to both k_f and K, the uncertainty in the value of K is coupled with the uncertainty in the value of k_f.

With regard to the possible nonlinear dependence of the dissolution rate on the Gibbs free energy of reaction discussed in Section 2.3, this value of K is relevant to the far-from-equilibrium term. The value of K for near-equilibrium conditions is better measured with tests designed to approach saturation rather than with these C1220 tests, which were designed to remain far from saturation. (The ASTM C1285 test method presented in the next section is recommended to generate saturated solutions for determining the value of K.)

Finally, note that the direct linear regression of the test results provides a better fit to the test results than the fit to Equation 3.9 in terms of the squared residuals (11.18 for the linear fit and 17.59 for the fit to the affinity equation). As will be shown in other results evaluated in this report, the results of a single test method are usually not adequate to determine the degradation mechanism of a material, and how well a model fits a particular data set may be misleading. For this example, many other test methods show borosilicate glasses degrade by an affinity-controlled mechanism. It is expected that including longer test durations would have shown obvious deviation from the straight-line fit, and such data should be collected when studying the dissolution behavior of a material to reliably discriminate between different mechanisms.

3.3.5 Example: ASTM C1285 Tests with Glass-Bonded Sodalite

A glass-bonded sodalite ceramic waste form (CWF) was developed to immobilize waste salt from the electrometallurgical treatment of spent sodium-bonded nuclear fuel (Ebert 2005a). Because chloride ions are not soluble in glass (< 1 mass% is soluble), the chloride waste salt is reacted with zeolite to generate the mineral sodalite, which is then encapsulated in a borosilicate glass. Dissolution of sodalite and the glass phase both occur through affinity-controlled mechanisms that are modeled using Equation 2.22 with the Q and K terms including only dissolved silica. The values of K were measured for the separate sodalite and glass phases and for CWF materials made by hot isostatic pressing (HIP CWF) with 25 mass% glass and 72 mass% sodalite and CWF materials made by pressureless consolidation (PC CWF) with about 50 mass% glass and 47 mass% sodalite (PC CWF). Both waste form materials contained about 3 mass% salt (primarily halite) that is not incorporated into the sodalite phases; this salt exists as inclusions in the glass phase. Tests were conducted with crushed and sized material following the ASTM C1285 Method B procedure at a S/V ratio of about 2300 m^{-1} for reaction times up to 1 year. The silica concentrations measured in tests with the four materials (expressed as orthosilicic acid) are plotted against the product of S/V ratio and the reaction time in Figure 3.2. Horizontal lines are drawn through the highest concentrations measured for the separate binder glass and sodalite phases, which are 280 and 47.7 mg L^{-1}, respectively.

Equation 3.2 is used to interpret the concentrations measured in tests with HIP CWF and PC CWF in terms of the two major component phases. Dashed lines are drawn in Figure 3.2 at the values calculated for 2-phase systems of 50% glass + 47% sodalite and 25% glass + 72% sodalite assuming the sodalite and binder glass phases dissolve at the same rate. The actual concentrations

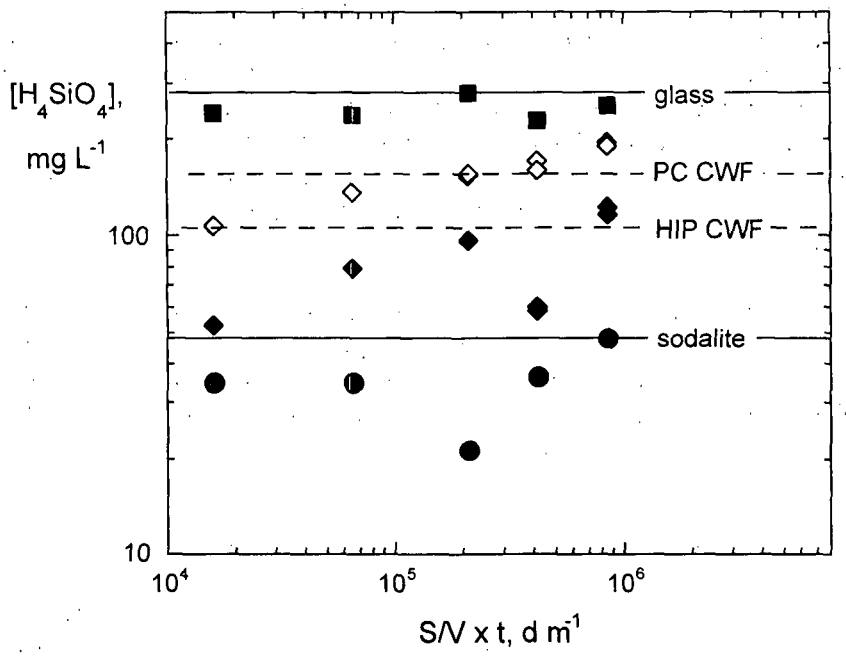

Figure 3.2. Results from Ebert (2005a): ASTM C1285 Method B tests with sodalite, binder glass, PC CWF, and HIP CWF materials.

measured for the PC CWF and HIP CWF materials are slightly higher than the calculated values. This can be attributed to the higher solution pH values attained in tests with PC CWF and HIP CWF: tests with binder glass and sodalite had average final pH values of 8.51 and 8.46, whereas tests with PC CWF and HIP CWF had average final pH values of 8.80 and 9.21, respectively. Based on the measured sensitivity of glass and sodalite dissolution rates to the pH (Ebert 2005a), pH differences of +0.3 and +0.7 units are expected to increase the glass dissolution rates by about 51% and 160%, and increase the sodalite dissolution rates by about 15% and 38%, respectively. The steady-state silica concentrations can be predicted for the dissolution of PC CWF and HIP CWF materials based on the fractional areas and the measured saturation concentrations of sodalite and binder glass in each material.

4 Mass Transport Equations

Mass transport in a solid waste form can occur through crystalline or amorphous grains, along grain boundaries and phase boundaries, through intra-particle and inter-particle voids, along pore surfaces, etc. The diffusion rates will differ significantly depending on the path, and transport is usually represented by an effective diffusion coefficient, D_e. The diffusion coefficient is an empirical coefficient that represents a complex diffusion mechanism involving several diffusion pathways and must be measured for the particular host material and diffusing component of interest. Diffusion that results in the release of a radionuclide from a waste form is distinct from the diffusion of the released radionuclide through the disposal medium. The mathematics are the same for both systems (the waste form and the disposal medium), but the boundary conditions and values of D_e will differ. The diffusion equations of present interest pertain to waste form diffusion in laboratory tests in the absence of other processes that affect behavior in a disposal system. The following sections address diffusional release from a test specimen.

4.1 Simple Diffusion-Controlled Release

If an amount of material a is lost during the time interval t from a specimen having an initial concentration A_o, surface area S, and volume V_{wf} (the subscript wf is used to distinguish the test specimen volume from the solution volume), the flux at the specimen surface ($x = 0$) is given by

$$\left.\frac{dq}{dt}\right|_{x=0} = \frac{A_o}{V_{wf}} \bullet \left(\frac{D_e}{\pi}\right)^{1/2} t^{-1/2}, \tag{4.1}$$

where

$$q = \frac{a}{S} \quad \text{and} \quad \frac{dq}{dt} = \frac{1}{S}\frac{da}{dt}. \tag{4.2}$$

Equation 4.1 can be written as

$$\frac{da}{S\,dt} = \frac{A_o}{V_{wf}} \bullet \left(\frac{D_e}{\pi}\right)^{1/2} t^{-1/2} \tag{4.3}$$

at the specimen surface. Consider a laboratory test in which the solution is completely replaced and analyzed periodically. In the limit of a very short solution renewal interval t_n, the amount a_n that is released can be approximated as the derivative:

$$\frac{a_n}{t_n} = \frac{\Delta a}{\Delta t} \; and \; \lim_{\Delta t \to 0} \frac{\Delta a}{\Delta t} = \frac{da}{dt}. \tag{4.4}$$

Upon substitution of Equation 4.4, Equation 4.3 becomes

$$\left(\frac{a_n}{t_n}\right)\left(\frac{1}{S}\right) = \frac{A_o}{V_{wf}}\left(\frac{D_e}{\pi}\right)^{1/2} t^{-1/2}. \tag{4.5}$$

Equation 4.5 relates the amount released within a test interval t_n to the diffusion coefficient and can be used to calculate values of D_e for individual test increments. There are advantages to following the trends in D_e over sequential test intervals to understand the time dependence and relating the test results to a mechanistic model. If the amount of a contaminant released over the interval t_n between samplings at t_{j-1} and t_j in a test is a_n, then the average release rate over the interval is $\frac{a_n}{t_n}$ and the incremental rate is $\left(\frac{a_n}{A_o\, t_n}\right)$. Even though the release during a test interval is modeled to have a square root time dependence for a diffusion controlled mechanism, the test data can provide only a linear (average) release rate over the test interval. The results of a series of consecutive test intervals must be plotted on the proper time axis to correctly model the mechanism. Neither the interval duration nor half the interval duration is appropriate. Instead, the time at which the tangent to the release curve (the differential rate) is equal to the linear release rate is appropriate. That point is the "generalized mean of the square root of the cumulative leaching time," T. The value of T can be calculated using the cumulative durations that define the sampling interval (ANS 2009)

$$T = \left[\frac{\left(t_j^{1/2} + t_{j-1}^{1/2}\right)}{2}\right]^2 . \tag{4.6}$$

Figure 4.1 illustrates the relationship between T and the experimental values for the testing interval from t_{j-1} to t_j, during which time the accumulated amount of contaminant released is a_n. The dashed line shows the theoretical release having a root-time dependence. The heavy solid line between the two points shows the average rate a_n/t_n that is measured in the test. For each test interval, the point at t_{j-1} gives the background concentration in the leachant and the point at t_j gives the concentration measured at the end of the test interval. The time T corresponds to the time at

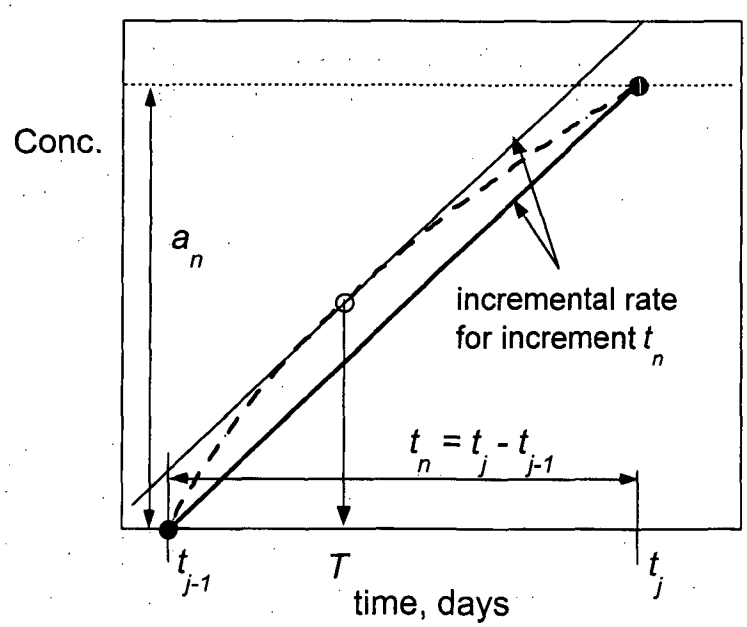

Figure 4.1. Schematic plot of testing increment.

which the tangent to the actual release curve (the dashed line) is equal to the average incremental rate (the heavy diagonal line); that point is located at the open circle whereat the lighter line drawn parallel to the heavy line giving the incremental rate intersects the dashed line showing the release behavior. The mean root-time (T) of the interval is the time at which the experimental rate during that interval should be plotted in the series of incremental rates for fitting with Equation 4.5.

The value of T will always be less than the average time of the interval early in the test (for time dependencies less than one) but will approach the average value at long test durations when the diffusion curve becomes more linear over the test interval. For example, if the 7-day sampling interval occurs between 3 and 10 days after the test was initiated, then $T = 5.99$ days and the arithmetic average is 6.5 days. If the 7-day sampling interval occurs between 20 and 27 days after the test was initiated, then $T = 23.4$ days and the arithmetic average is 23.5 days. The use of T is necessary to properly plot the time dependence of the early incremental releases that are measured in a series of consecutive static leaching intervals for analyses using dynamic leaching models using the diffusion equation. By bringing the initial concentration A_o and the specimen volume to the left-hand side of the equation and substituting T for t, Equation 4.5 can be rewritten in a form convenient for evaluating test data as

$$\left(\frac{a_n}{A_o}\right)\left(\frac{V_{wf}}{S}\right)\left(\frac{1}{t_n}\right) = \left(\frac{D_e}{\pi}\right)^{1/2} T^{-1/2} . \tag{4.7}$$

The value of D_e determined from a test of finite duration t_n is based on the instantaneous rate occurring at time T. The first term in parentheses on the left-hand side gives the incremental fraction released during interval n, and this fraction divided by the interval time gives the incremental release rate for interval n. Using this equation, the incremental leach rates determined from a series of samplings and leachate replacements can be used to calculate the effective diffusion coefficient. For purely diffusion-controlled release, plotting the product from the left-hand side of Equation 4.7 against $T^{1/2}$ will give a line with the slope $\left(\frac{D_e}{\pi}\right)^{1/2}$. Using the incremental release to determine D_e has an advantage in that uncertainties are not accrued in subsequent sampling results, as they are when the cumulative releases are used.

Despite the advantage of using the incremental releases, most analyses use the cumulative release and the integrated form of Equation 4.3 to determine the diffusion coefficient. Equation 4.3 has the standard form $\int x^n dx = \frac{1}{n+1} x^{n+1}$, with $n = -1/2$, which when integrated gives

$$\left(\frac{\sum a_n}{A_o}\right)\left(\frac{V_{wf}}{S}\right) = 2\left(\frac{D_e}{\pi}\right)^{1/2} t^{1/2} . \tag{4.8}$$

This step approximates t_n with dt and $\int a_n$ with $\sum a_n$. In Equation 4.8, t represents the cumulative test duration and $\sum a_n$ gives the cumulative release. A plot of the cumulative amount leached against the square root of the (cumulative) reaction time has a slope that represents $2\left(\frac{D_e}{\pi}\right)^{1/2}$.

4.2 Semi-Static Laboratory Test Methods

The general test method used to characterize the diffusive release that was discussed in Section 4.1 is referred to herein as a semi-static method. This testing approach differs from the static tests that were discussed in Section 3.3 in that the release of contaminants from a single test specimen are tracked as a function of reaction time for discrete and sequential intervals. The solution is replaced with fresh leachant after each interval. This approach is appropriate when the contaminant release is controlled by the solid and not affected by solution feedback effects. Two versions of that test method that are commonly used today are summarized below: the ANS 16.1 and ASTM C1308 methods. Examples from the literature are used to support discussion of each method.

4.2.1 ANS 16.1

The American Nuclear Society test method ANSI/ANS 16.1 *Measurement of the Leachability of Solidified Low-Level Radioactive Wastes by a Short-Term Test Procedure* provides a method for "indexing radionuclide release from solidified low-level radioactive waste forms in a short-term (5-day) test under controlled conditions in a well-defined leachant" (ANS 2009). The test method is widely used to evaluate the performance of low-level radioactive waste forms, but is not intended to represent any disposal system or provide insights into long-term leaching behavior. Instead, it provides a measure of the release of soluble components from a monolithic test specimen of known geometric area and volume into demineralized water over various durations at room temperature. The method recommends the use of cylindrical or parallelepiped specimens. The test method is similar to the International Atomic Energy Agency method ISO 6961-1982 (ISO 1982), which is no longer an active ISO standard.

In the ANS 16.1 test method, the leachate solution is replaced with fresh leachant (demineralized water) after consecutive intervals of 2, 5, 17, 24, 24, 24, and 24 hours; the extended test includes three additional exchanges after intervals of 336, 672, and 1032 hours (14, 28, and 43 days) for a cumulative test duration of 90 days. The rationale for the range of exchange intervals is not discussed in the procedure. It may be to ensure that the solutions in the initial intervals are not so concentrated in leached components that they affect the release and that the solutions in the later intervals become sufficiently concentrated to be analyzed. As will be shown later in this report, the test results and value of the diffusion coefficient are affected by the exchange interval.

The test data are evaluated presuming the release is controlled by diffusion, although the validity of the assumption is not evaluated as part of the test method. Instead, the results of each interval are used to calculate a leaching index and then those values are averaged to provide the test response. The data set that is provided in the ANS 16.1 standard test method as an example of the procedure is reproduced in Table 4.1. (Note that the test intervals in this example differ from those specified in the method.) The value of the diffusion coefficient is calculated from data at each exchange interval as

$$D_e = \pi \left[\frac{a_n / A_o}{t_n} \right]^2 \left[\frac{V_{wf}}{S} \right]^2 T . \tag{4.9}$$

Table 4.1. Data from ANS 16.1 Table A.2 for Example 1, expressed in hours.

Incremental time Δt, hours	Cumulative time t, hours	T, hours	$t^{1/2}$, hours$^{1/2}$	Incremental release, fraction	Cumulative release, fraction	Incremental release/Δt, fraction h^{-1}	Leachability Index (L)
21.61	21.61	5.40	4.65	2.81E-03	2.81E-03	1.30E-04	7.2
28.89	50.50	34.55	7.11	2.43E-03	5.24E-03	8.41E-05	6.8
182.50	233.00	125.11	15.26	4.18E-02	4.70E-02	2.29E-04	5.4
240.00	473.00	342.49	21.75	2.27E-02	6.97E-02	9.46E-05	5.7
240.00	713.00	586.87	26.70	1.90E-02	8.87E-02	7.92E-05	5.6
240.00	953.00	828.66	30.87	2.98E-03	9.17E-02	1.24E-05	7.1
719.44	1672.44	1287.60	40.90	1.13E-02	1.03E-01	1.57E-05	6.7
3611.11	5283.56	3225.31	72.69	1.36E-02	1.17E-01	3.77E-06	7.5
6722.22	12005.78	8304.58	109.57	2.10E-02	1.38E-01	3.12E-06	7.3
11750.00	23755.78	17384.42	154.13	1.70E-02	1.55E-01	1.45E-06	7.6

This is identical to Equation4.8 but rearranged to solve for D_e; t_n is the duration of the test interval and the "mean time" T is calculated using Equation 4.6. The leachability index (L) is calculated as the negative logarithm of the diffusion coefficient divided by the constant 1.0 cm^2 s^{-1} (so as to take the logarithm of a unitless number). The values of L reported for the individual samplings are included in Table 4.1. To better assess the results, the cumulative fractional release results are plotted against the square root of the cumulative test time in Figure 4.2. Based on Equation 4.8, such a plot is expected to be linear with a slope equal to $\frac{2S}{V_{wf}}\left(\frac{D_e}{\pi}\right)^{1/2}$. There is an obvious change in slope between results obtained before and beyond about 720 hours (30 days) cumulative duration: the slope for the first 713 hours (about 30 days) is about 8 times the slope for data beyond 713 hours. The change is not addressed in the ANS 16.1 standard.

The leachability index (L) values are included in the plot. They are not correlated with the time dependence of the release. The L value reported in the standard is $L = 6.3$, which is the average of the initial 7 test intervals. The average for all 10 intervals is $\bar{L} = 6.7$. The second example provided in ANS 16.1 showed more diffusion-like release behavior, but shows a very slight change in slope beyond 30 days. The source data used for the examples provided in the ANS 16.1 procedure are further analyzed in Section 5.1.4 as examples of contaminant release from cements.

As will be demonstrated in this report, an important conclusion of the analyses and evaluations conducted for and summarized here is that the response of diffusional release in a test interval is dependent on the duration of the interval. The guidance in ANS 16.1 to average the leachability indexes calculated from the results of samplings taken after different test intervals cannot be justified technically.

4.2.2 ASTM C1308

The ASTM C1308 test method is a modification of the American Nuclear Society (ANS) ANS 16.1 method designed to facilitate mechanistic modeling of the test results using various diffusion and solubility limit models (Colombo et al. 1985; ASTM 2009a). The ALT can be conducted at various temperatures to determine an effective activation energy for diffusion-controlled release and test results can be extrapolated with respect to time, temperature, and scale. Extrapolations in temperature are limited to the range over which the release mechanism is not expected to change.

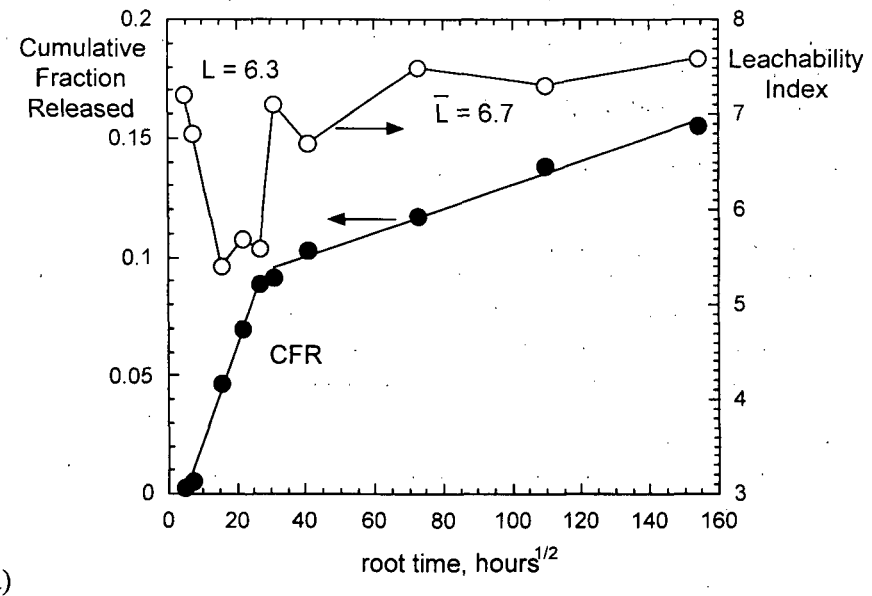

(a)

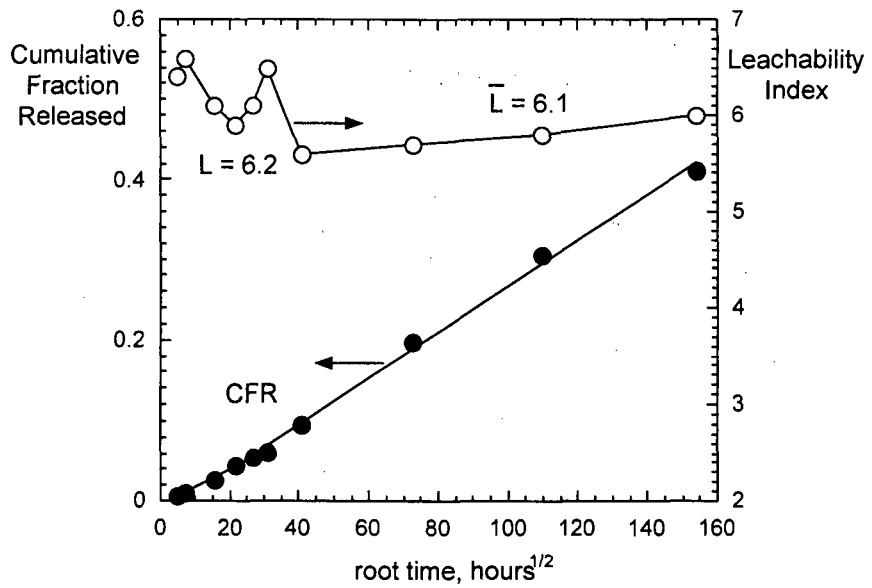

(b)

Figure 4.2. Results from ANS 16.1 test procedure: (a) Example 1 and (b) from Example 2 for cumulative fractional release (CFR, filled circles) and leachability index (L, open circles).

The activation energy that is measured may not represent a single process. For example, a reaction to release the contaminant from the matrix may occur prior to its diffusive release such that the test response reflects both the reaction and diffusion processes. The standard exchange intervals in the ALT are 2 hours, 5 hours, 17 hours, and then daily for the next 10 days, for a total test duration of 11 days. The advantage of the ALT over similar solution exchange procedures (including ANS 16.1) is the linkage to the models used to calculate the effective diffusion coefficient. A computer program is provided with the procedure that can be used to regress the test results to equations for release from a semi-infinite solid (using Equation 4.8) and from a finite cylindrical solid (see Appendix D). The computer program can also be used to analyze the test results for evidence that the leached component is partitioned between mobile and immobile fractions and for

solution saturation effects. While the same models can be used to analyze the results of ANS 16.1 tests, the testing parameters called for in the ASTM C1308 method are coordinated with the computer program data inputs and default values. The computer program allows for test intervals other than those called for in the test procedure.

4.2.3 Solution Feedback Effects in Semi-Static Tests

The derivation of Equation 4.8 presumes that the solution concentration of the diffusing species is zero at the boundary of the test specimen. In practice, the concentration will increase during the test interval because the released species are not removed by advection (each interval is a static test). Spence and Cox (1990) evaluated the error introduced by analyzing the results of static testing intervals with a model based on dynamic leaching conditions that assumes a zero-concentration boundary condition. This is an important difference because the concentration gradient establishes the free energy difference that drives the diffusion. The actual concentration in the solution contacting the test specimen will depend on the release rate from the test specimen, the diffusion rate of the released species in the solution away from the surface, and, of course, the frequency of solution exchange. Calculations were performed by Spence and Cox (1990) for test specimens having V_{wf}/S ratios of 1 cm and 10 cm, and for values of -log D_e = 5, 6, 7, 8, and 10 to estimate the error (in terms of percent difference in contaminant release) generated by analyzing test data using a model based on zero-concentration boundary condition. Some of the results are plotted in Figure 4.3 to compare the effects of the V_{wf}/S ratio and D_e on the cumulative release.

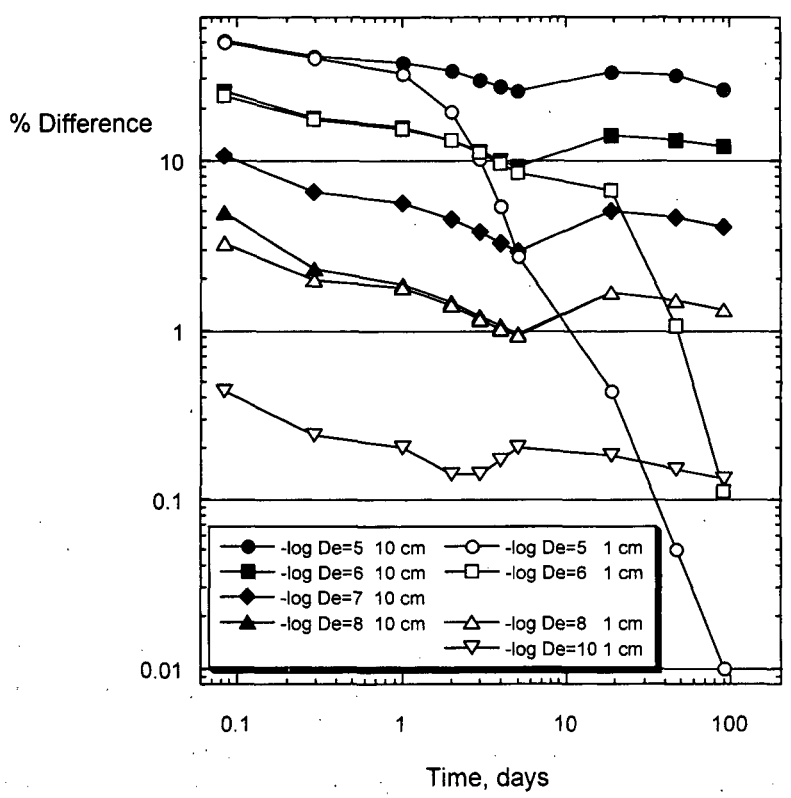

Figure 4.3. Results from Spence and Cox (1990): Impact of assuming zero surface concentration on cumulative release for four diffusion coefficients and two specimen V_{wf}/S ratios.

Comparing open and filled symbols for -log D_e = 5 and 6, the effect of the V_{wf}/S ratio of the specimen appears to become more significant with time, but this is a result of the specimens becoming depleted of the contaminant rather than the nonzero surface concentration. The differences with V_{wf}/S ratio are insignificant at smaller D_e values (larger values of –log D_e). This does show the potential effect specimen geometry on the test response at high diffusion rates. The ANS 16.1 method recommends using cylindrical test specimens having height/diameter ratios in the range 0.2 to 5, which results in V_{wf}/S ratios less than 1. The user should be aware of the possible depletion of contaminants in the specimen (i.e., a decrease in the bulk concentration) after long test durations, which could be misinterpreted as a lower release rate.

The error due to the nonzero solution concentrations is high for contaminants with high values of D_e initially but it decreases and becomes relatively constant over time. The calculations at -log D_e = 5 represent the situation in which the diffusion rate in the specimen equals the diffusion rate in the solution. At this high diffusion rate, the test specimen used in the simulation at V_{wf}/S = 1 cm was depleted of the contaminant after a few days (this leads to a rapid decrease in the percent difference because the concentrations in the test approach zero as the specimen is depleted). The specimen at -log D_e = 6 and V_{wf}/S = 1 cm was depleted after about 20 days.

The slight increases in the percent differences between 5 and 20 days for -log D_e = 5, 6, 7, and 8 (except for the V_{wf}/S ratio of 1 cm) and between 3 and 5 days for -log D_e = 10 are attributed to the opposing effects of the concentration at the surface (1) increasing due to diffusion out of the specimen and into solution at the interface—which slows with time—and (2) decreasing due to diffusion away from the specimen—which remains nearly constant with time. Since the effective D_e values for radionuclide diffusion in waste forms are expected to be less than 1×10^{-6} cm^2 s^{-1}, the effect of nonzero concentrations of the diffusing species in the solution at the specimen surface on the accuracy of the cumulative release that is calculated assuming zero concentrations will decrease from about 20% for the initial test intervals to less than 10% for the extended intervals when the specimen V_{wf}/S ratio is within the recommended range of 0.2 to 5 cm. The specimen dimensions recommended in ASTM C1308 (a cylinder 2.5 cm in diameter and 2.5 cm in height) give a V_{wf}/S ratio of 0.42 cm and are expected to generate a similar error relative to the assumption of zero concentrations at the surface as that generated in the ANS 16.1 method.

4.2.4 Example: Release of Cs from a Cement-Sludge Waste Form

The results of solution exchange tests with a cement-sludge waste form that were conducted by Smith (1969) and later evaluated by Godbee and Joy (1974) are considered as an example of determining the diffusion coefficient from experimental data. Table 4.2 presents the time and cumulative release results and several calculated values. The specimen was reported to have a volume of 1049 cm^3 and a surface area of 619 cm^2, which gives a V_{wf}/S ratio of 1.6949 cm. Consideration of these values indicates that the specimen was *not* a cylinder. That is, no combination of height and diameter provides the reported values of S and V_{wf}. However, as pointed out in the ANS 16.1 procedure, cumulative releases less than about 20% can be approximated as release from a semi-infinite surface regardless of the specimen geometry. Values of root-time, T, the products of the cumulative amounts leached × (V_{wf}/S), and the products of the incremental amounts leached × (V_{wf}/S) × ($1/t_n$) were calculated for use in the plots.

Table 4.2. Test data from Godbee and Joy (1974).

time[a], d	t_n, days	root time, $(days)^{1/2}$	T^b, d	Cumulative fraction	Cumulative x $(V_{wf}/S)^a$, cm	Incremental x $(V_{wf}/S)(1/t_n)$, cm d^{-1}
1	1	1.000	0.25	0.000425	0.00072	0.00072
2	1	1.414	1.46	0.000649	0.0011	0.00038
3	1	1.732	2.47	0.000826	0.0014	0.00030
6	3	2.449	4.37	0.001121	0.0019	0.00017
7	1	2.646	6.49	0.001239	0.0021	0.00020
14	7	3.742	10.20	0.001711	0.0029	0.00011
21	7	4.583	17.32	0.002183	0.0037	0.00011
28	7	5.292	24.37	0.002655	0.0045	0.00011
35	7	5.916	31.40	0.003068	0.0052	0.00010
42	7	6.481	38.42	0.003541	0.0060	0.00011
50	8	7.071	45.91	0.004013	0.0068	0.00010
56	6	7.483	52.96	0.004367	0.0074	0.00010
64	8	8.000	59.93	0.004721	0.0080	0.000075
70	6	8.367	66.97	0.004957	0.0084	0.000067
84	14	9.165	76.84	0.005547	0.0094	0.000071
91	7	9.539	87.46	0.005783	0.0098	0.000057

[a]Values provided in Table 1 of Godbee and Joy (1974).
[b]Calculated using Equation 4-6.

Using Cumulative Release

Figure 4.4a shows the cumulative amount leached x (V_{wf}/S) plotted against the cumulative test duration. The shape of the curve is typical for diffusive release, but the trend line does not pass through the origin. Figure 4.4b shows the cumulative amount leached x (V_{wf}/S) plotted against the square root of the reaction time. The fit of the entire data set (solid line) indicates the correlation may not be linear over the entire test duration. Data for times through about 25 days are well fitted by a regression line passing very near the origin (the dashed line and solid circles in Figure 4.4b), but results for longer durations deviate positively from that line. Separate regressions of the entire data set (solid line) and of only the long-term data (dotted line and open circles) show good correlations, but both have negative y-intercepts. The effective diffusion coefficient calculated from the regression to the entire data set (solid line in the figure) using Equation 4.9 is 8.82×10^{-7} cm^2 d^{-1}. The values from the short-term and long-term results (dotted and dashed lines in the figure) are 5.23×10^{-7} cm^2 d^{-1}and 1.13×10^{-6} cm^2 d^{-1}, respectively. An important difference between the short-term and long-term results is that the test intervals for the first five samplings were 1, 1, 1, 3, and 1 days, whereas subsequent sampling intervals were 7 days or longer.

Why a longer sampling interval would result in greater releases from a diffusion-controlled mechanism is not obvious. It could occur coincidentally with the medium becoming a less-efficient diffusion barrier as the reaction continues, e.g., due to increasing porosity, or it could instead indicate a change in the mechanism and the effective time-dependence of the release. However, the difference is most likely an artifact of the sampling and solution exchange interval t_n and using a linearly averaged rate (for each interval) to represent root-time reaction kinetics.

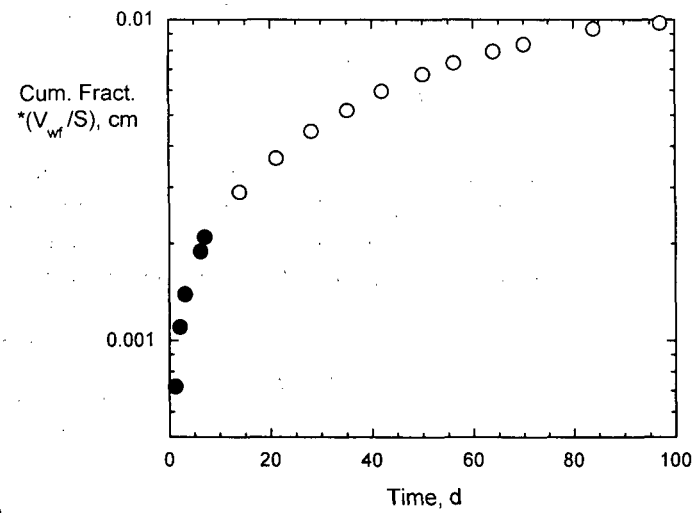

(a)

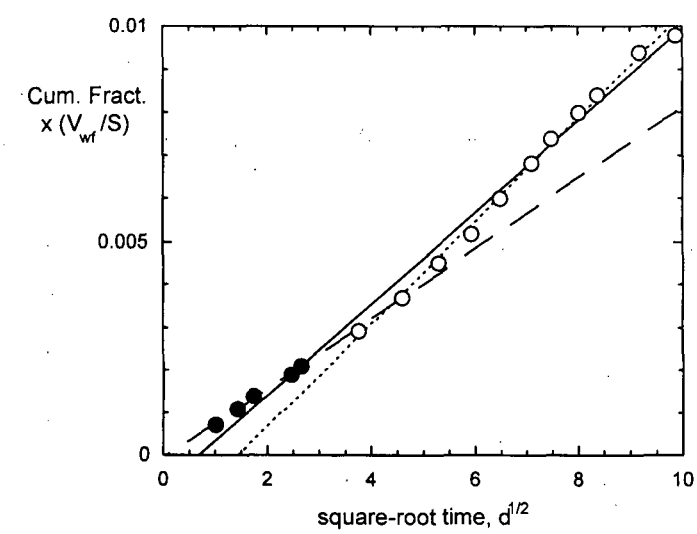

(b)

Figure 4.4. Data from Godbee and Joy (1974): (a) Cumulative release x (V/S) vs. time and (b) cumulative fraction leached vs. root time with analytical fits. Filled symbols represent exchange intervals ≤3 days and open symbols represent exchange frequencies ≥7 days.

Using Incremental Release

To use a set of test results to distinguish between optional mechanisms, it is necessary to understand the uncertainty in the data. A major issue that must be addressed is the accrual of uncertainty in the cumulative results used to measure the release behavior. An alternative plotting method that avoids accruing uncertainties in subsequent intervals was suggested by Godbee and Joy (1974) wherein the product of the incremental leach rate and V_{wf}/S ratio of the test specimen (see Equation 4.7) is plotted against the generalized mean of the square root of the cumulative leaching time term T. As discussed in Section 4.1, using T places the data point at the time corresponding to the average release over that interval (not the average time). The use of such a plot helps identify suspect data. The time dependence of the incremental leach rate is calculated as

$$Incremental\ leach\ rate \times \left(\frac{V_{wf}}{S}\right) = \left(\frac{D_e}{\pi}\right)^{1/2} T^{-1/2} . \tag{4.10}$$

Figure 4.5 shows a plot of the incremental leach rate times V_{wf}/S against the mean root time T (data from columns 7 and 4 in Table 4.2, respectively) with a regression fit to the equation $y = b\ T^{-0.5}$, which is the form expected for diffusive release from a nonreactive substrate per Equation 4.10. (The term y represents the left-hand side of Equation 4.10 and the parameter b represents $\left(\frac{D_e}{\pi}\right)^{1/2}$.) The data appear to be consistent with the reciprocal root-time dependence with no obvious outlying results. For example, none of the results are anomalously high enough to cause the slight increase in cumulative values at long times that was seen in Figure 4.4b. Because the uncertainty in the data up to about 7 days is hard to judge, these data were excluded from the regression. The value of b in the fit is 0.00052 and the effective diffusion coefficient from this fit is 8.49×10^{-7} cm^2 d^{-1}. This is similar to the value determined from regressing all data in the plot in Figure 4.4b. The change in slope seen in Figure 4.4b occurs at about 4 d$^{1/2}$ (16 days), which is the sixth data point in Figure 4.5. In Figure 4.5, this point (which is plotted as the open circle) falls below the fitted curve near the point of greatest curvature. The data points before and after that point appear to be equally well represented by the curve representing the diffusion model.

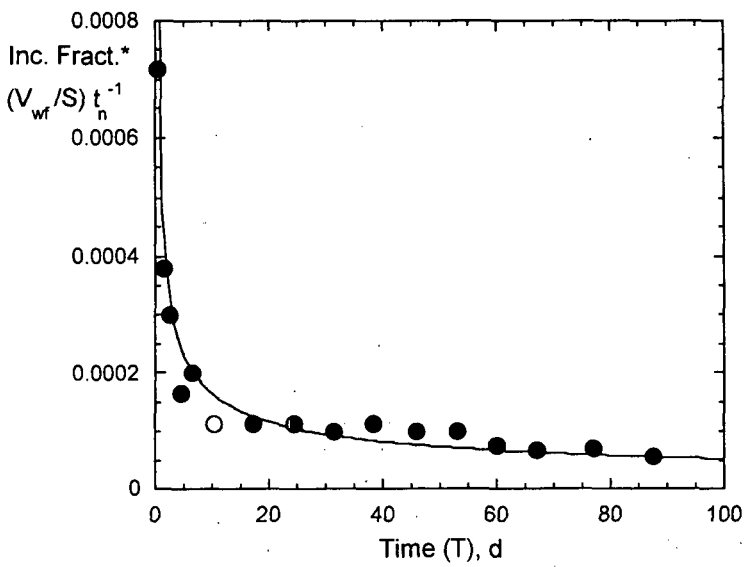

Figure 4.5. Data from Godbee and Joy (1974): Incremental leach rate vs. mean root time with regression fit.

As pointed out by Ogard and Bryant (1982), plotting the incremental release values vs. $t - (t_n/2)$ (or vs. T) is not equivalent to plotting them vs. Σt_n, where t_n is the duration of increment n, and the two curves may differ considerably. Ogard and Bryant (1982) suggested plotting the test results (the incremental release) vs. the increment duration t_n. Such a plot will show a group of rates for a particular test interval that decrease slightly as the interval occurs later in the test if the release rate

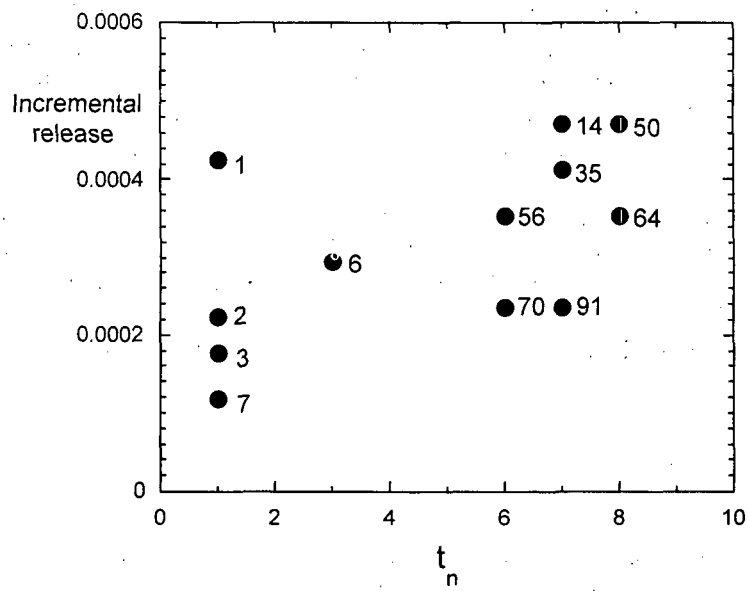

Figure 4.6. Data from Godbee and Joy (1974): Plot of incremental release values vs. duration of increment.

is diffusion controlled. This is because the diffusion path for release increases as the square root of the cumulative time; the difference will be much greater at the beginning of the test. For example, Figure 4.6 presents the results of tests with the cement-sludge waste discussed earlier plotted in this way. Values next to points give cumulative duration at the end of each increment. The releases measured in intervals of the same duration are seen to decrease with increasing test time in most cases. The amount released in the second day is about half that released in the first day, but the 7-day intervals that end after 14, 21, 28, and 42 days cumulative durations all had incremental releases of 0.000472. The amount released in a 7-day interval after 91 days cumulative reaction time was about half the amount released in the 7-day interval at 14 days cumulative reaction. This is consistent with the sub-linear time dependence of the release, but the plot provides no added insight.

4.2.5 Partition Model

The distribution of a contaminant in a material may be heterogeneous such that different fractions have different release behaviors, including not being leached at all. The computer program provided in the User's Guide for the ALT computer program (developed to evaluate data from ASTM C1308) includes a partition model in which a fraction of the contaminant is considered to be immobile and not leachable (Fuhrmann et al. 1990; page 80). The ALT User's Guide states: The partition model uses the model for diffusion from a finite cylinder (or from a semi-infinite cylinder if the [cumulative fraction leached] CFL<0.0124), but alters the result by reducing the original source term so that the cumulative fraction leached is determined as follows:

$$CFL = \frac{\sum a_n}{A_o P} = 2\frac{S}{V_{wf}}\left[\frac{D_e t}{\pi}\right]^{1/2} \tag{4.11}$$

where a_n is the total amount of radioactive material released in all leaching periods up to time t, A_0 is the initial source term which is the amount of radioactive material originally present in the solid sample, P is the source term partitioning factor, which is $0<P<1$, $[V_{wf}]$ is the volume of the solid sample, S is the geometric surface area of the solid sample, and D_e is the effective diffusion coefficient" (Fuhrmann et al. 1990; page A5).

In the ALT computer program, values of CFL calculated with the semi-infinite or finite cylinder model are scaled by trial values of P to minimize the residuals between the calculated values and the measured CFL values to within a specified tolerance. Figure A1 from Fuhrmann et al. (1990) gives the results of ASTM C1308 tests measuring the release of ^{137}Cs from cement. That figure is reproduced as Figure 4.7 with the test data and regression fit to the diffusion equation, which is

$$CFL = 1060 \times \left(\frac{1.33 \times 10^{-7}}{\pi} t \right)^{1/2} \tag{4.12}$$

where the value 1.33×10^{-7} ($cm^2\ d^{-1}$) is the diffusion coefficient given for this data on page 80 of Fuhrmann et al. (1990). (The method used to reproduce this and other plots taken from literature sources in which the data were not provided is described in Appendix B.) The fit of the entire data set to the diffusion model shown in Figure 4.7a (solid line) is similar to that shown in Fuhrmann et al. (1990), but the time dependence of the data (shown empirically by the dotted line) is not consistent with the $t^{1/2}$ time dependence expect for diffusion-controlled release. Regression of the subsets of data for samplings less than 2 days and for samplings after 2 days or longer cumulative test duration to power-law equations indicates that the time dependence of the longer-term data (filled squares in Figure 4.7b) is best represented by the equation

$$CFL = 0.297 \times t^{0.341}. \tag{4.13}$$

The data for the three early samplings are well fit by the diffusion equation with root time dependence and $D_e = 1.97 \times 10^{-7}$. $cm^2\ d^{-1}$. The apparent change in behavior beyond 1 day (cumulative) coincides with a change in sampling interval. Empirically, the best regression fits are power-law fits to samplings through 3 days and beyond 3 days, which show time dependencies of $t^{0.506}$ and $t^{0.304}$, respectively. This implies that the initial release is diffusion-controlled but releases after longer durations are complicated by another process that affects the time dependence. The combined effects of diffusion and reaction are considered in the next section.

4.3 Diffusion-Controlled Release with Concentration-Dependent Reactions

Amarantos cautioned against "the danger inherent in the uncritical use of Fick's law for long-term prediction of leaching rates" (Amarantos, 1976). Several factors that will likely be important in practical situations are ignored in theoretical models due to either the complexity they would introduce or the fact that the impacts are not well understood. These include the initial heterogeneity of the specimen itself, changes in the structure and composition of the specimen as it degrades, the non-uniform distribution of waste components in the test specimen, and swelling that may occur in some materials due to water uptake. In addition to (or because of) changes in the system, the values of the rate coefficient and diffusion coefficient may not remain constant over the test duration. The conceptual model developed by Amarantos and Petropoulos (1972) takes

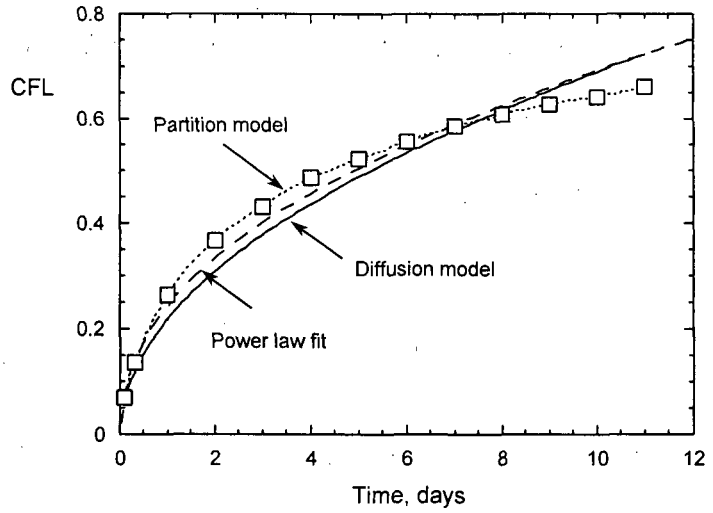

(a)

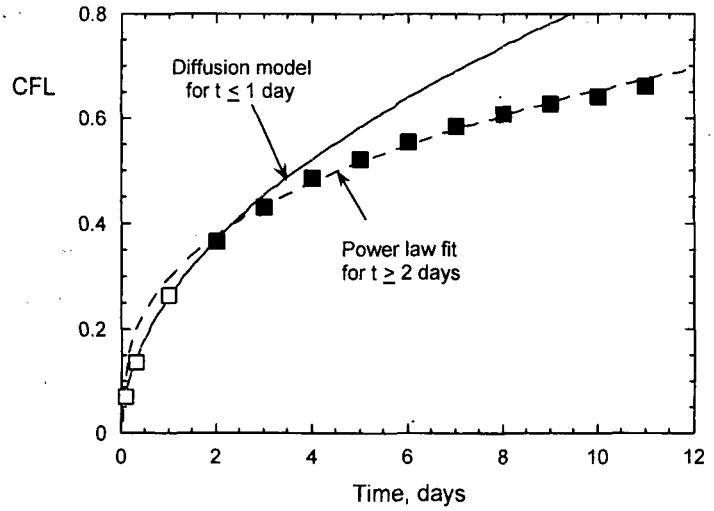

(b)

Figure 4.7. Results from Fuhrmann et al. (1990): (a) Regressed to diffusion model and power-law fit and expected partition model fit, and (b) data for cumulative durations $t \leq 1$ day regressed to diffusion model and data for cumulative durations $t \geq 2$ days regressed to power-law fit.

into account the possibility that a species bound in a waste form must first be mobilized by a reaction and then diffuse through the encapsulating matrix. The model couples a first order reaction to mobilize the contaminant with diffusion. The mobilizing reaction could be dissolution of the phase containing the species, oxidation of the species to a mobile oxidation state, etc.

A solution to the diffusion problem for a system in which the diffusing species is generated or consumed by reaction at a rate that depends on its concentration was given by Danckwerts (1950) for the absorption and subsequent uptake of a species. This analytical solution was later modified by Godbee and Joy (1974) to represent a dissolution reaction coupled with diffusion in a system with boundary conditions appropriate for the conceptual model given in Amarantos and Petropoulos (1972). The Danckwerts (1950) solution and Godbee and Joy (1974) adaptations are

presented in detail in Appendix C for the important model of diffusion with a concentration-dependent reaction. For a contaminant mobilized at a rate that depends on its concentration as

$$rate = k_f\left(C_s - C\right) \tag{4.14}$$

and the incremental leach rate at the surface is given by

$$\left(\frac{a_n}{A_o}\right)\left(\frac{V_{wf}}{S}\right)\left(\frac{1}{t_n}\right) = \left(D_e\, k_f\right)^{1/2} \bullet \left[erf\left(k_f T\right)^{1/2} + \frac{e^{-k_f T}}{\left(\pi\, k_f T\right)^{1/2}}\right], \tag{4.15}$$

where k_f is the rate coefficient for the mobilizing reaction and $T = \left[\frac{\left(t_j^{\,1/2} + t_{j-1}^{\,1/2}\right)}{2}\right]^2$. The complicated time-dependence is due to the interaction of the root-time time dependence for diffusion and linear time dependence for reaction. Consider the limiting extremes. At large values of $k_f T$ (for fast reactions and/or after long time), Equation 4.15 reduces to

$$\left(\frac{a_n}{A_o}\right)\left(\frac{V_{wf}}{S}\right)\left(\frac{1}{t_n}\right) \approx \left(D_e\, k_f\right)^{1/2} . \tag{4.16}$$

At small $k_f T$ (e.g, $k_f T$ <0.5) due to a low dissolution rate and/or short durations (noting that the value of $erf(x)$ approaches $\frac{2x}{\pi^{1/2}}$ for small values of x), the error function term in Equation 4.15 can be written as $\frac{2\left(k_f T\right)^{1/2}}{\pi^{1/2}}$ and the exponential term can be approximated as $1 - k_f t$. With these substitutions, Equation 4.15 for small $k_f T$ can be reduced to

$$\left(\frac{a_n}{A_o}\right)\left(\frac{V_{wf}}{S}\right)\left(\frac{1}{t_n}\right) \approx \left(\frac{D_e}{\pi}\right)^{1/2} \left(1 + k_f T\right) \bullet T^{-1/2} . \tag{4.17}$$

At the limit $k_f = 0$, Equation 4.17 reduces to Equation 4.7, the diffusion equation for a semi-infinite solid. Now consider the integrated rate. Integrating Equation 4.15 over time gives (see Appendix C)

$$\left(\frac{\sum a_n}{A_o}\right)\left(\frac{V_{wf}}{S}\right) = \left(\frac{D_e}{k_f}\right)^{1/2} \bullet \left[\left(k_f t + \frac{1}{2}\right) erf\left(\left(k_f t\right)^{1/2}\right) + \left(\frac{k_f t}{\pi}\right)^{1/2} e^{-k_f t}\right]. \tag{4.18}$$

When $k_f t$ is large due to either high dissolution rates or long durations, the second term in brackets becomes negligible, the value of the error function approaches one, and Equation 4.18 reduces to

$$\left(\frac{\sum a_n}{A_o}\right)\left(\frac{V_{wf}}{S}\right) \approx \left(\frac{D_e}{k_f}\right)^{1/2} \bullet \left(k_f t + \frac{1}{2}\right). \tag{4.19}$$

This gives a linear time dependence for the cumulative release and a nonzero intercept:

$$\left(\frac{\sum a_n}{A_o}\right)\left(\frac{V_{wf}}{S}\right) \approx \left(D_e k_f\right)^{1/2} t + \left(\frac{D_e}{4k_f}\right)^{1/2} . \tag{4.20}$$

When the product $k_f t$ is small (e.g, <0.5) due to either a low reaction rate or short durations, Equation 4.18 can be simplified by approximating the error function and exponential terms—the value of $erf(x)$ approaches $\frac{2x}{\pi^{1/2}}$ and the value of $exp(-k_f t)$ approaches $(1-k_f t)$—as

$$\left(\frac{\sum a_n}{A_o}\right)\left(\frac{V_{wf}}{S}\right) = k_f t \bullet \left(\frac{D_e t}{\pi}\right)^{1/2} + 2\left(\frac{D_e t}{\pi}\right)^{1/2} . \tag{4.21}$$

For a given value of k_f, short leaching times are predicted to show a nearly root-time dependence and long leaching times are predicted to show a linear time dependence by Equation 4.21. For systems with $k_f t << 2$, Equation 4.21 can be further reduced to

$$\left(\frac{\sum a_n}{A_o}\right)\left(\frac{V_{wf}}{S}\right) = 2\left(\frac{D_e t}{\pi}\right)^{1/2} , \tag{4.22}$$

which is the expression for cumulative release from a semi-infinite solid (Equation 4.8). Figure 4.8 shows the CFL values calculated with Equation 4-15 for $D_e = 1 \times 10^{-7}$ cm^2 d^{-1} and various values of k_f. The curve for $k_f = 5$ is essentially linear with time (in agreement with Equation 4.20) and the curve for $k_f = 0.001$ has essentially root-time dependence (in agreement with Equation 4.22). Curves for k_f values of 0.05, 0.1, and 0.5 have a square root time dependence at short times and approach a linear time dependence at longer times. Long leaching intervals are needed to quantify small values of k_f. Values are needed for both D_e and k_f to apply Equation 4.18. These can be determined by regression analysis of the appropriate experimental results.

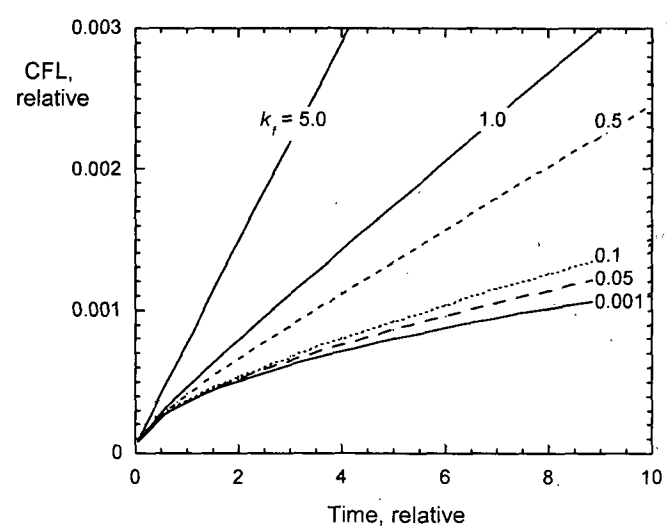

Figure 4.8. Plots of Equation 4.18 with $D_e = 1 \times 10^{-7}$ and various values of k_f.

4.3.1 Example: Release of Cs from a Cement-Sludge Waste Form

The results of the test with the cement-sludge material shown in Figure 4.4a were fitted with Equation 4.8 using the value $D_e = 8.82 \times 10^{-7}$ cm^2 d^{-1}, which was determined by fitting the complete set of results in Figure 4.4b (dashed line; see NOTE 1 below). The results were also fitted with Equation 4.18 using values $D_e = 4.75 \times 10^{-7}$ cm^2 d^{-1} and $k = 0.012$ d^{-1}, which were taken from Godbee and Joy (1974) (solid line; see NOTE 2 below). The results and fits are shown in Figure 4.9. The goodness of fit measured by the square of the residuals is 8.70×10^{-6} for the fit with Equation 4.8 and 3.04×10^{-7} for the fit with Equation 4.18. Although the solid line gives the better regression, the dashed line is visually more representative of the expected longer-term behavior based on results for the six longest durations. The curves diverge beyond about 100 days and the long-term behaviors calculated with the two equations will differ significantly. For example, the cumulative loss will be 20% higher using Equation 4.18 (solid line fit) than using Equation 4.8 after only 176 days. That is, a 176-day test would be required to differentiate the models assuming 20% uncertainty in the results (e.g., the combined uncertainty in test execution and analysis). Neither model can be selected with confidence for the purpose of calculating releases over hundreds of years based on this data set alone. Within the uncertainty in the data, other values of D_e and k_f could be selected using values of k_f that approach zero, at which point the model expressed by Equation 4.18 converges with Equation 4.8. The important point is that the uncertainty of using a single data set can significantly affect the confidence in model selection and long-term predictions.

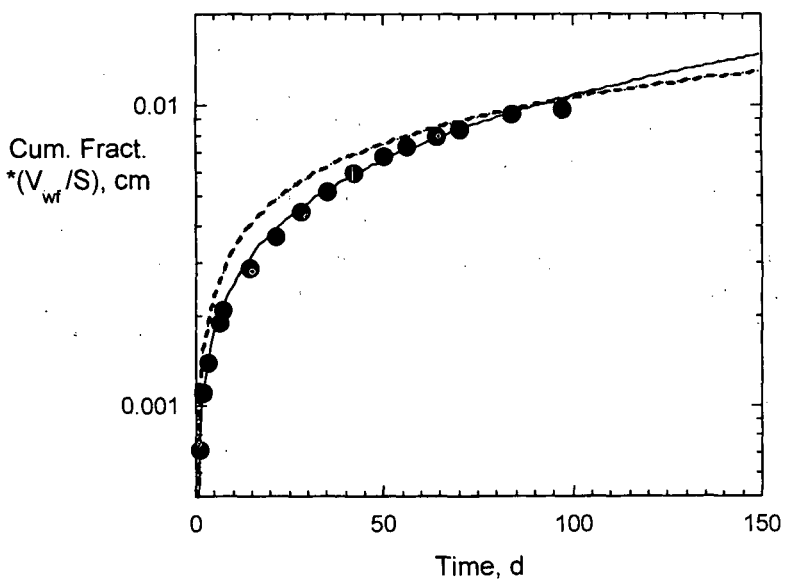

Figure 4.9. Data from Godbee and Joy (1974): Plot of cumulative release vs. cumulative time for cement-sludge material. Dashed line shows fit with the simple diffusion equation given in Equation 4.8 and solid line shows fit with the coupled diffusion-reaction equation Equation 4.18.

NOTE 1: Fits using Equation 4.8 with values of D_e determined from regressions to only the short-term or long-term results in Figure 4.4b significantly underestimate the releases. The root-time fits in Figure 4.4b all had negative y-intercepts that were not taken into account in the fit in Figure 4.9. The y-intercepts in the plots can be represented by recasting Equation 4.8 with an *ad hoc* adjustment term as

$$\left(\frac{\sum a_n}{A_o}\right)\left(\frac{V_{wf}}{S}\right) = 2\left(\frac{D_e\, t}{\pi}\right)^{1/2} + \left[\left(\frac{\sum a_n}{A_o}\right)\left(\frac{V_{wf}}{S}\right)\right]_{t=0} . \tag{4.23}$$

The value of the y-intercept in the plot could be subtracted from the calculated cumulative releases in Figure 4.9. This would shift the dashed curve down by 0.0001 cm and improve the fit to short-term results (<50 days) slightly but worsen the fit to the longer-term results.

NOTE 2: To determine the values of D_e and k_f for the model in Equation 4.18, the value of D_e determined from Equation 4.8 was used as an initial guess with trial values of k_f to determine the value that minimized the square of the residuals between the release calculated with Equation 4.18 and the measured release. That value of k_f was then used with trial values of D_e to again minimize the value of the residuals to select a better value of D_e. Values of D_e and k were alternatively refined until the sum of the squared residuals became constant at the precision deemed appropriate for the scatter in the data. This method yielded the same values that are given in Godbee and Joy (1974): $D_e = 5.5 \times 10^{12}$ cm^2 s^{-1} and $k_f = 1.5 \times 10^{-7}$ sec^{-1}.

4.3.2 Linking Reaction and Diffusion

The general expression for the release of a mobile constituent given in Equation 4.18 can be applied to complex release modes if the mobilizing reaction can be expressed as a first order reaction. For example, it could represent the dissolution of a phase embedded in a second matrix, such as $CaCO_3$ embedded in concrete. Although diffusive transport occurs through the pore structure of the concrete, Ca^{2+} must be mobilized by the dissolution of $CaCO_3$ prior to being transported. The dissolution of most materials can be expressed using an affinity-controlled rate law such as those discussed above.
The concentration-dependent reaction rate at which species are mobilized or immobilized (generated or annihilated) that was considered above can be rewritten as

$$rate = k_f\left(C_s - C\right) = k_f\, C_s\left(1 - \frac{C}{C_s}\right) = k_f'\left(1 - \frac{C}{C_s}\right). \tag{4.24}$$

This is the same form as the affinity-controlled dissolution reaction in Equation 2.22, where C is equivalent to Q and C_s is equivalent to K; the saturation concentration C_s must also included in the rate coefficient k_f' for this correspondence. As discussed in Section 3.1, the rate coefficient may include expressions for the kinetic dependencies on the pH and temperature (e.g., Equation 3.3), and perhaps other variables.

Equation 4.24 (and Equation 2.22) can be used to approximate the dissolution behavior of glassy phases, which are thermodynamically unstable but durable due to slow dissolution kinetics. The mechanism for glass dissolution includes simultaneous hydrolysis reactions to break the bonds between various constituent elements and oxygen that are coupled with the diffusion of water into the glass to access reaction sites. The hydrolysis of Si-O bonds is usually considered to be the rate-controlling reaction for glass dissolution. Hydrolysis of B-O and alkali metal-O bonds (the latter are sometimes referred to as ion exchange reactions) occurs faster than hydrolysis of Si-O bonds and the hydrolysis of other metal-O bonds may occur faster or slower depending on the reaction conditions. The structures of most silicate glasses are established by a network of Si-O bonds and the dissolution behaviors of many glasses have been well modeled by considering only

Si-O hydrolysis in the mechanism. The hydrolysis reaction to release orthosilicic acid from the surface of a silicate glass can be written as

$$\text{glass}\equiv\text{Si-O-Si(OH)}_3 + H_2O \leftrightarrows \text{glass}\equiv\text{Si-OH} + \text{Si(OH)}_4 \tag{4.25}$$

Application of Equation 2.22 (or Equation 4.24) to a glass will be inexact because the standard state of Si (and other components) is different in the glass and in solution. In addition, the principle of detailed balance that is applied on the atomic scale in Equation 4.25 with regard to the breaking and reforming of the Si-O bond does not hold on a macroscopic scale because the dissolving glass cannot be reformed. Instead, either the equilibrium constant for a simple silicate such as chalcedony is assumed to represent the equilibrium constant of the glass for modeling purposes, or the value of the equilibrium constant is assigned empirically based on experimental results.

The value of k_f will depend on the species of interest, how it is immobilized in the waste form, and how it becomes mobilized. The value of D_e will depend on how readily water can access the leachable species in the waste form and the released species can migrate out of the waste form; this will likely change if the waste form degrades as leaching occurs. The values of D_e and k_f determined by regression of test data are likely to represent effective values that must be de-coupled. That is, the measured value of k_f will probably depend on water accessibility and the measured value of D_e will probably depend on the distribution of the species in the material. It may be impossible to distinguish the effects of mobilization and diffusion using the results from a single test method. For example, a small fraction of a waste component may be more readily accessible to water during the tests than the rest of that component so that the measured value of k_f will decrease as the accessible amount of that component decreases. In that case, the value of k_f measured in short-term tests will be too high to represent mobilization of the majority of waste. The opposite situation could also occur, wherein the amount of water that penetrates the matrix is not sufficient to dissolve all of the accessible waste. In this case, the observed release would be expected to follow the simple diffusion model as if the value of k_f was small (i.e., Equation 4.21), although this is due to the slowing effect of chemical affinity (solubility limit) at the reaction site, which may be within the pore structure. Likewise, the measured value of D_e will represent a range of pore sizes, fractures, etc. in the test specimens, which can change over the course of the test. This is also very sensitive to the surface properties of test specimens, which can differ from bulk material properties due to preparation artifacts, the formation of surface skins on prepared lab samples, etc. Confidence in projecting the release kinetics measured in short-term tests to long times requires additional insight into the reaction being represented by k_f and the transport represented by D_e and possible testing interactions and artifacts. Some of these are discussed in the following sections.

4.3.3 Solution Exchange Tests for Affinity-Controlled Release

It is of interest to understand how the release of a contaminant that is controlled by chemical affinity responds in a solution exchange test. As an extreme example of coupled diffusion and reaction in a semi-static test, consider the reaction of a glass-bonded sodalite waste form material. The material is composed of two predominant phases: about 70 volume% sodalite and 25 volume% borosilicate glass. The remaining volume is occupied by insoluble oxides and halite inclusions. The sodalite and glass phases both dissolve by a dissolution-controlled mechanism, but have different solubilities. The halite dissolves immediately when contacted by water and the oxide inclusions are essentially insoluble. Tests were conducted with a leachant having a dissolved silica content known to exceed the solubility concentration of sodalite and to be unsaturated with respect to the glass phase. A series of solution exchange tests was conducted in

which monolithic samples of two glass-bonded sodalite materials made by hot isotatic pressing (HIP CWF) and by heating under atmospheric pressure (PC CWF) were reacted in a solution made with 110 mg L^{-1} H_4SiO_4 (32 ppm Si) with a test method similar to the ASTM C1308 method (Ebert 2005a; section IV.B.4). The tests were conducted at 90°C at a *S/V* ratio of 10 m^{-1}. This solution is saturated with respect to sodalite, but under-saturated with respect to the binder glass (see Section 3.3.5).

The entire solution was exchanged periodically to maintain the dissolved silica concentration near a particular value rather than maintaining a highly dilute composition, which is the usual objective of the C1308 test method. The tests were interrupted every 10 or 11 days for the first five exchanges. The solutions were recovered for analysis and replaced with an equal amount of fresh leachant solution, and then the test was continued without disturbing until the next exchange. The exchange period was extended to 21 days for the following six exchanges to study the effect of the test interval, and the final exchange was made after 11 days. The cumulative release of B is plotted against the cumulative reaction time in Figure 4.10 for tests with PC CWF and HIP CWF. Expressing the released mass as *NL*(B) normalizes the solution concentrations to the surface area and the boron content of the test specimens and permits direct comparisons of the releases from the two materials (see discussion in Section 3.2). The results for 10- or 11-day test intervals are shown by open symbols and the results for 21-day test intervals are shown by filled symbols. The increases in *NL*(B) are linear in time for both materials, but the rates of increase differ with the exchange interval. The lower release rate at longer exchange intervals can be attributed to the greater increase in the Si concentrations that occurs during the 21-day intervals compared to the 10- and 11-day intervals. This decreases the value of the affinity term and lowers the rate. The Si concentrations increase to 38.4 ± 0.8 ppm Si during the 21-day intervals in tests with PC CWF and 37.9 ± 0.4 ppm Si for tests with HIP CWF, but only increase to 33.9 ± 0.6 mg L^{-1} Si for tests with PC CWF and 34.6 ± 1.0 mg L^{-1} Si for tests with HIP CWF during the 10- and 11-day intervals. Separate regression lines are drawn for the different exchange intervals to show their impact on the dissolution rates. The rates for the short and long exchange intervals are 0.21 and 0.13 g m^{-2} d^{-1} in tests with HIP CWF, and 0.17 and 0.087 g m^{-2} d^{-1} in tests with PC CWF. These values represent

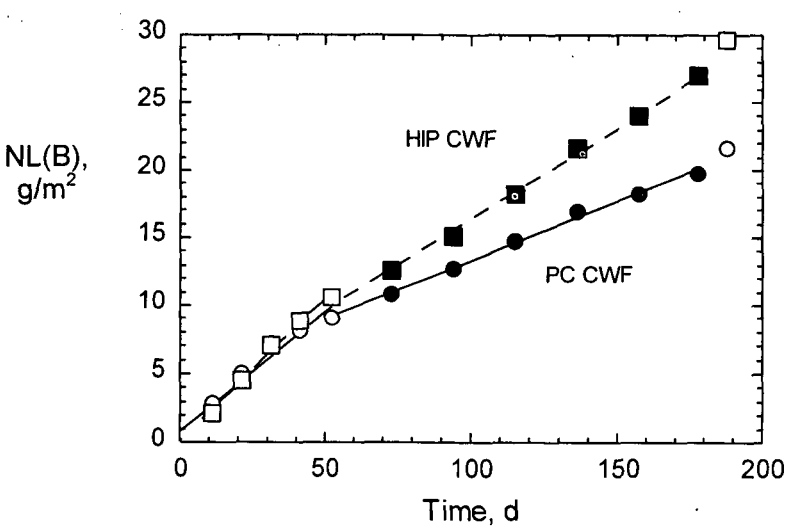

Figure 4.10.Results from Ebert (2005a): Solution exchange tests with HIP CWF and PC CWF in 110 mg L^{-1} H_4SiO_4 leachant solution. Open symbols represent 10- or 11-day exchange intervals and filled symbols represent 21-day exchange intervals.

the average rates over each test interval, but are not intrinsic properties of the materials. They provide insight into the relative effects of solution feedback for the two materials at a particular value of the saturation index.

Boron is only present in the binder glass and the rates determined from the release of B indicate dissolution of the binder glass only. It is presumed that net dissolution of sodalite does not occur in the supersaturated test solutions. Figure 4.11 shows scanning electron microscopy (SEM) photomicrographs of polished cross-sections of reacted samples recovered from the solution exchange tests. Dissolution of binder glass in the HIP CWF occurs primarily near the boundaries with sodalite, although a slight retreat of the glass surface is seen, whereas dissolution of the binder glass in the PC CWF is fairly uniform. The dissolution of glass from pores within the sodalite is seen in Figure 4.11b, where the flat sodalite surface is the original surface of the specimen. The difference is attributed to differences in the distribution of pores and halite inclusions in the two materials. Most pores and inclusion phases are located in the binder glass near sodalite domains in the HIP CWF materials but are more uniformly distributed throughout the binder glass in PC CWF. Preferential dissolution at the sodalite/glass interface has been observed in other tests with HIP CWF (Ebert 2005a).

The point of this example is that solution exchange tests such as ASTM C1308 can be used to distinguish between affinity-controlled and diffusion-controlled release mechanisms from waste materials. For constant test intervals, affinity-controlled dissolution will give cumulative releases that are linear in time, whereas diffusion-controlled dissolution will give cumulative releases that are linear with the square root of the reaction time. The rates of both release processes will depend on the solution replacement interval.

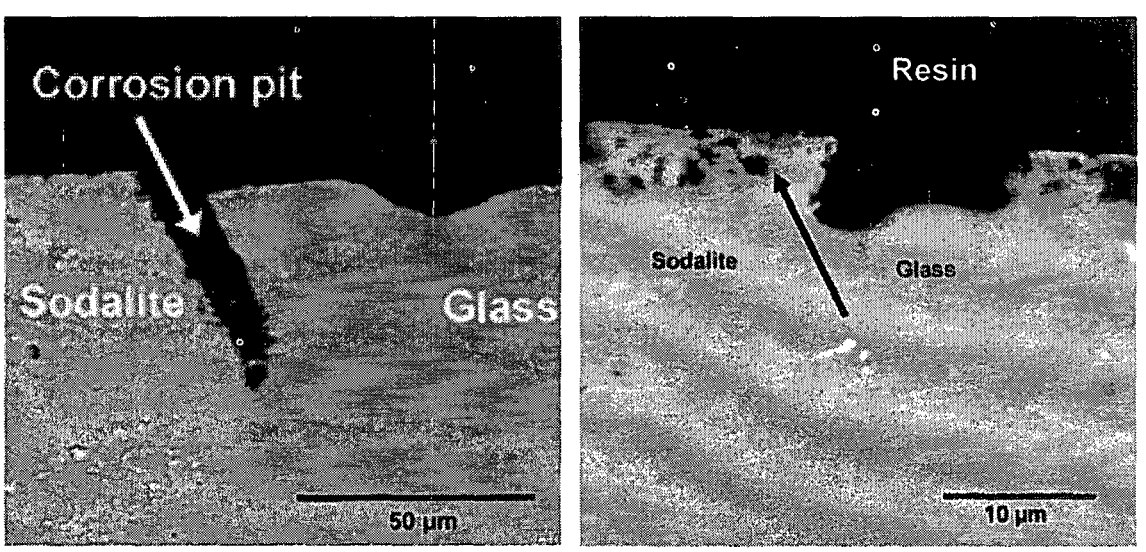

(a) (b)

Figure 4.11. Results from Ebert (2005a): SEM photomicrograph of (a) HIPCWF and (b) PC CWF materials reacted with 110 mg L^{-1} H_4SiO_4 at 90°C.

5 Static and Semi-Static Laboratory Test Results

The theoretical backgrounds for diffusive and affinity-controlled release processes and for the laboratory test methods discussed in the preceding sections are applied to the results of tests with portland cement-based (grouted) and slag materials that are available in the literature. This is not intended to be a thorough review of the literature rather, it is used to demonstrate and evaluate the application of the test methods and models to these materials. In the following sections, data were taken from publications and reports available in the open literature. Some of the data were estimated from published plots and charts and then replotted for regression analysis or fitting to model equations using Microsoft Excel or KaleidaGraph from Synergy Software. That procedure is summarized in Appendix B. In all cases, the reproduced plots were compared visually with the source plots for verification, but small errors are likely. These small errors do not compromise the objective of the plots, which is to evaluate the trends in the data and the fits to various equations used to identify and model the release mechanism. Interpretations and critiques of the model fits are provided as a part of this report unless specifically cited as an interpretation provided by the authors who published the data set.

5.1 Tests with Grouted Wastes

Various waste solutions with low levels of radioactivity have been solidified by mixing with portland cement and additives (such as active silica fume and fly ash) to form cements, grouts, and concretes. Portland cement is a porous inhomogeneous material containing micropores, microfractures, and grain boundaries that provide diffusion paths along which ions can migrate. These include a variety of connected and nonconnected pathways that are collectively referred to as the pore structure. The pore structure of a cement that is made with a volume of water exceeding the amount needed to hydrate the component phases will retain some of the excess water as alkaline pore water typically containing dissolved $Ca(OH)_2$, NaOH, and KOH. Both the pore structure and pore water are affected by additives such as active silica fume and fly ash. The relative amounts of cement and water used to prepare a grout have a significant effect on its performance. When a grout is immersed in water, the connected pore and fracture structures provide preferred pathways for water to diffuse into the cement and for dissolved cement components to diffuse out. The diffusivity of species will be affected by constrictions and tortuosity in the pore structure and transport may be further retarded by interactions with constituent phases. For example, the sorption of Cs is negligible within ordinary portland cement but may be appreciable in cements with additives. These interactions are usually modeled empirically using a distribution coefficient.

Portland cement–based materials including various grouts and concrete are considered together in the present analyses. Grout can be modeled as an assemblage of four dominant phases: tobermorite-14A [$Ca_5Si_6O_{16}(OH)_2 \bullet 4H_2O$], ettringite [$(CaO)_3(Al_2O_3)(CaSO_4)_3 \bullet 32H_2O$], portlandite [$Ca(OH)_2$], and sodium hydroxide [NaOH] (e.g., Bacon and McGrail 2005). Tobermorite-14A represents the calcium silicate hydroxide (CSH) gel phase $1.7CaOSiO_2 \bullet 2H_2O$. The added aggregate materials in concretes will provide additional mineral phases with which contaminant species may interact. The dissolution of portlandite dominates the leaching behavior of the grout itself and leads to increasing porosity. In addition to leaching, interactions with sulfate and CO_2 will affect the retention of contaminants. Carbonation will be important for some waste forms, especially those containing uranium and steel-reinforced concretes, and will depend on the diffusion rate of CO_2 through the concrete and the extents of reactions with alkaline constituents.

Immersion of a cement (or grout or concrete) in contaminated water can result in contaminants diffusing through the pore water and into the pore structure of the material. In fact, the uptake of contaminants is sometimes measured in laboratory tests to assess the performance of a grout waste form instead of the release of contaminants from the grout. An important factor in the case of contaminated cements is the depth to which the contaminants have penetrated. A heterogenous distribution of contaminants will complicate the interpretation of laboratory tests and add uncertainty to assessment models. In this report, the results of tests conducted with materials presumed to have uniform bulk contamination levels are considered to evaluate the efficacy of current test methods and models. The impacts of non-uniform contamination will be considered in subsequent reports.

In the following sections, several data sets from the literature are analyzed to assess the application of test methods to cement-based waste materials and the application of diffusion models to the interpretation of those results. In the cases of examples for which the data were not published, results were estimated from the plotted data and replotted for use in the analyses. This undoubtedly introduced small errors with respect to the data itself, but the impact on the trends in the data and how well models represent the data is insignificant.

5.1.1 Christensen

Solution exchange tests were conducted with cement-solidified ion exchange bead resins following a procedure similar to the ANS 16.1 test method (Christensen 1982). Values read from a plot of the cumulative fraction ^{137}Cs released from cements with boiling water reactor (BWR) resins against root-time (provided as Figure 1 in Christensen 1982) were used to estimate the cumulative reaction time and intervals. The estimated data (by measurement of the plotted data, see Appendix B) for grouts with and without added vermiculite are summarized in Table 5.1. The cumulative fractional releases are plotted against cumulative time in Figure 5.1a. Both sets of results have the characteristic root-time dependence expected for diffusional release, and the cumulative fractional release values are plotted against the square root of the cumulative reaction time in Figure 5.1b. Linear regression fits are shown for three groups of data in each test series. The sets of data at short and intermediate test durations are separated by test intervals that are significantly shorter than those that either precede or follow the 4th sampling of the test with grout and the 6th sampling of the test with grout + 2% vermiculite. The effect of the test interval on the release is significant for the grout, but less significant for the grout + 2% vermiculite. Fits to the series of tests are also discontinuous after about 11 days (3.2 $d^{1/2}$) when the exchange interval was changed from about 1 day to about 5 days. Christensen (1982) noted that there was not a linear relationship between the cumulative fractions released and the square root of the cumulative test intervals. Nevertheless, he fit the results from the longest test durations to the semi-empirical expression derived above as Equation 4.23

$$\left(\frac{\sum a_n}{A_o}\right)\left(\frac{V_{wf}}{S}\right) = 2\left(\frac{D_e t}{\pi}\right)^{1/2} + \left[\left(\frac{\sum a_n}{A_o}\right)\left(\frac{V_{wf}}{S}\right)\right]_0 \tag{4.23}$$

to determine effective diffusivities. A linear fit to only the long-term data for grout in Figure 5.1b gives the equation $y = 0.1261 + 0.03435x$, from which

$$D_e = \pi\left(\frac{0.03435}{2}\right)^2 = 9.27 \times 10^{-4}\ \mathrm{cm^2\ d^{-1}}. \tag{5.1}$$

Table 5.1. Estimated data for tests by Christensen (1982).

Root time, $d^{1/2}$	Time, d	Interval, d	Cumulative Fractional Release	Root time, $d^{1/2}$	Time, d	Interval, d	Cumulative Fractional Release
Grout without Additives				Grout with 2% Vermiculite			
1.01	1.02	1.02	0.09	1.01	1.02	1.02	0.04
1.43	2.05	1.03	0.13	1.43	2.05	1.03	0.06
1.82	3.30	1.25	0.16	1.74	3.04	0.99	0.07
2.03	4.13	0.83	0.17	2.02	4.08	1.04	0.08
2.26	5.11	0.98	0.18	2.31	5.33	1.25	0.09
2.48	6.14	1.03	0.19	2.44	5.96	0.63	0.10
2.67	7.13	0.99	0.20	2.67	7.13	1.17	0.11
2.85	8.13	1.00	0.21	2.84	8.06	0.93	0.11
3.02	9.11	0.99	0.22	3.02	9.11	1.06	0.12
3.19	10.16	1.05	0.23	3.20	10.24	1.12	0.12
3.88	15.09	4.93	0.26	3.88	15.09	4.86	0.14
4.50	20.23	5.14	0.28	4.58	21.00	5.91	0.16
5.14	26.38	6.14	0.30	5.03	25.28	4.28	0.16
5.76	33.19	6.82	0.32	5.51	30.34	5.07	0.18
6.36	40.48	7.29	0.35	6.10	37.18	6.84	0.19
7.05	49.68	9.19	0.37	6.68	44.56	7.37	0.20
				7.19	51.73	7.17	0.21

The slope is 0.022 cm $d^{-1/2}$ for the long-term tests with grout + 2% vermiculite and the diffusion coefficient $D_e = 3.80 \times 10^{-4}$ cm^2 d^{-1}. Christensen (1982) gives values of 8.7×10^{-4} cm^2 d^{-1} for grout and 3.9×10^{-4} cm^2 d^{-1} for grout + 2% vermiculite. The small difference is due in part to the number of data points included in the regression in Figure 5.1b and the number included by Christensen (1982). If linear fits to the short-term results are used instead of fits to the long-term results, the values of D_e are 4.67×10^{-3} cm^2 d^{-1} for grout and 1.22×10^{-3} cm^2 d^{-1} for grout + 2% vermiculite. As will be discussed in following sections, the value of D_e determined from the short-term intervals are expected to be more characteristic of the intrinsic material behavior.

As shown in Figure 5.2a, the long-term results can be fit with the diffusion equation if the results for tests with grout are uniformly increased by 0.1318 cm and the results for tests with grout + 2% vermiculite are increased by 0.0515 cm. These adjustments yield the values of D_e given by Christensen, but the fits are not consistent with the short-term results. This *ad hoc* adjustment may indicate that the near-surface regions of the test specimens were partially depleted of contaminants during preparation or have a different morphology than the underlying bulk, but it does not provide confidence that the release is controlled by diffusion. The dashed curves in Figure 5.2a show the fits using the D_e values from the short-term data. The curve for the tests with the grout has been shifted by 0.020 cm to coincide with the data at 3 days. Clearly, the data collected at different sampling intervals can be fit using different D_e values; the value of D_e determined from solution exchange tests appears to depend on the sampling interval. The fits by regression *of all results* with the simple diffusion equation and with the combined diffusion/reaction equation are also poor, as shown in Figure 5.2b for the tests with grout. The dashed curve shows the fit using Equation 4.8 for simple diffusion and the solid curve shows the fit using Equation 4.18 for coupled diffusion and reaction. The release behavior described by the complete data set is not well modeled with either simple diffusion or diffusion with reaction.

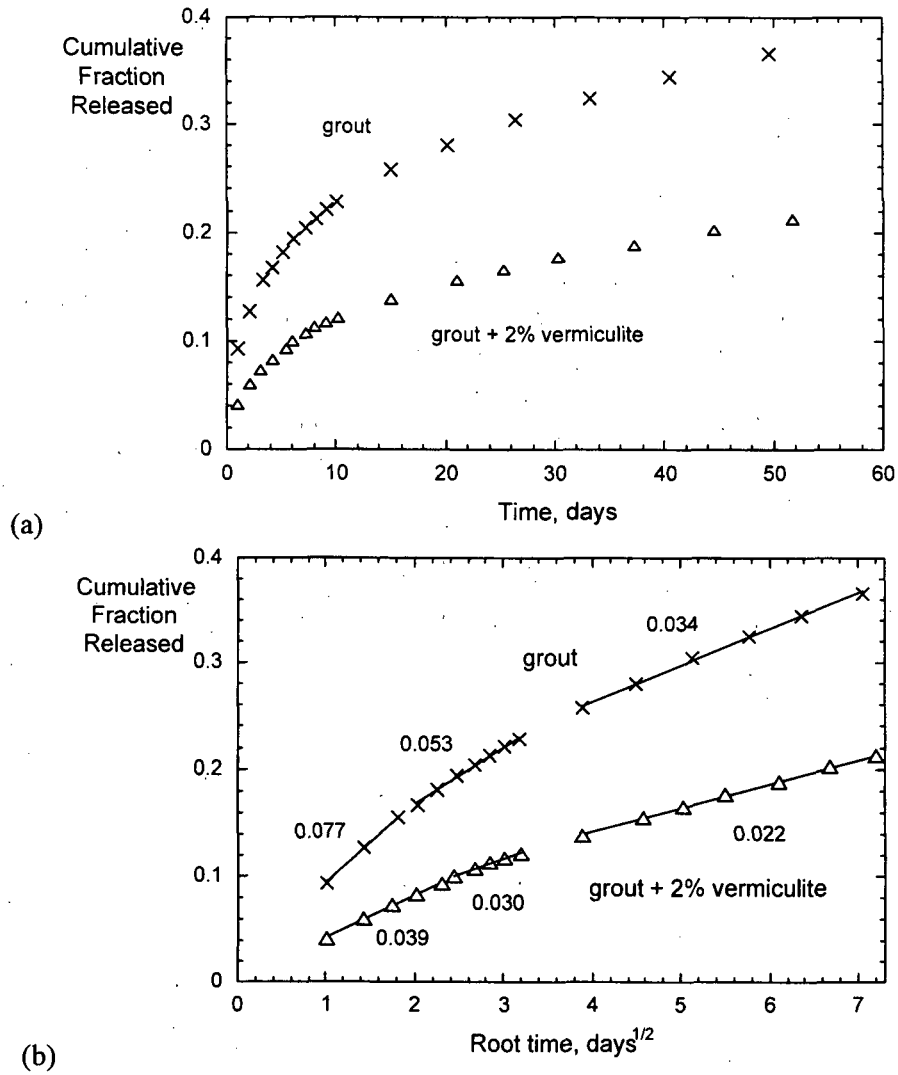

Figure 5.1. Results from Christensen (1982): ANS 16.1-like tests with BWR bead resins immobilized in cement (a) cumulative release ^{137}Cs vs. cumulative time and (b) cumulative release ^{137}Cs vs. root cumulative time.

5.1.2 Habayeb

Five decontamination solutions were immobilized in portland Type III cement and subjected to the International Atomic Energy Agency (IAEA) static leach test, which was a forerunner of the ANS 16.1 procedure (Habayeb 1985). Five solutions simulating decontamination wastes were spiked with ^{134}Cs at a level of 304 nCi mL^{-1} and then mixed with the portland cement. The mixture was cast in leach cups and cured for 32 days at room temperature and 50% relative humidity. The surface areas of the test specimens ranged from 58.1 cm^2 to 78.5 cm^2. Each cast specimen was immersed in 350 mL of demineralized water sequentially for four 1-day increments, one 3-day increment, three 7-day increments, and then several increments of 14 days and longer. Test results were provided as incremental release rates of ^{134}Cs vs. root cumulative time for durations of 1, 2,

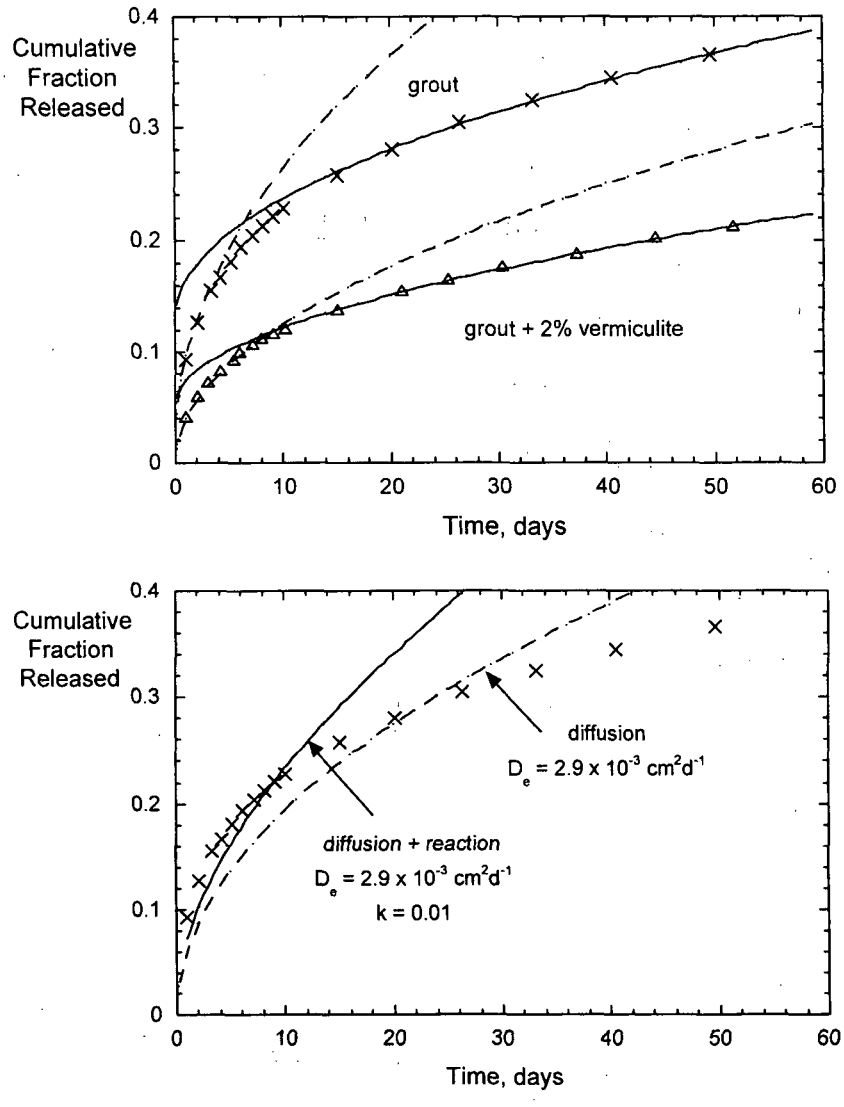

Figure 5.2. Results from Christensen (1982): ANS 16.1-like tests with BWR bead resins immobilized in cement fit (a) by shifting diffusion equation to fit the long-term results, and (b) with regressed diffusion equation (Equation 4.8) and the diffusion + reaction equation (Equation 4.18).

3, 4, 7, 14, 21, 28, and 77 days. The data are plotted as cumulative fractional release vs. cumulative time and vs. root cumulative time in Figs. 5.3a and 5.3b, respectively. (The plotted results were calculated from the incremental rates provided in Figure 1 of Habayeb (1985).) The cumulative results show smoothly decreasing amounts of ^{134}Cs to be released in successive samplings. Plots of CFR against the square root of time are linear for samplings at common intervals, but the slopes decrease with increasing interval time between samplings. The first four 1-day samplings and the three 7-day samplings each show linear root-time behavior, but the slopes are significantly lower for the 7-day sampling intervals. The single samplings at 3 intervals could have been included in the fits with either the 1-day or 7-day intervals within testing uncertainty. This suggests that a variance of 2 to 4 days in the sampling interval may not be significant relative to the testing uncertainty. The CFR values for 49-day intervals of the final data points all fall below the values predicted by the rates from 7-day intervals, albeit only slightly.

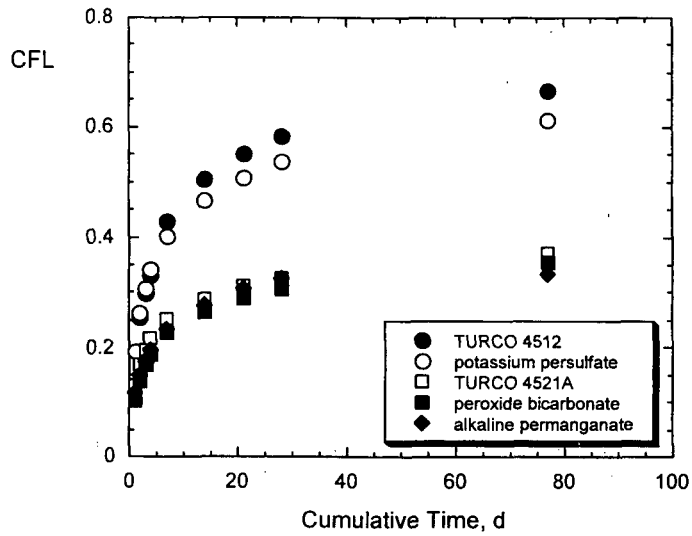

(a)

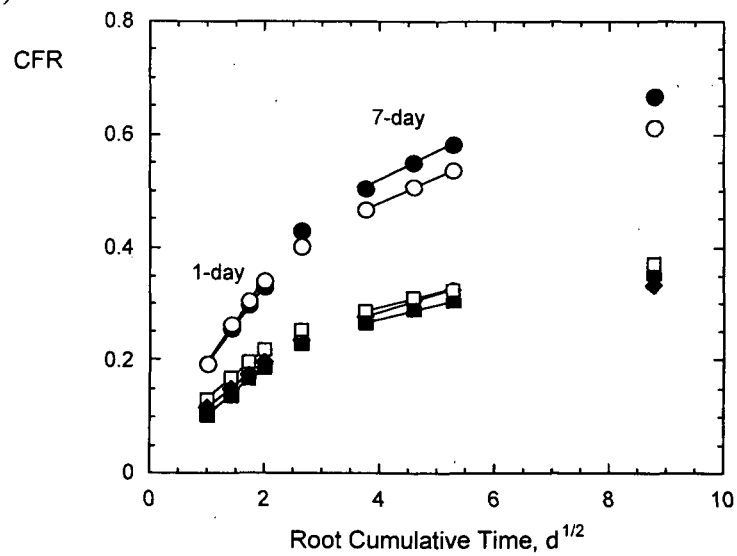

(b)

Figure 5.3. Results from Habayeb (1985): ANS 16.1-type tests with portland cement (a) cumulative ^{134}Cs release vs. cumulative time and (b) cumulative ^{134}Cs release vs. root time.

5.1.3 Crawford et al.

A series of static leach tests were conducted with ordinary portland cement doped with ^{134}Cs and cured for various times before testing (Crawford et al. 1984). In the first test, the surface of a 4.5 cm diameter × 7 cm high cylindrical specimen cured 28 days was sealed with bitumen except for one exposed end (about 16 cm^2). This was immersed in 1 L of distilled water for a total of 27 days, during which time seven 6-mL aliquots were removed and analyzed. The fraction of doped ^{134}Cs that was released into the solution is plotted against time in Figure 5.4a. The results show typical behavior for diffusive release and are linear with the square root of the reaction time, as shown in Figure 5.4b. The effective diffusion constant is 1.3×10^{-3} cm^2 d^{-1} (1.5×10^{-8} cm^2 s^{-1}).

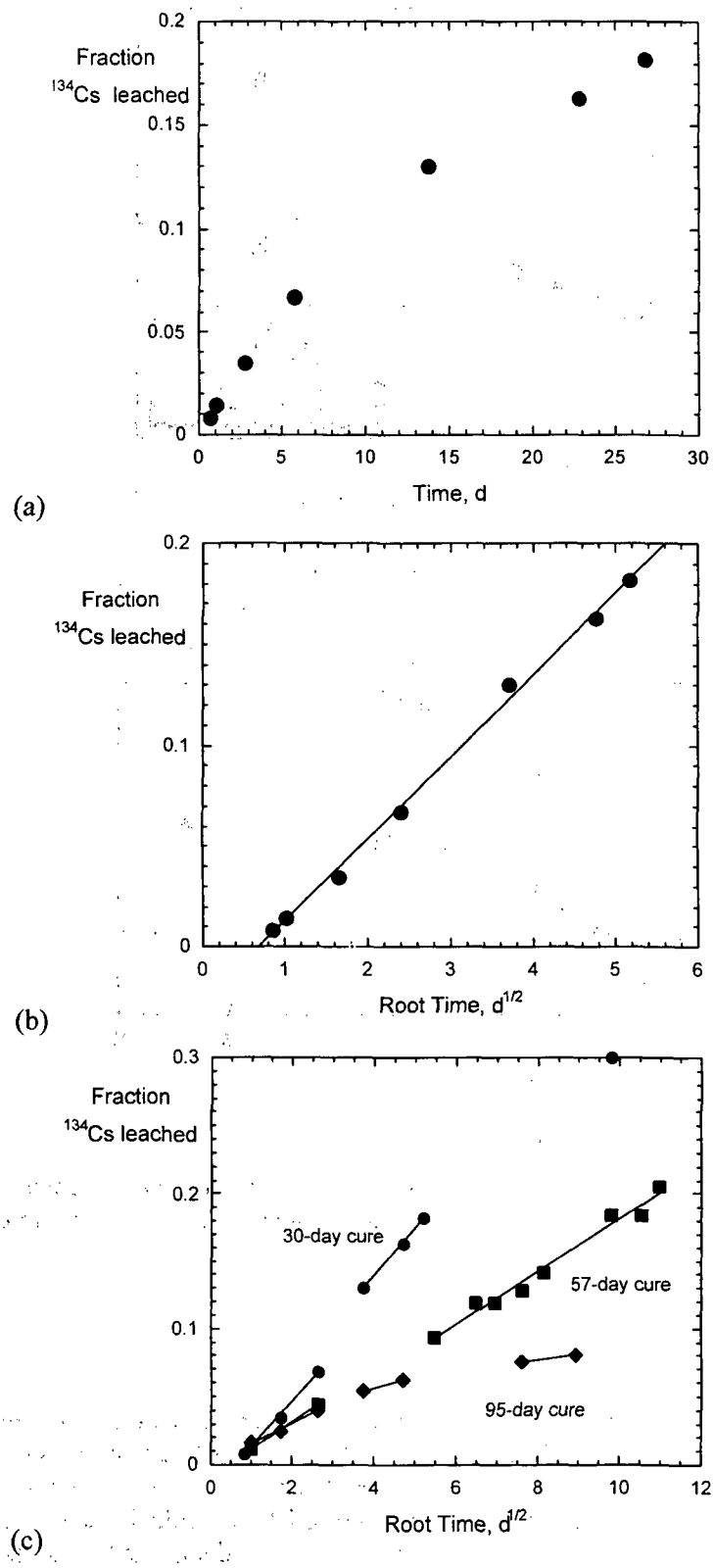

Figure 5.4. Results of tests from Crawford et al. (1984): (a) Cumulative release vs. time and (b) cumulative release vs. root time of ^{134}Cs from 28-day grout, and (c) cumulative releases from materials cured for three different durations vs. root time.

Another series of tests was conducted with cement specimens that had been cured for different times prior to testing. The cure time affects the pore structure and crystal content of the grout. These results are shown plotted against the square root of the reaction time in Figure 5.4c. The effect of curing time is thought to be through constriction of the pore structure due to the continued development (growth) of hydration products, which is expected to decrease the diffusion coefficient. Crawford et al. (1984) fit the samples taken between 1 and 7 days, 8 and 28 days and beyond 28 days separately to determine separate diffusion coefficients. Fits to results at different time intervals are shown in Figure 5.4c. The slopes from the plots and the effective diffusion coefficients reported by Crawford et al. (1984) are summarized in Table 5.2. (The coefficients reported for ranges with one data point or no data points are presumed to have been determined using the last data point from the earlier time range and the first data point from the later time range.) The authors attributed the observed behavior to two successive processes: "surface wash-off, which is not diffusion-controlled, followed by a static diffusion stage" (Crawford et al. 1984, p. 188). The authors interpreted the initial release (during the first 7 days) to represent the surface wash-off stage in which contaminants in the surface pores equilibrating with the solution, and that this stage was independent of the curing time. The second stage (beyond 7 days) was interpreted to represent the diffusion of contaminants from the bulk through the depleted surface layer.

Table 5.2. Results from tests by Crawford et al. (1984).

Time Range, d	30-day Cure		56-day Cure		95-day Cure	
	slope, $s^{-1/2}$	D_e, $cm^2\ s^{-1}$	slope, $s^{-1/2}$	D_e, $cm^2\ s^{-1}$	slope, $s^{-1/2}$	D_e, $cm^2\ s^{-1}$
1–7	0.0326	6.08×10^{-8}	0.0201	1.76×10^{-8}	0.0148	1.32×10^{-8}
8–28	0.0356	2.06×10^{-8}	—	2.04×10^{-9}	0.00874	3.98×10^{-10}
>28	—	1.15×10^{-9}	0.0197	5.86×10^{-10}	0.00361	4.18×10^{-11}

An alternative interpretation of the test results in Figure 5.4c is that the decreasing slopes are due simply to the effect of increasing the sampling intervals. The intervals during the first 7 days ranged from 0.7 to 6 days, the intervals between 8 and 28 cumulative days ranged from 5 to 8 days, and the intervals beyond 28 cumulative days ranged (randomly) from 6 to 69 days. The relative scatter in the results within a range of sampling intervals is consistent with the expected effects of the sampling interval (based on the effects seen in the results discussed above). That the fits to the short-term results of the 30-day and 57-day cured specimens have negative y-intercepts suggests that the specimen surfaces were depleted of Cs prior to testing. The results from the initial 7 days of testing with short sampling intervals indicate that longer curing times do lead to smaller diffusion coefficients. The shapes of the release curves at longer times are significantly affected by the different sampling intervals.

5.1.4 Neilson et al.

Large-scale ANS 16.1-like tests were conducted with specimens of pressurized water reactor (PWR) evaporator concentrate waste that had been immobilized in masonry cement and BWR evaporator concentrate waste that had been immobilized in portland Type III cement, both in 55-gallon drums (Neilson et al. 1982). Table 5.3 provides a summary of the waste form and testing data and Table 5.4 summarizes the test results that were determined from the plots in Neilson et al. (1982). The releases of ^{134}Cs and ^{137}Cs could not be distinguished. Although the sampling

Table 5.3. Waste form and testing data for Neilson et al. (1982).

Waste	Cement	Tank #	Waste Form #	Surface Area, cm^2	Leachant Volume, L	V_{wf}/S, cm
PWR	Masonry	1	4-3	14130	240	17.0
BWR	Portland III	4	1-3	16862	216	12.8

intervals differed significantly from those specified in the ANS 16.1 test procedure, this data set provides a valuable insight regarding the application of the laboratory-scale test method to large-scale. The V_{wf}/S ratios used in these tests are higher than the ratio of 10 cm that is called for in the ANS 16.1 method and the sampling intervals differed. Figures 5.5a and 5.5b show the results as the cumulative fraction releases of ^{137}Cs from cement with PWR waste vs. cumulative time and vs. root-time, respectively. Subsets of the data are fit according to the sampling interval. The linearity of the release data as a function of the square root of the cumulative time indicates simple diffusion-controlled release. The data for release from the masonry cement (Figure 5.5b) are linear with root-time, but the slope varies only slightly with the different sampling intervals. The negative *y*-intercept of the initial results suggest that either the outer surface was depleted of contaminants prior to testing or the outermost surface had to degrade prior to diffusion-controlled release, e.g., by opening pores. These test results are cited as the source for the data given in the examples of the ANS 16.1 procedure. (Data in the example in the ANS 16.1 procedure are reported to be adapted from the data given in this reference.)

Table 5.4. Data read from plots for release of ^{137}Cs.

PWR Evaporator Concentrate Waste in Masonry Cement[a]				BWR Evaporator Concentrate Waste in Portland Type III Cement[b]			
Time, d	root time	CFR	Interval, d	Time, d	root time	CFR	Interval, d
1.2	-2.629	0.0023	1.2	1.6	1.265	0.0029	1.6
2.4	-2.452	0.0035	1.2	2.4	1.549	0.0512	0.8
2.8	-2.371	0.0043	0.4	3.6	1.897	0.1000	1.2
4.4	-2.290	0.0051	1.6	6.8	2.608	0.1077	3.2
6.9	-2.081	0.0083	2.4	9.6	3.098	0.1118	2.8
9.7	-1.984	0.0104	2.8	14.8	3.847	0.1160	5.2
14.5	-1.903	0.0125	4.8	21.6	4.648	0.1250	6.8
21.8	-1.807	0.0156	7.3	28.4	5.329	0.1273	6.8
28.2	-1.726	0.0188	6.5	35.6	5.967	0.1297	7.2
35.9	-1.661	0.0218	7.7	42.4	6.512	0.1297	6.8
42.3	-1.645	0.0226	6.5	49.6	7.043	0.1346	7.2
49.2	-1.629	0.0235	6.8	56.4	7.510	0.1397	6.8
56.1	-1.581	0.0263	6.9	70.4	8.391	0.1450	14
70.2	-1.548	0.0283	14.1	84.4	9.187	0.1505	14
84.7	-1.500	0.0316	14.5	98.4	9.920	0.1621	14
98.4	-1.484	0.0328	13.7	112.4	10.602	0.1621	14
112.5	-1.452	0.0354	14.1	126.8	11.261	0.1682	14.4
126.2	-1.436	0.0367	13.7				

[a]Data from Neilson et al. (1982) Figure 4.1.
[b]Data from Neilson et al. (1982) Figure 4.4.

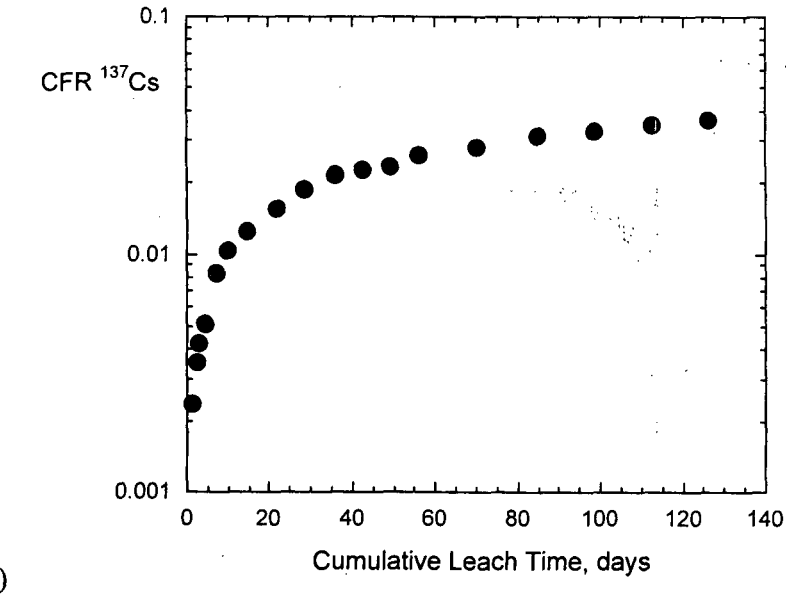

(a)

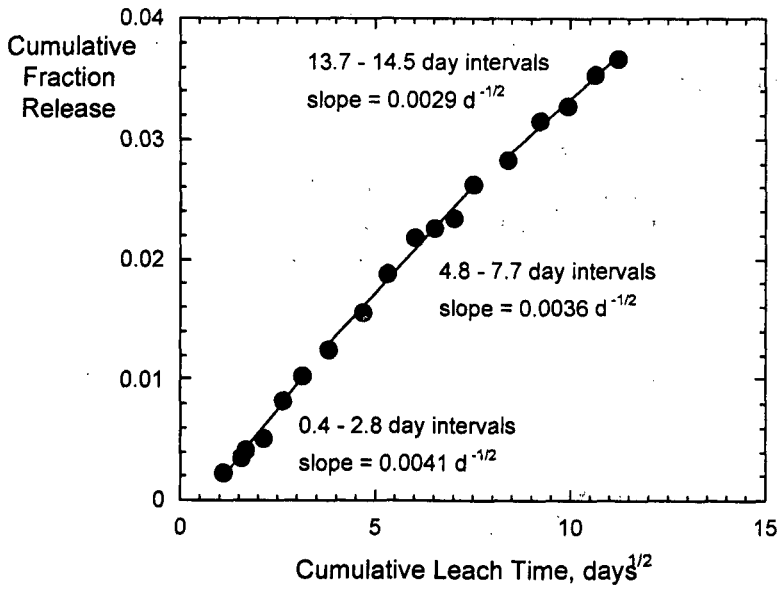

(b)

Figure 5.5. Results from Neilson et al. (1982): Full-scale ANS16.1 tests with PWR evaporator concentrate waste in masonry cement (a) cumulative fraction release ^{137}Cs vs. cumulative time and (b) cumulative fraction release ^{137}Cs vs. root-time.

The release from the portland cement made with BWR waste (Figs. 5.6a and 5.6b) shows somewhat different behavior than release from the masonry cement. Little release is seen in the first sampling, relatively high releases occur in the next two samplings, and then little release is seen in each subsequent sampling. The initial 30-second rinse called for in the ANS 16.1 procedure to remove loosely held activity at the surface was omitted for these tests. However, that is probably not the cause of the rapid release seen in Figs. 5.6a and 5.6b because the majority of the release occurs in the second and third replacements rather than the first. A linear fit of the first three data points against the square root of the cumulative reaction time is 0.15 d$^{-1/2}$. Regressions of the results of samplings beyond the first three in the plots vs. time and vs. root time give similar

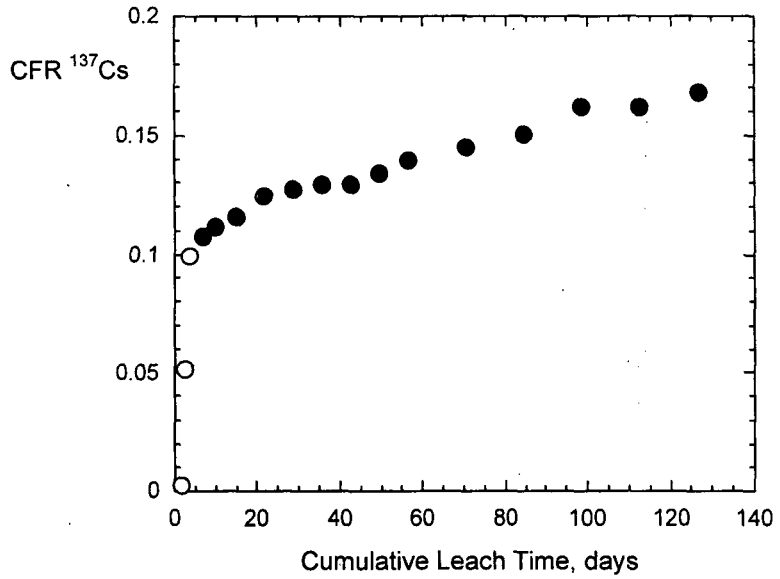

(a)

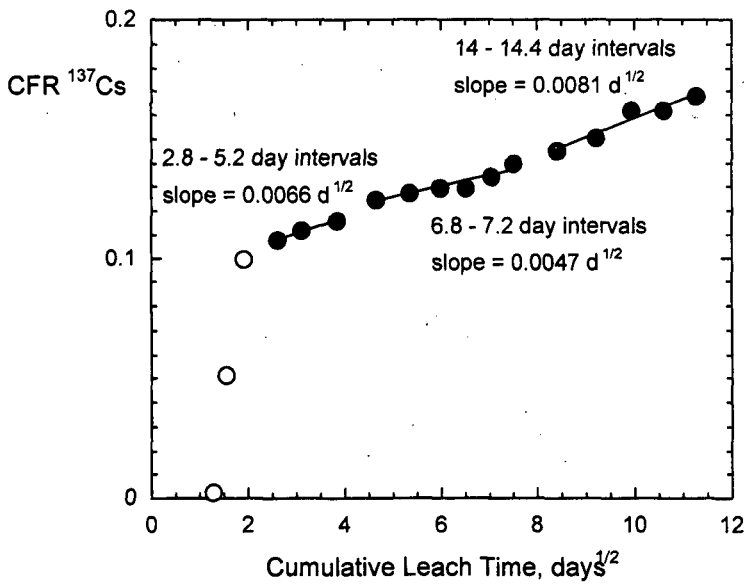

(b)

Figure 5.6. Results from Neilson et al. (1982): Full-scale ANS16.1 tests with BWR evaporator concentrate waste in portland Type III cement (a) cumulative fraction release ^{137}Cs vs. cumulative time and (b) cumulative fraction release ^{137}Cs vs. root-time.

coefficients (R^2 = 0.974 for the fit with time and R^2 = 0.983 for the fit with root-time). Note that separate fits to data collected at different intervals give similar slopes in the root-time plot, whereas other diffusion-controlled releases considered in the previous examples show a pronounced dependence on the sampling interval. The difference may be that long sampling intervals did not occur until after relative long cumulative duration: 7-day intervals after about 21 days and 14-day intervals after about 70 days. At this stage of the reaction, the release is nearly linear with time.

The large scale of these tests may affect the interpretation of the results compared to bench-scale experiments because the near-surface region that reacts is a much smaller fraction of the specimen volume than for typical laboratory-scale specimens. The test results are normalized to the volume-to-surface area ratio of the test specimen to extract the diffusion coefficient. Using test specimens having high V_{wf}/S ratios will result in CFR that are very insensitive to the effective diffusion coefficient and (root) time. This may be another reason the slopes in Figure 5.5b are much less sensitive to differences in the sampling intervals than the other tests that have been considered.

5.1.5 Mattigod et al.

The ANS 16.1 method and a partial replacement test method were used by Mattigod et al. (2001) to measure the leaching of I and Tc from a grout due to reaction with a simulated Hanford groundwater. The standardized ANS 16.1 procedure was followed at the recommended exchange intervals through 92 days. The partial replacement test was conducted by removing 50-mL aliquots of the leachate for analysis and replacing that with 50 mL of fresh leachant. (The total volume of solution was maintained at 350 mL.) Although Mattigod et al. (2001) referred to this procedure as a static test, it is better described as a semi-static partial replacement test because the solution concentrations of the contaminants are decreased at the beginning of each interval due to the addition of fresh leachant, albeit not to zero as in the ANS 16.1 tests. The concrete mixture was made with cement, fly ash, aggregate, and water spiked with ^{125}I, stable I, ^{99}Tc, and U. The approximate activities in the concrete were 0.35 mCi kg^{-1}, 460 mg/kg, 0.03 mCi kg^{-1}, and 10.3 mCi kg^{-1}, respectively. The chemical forms of the additives were not reported; it is presumed that Tc was added as the pertechnetate ion, I was added as iodate, and U was added as the uranyl ion. A portion of the concrete mixture was poured into 5 molds to produce 5 replicate test specimens (specimen numbers 1–5). Type I steel fibers were mixed with the remaining mixture, which was then poured into 5 other molds to produce replicate specimens with steel for testing (specimen numbers 6–10). Type I steel is a low-carbon steel commonly used to reinforce cement mortar and concrete.

Figure 5.7 shows the results for two ANS 16.1 tests (tests with specimen numbers 1 and 2) and two static tests with specimens of concrete without added steel (tests with specimen numbers 3 and 5) as CFL vs. cumulative reaction time. The releases in the static (partial replacement) test with specimen 3 were more than 3 times the releases in the other tests and have been scaled (divided by 3) to better compare the release behavior with other tests; the authors speculated that specimen 3 had more extensive cracking. (Note that the label "static (3)/3" indicates a static test with specimen no. 3 for which the results have been divided by 3 in the plot.) The releases of ^{99}Tc and ^{125}I in the static (partial replacement) test with specimen 5 are similar to the releases in the ANS 16.1 tests, except for the increased release of ^{125}I seen in both ANS 16.1 tests sampled at 92 days. Anomalously high releases of ^{125}I occurred in both ANS 16.1 tests after 92 days. Although it is certainly possible that encapsulated pockets of material rich in I were accessed in both samples and dissolved in the final test interval, it is more likely that the increase reflects an analytical or procedural error than the material behaviors of the four specimens, especially since the ^{99}Tc releases do not show corresponding increases. The results of tests with concrete and added steel are shown in Figure 5.8. The ANS 16.1 and static (partial replacement) test methods yield similar results, except note the increases in the ^{125}I releases in the final samplings of the ANS 16.1 tests, as was seen in Figure 5.7b. The similar test responses of cements with and without steel indicate that the presence of Type I steel did not affect the release behaviors of either ^{99}Tc or ^{125}I beyond testing uncertainty.

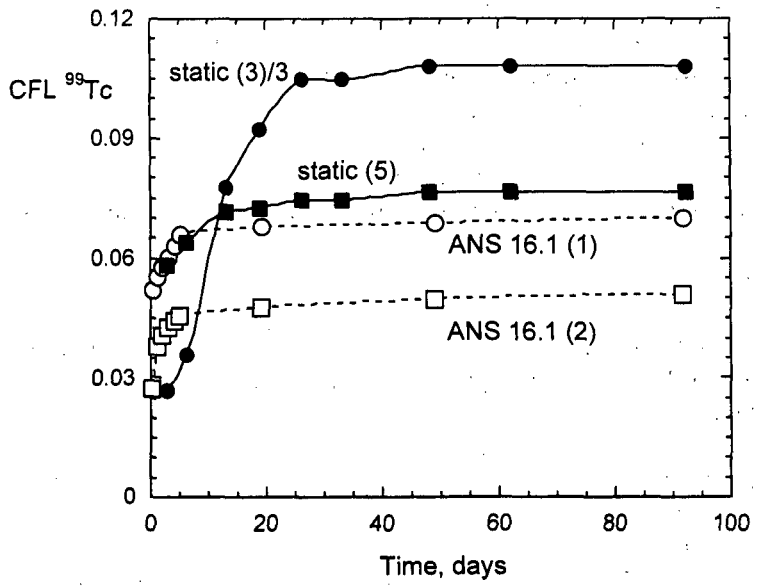

(a)

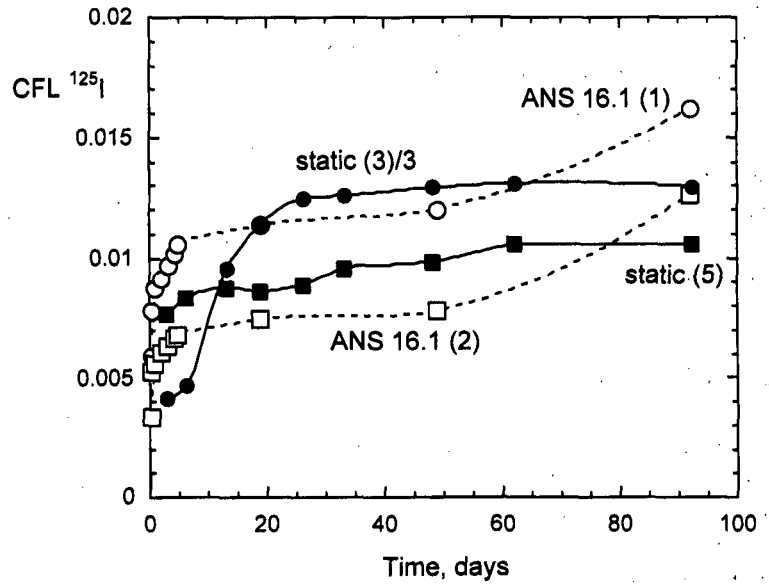

(b)

Figure 5.7. Results of tests by Mattigod et al. (2001): Cumulative fractions released from cement without added steel vs. time for (a) ^{99}Tc and (b) ^{125}I.

The similarity of the ANS 16.1 and static (partial replacement) test results is of particular interest. The similar test responses (apart from the higher releases from specimen number 3 after about 10 days in Figure 5.7) indicate that the accumulation of leached and dissolved components in the static test leachates does not affect the release of ^{99}Tc or ^{125}I during the first 20 days. The subsequent releases of each radionuclide are essentially nil at longer durations (until additional ^{125}I appears to be released between 50 and 92 days). Figure 5.9 shows the results of tests with cement without steel plotted against the square root of the cumulative reaction time. The ^{99}Tc and ^{125}I releases in the ~1-day intervals of the third through sixth samplings in the ANS 16.1 test are linear with the square root of the reaction time. The longer-term results also appear to be linear, but with

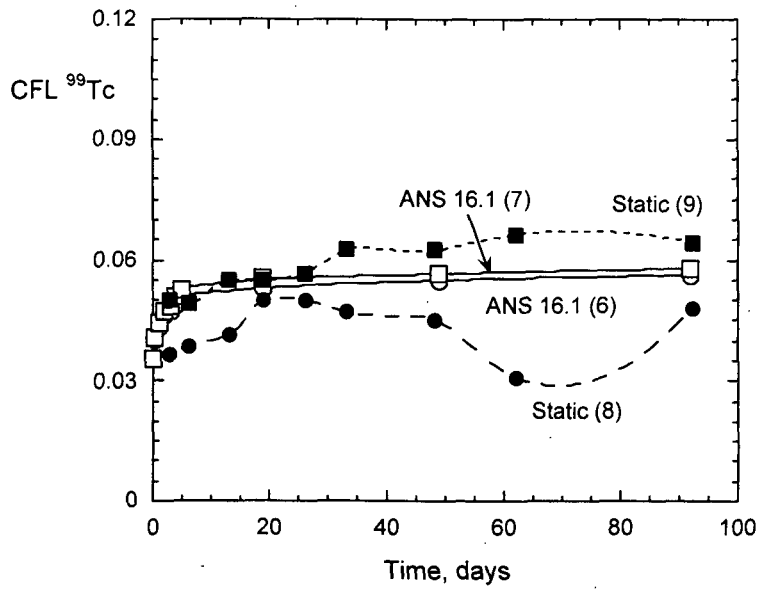

(a)

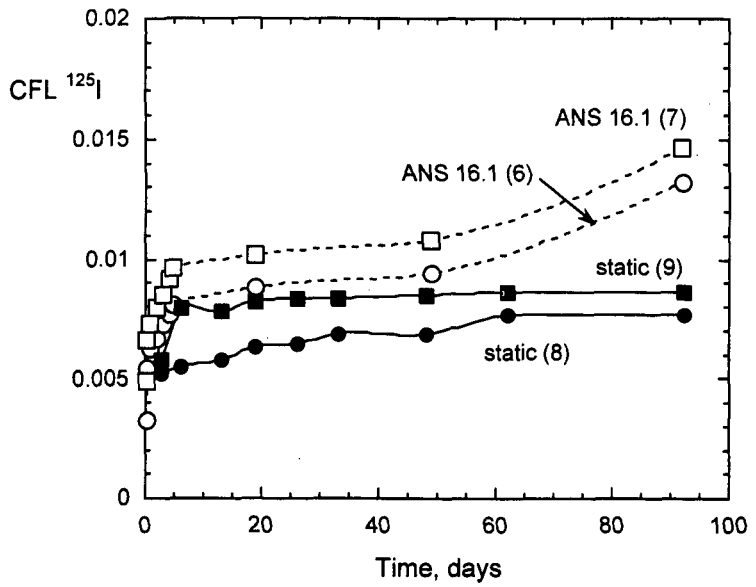

(b)

Figure 5.8. Results of tests by Mattigod et al. (2001): Cumulative fractions released from cement with added steel vs. time for (a) ^{99}Tc and (b) ^{125}I.

slopes more than 10-times lower than for the early results. The apparent linearity of the long-term ANS 16.1 results despite the different sampling intervals (approximately 14, 30, and 43 days) is a consequence of the negligible releases.

Diffusion coefficients were calculated by Mattigod et al. (2001) from results of each test method, with data from static tests yielding lower values than data from ANS 16.1 tests. The authors did note that the diffusion coefficient values calculated with the incremental fractional releases were about 50% less than the values calculated with the cumulative fractional releases. This may indicate accumulating error in the sequential samplings, but more likely is a random outcome of extracting a diffusion coefficient from a data set (for the static tests) that does not show diffusive behavior.

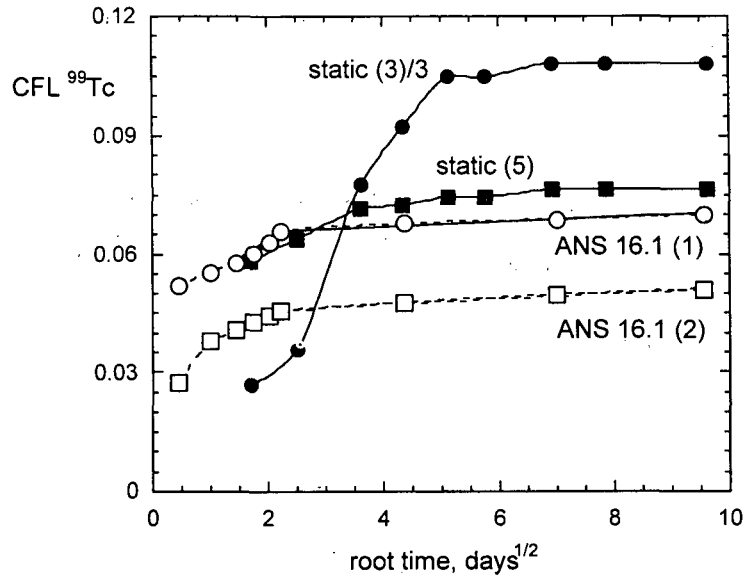

(a)

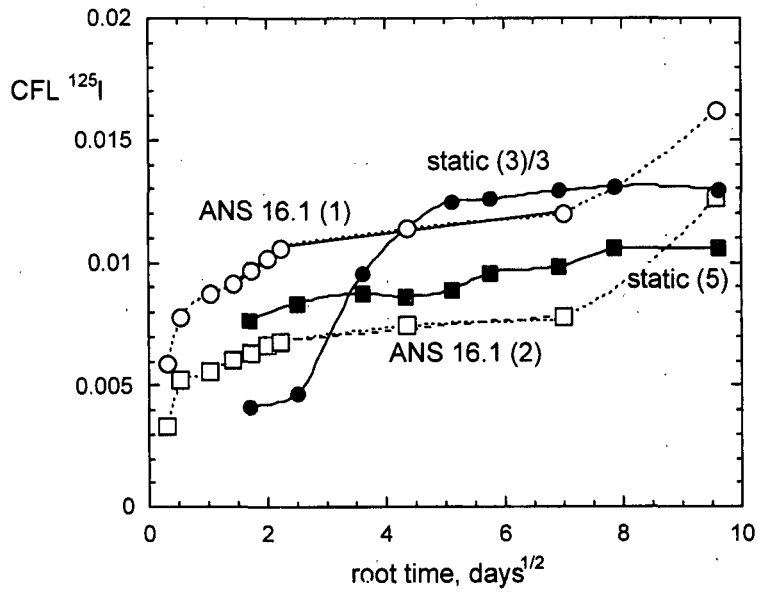

(b)

Figure 5.9. Results of tests by Mattigod et al. (2001): Cumulative fraction released from cement without added steel: vs. root time for (a) ^{99}Tc and (b) ^{125}I.

Perhaps the key insight to be derived from these test results is the good agreement between some ANS 16.1 and static (partial replacement) test results and the poor reproducibility of replicate tests conducted with either of the test methods. The poor reproducibility is attributed to differences in the pore structures of the different test specimens and the distributions of Tc and I. The agreement in test methods suggests that the accumulation of Tc and I in the solution does not affect their continued release from these materials.

5.1.6 Rorif et al.

The releases of Cs and Ca from an ion exchange resin in ordinary portland cement with blast furnace slag were compared in solution exchange tests following the exchange intervals in the ANS 16.1 and ISO 6961 standardized methods, and those in a method called for by the NIRAS/ONDRAF (OND 1991), which is the agency regulating high-level waste in Belgium. The sampling intervals for the three test methods are summarized in Table 5.5, and the cumulative fractional releases of Cs in triplicate ANS 16.1 and OND tests and duplicate ISO tests are reproduced in Figure 5.10a (Rorif et al. 2005). The trends in the data are the same for the three methods. The results of the ANS 16.1 tests fall within the range of the triplicate OND tests, whereas the release is slightly higher in the ISO tests. Figure 5.10b shows the results of the ANS 16.1 and ISO tests plotted against the square root of the cumulative test duration with each set of replicate data points labeled with the duration of the sampling interval. The results of the short-term tests are linear for both methods; the three ANS 16.1 tests give slopes of 0.30, 0.31, and 0.29 $d^{-1/2}$ and the two ISO tests give slopes of 0.26 and 0.27 $d^{-1/2}$. The diagonal line in Figure 5.10b is drawn with the average of these five slopes. As can be seen, the test responses decrease significantly at longer cumulative times as the sampling interval increases. The decrease is subtle for the ISO tests with sampling intervals of 5 and 6 days, but quite obvious for the sixth samplings of the three ANS 16.1 tests after an interval of 14 days. The impact of the sampling interval is

Table 5.5. Sampling intervals used in ANS 16.1, ISO 6961, and OND test methods.

ANS 16.1		ISO 6961		OND	
Cumulative time, days	Time Interval, days	Cumulative time, days	Time Interval, days	Cumulative time, days	Time Interval, days
0.083	0.083				
1	0.92	1	1		
2	1				
3	1	3	2		
4	1				
7	3	7	4		
		10	3		
		15	5		
				16	16
21	14	21	6		
		30	9	30	14
		35	5		
		42	7		
45	24				
				59	29
		73	31		
				88	29
90	45				
		100	27		
				179	91
				269	90
				366	97
				455	89

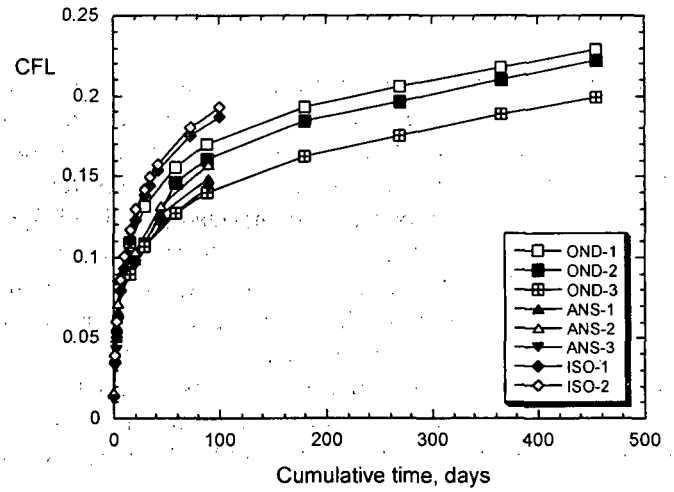

(a)

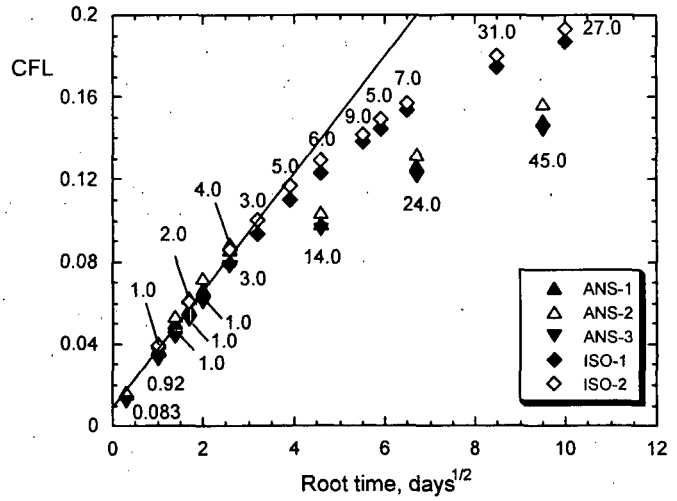

(b)

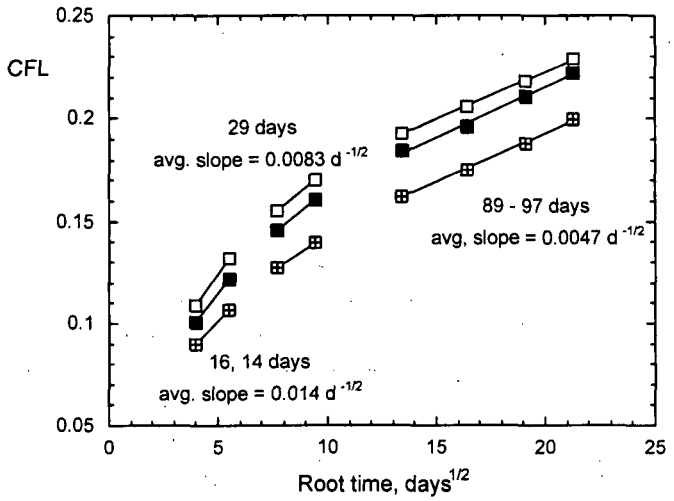

(c)

Figure 5.10.Results from Rorif et al. (2005): Solution exchange tests conducted following the ANS 16.1, ISO 6961, and OND sampling schedules: (a) CFL vs. cumulative time, (b) CFL vs. root time for ANS 16.1 and ISO 6961 tests with identified sampling intervals, and (c) linear fits to OND test results for different sampling intervals.

shown to persist through much longer cumulative durations of the OND tests. Figure 5.10c shows the OND test results fitted separately for different sampling intervals. The root-time dependence persists through 455 days for subsets of data with uniform sampling intervals. The authors concluded that the "diffusional stage [was] reached faster in the case of ANSI and ISO compared to OND due to the more frequent renewal of the leachant (faster wash-off) [and the] results of ANSI and ISO are similar and higher (conservative) than those of OND. This acts in favor of the short-term tests" (Van Iseghem 2005). That is, the authors viewed the more rapid attainment of the diffusion-controlled mechanism by the ANSI and ISO test methods as being advantageous.

Based on evaluation of these and other solution exchange test results, the *time* at which the "diffusional stage" is reached is not a function of the sampling intervals that are used in the test. The releases are controlled by diffusion throughout the test. Rather, the slopes and the values of the effective diffusion coefficients that are extracted from the data depend on the *sampling interval*. It follows that the diffusion coefficient that is extracted from the test data differs from the effective diffusion coefficient by a factor related to the sampling interval (which necessarily and artificially models the release as being linear in time). This is not an effect of solution feedback, as in the case of affinity-controlled release, but is simply an artifact of a non-linear release being averaged over the linear testing interval. The release is not linear over the interval because the diffusion barrier at the specimen surface that controls the release changes over the test interval and is evolving as components are leached. The diffusion length generally increases with time, but the density and the tortuosity can either increase or decrease as degradation progresses. Note that the effective diffusion coefficient is proportional to the square of the slope, so even small variances in the sampling interval can have a significant effect on the extracted diffusion coefficient.

Another observation from these test results is that the CFL measured in the first sampling of the OND series after 16 days was essentially the same as the cumulative fractions measured in the ISO series after 15 days and five solution exchanges and the ANS 16.1 series after 21 days and seven solution exchanges. This indicates that the exchanges (and exchange frequency) have little effect on the actual release of Cs, as is expected due to the very high solubility limit of Cs, and that *they only affect how accurately the release is being measured.* This is consistent with the hypothesis that the rate is being controlled by diffusion through the near-surface region of the test specimen and is not significantly affected by the Cs concentration.

5.1.7 Côté et al.

Côté et al. (1987) measured the amounts of As, Cd, Cr, and Pb leached from four waste forms that had been made with 0.04 M solutions of $NaAsO_2$, $Cd(NO_3)_2$, $CrCl_3$, and $Pb(NO_3)_2$ mixed with type N soluble silicates and Type 1 portland cement, with fly ash and portland cement, with fly ash and hydrated lime, and with Na-bentonite clay and portland cement. Experiments were conducted following the general ANS 16.1 procedure for 665 days. The results are plotted in Figure 5.11 to compare the releases of each element from the different waste forms and in Figure 5.12 to compare the relative releases of Cd, Cr, and Pb from each waste form (note that the y-axis is a logarithmic scale). The results for As provided in Côté et al. (1987) were not evaluated for this report because the plotted values for samples taken prior to about 300 days for three of the waste forms could not be discerned. Each set of results was regressed with a power law fit as $y = bx^m$. The fits are shown by the curves in Figure 5.11 and Figure 5.12 and the coefficients are given in Table 5.6. Fits with values of m near ½ are assumed to indicate release that is predominantly diffusion-controlled. Fits with higher or lower values of m indicate other processes are important. The releases of Cd and Cr from the fly ash-cement and clay-cement are well-described by bulk diffusion, as are the releases of Pb from the soluble silicates-cement and clay-cement.

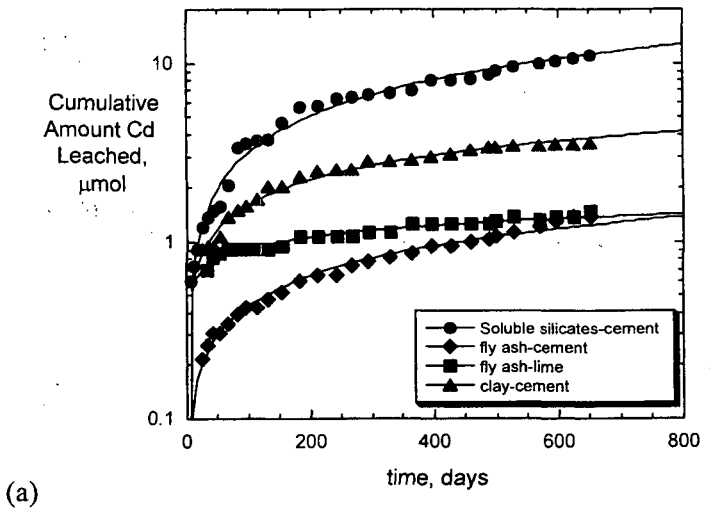

(a)

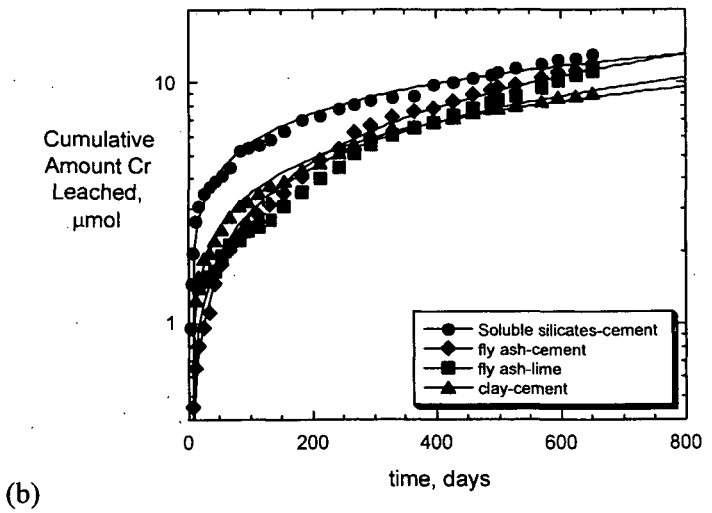

(b)

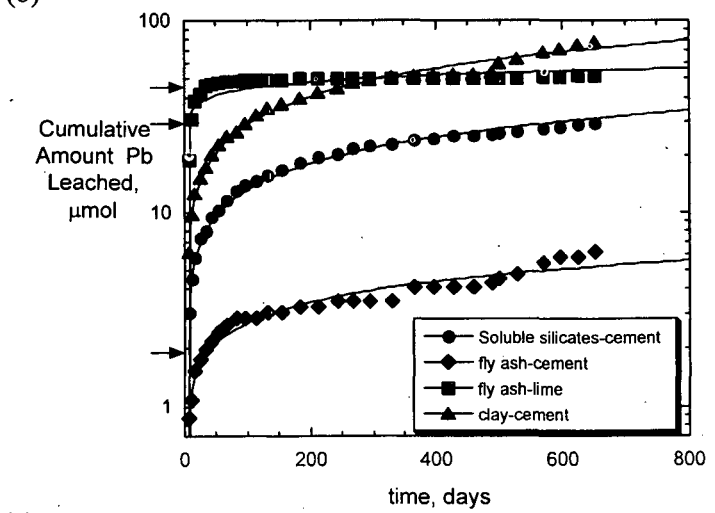

(c)

Figure 5.11. Results from Côté et al. (1987): Cumulative amounts of (a) Cd, (b) Cr, and (c) Pb leached from soluble silicate-cement, Fly ash-cement, and fly ash-lime waste forms.

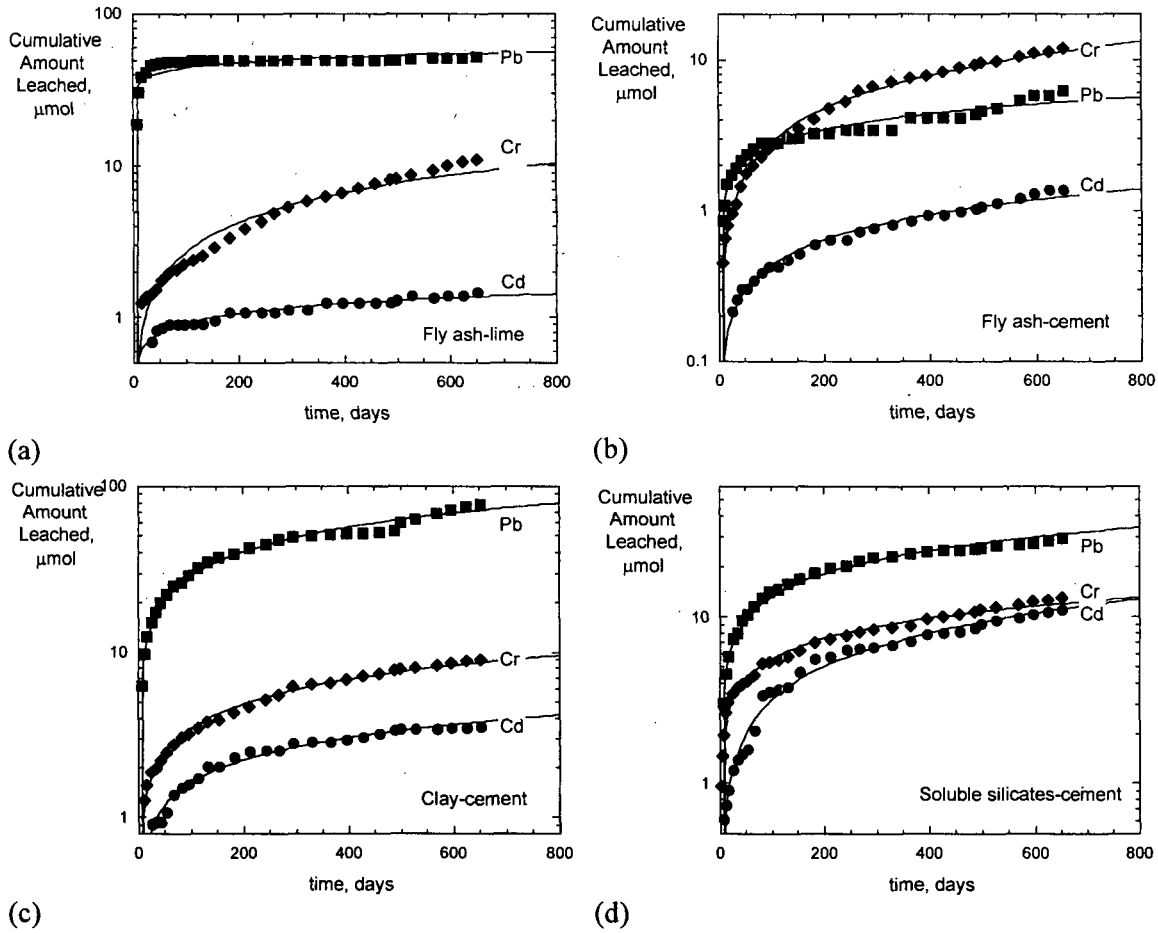

Figure 5.12. Results from Côté et al. (1987): Cumulative amounts of Cd, Cr, and Pb leached from (a) Fly ash-lime, (b) fly-ash-cement, (c) clay-cement, and (d) soluble silicates-cement waste forms.

Table 5.6. Coefficients regressed with power-law fits.

Waste Form	Cd		Cr		Pb	
	m	*b*	*m*	*b*	*m*	*b*
Soluble silicates – cement	0.67	0.14	0.41	0.86	0.46	1.6
Fly ash – cement	0.55	0.035	0.74	0.096	0.36	0.52
Fly ash – lime	0.21	0.35	0.65	0.14	0.12	26
Clay – cement	0.45	0.20	0.49	0.37	0.49	3.1

Côté et al. (1987) regressed the cumulative amounts that were leached using an empirical expression that included terms for dissolution with solution feedback effects, diffusion-controlled release, and diffusion coupled with a mobilizing reaction. The cumulative amount of each element leached was expressed as a function of time as

$$CAL(t) = k_1\left(1-e^{-k_2 t}\right) + k_3 t^{1/2} + k_4 t \tag{5.2}$$

where $CAL(t)$ is the cumulative amount leached. Model coefficients k_1 and k_2 represent the intrinsic release rate and a solution feedback term, k_3 represents bulk diffusion from a semi-infinite source, and k_4 represents constant dissolution. (Note: these terms correspond to modes 1 and 6, mode 3, and mode 4, which were described in Section 2.) The coefficient values reported by Côté et al. (1987) are summarized in Table 5.7. Large k_1 values with $k_2 = \infty$ indicate an initial time-independent, instantaneous release due to surface wash-off. The value of the term in parentheses is greater than 0.97 after 20 days when $k_2 = 0.178$, after 39 days when $k_2 = 0.092$, and after 293 days when $k_2 = 0.012$, so the first term impacts the early release of Pb from both fly ash-lime and fly ash-cement waste forms, and impacts the release of Pb from the clay-cement waste form through moderate times. The initial release of Pb from the fly ash-lime waste form is significant and dominates the release behavior seen in Figure 5.11 and Figure 5.12. The value of k_1 for the release of Pb from the clay-cement waste form is also large, but the effect of k_1 on the overall release behavior is not as obvious. Arrows on the y-axis in Figure 5.11c locate 45.55, 29.39, and 1.99 μmol, which represent the amounts of Pb released from the surfaces of the fly ash-lime, clay-cement, and fly ash-cement materials, respectively, at $t = 0$ in the model. This release mode is responsible for the release of essentially all of the Pb from the fly ash-lime and about 30% of the Pb from the fly-ash-cement and clay-cement waste forms over the test duration, but only about 7% of the Pb released from the soluble silicates-cement.

Table 5.7. Coefficients from the regression analyses by Côté et al. (1987).

Element/Waste Form	Surface Phenomena $k_1(1-e^{-k_2 t})$		Diffusion $k_3 t^{1/2}$	Diffusion with reaction $k_4 t$
	k_1	k_2	k_3	k_4
Cadmium				
Fly ash – cement	0.035	∞	0.054	—
Fly ash – lime	0.380	∞	0.044	—
Clay - cement	0.177	∞	0.144	—
Soluble silicates – cement	-0.843	∞	0.477	—
Chromium				
Fly ash – cement	0.037	∞	0.168	0.017*
Fly ash – lime	0.703	∞	—	0.015
Clay - cement	-0.041	∞	0.384	—
Soluble silicates – cement	0.759	∞	0.461	—
Lead				
Fly ash – cement	1.992	0.092	0.149	—
Fly ash – lime	45.55	0.178	0.235	—
Clay - cement	29.39	0.012	1.09	—
Soluble silicates – cement	1.666	∞	1.122	—

*The value of 0.177 given in Côté et al. (1987) should be 0.017.

Diffusion-controlled release is a significant contributor to the releases from the soluble silicates-cement and clay-cement waste forms, as indicated by the relatively large values of k_3. Negative values of k_1 values indicate a time delay in leaching, which is probably an artifact of the regressions.

The linear term quantified by k_4 is not significant except for the release of Cr from the fly ash-cement and fly ash-lime waste forms. Those results are shown in Figure 5.13 plotted on a linear

scale. A slight change in slope occurs after about 350 days for both data sets. The regressed slope for the fly ash-lime waste form in Figure 5.13 for long durations agrees with the value of k_4 in Table 5.7, but the regressed slope for the fly ash-cement waste form (0.015 for long durations) is about 10 times lower than the value given in Côté et al. (1987). The Cr releases from the fly ash-cement and fly ash-lime in Figure 5.11b are almost the same beyond about 200 days, so the value reported by Côté et al. (1987) for the release of Cr from the fly-ash-cement waste form is probably in error. Linear regressions of the full data sets give slopes of 0.0175 and 0.0152 for Cr release from the fly ash-cement and fly ash-lime waste forms, respectively.

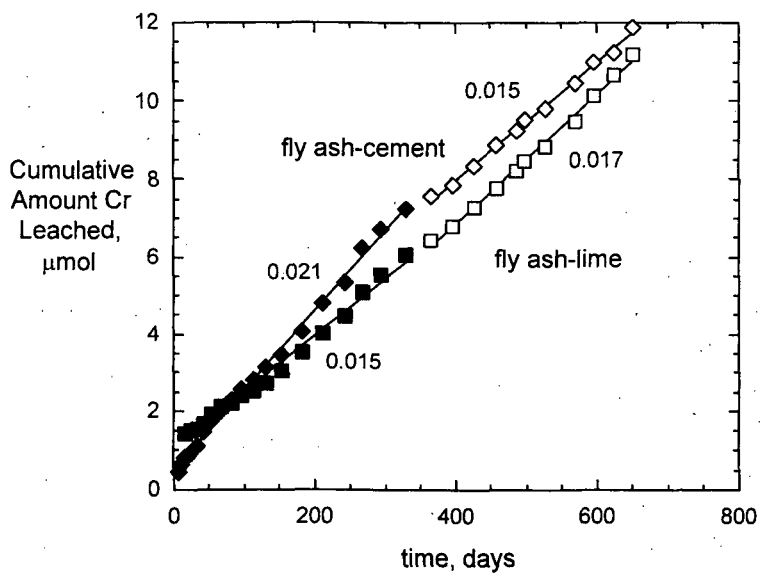

Figure 5.13. Results from Côté et al. (1987): Releases of Cr from fly ash-cement and fly ash-lime waste forms.

Although the leaching of As is not evaluated in this report, the discussion in Côté et al. (1987) regarding the release of As raises an important point: the impact of solution replacement on gas constituents within the test vessel. In the case of As, reactions involving H_2CO_3 were hypothesized to mobilize As from the precipitated basic calcium arsenite to arsenious acid:

$$Ca(AsO_2)_2 \cdot Ca(OH)_2 + H_2CO_3 \rightarrow Ca(AsO_2)_2 + CaCO_3 + 2\ H_2O \tag{5.3}$$

$$Ca(AsO_2)_2 + H_2CO_3 \rightarrow 2\ HAsO_2 + CaCO_3 \tag{5.4}$$

The CO_2 content of the test vessel is refreshed every time the solution is replaced, so the exchange frequency could affect or even control the As release rate. The refreshment of air also supplies O_2 for oxidation reactions. Small amounts of both CO_2 and O_2 may enter test vessels that are not continuously air tight.

The approach used by Côté et al. (1987) of regressing the results of ANS 16.1 solution replacement tests to estimate the contributions of potential release modes and model parameter values, while seemingly efficient, is not recommended. First, the non-constant replacement frequency does not provide a reliable measure of the diffusive release, as demonstrated in the preceding sections. Second, the accumulated uncertainties inherent with the cumulative release values do not provide best values for model parameters. Third, multivariable regression may not

provide reliable parameter values for the individual processes. As stated in the ANS 16.1 procedure, the kinetics of many processes are fairly well described by a diffusion equation at the early stages of reactions. The difficulties of distinguishing between diffusion-controlled and affinity-controlled reactions are discussed in greater detail in Section 7.4. Instead, several test methods should be used to distinguish the effects of surface phenomena, diffusion, and diffusion with reaction on contaminant release and the method or methods that are appropriate for the rate-controlling mechanism should be used to parameterize the rate law.

5.2 Tests with Contaminated Slags

In general, a slag is a byproduct of smelting an ore to purify the metal. Slags usually contain glassy phases (from silica added to adjust the melt chemistry and sequester contaminants during the smelting process) mixed with various metals, metal oxides, metal carbides, and metal sulfides, depending on the ore and additives. Most of the slags generated during normal steel-making operations pose no health or ecological risks and are commonly recycled for use in concrete and bituminous mixtures, soil conditioning, and fill. About 13 million tons of blast furnace slag was produced in the US in 1997 during the production of about 130 million tons of steel. The conditions under which the constituent phases of the slag are formed (e.g., the redox conditions) will be controlled by the chemistry of the melt and, to a lesser degree, the atmosphere within the furnace. Because slags usually form on the surfaces of molten metals, the chemistry of the molten slag and how quickly it cools will likely affect physical and textural attributes of the slag such as porosity. The presence of a glassy phase provides a sink for elements not incorporated into crystalline phases. The glassy phase usually microencapsulates the crystalline phases, although typically about 30 volume% glass is required to completely encapsulate other phases. Slags containing non-negligible concentrations of radionuclides such as Th, U, and their daughters, present either in the ore, recycled materials, or as additives, are referred to herein as contaminated slags. The results of laboratory tests conducted with various contaminated slags are reviewed in the following section. Although the focus of the testing programs was to characterize the behavior of the contaminants, the focus here is to evaluate the degradation behavior of the slags and the applicability of the test methods and models to these materials.

5.2.1 Pickett et al.

Leaching tests were conducted with slag specimens from the Molycorp-Washington site (Molycorp, Inc., Washington, PA), the Cabot-Reading site (Cabot Industries, Reading, PA), and the Whitaker-Greenville site (Whittaker Metals Corporation, Greenville, PA) following the ANS 16.1, EPA Method 1311, and EPA Method 1312 protocols (Pickett et al., 1998). These slags resulted from alloy production at the different sites using ores containing licensable levels of Th and U. These slags have been described as being rocklike, cemented sandstone-like, or glassy. At least 28 phases were identified in specimens that were analyzed with optical and electron microscopy, X-ray diffraction, X-ray fluorescence, radiography, and chemical analyses (Veblen et al. 2004), including perovskite ($CaTiO_3$), variously substituted zirconolites ($CaZrTi_2O_7$), pyrochlore ($Ca_2Ti_2O_6$), various spinels ($FeAl_2O_4$), and silica glass. Many of these phases are radioactive due to the presence of U, Th, and their daughters. The gross compositions of samples of the three slags are given in Table 5.8.

Results of ANS 16.1 tests with slag from the Whittaker-Greenville site are shown in Figure 5.14. The slags from this site were described as having "several different appearances, including both black and green glassy slag, and a porous, rock-like slag" (Craig and Reisenweaver cited in

Table 5.8. Chemical compositions of Molycorp-Washington, Whittaker-Greenville, and Cabot-Reading site slags.

Oxide, mass%	Molycorp-Washington average	Whittiker-Greenville WH-6a	Cabot-Reading C-B5-5	Element Conc.	Molycorp-Washington average	Whittiker-Greenville WH-6a	Cabot-Reading C-B5-5
SiO_2	10.1	9.18	19.10	Mo, ppm	334	137	<5
TiO_2	2.36	0.539	9.41	U, ppm	157	<20	580
Al_2O_3	39.0	17.2	16.21	Sr, ppm	503	38.7	262
FeO	0.492	12.7	0.159	Cu, ppm	201	265	<75
BaO	6.85	0.0055	0.0610	Li, ppm	1.29	25.6	121
MnO	0.0558	0.213	0.606	Ni, ppm	3.62	37100	10.3
MgO	0.063	29.4	1.45	P, ppm	<5	124	40.2
CaO	9.09	3.37	29.38	S, ppm	329	<100	660
Na_2O	1.65	0.0798	0.0774	V, ppm	<5	329	21.7
K_2O	0.0106	0.0769	0.286	Y, ppm	92.8	<25	2230
Cr_2O_3	<0.004	10.7	0.0304	Zn, ppm	12.1	135	7.33
ZrO_2	0.165	0.0342	4.31	Ra, pCi g^{-1}	1017	235	1040
La_2O_3	0.359	0.0033	0.613	Th, pCi g^{-1}	1467	99.1	314
ThO_2	1.51	0.102	0.322	U, pCi g^{-1}	52	<7	194

Pickett et al. (1998)). The material used in the tests had been weathered to the extent that the glass was completely altered and replaced by alteration phases. The ANS 16.1 tests were conducted through 19 days (cumulative) with a specimen having a surface area of 45 cm^2 and a volume of 16.7 cm^3. Releases of Ba, Ca, Mg, Mo, and Si are linear in time for the first 5 days but the release rates are much lower over the following 14-day interval. This suggests that the releases are slowed by solution feedback effects and are affinity controlled. The pH values were reported for all leachates in this test series. The pH values after the 2-hour and 5-hour intervals increased to 8.03 and 9.4, and the pH values for longer intervals were greater than 10. The root-time plot in Figure 5.14b shows that the results for 1-day test intervals are linear with root-time, but the slopes for each element are greater than those for the preceding samplings at shorter intervals. The 19-day results, after a 15-day interval, show lower release rates.

The release of components from Whittaker-Greenville site slag appears to be affinity controlled. An alternative explanation for the decreased release at long times is the formation of a surface layer that restricts element releases. This is unlikely in an ANS 16.1 test because the solution is replaced periodically to mitigate the concentration of elements in the solution.

The slag materials from the Molycorp-Washington site consisted of 0.1-mm-sized metallic and non-metallic phases encapsulated in glass. A test specimen of that slag was cut in the shape of a parallelepiped for leach testing. The specimen dimensions were 1.7 x 1.8 x 4.8 cm, which has a calculated geometric surface area of 39.72 cm^2. The ANS 16.1 protocol calls for a leachant volume/specimen area ratio of 10 cm, so it is assumed that tests were conducted using leachant volumes of about 400 mL at each exchange (the leachant volumes were not reported). Whereas the leach rates of contaminants during each interval are computed in the ANS 16.1 method and were the focus of the Pickett et al. (1998) report, the present interest is in the release behavior revealed in the series of test intervals. The cumulative released masses were calculated from the solution concentrations reported for each test interval, and these are plotted in Figure 5.15. The data for different elements have been scaled to facilitate direct comparison of the release behaviors

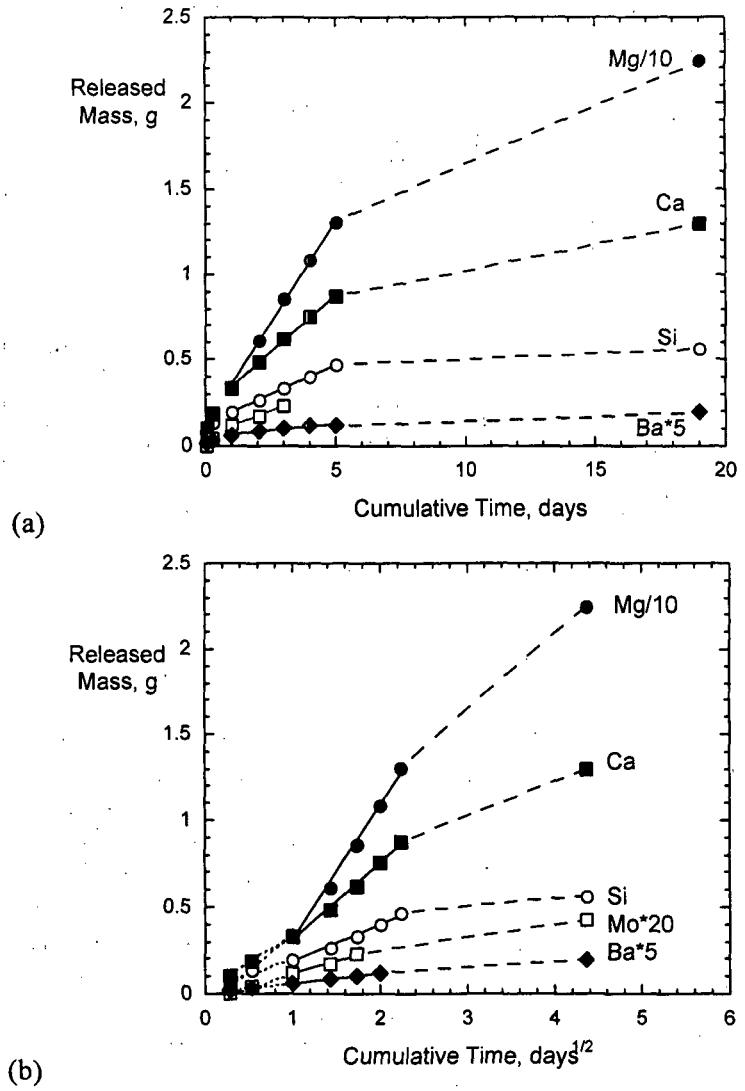

Figure 5.14. Results from Pickett et al. (1998): ANS 16.1 tests with Whittaker-Greenville site slag plotted as (a) cumulative release vs. cumulative time, and (b) cumulative release vs. cumulative root-time.

on a single plot. Figures 5.15a and 5.15b show the cumulative release plotted against the cumulative test duration highlighting the short-term and long-term results, respectively. Consider first the initial seven samplings. The first three are taken after intervals of 2, 5, and 17 hours and then the next four after intervals of 24 hours. The cumulative releases for the fourth through seventh samplings are linear in time, as shown by the solid line fits. (The third point can be thought of as the origin for the linear fit to the next four points.) Releases prior to this are non-linear, as illustrated by the Na release. The releases beyond the seventh sampling are fairly well described with a linear fit, although the data deviate negatively. This is attributed to the increasing interval for each successive sample. The largest deviation is between the points at 5 and 19 days. Figure 5.15c shows the cumulative releases plotted against the square root of the cumulative test duration. The Na release in tests through about 20 days (cumulative) is linear with root-time, but

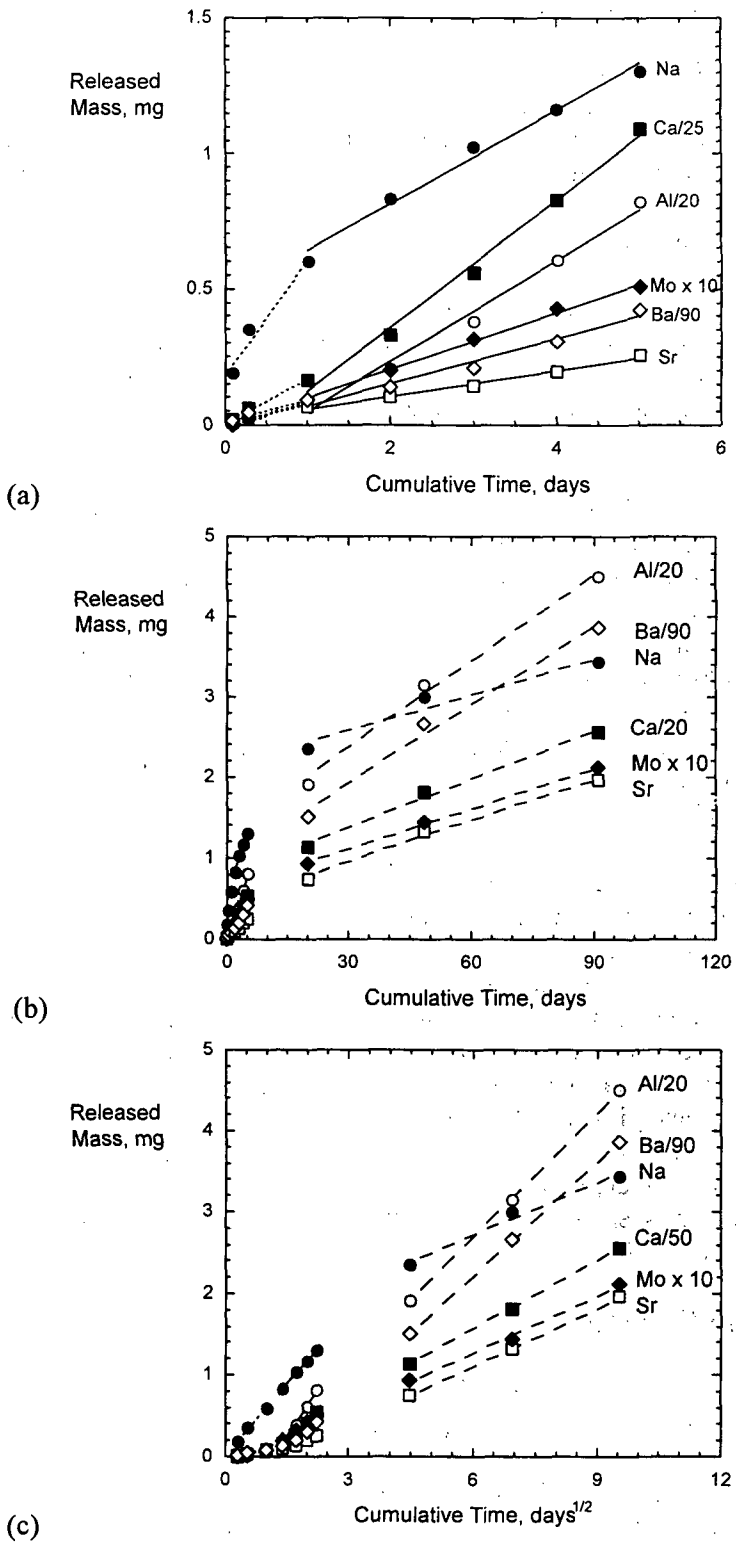

Figure 5.15. Results from Pickett et al. (1998): ANS 16.1 tests with Molycorp-Washington site slag plotted against (a) and (b) cumulative time and (c) cumulative root-time.

then deviates negatively. This is probably due to depletion of Na in one or more of the dissolving phases, since Na is a minor component of the slag. The releases of the other plotted elements are linear with root time beyond the first 3 days. Although the root-time dependence of the releases beyond about 3 days is consistent with diffusion control, it is probably a fortuitous result of solution feedback effects due to the increasingly long sampling intervals. As will be discussed in Section 7.4, diffusion-controlled and affinity-controlled release can be difficult to distinguish in short-term tests. The observation that the early release was not consistent with diffusion control makes it unlikely that the later release is diffusion controlled. The pH values of the 20- and 91-day leachates were reported to be 11.42 and 11.45. The pH values of other leachates were not reported, but the tests were conducted with demineralized water as the leachant, which has a slightly acidic pH due to dissolved CO_2. The significant increase in solution pH over moderate test intervals (e.g., an increase to pH 11.42 after only 20 days) could contribute to the faster release beyond the initial 3 days, since the dissolution rates of many materials increase with pH in alkaline solutions.

The data set for ANS 16.1 tests with the Cabot-Reading site slag was incomplete in that samplings prior to 20 days were not analyzed for all components. Only the behavior in samplings at about 20, 48, and 91 days are evaluated for multiple components. These results are shown plotted against time and root-time in Figs. 5.16a and 5.16b. As for the other slags evaluated by Pickett et al. (1998), the long-term results are equally well fit by the affinity-controlled and diffusion-controlled models. The different interval durations add uncertainty to the evaluations with both models. Only the Ca concentration was measured in all samplings and the short-term results show release is linear in time with a slope greater than the slope for the long-term releases. (Note that the cumulative releases in Figs. 5.16a and 5.16b only include the increments measured at 20, 48, and 91 days, whereas the releases in Figure 5.16c include the releases in all ten increments.)

The test schedule used by Pickett et al. (1998) provides information regarding the release mechanism. Initial short-term tests with uniform replacement intervals would indicate that an affinity-controlled mechanism is operative for a homogeneous material if the results were linear. The use of a longer interval for subsequent samplings would indicate an affinity-controlled mechanism if the release is linear but slower than the release rate measured with shorter intervals. A diffusion-controlled mechanism would show releases following root-time kinetics over the cumulative test duration, with the rate depending on the exchange frequency. It would be easier to distinguish between affinity and diffusion control if all of the longer intervals were of the same duration. There is no obvious benefit to using different long-term intervals but there is an obvious detriment: the increasing interval durations can give affinity-controlled releases the appearance of diffusion-controlled release, as seen in the results for the Whittaker-Greenville site slag. The effect of the testing interval durations is discussed further in Sections 5.2.3 and 7.4.3.

5.2.2 Fuhrmann and Schoonen

Several series of ASTM C1308 accelerated leach tests (ALTs) were conducted with slags that had been recovered during steel recycling operations (Fuhrmann and Schoonen, 1997). The results of the ASTM C1308 tests conducted with non-radioactive slag E-1 (Steel Slag Coalition, Washington, D.C.) at 60°C are shown in Figure 5.17. The cumulative mass loss is plotted against time in Figure 5.17a and against root-time in Figure 5.17b. The results for different components have been scaled to better compare the release trends over time. The early releases of Ca, Na, Si, and Sr (through the first 24 hours) show root-time dependence within the testing uncertainty, with regressed slopes of 13, 0.24, 0.12, and 0.015 mg $d^{-1/2}$, respectively (adjusted for scaling factors). However, these fits have significant positive y-intercept values that are inconsistent with diffusion-

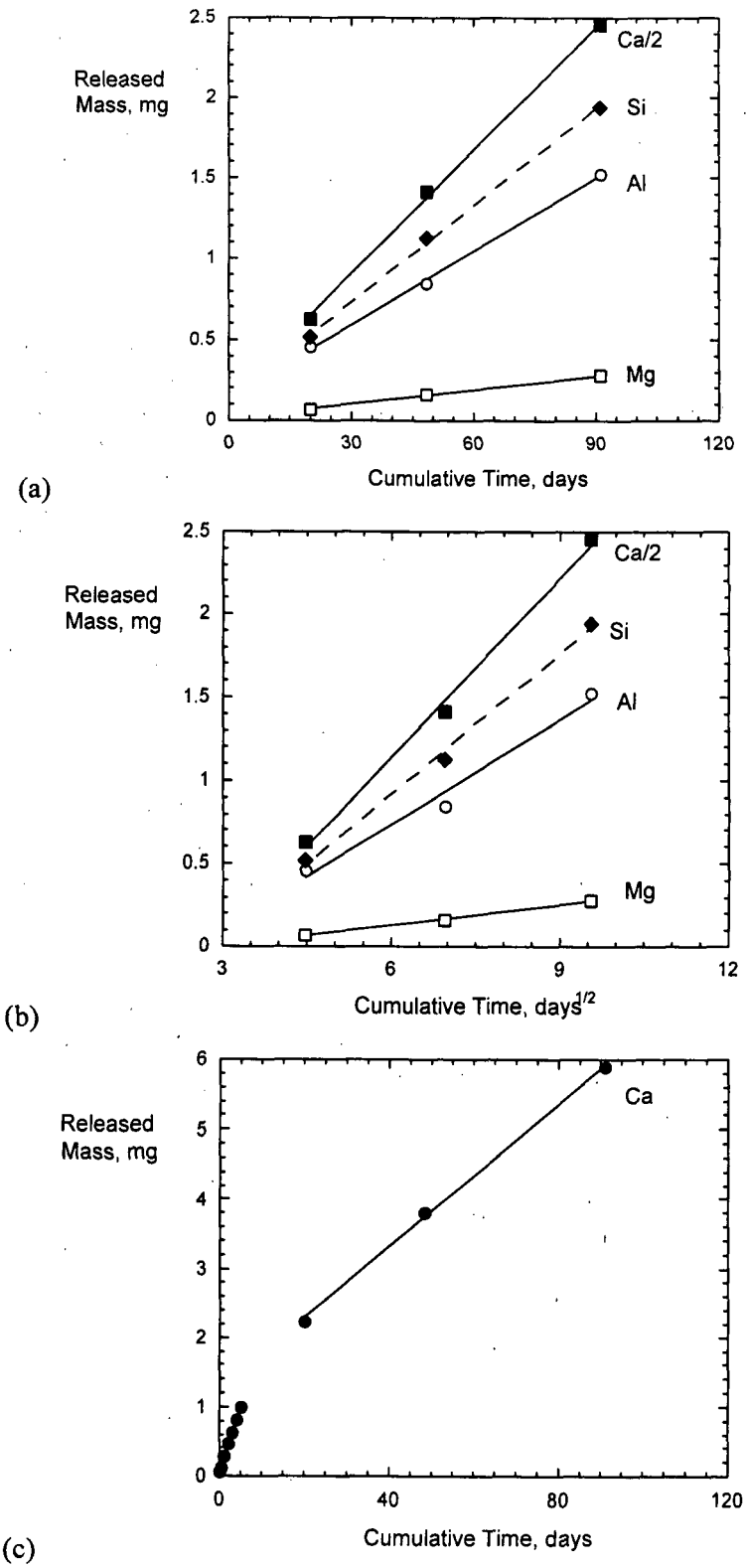

Figure 5.16. Results from Pickett et al. (1998): ANS 16.1 tests with Cabot-Reading site slag plotted against (a) cumulative time and (b) cumulative root-time, and (c) release of Ca.

controlled release. The longer-term samplings are also linear with root-time, but the fits to Ca, Si, and Sr releases beyond 6 $d^{1/2}$ for tests with 1-day sampling intervals have greater slopes than the fits to the short-term tests with shorter sampling intervals: 15, 0.94, and 0.018 mg $d^{-1/2}$, respectively. This is not consistent with diffusion-controlled release, because longer intervals should give lower slopes. The releases of all elements are also linear with the reaction time for samplings taken beyond 48 hours (see Figure 5.17c) at 1-day intervals. The test results beyond 48 hours are fit equally well with linear and root-time time dependencies (all Si releases are well fit with time).

The data set is not sufficient to distinguish whether the release is controlled by diffusion or reaction affinity. However, comparing the release behaviors of Ca, Si and Sr in the initial short sampling intervals with the behaviors in the longer constant sampling intervals and noting the *y*-intercepts of the short-term root-time fits both suggest that the release is most likely controlled by dissolution. This is because longer sampling intervals should result in lower average release rates for both diffusion- and affinity-controlled reactions. Figure 5.17c shows lower release rates for the longer intervals than for the individual short-term samplings. The releases of Ca, Si, and Sr increase slightly with the sampling interval on the root-time plots.

Modified ALTs were conducted with non-radioactive slag AS-3 (Ameristeel, Knoxville, TN) in the form of a powder that was contained in a membrane during the test. The results are shown in Figs. 5.18a and 5.18b in linear and root-time plots, respectively. The early releases of Al, Ca, and Si are described equally well with linear and root-time fits. A change in the release behaviors of Al and Si occurs after about 120 hours (5 days) of testing that results in a significant change in the slopes of both the linear and root-time fits. The release rate of Si increases and the release rates of Al and Na decrease on both scales. This may indicate a change in the phase composition at the sample surface, such as the most soluble phase being completely dissolved after 120 hours. It could instead be an artifact of using powdered slag in the test. Crushing most materials generates particles with sharp fractured edges that are more reactive than the smooth surfaces (e.g., Petrovich 1981). Dissolution rates are expected to be artificially high (with respect to the bulk material) until the sharp edges have been dissolved. As discussed later (see Section 6.1.2), the influence of the edges on the measured dissolution rate can decrease quickly after the sharp edges are removed. Regardless, the release behaviors before and after the discontinuity can be well represented with either linear or root-time dependencies. As discussed for the E-1 slag, the relative slopes for the three short-duration samplings and the subsequent 1-day samplings favors dissolution control: longer intervals should result in lower release rates under both diffusion-controlled and affinity-controlled mechanisms. The releases of most elements increase on the root-time basis, contrary to the expectation for diffusion control, but decrease on the linear time basis, consistent with the expectation for affinity control. Therefore, the process controlling the releases is suspected to be affinity controlled.

The release of Na shows more scatter than the releases of other elements in early samplings, probably because Na is present in the solutions at significantly lower concentrations than other components. The early release of Na could be a diffusion-controlled process while the releases of other components are controlled by dissolution. The early release behavior of Na from silicate glasses is usually seen to be diffusion-like, which may indicate that the reaction is controlled by the diffusion of water into the glass where reaction occurs with sodium in the glass. In these tests, the Na behavior before about 96 hours is not represented well by either model, whereas the Na release beyond about 96 hours is described equally well with time and root-time fits.

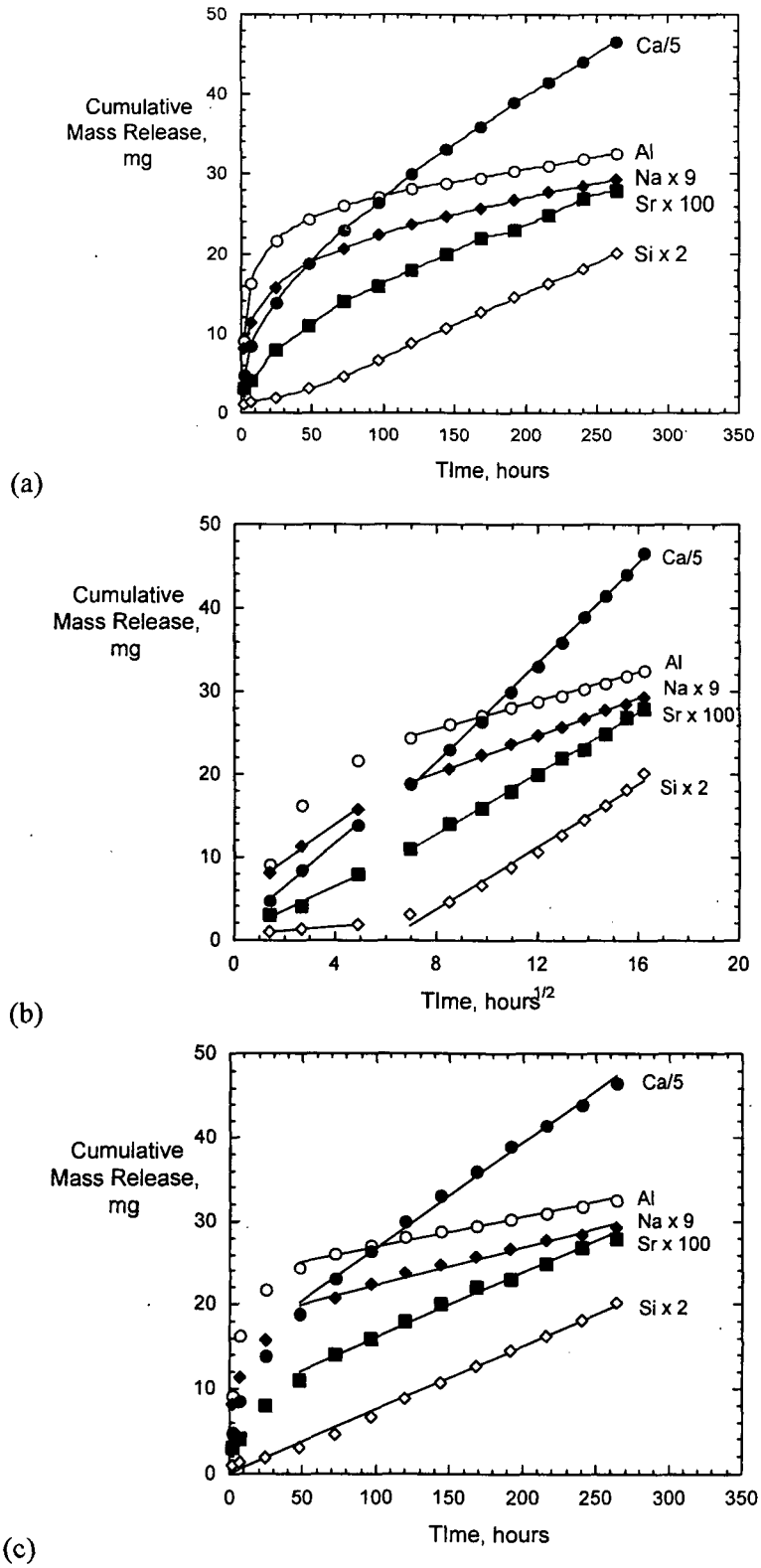

Figure 5.17. Results from Fuhrmann and Schoonen (1997): ALT at 60°C with slag E-1 plotted against (a) cumulative time, (b) cumulative root-time, and (c) cumulative time with linear fits.

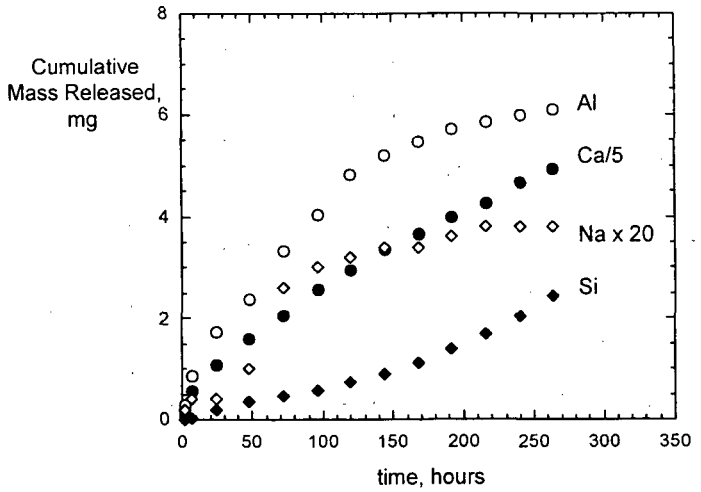

(a)

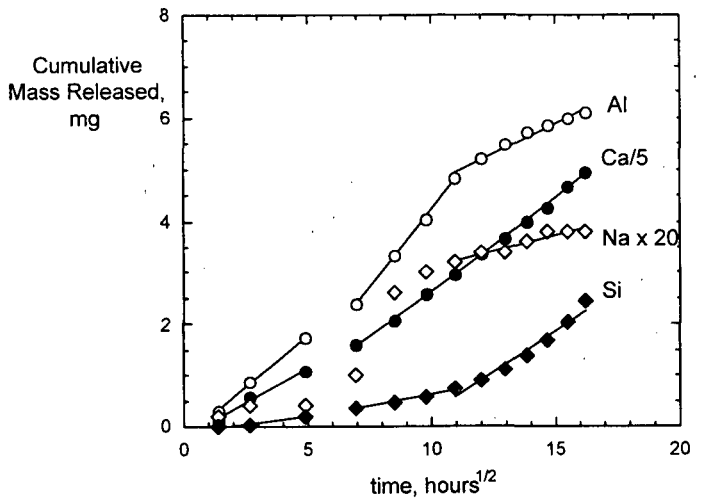

(b)

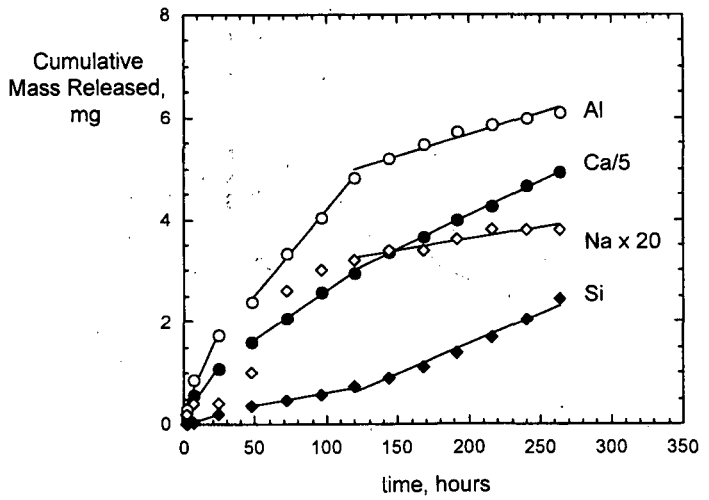

(c)

Figure 5.18. Results from Fuhrmann and Schoonen (1997): ALT at 60°C with slag AS-3 plotted against (a) cumulative time, (b) cumulative root-time, and (c) cumulative time with regression fits.

5.2.3 Sampling Interval

The different exchange/sampling intervals in the ANS 16.1 and C1308 test methods were utilized to distinguish between diffusion control and dissolution control for both the AS-3 and E1 slags. Without varying the exchange intervals, the curvature in the sequential results caused by changing affinity effects can be misinterpreted as reflecting diffusion control. The use of a single constant interval results in solution feedback effects that are essentially constant for all intervals and a constant release rate for an affinity-controlled dissolution mechanism (i.e., linear in time). As evidenced by the tests with the E1 and AS-3 slags, some test results can be equally well described by diffusion or affinity control. Continuing the test by using longer (constant) sampling intervals may help distinguish which process dominates the mechanism and is appropriate for long-term projections: diffusion control is expected to retain the root-time behavior, but with a smaller slope (as discussed regarding the test results evaluated in Section 5.1); affinity-controlled dissolution would remain linear (with time) with a lower slope. The expectation is that either the higher slopes from short intervals or the lower slopes from longer intervals would distinguish between the mechanisms.

The examples discussed in Section 5.1 indicated that short and constant exchange intervals are needed to provide a reliable measure of the diffusion constant, and that the interval duration affects the measured value. The examples in Section 5.2 show that diffusion-controlled and affinity-controlled release mechanisms cannot be distinguished by using a single constant exchange interval. At the high solution volume-to-surface area ratio used in the ANS 16.1 and C1308 test methods, the reaction affinity decreases slightly over the test interval, but by about the same extent for each sampling. Therefore, the extent of dissolution is about the same for each test interval. The computer program available for the ASTM C1308 test method includes a routine to evaluate the similarity of concentrations in successive sampling intervals as an indication that the concentration is solubility limited. In fact, consistent solution concentrations indicate a consistent extent of dissolution over each interval and a constant dissolution rate regardless of the degree of saturation. As discussed elsewhere, this is valuable information provided by constant sampling intervals.

6 Dynamic Test Methods

Dynamic tests in which leachant flows continuously through a bed of crushed material (or around a monolithic test specimen) are used to control the leachate chemistry as the specimen dissolves or to simulate natural environments. Simple column tests are conducted using gravity-induced flow through the column, whereas other tests are performed with the leachant forced through the column by using a pump. Upward flow minimizes the possibility of channeling and ensures all surfaces are contacted by the leachant. The dimensions of the column are usually selected based on practical considerations such as the amount of material available, the radioactivity of the material, the planned duration of the test, the need to minimize waste solutions, etc. Most laboratory tests are conducted using <2 mm particles because of the relatively high specific surface area and greater homogeneity expected for small particles. Although arbitrary, separating site materials into fractions that are greater than and less than 2 mm facilitates reliable characterization of the surface properties of the very large volumes of material that are of interest to field analyses by using laboratory-scale samples. This is because small particles have a proportionately higher specific surface area (i.e., surface area per unit mass) than large particles, which is easy to scale. For example, a spherical particle with diameter d and density ρ has a surface area–to–volume ratio of $6/d$ and a specific surface area of $6/(d \times \rho)$. The densities of metallic and non-metallic minerals range from about 1 g cm^{-3} to about 12 g cm^{-3}, with a peak in the distribution between 2.5 g cm^{-3} and 5 g cm^{-3} (Hillel 1980). Most silicate minerals have a density between about 2 g cm^{-3} and 4 g cm^{-3}. Using a nominal density of 3 g cm^{-3} for a geological specimen, the specific surface area will scale as $2/d$. From this relationship, the specific surface area decreases rapidly with particle diameter, such that a particle 20 mm in diameter has a specific surface area that is only 10% that of a 2-mm particle. On the other hand, a particle that is 0.2 mm in diameter has 10 times the specific surface area of a 2-mm particle. Therefore, conducting laboratory tests with particles that are 2 mm and smaller provides the maximum surface area (and representation of the mineralogy) with the minimum volume. As an example of experimental convenience, a column diameter at least 30 times the maximum particle size is recommended to avoid local velocity effects such as channeling (Relyea 1982). Particles that are 2 mm or smaller require a 6-cm diameter column, which is available as standard laboratory ware.

Note that the fluid flows through the specimen chamber but around the particles of test specimen in these dynamic tests, so that reaction occurs at the surfaces of the particles. A different test method is conducted wherein the fluid is forced to pass through a porous test specimen using high pressure. That method is discussed separately in Section 6.6. Note also that the term "steady state" is often used in the literature to denote a constant release rate or constant concentration. In this report, steady state refers specifically to the kinetic condition of no change in the concentration of solution exiting the reaction cell over time. That is, the amount of a contaminant released from the specimen due to dissolution or leaching equals the amount of that contaminant that is removed from the system due to flow at steady state. Steady-state conditions in the reactor lead to constant release into the effluent and concentrations that are constant with the reaction time. The important difference is that the constant rate is *a direct function of the solution flow rate and exposed surface area*, and not an intrinsic or characteristic property of the dissolving specimen that occurs under equilibrium conditions. This is discussed in detail in Section 6.2.2.

Dyanamic test methods are usually classified according to the apparatus used to control the flow rate and interaction with the test specimen. Six testing methods using different reactors are considered in detail in this report: column reactor, SPFT reactor, fluidized bed recirculating reactor, pressurized unsaturated flow reactor, forced-through reactor, and Soxhlet reactor. The

column reactor is discussed first and results are presented for tests conducted with minerals and various slag materials. The other methods are discussed with regard to the interpretation and modeling of dynamic test results.

6.1 Column Reactors

Column reactor tests are often used to measure the degradation rates of minerals and waste materials. A good description of column and flow-through reactors and how they are used to measure the weathering rates of minerals is provided by White and Brantley (2003). Their description and application of the test data are used here as an introduction and basis for comment and critique:

> The weathering rate of a silicate mineral, R (mol m^{-2} s^{-1}), is commonly defined by the relationship
>
> $$R = \frac{Q}{St} \tag{6.1}$$
>
> where Q (mol) is the moles of a mineral reacted, S (m^2) is the surface area and t (s) is time. In well-stirred flow-through experiments, such as fluidized bed reactors, e.g., Chou and Wollast (1984), the weathering rate can be defined explicitly as
>
> $$R = \frac{(C_i - C_0)}{\beta S}\frac{dV}{dt} \tag{6.2}$$
>
> where C_i and C_0 (mol L^{-1}) are inlet and outlet solute concentrations, β (mol mol^{-1}) is the stoichiometric coefficient describing the number of atoms of solute released per formula unit of the dissolving mineral, and dV/dt is the rate of flow of fluid through the reactor (L s^{-1}). With C_i as a constant, the weathering rate is proportional to the product [of] the effluent concentration and flow rate.
>
> Plug-flow or column reactors have an advantage over stirred and fluidized bed reactors in that they are easily designed as passive gravity flow systems with no mechanical parts, a major consideration for long-term experimental studies. In addition, column reactors are closer analogs to weathering in natural regoliths in which solutes in a volume of infiltrating water progressively react with a continuum of mineral phases.
>
> The disadvantage of column reactors is that [Equation 6.2] is only an approximation of experimental weathering conditions. Solute gradients are produced in which reactant and product concentrations change with distance within the column, i.e., C_i-C_0 is not spatially constant [...] In the present study, solute gradients within the columns were minimized by the long duration and slow rates of the reaction that produced very dilute effluent concentrations [...] In addition, relatively large grain sizes of similar dimensions were used to produce high porosities and relatively homogenous flow in the column bed. White and Brantley (2003)

It is sometimes stated (as above) that the conditions used in a column test represent a natural weathering site or that column tests, in general, provide a closer analogue to a natural site than other laboratory tests. Although this could be true, an important question to be asked is whether the similarity is sufficiently accurate to justify empirically extrapolating the results of tests collected over a few years to geologic timescales. As the evaluation of data in this section will

show, the answer is usually no. Instead, a suite of laboratory tests must be conducted to develop and parameterize a mechanistic model that can be used to link laboratory measurements with calculations of long-term behavior as a function of environmental conditions rather than relying on empirical extrapolations. Although this requires a fairly extensive characterization of the waste and a relatively large number of tests, for example, as recommended in ASTM method C1174 (ASTM 2009a), mechanistically based models are usually considered to provide more defensible long-term projections. A standardized procedure for conducting a column test is available as ASTM D4874 Standard Test Method for Leaching Solid Material in a Column Apparatus (ASTM 2009d). That procedure specifies an up-flowing solution and provides for calculating the void volume and porosity of the column. The void volume provides a convenient unit for quantifying the amount of effluent solution. Recommendations for sampling and reporting are provided in the procedure, for example, it specifies that the flow rate be adjusted to completely replace the solution in the column (one void volume) within a 24-hour period and that void volumes 1, 2, 4, and 8 be collected and analyzed. Instead of the test methodology *per se*, the focus of this evaluation is on the application of test results to material behavior and modeling.

6.1.1 White and Brantley

White and Brantley (2003) measured the dissolution rates of fresh plagioclase and weathered plagioclase that had been recovered from the Panola watershed in the Piedmont province of Georgia, USA. Tests were conducted with 750 g crushed material in a size fraction <2 mm that was placed in a 2.4 cm id × 1.0 m long Pyrex glass column using distilled deionized water that was saturated with a 5% CO_2/95% air mixture at 20°C (pH = 4.5) prior to use. The leachant flow rates were controlled by gravity and were measured throughout the test; the average flow rate was 10 mL h^{-1}. The dissolution rate was calculated with Equation 6.2 using the measured Na concentration and the flow rate measured at the time the sample was collected. The specific surface area of the crushed plagioclase was measured to be 0.084 m^2 g^{-1} prior to testing (BET surface area) and 0.126 and 0.298 m^2 g^{-1} after 1.66 and 6.21 years, respectively. The increase in specific surface area may result from the particles shrinking as they dissolve or the formation of secondary phases having higher specific surface areas than the dissolving phase (e.g., clays). Although the specific surface area of the test material increased during the test, the mass decreased. The reactive surface area cannot currently be quantified or distinguished from the total surface area. The results for dissolution of fresh plagioclase are plotted in Figure 6.1a with a regressed power-law fit:

$$rate\left(mol\ m^{-2}s^{-1}\right) = 1.49\times10^{-13}\ t^{-0.51}\ . \tag{6.3}$$

The dissolution rate of the weathered plagioclase was measured to be nearly constant over the test duration (see Figure 6.1b) and the results were fit to a linear (with respect to time) release equation:

$$rate\left(mol\ m^{-2}s^{-1}\right) = 1.4\times10^{-15} + 1.71\times10^{-18}\ t\ . \tag{6.4}$$

(Note that Equation 6.4 differs from Equation 7 in White and Brantley (2003), wherein the constant term is wrongly given as 0.0014 and the coefficient for the time dependence fails to account for the multiplication factor of 10^{13} in the results.) The linear fit is shown by the dashed line in Figure 6.1b. The power-law regression of the entire data set may provide a more realistic fit, as shown by the solid curve in Figure 6.1b. Using Equation 6.4, White and Brantley (2003)

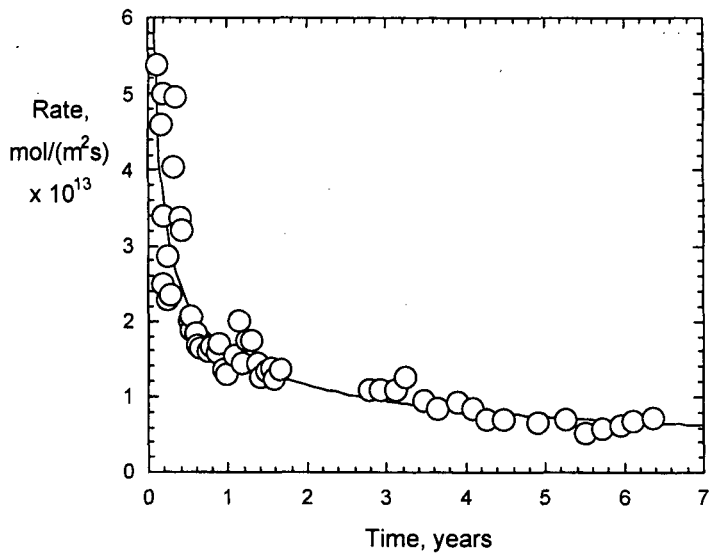

(a)

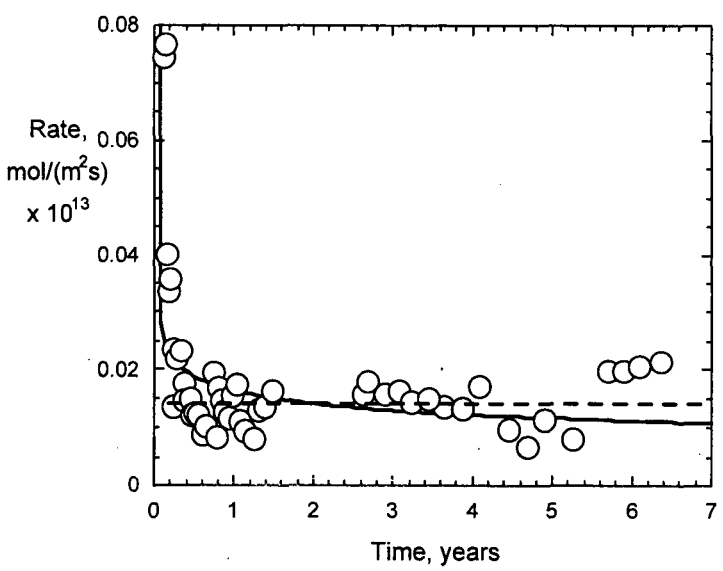

(b)

Figure 6.1. Results from White and Brantley (2003): Measured dissolution rate of (a) fresh plagioclase and (b) weathered plagioclase based on release of Na.

calculated a reaction time of 22,000 years for the dissolution rate of fresh plagioclase to decrease to the rate that was measured for weathered plagioclase under the particular test conditions.

Granite is an igneous rock composed of aggregated minerals, including quartz, alkali feldspar (e.g., orthoclase), and plagioclase feldspar. The dissolution rates of most (if not all) of these phases are expected to be affected by the dissolved silica concentration through a chemical affinity dependence. Therefore, the dissolution rates measured in the column tests of White and Brantley (2003) probably depend on the flow rate that was used in the test. The authors noted that "lower flow rates generally resulted in increased effluent Na" (White and Brantley 2003, p. 484), but the effect of flow rate was not discussed further. The dissolution (weathering) rate is proportional to the product of the effluent concentration and the flow rate (dV/dt) in Equation 6.2, but this only

takes into account the diluting effect of the flow rate. It does not account for any dependence of the rate on the solution composition. The relationship between an affinity-controlled dissolution rate and the response of a dynamic dissolution test is discussed in Section 6.2. The consequence of the flow dependence is that the dissolution rate measured at any particular flow rate is not a characteristic rate of a material that should be used to predict its long-term behavior. The effect of the leachant flow rate on the dissolution rate should be taken into account for long-term projections. (See also Section 7.4.6.) Even if the experimental flow rate accurately mimicked the infiltration rate of meteoric water, flow through the geologic environment would not have been simulated by flow through the <2 mm particles used in the column tests. The <2 mm particles provide a representative reactive surface for use in the test, but not a representative flow path.

In this solids-dominating test configuration, the solution composition varies continuously through the column and becomes increasingly concentrated as it passes through the crushed material. At high percolation (advection) rates, the material near where the leachant enters the column will react in nearly pure leachant (without components from dissolved plagioclase) whereas the material near the exit will react in nearly pure leachate (with the highest concentrations of components from dissolved plagioclase attained in the column). The chemistry of the solution changes while passing through the column. White and Brantley (2003) suggest that the long test duration and low flow rates occurring in these tests minimized solution gradients. This may have been true with regard to gradients normal to the advective flow, but not along the length of the column. Concentration gradients will remain along the length of the column even after steady state is attained. They also suggested that their use of relatively large and similar grain sizes lead to relatively homogeneous flow through the bed. Particle sizes 0.25–0.85 mm in a column having a 2.4-cm inside diameter are small enough to maintain even flow in column tests to measure K_d values (e.g., Relyea 1982). Using an average particle size of 0.5 mm and assuming cubic geometry gives a specific surface area of 0.0044 $m^2\ g^{-1}$ and 3.3 m^2/750 g in the packed column. The surface area/solution volume ratio in the column is about 19,000 m^{-1}. The fluid exiting the column was not exposed to this area for the entire residence time and the effective S/V ratio is much lower. Contrasting this with the 10 m^{-1} ratio called for in the ANS 16.1 and ASTM C1308 test methods to maintain highly dilute conditions and the ASTM C1285 test method to generate concentrated solutions, these column test conditions are likely to result in far-from-equilibrium conditions at the entrance of the column and near-equilibrium concentrations near the column exit. The output concentrations are expected to be insensitive to the intrinsic plagioclase dissolution rate but reflect the solubility limits.

6.1.2 Fuhrmann and Schoonen

Column tests were conducted with three different slags resulting from steel recycling (Fuhrmann and Schoonen, 1997). Samples of the same slags were used in ASTM C1308 ALT tests that were discussed in Section 5.2.2. The slags were crushed, but the particle size range was not reported. Distilled water was pumped upwards through the columns at average flow rates calculated to be 63, 66, and 69 mL/day in tests with the E-1, Q-BOPA (Heckett Multiserve, Provo, UT), and AS-1 slags, respectively. The void volume of each packed column is estimated to be about 20 mL based on the column volumes and reported porosities, so the solution in each column is exchanged more than three times daily at these flow rates. The test results are plotted in Figure 6.2 as the cumulative fraction released. Note that the results have been scaled to facilitate comparisons of the release patterns of different elements over time on the same scale. The initial concentrations of the tracked components in the slags are given in Table 6.1. The cumulative releases in the test with slag E-1 shown in Figure 6.2a are fairly linear between nodes occurring at 6.4, 10.2, 17.3, and 24.4 days, which are indicated by the vertical dashed lines. Changes in slope occur for Na, Sr, and Al at 6.4 and 10.2 days, for Sr, Al, Ca and Si at 17.3 days, and for Ca and Si at 24.4 days. The

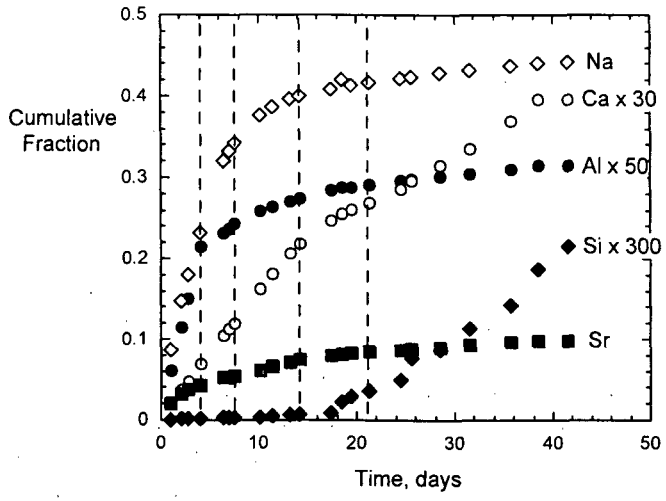

(a)

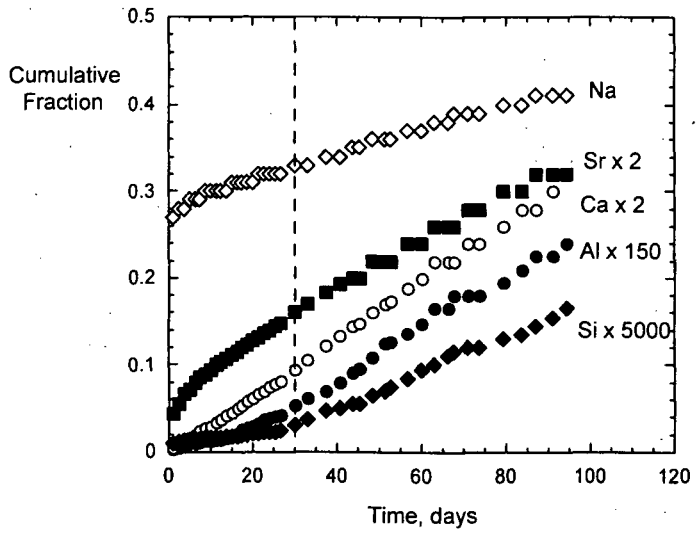

(b)

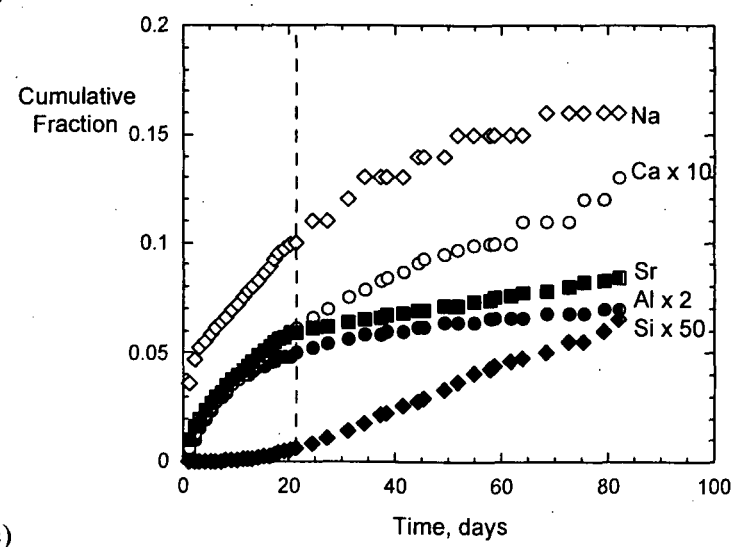

(c)

Figure 6.2. Results from Fuhrmann and Schoonen (1997): Column tests with slags (a) E-1, (b) Q-BOPA, and (c) AS-3. The vertical dashed lines locate changes in sampling frequencies.

Table 6.1. Initial concentrations in slags,[a] as elemental mass%.

Specimen	Al	Ca	Na	Si	Sr
E-1	8.3	32.0	0.064	6.0	0.021
Q-BOPA	0.69	31.7	0.016	7.6	0.017
AS-3	4.9	29.3	0.031	8.6	0.027

[a]Normalized to 100% total oxides.

release rate of Si increases, whereas the release rates of the other elements decrease at each node (the Ca release rate may increase beyond 24.4 days, or this may be experimental uncertainty). These changes correlate with an increase in the interval between effluent collection time and may indicate a dependence of the measured release rates on the sampling interval. The sampling intervals in tests with slags Q-BOP and AS-3 were more regular, as seen in Figs. 6.2b and 6.2c, but the slightly longer interval between 21.3 and 24.4 days does result in a noticeable change in the releases of Na and Sr, which decrease, and an increase in the Si release. The impact of when and how long the effluent solutions were collected for analysis suggests the system was not at steady-state during the initial samplings. That is, the solution concentrations varied with time.

A better understanding of the test results is gained by plotting the solution concentrations at every sampling against the cumulative test duration, as shown in Figs. 6.3a, 6.3b, and 6.3c. (The final page of the report BNL-71445 was missing and the measured concentrations are only available for the initial samplings of the column test with AS-3 slag. The concentrations were estimated from the reported CFL values.) The releases of particular elements have common behaviors during the tests, (1) The concentrations of Al, Na, and Sr decrease during the first ~20 days of each test. (2) The solution concentration of Ca remains fairly constant during the three tests. (3) The concentrations of Si *increase* during the first ~20 days of all tests whereas the releases of other components decrease. The solution concentrations decrease at similar rates beyond 20 days in tests with E-1 and Q-BOP slags. The observed behaviors can be understood as follows. As the demineralized water is pumped into the column, it reacts with and dissolves the phases in the slags. Minute particles are dissolved quickly, due to their high specific surface areas, and the initial samplings attain high concentrations as they pass through the column. As the small particles dissolve completely, less surface area is available to react with the fluid that is collected in subsequent samplings, so the solution concentrations decrease with time. Why the solution concentrations of Si increase during the first 20 days while the releases of other components decrease is not understood. It may indicate delayed transport of Si through the column due to interactions with the solids. Silicon is a minor component of all three slags. After about 20 days, the test systems attain nearly steady-state conditions when the dissolution rates of the phases become fixed by the flow rate of the fluid. The continued decrease in solution concentrations at longer sampling times is probably due to the loss of surface area as the particles dissolve.

The test responses depend on the phase compositions of the slags and the intrinsic dissolution behaviors of these phases, but also on test conditions including the fluid flow rate, particle size distribution, column porosity, and transport properties of the released species. Although the collected eluates represent the solutions contacting the slag materials at the end of the column, the chemistry of the fluid in the column (and the surface state of the slags) changes significantly over the length of the column. Slag phases at the entrance of the column are reacting with demineralized water and phases at the exits are reacting with highly alkaline solutions. At steady state, the composition of the fluid will still vary through the column, but the concentration at any particular location will not vary with time except in response to the loss of surface area or upon the precipitation of secondary phases. This is considered further in the following section.

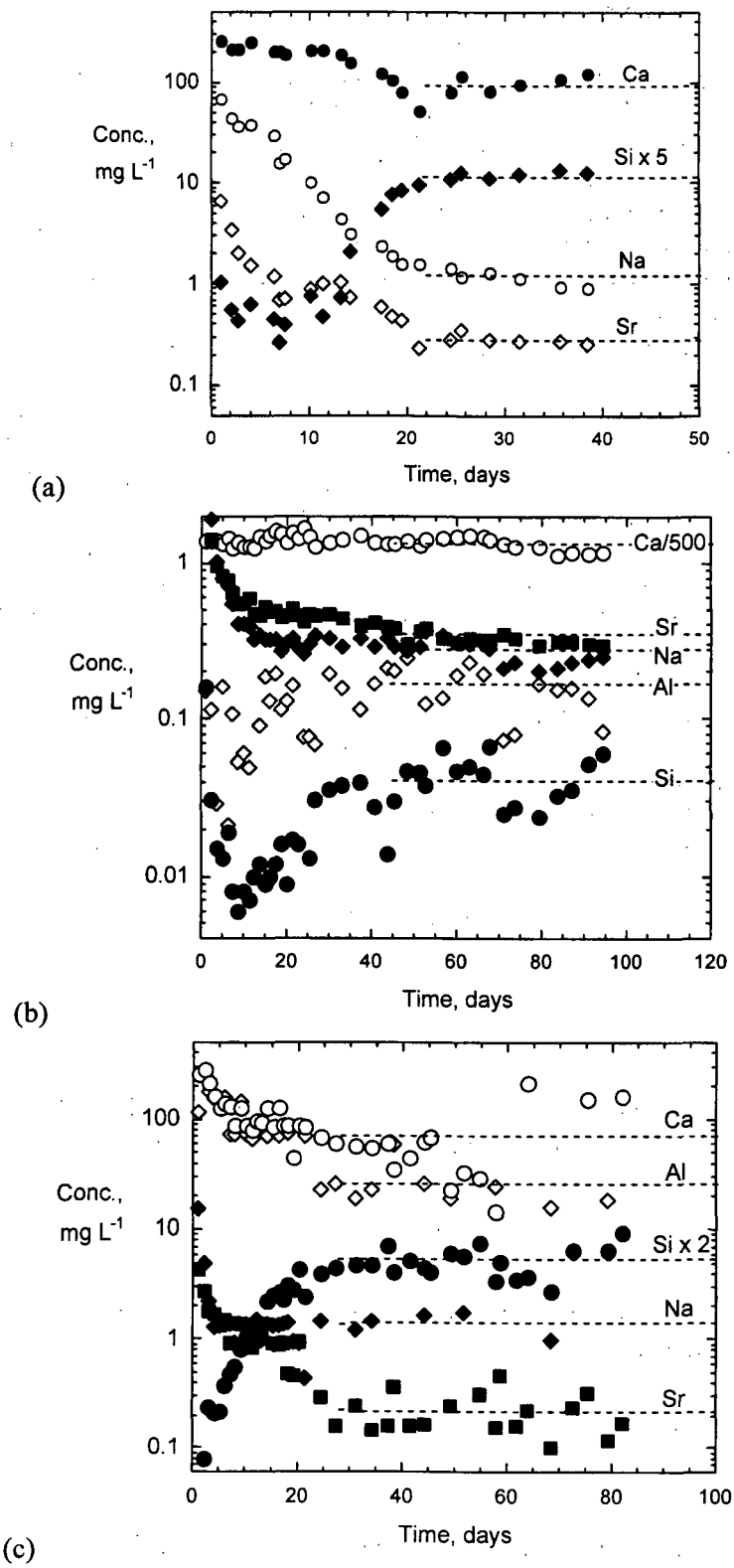

Figure 6.3. Results from Fuhrmann and Schoonen (1997): Solution concentrations in column tests with slag (a) E1, (b) Q-BOP, and (c) AS-3.

6.1.3. Steady State in Column Reactors

Column reactors present a more complicated system than static reactors in that the time that fluid contacts the material surface depends on the flow rate and length of the column. In static tests, the fluid contacts all surfaces throughout the test, released components accumulate in the solution over time, and all surfaces are contacted by a similar solution chemistry. In column tests, the fluid contacts a particular surface for a limited duration and the solution chemistry changes over the length of the column. Material at the entrance of the column is continuously contacted by fresh leachant solution and material at the exit of the column is contacted by solution carrying dissolved components and having a chemistry that may differ significantly from the input leachant. The effluent solution that is analyzed represents the solution contacting the material very near the exit.

The transport of dissolved components through the column provides opportunity for species-specific retardation due to adsorption, precipitation, or other reactions with the solid materials in the evolving solution chemistries. For example, the solution pH and Eh will likely change throughout the transport pathway to affect the solubilities of released components. These differences will exist throughout the column even after steady-state conditions are attained. As in SPFT-type experiments, steady-state conditions cannot be maintained in tests with small particulate solids due to the continuing loss of material mass and reactive surface area as the materials dissolve.

To determine dissolution rates from experiments with packed columns, both chemical reaction and fluid transport must be taken into account. This is because the solution chemistry of the fluid changes as it passes through the column and contacts additional surfaces. Those surfaces will also vary throughout the column. In the batch tests, fluidized bed, stirred reactor, and SPFT methods discussed above, the effect of mass transport can be neglected in the fluid-dominated environments present under most test conditions. The general equation for coupled reaction and transport can be written as (Mogollon et al. 1996; Taylor et al. 2000a, Taylor et al. 2000b)

$$\frac{\partial(\Phi C_i)}{\partial t} = -\nabla(\Phi J_i) + \Phi\, Rate_i \tag{6.5}$$

where Φ is the porosity of the medium, C_i is the concentration of species i, J_i is the flux of solute i, and $Rate_i$ is the net rate of all reactions involving i. Consider the dissolution of gibbsite in acidic solutions

$$Al(OH)_3 + 3\ H^+ = Al^{3+} + 3\ H_2O. \tag{6.6}$$

For constant flow through a homogeneous column of gibbsite, the one-dimensional reaction-transport equation can be written in terms of dissolved Al (Mogollon et al. 1996),

$$\frac{\partial C_{Al}}{\partial t} = D\frac{\partial^2 C_{Al}}{\partial x^2} - v\frac{\partial C_{Al}}{\partial x} + Rate_{Al}, \tag{6.7}$$

where x is the distance along the column (m), v is the true fluid velocity (m s^{-1}), and D is the combined diffusion-dispersion coefficient ($m^2\ s^{-1}$). In Equation 6.7, the true fluid velocity is the ratio of the Darcy velocity and porosity. C_{Al} represents the total concentration of Al in solution (mol m^{-3} fluid), and $Rate_{Al}$ (mol m^{-3} fluid s^{-1}) is the net rate of all reactions affecting the Al

concentration. If the Al concentration is only affected by reactions involving gibbsite (i.e., dissolution and precipitation), then $Rate_{Al}$ can be replaced with $a_{Al,\ gibbsite}\ Rate_{gibbsite}$, where the term $a_{Al,\ gibbsite}$ is the stoichiometric coefficient for Al in the gibbsite dissolution reaction, which from Equation 6.6 is 1. If dissolution of another mineral in the system generated Al^{3+}, the rate of that reaction would be added to the right-hand side of Equation 6.7 as $a_{Al,\ mineral}\ Rate_{mineral}$. The change in Al concentration at any location in the column due to the dissolution and precipitation of gibbsite will depend on the surface area of gibbsite that is contacted by the fluid, and that surface area will depend on the distance along the column. The dissolution rate of gibbsite will also depend on the temperature and pH at that location. If the advection is sufficiently high that diffusion and dispersion can be neglected, the reaction-transport equation can be simplified *under steady-state conditions*, where $\frac{\partial C_{Al}}{\partial t} = 0$, as

$$\frac{\partial C_{Al}}{\partial x} = \frac{a_{Al,gibbsite}\, Rate_{gibbsite}(C_{Al}, pH, x)}{v}. \tag{6.8}$$

Consider first reaction conditions that are far from equilibrium for gibbsite. The dissolution rate constant with respect to the Al concentration and can be written as

$$Rate_{gibbsite} = k_{gibbsite}\frac{S}{V} \tag{6.9}$$

where $k_{gibbsite}$ is the forward dissolution rate at the temperature and pH), S is the gibbsite surface area and V is the solution volume in the column. Note that the ratio S/V is used to relate $Rate_{gibbsite}$ (mol m^{-3} s^{-1}) to $k_{gibbsite}$ (mol m^{-2} s^{-1}). Substituting Equation 6.9 into Equation 6.8 and integrating gives

$$C_{out} - C_{in} = \int_0^L \frac{k_{gibbsite}}{vV} S(x)\,dx \tag{6.10}$$

where the gibbsite surface area has been discretized along the column length. By defining the average surface area at any point along the column length as

$$\overline{S} = \frac{1}{L}\int_0^L S(x)\,dx. \tag{6.11}$$

The output concentration is related to the gibbsite dissolution rate as

$$\Delta C_{Al} = \frac{k_{gibbsite}}{vV} L\overline{S}, \tag{6.12}$$

and the kinetic rate coefficient for gibbsite dissolution (mol m^{-2} s^{-1}) can be written as

$$k_{gibbsite} = \frac{\Delta C_{Al}\, vV}{L\overline{S}}. \tag{6.13}$$

Under far-from-equilibrium conditions, the output Al concentration depends linearly on the ratios of the column length and mineral area to the fluid velocity as $L\bar{S}/v$. At the other extreme, the output Al concentration will become independent of the fluid flow as the solution *at the end of the column* approaches equilibrium with gibbsite. In practice, it is difficult to reach equilibrium in column tests at even the slowest flows. Figure 6.4 shows the results of column tests with gibbsite conducted with leachants having four different pH values conducted at various flow rates. Solutions in tests with pH 4.0 and pH 4.5 leachants reached equilibrium prior to exiting the column and maintained constant Al concentrations that were independent of the flow rate (but sensitive to the pH). Tests with pH 3.2 and pH 3.5 leachants conducted at high flow rates ($L/v < 0.5 \times 10^{-4}$ yr) maintained far-from-equilibrium conditions and show the linear dependence predicted by Equation 6.13. However, note that the fitted lines both have positive y-intercepts, whereas Equation 6.12 predicts a zero intercept as $v \rightarrow \infty$. This may indicate that the data are approaching the linear rate asymptotically. The steady state Al concentrations fall well below these lines at higher values of L/v. Dissolution at these pH values shows nonlinear behavior at lower flow rates, which indicates a sensitivity of the rate to the solution chemistry and to ΔG_r.

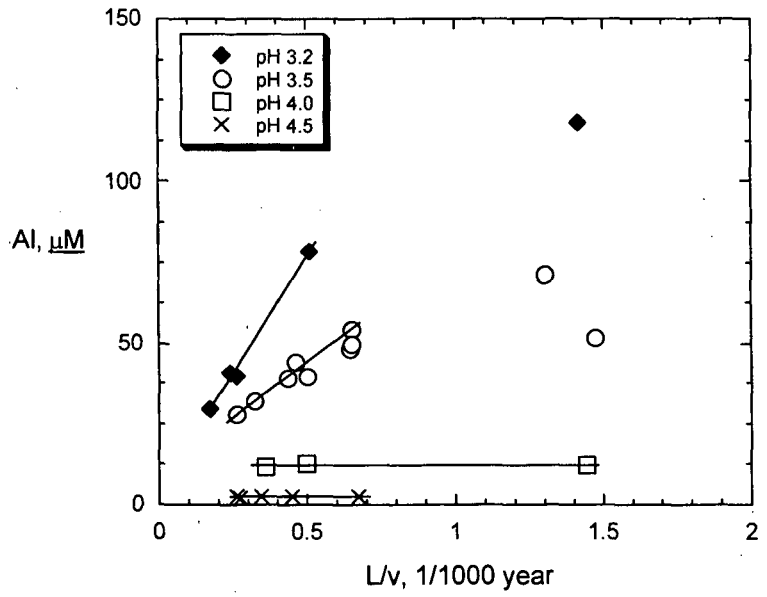

Figure 6.4. Results from Mogollon et al. (1996): Measured Al concentrations vs. L/v for tests conducted with leachant having four different pH values.

Figures 6.5 and 6.6 show the results of similar tests with plagioclase using columns that were 3.5 cm and 5.0 cm long (Taylor et al. 2000b). The dissolution reaction is written as

$$Na_{0.4}Ca_{0.6}Al_{1.6}Si_{2.4}O_8 + 1.6\ H_2O + 6.5\ H^+ \rightarrow 0.4\ Na^+\ 0.6\ Ca^{2+} + 1.6\ Al^{3+} + 2.4\ H_4SiO_4 \qquad (6.14)$$

where a small amount of Sr substitutes for Ca: the plagioclase was reported in Taylor et al. (2000a) to contain 0.3 mass% CaO and 12.9 ppm Sr. Figure 6.5 shows the Si and Sr solution concentrations and flow rates measured in successive samplings as a function of the cumulative reaction time for tests in the 5.0 cm column. The rapid decreases in Si and Sr concentrations during the first ~750 hours indicate the dissolution of highly reactive surface sites; tests were conducted using the 43–110 µm size fraction of crushed plagioclase. Steady-state concentrations

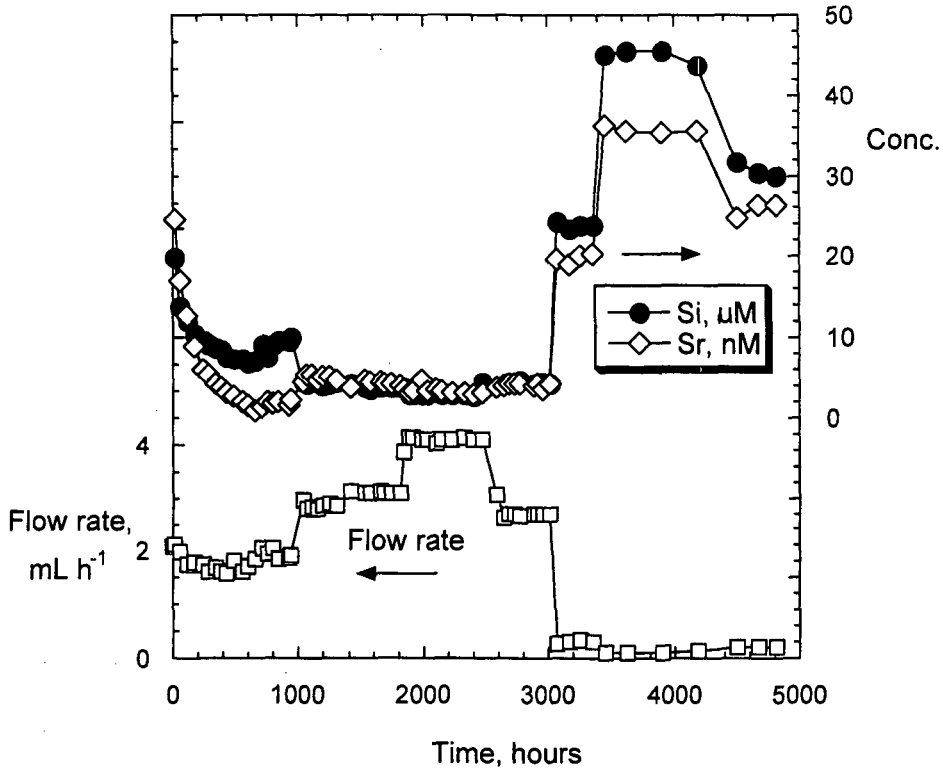

Figure 6.5. Results from Taylor et al. (2000a): Measured flow rate, Si, and Sr concentrations vs. *L/v* for 5.0 cm column tests with plagioclase.

are thereafter inversely related to the flow rate. The authors used the BET-measured specific surface area to normalize the rates and reported no significant change in the specific surface area before and after testing. They did not report the mass loss, which would indicate the change in available surface area in the reactor. The plagioclase dissolution rate is related to the Si release rate by the stoichiometric coefficients from Equation 6.14, where 2.4 moles of Si are released per mole of plagioclase dissolved. The release of Sr is not used to calculate the dissolution rate of plagioclase because Sr is a minor contaminant that may not be uniformly distributed. Nevertheless, the release of Sr is quite uniform in these experiments, although the steady-state Sr concentrations are very low at the higher flow rates.

Figure 6.6 shows the steady-state Si concentrations at various *L/v* for tests in both columns (Taylor et al. 2000a). The diagonal line shows the limiting far-from-equilibrium constant rate that is approached at high flow rates. The steady-state concentrations deviate negatively from this line representing a constant rate at lower flow rates and approach the Si saturation limit as the flow rate approaches zero (*L/v* becomes very large). Longer columns can be used to attain higher *L/v* conditions and determine rates under near-to-equilibrium test conditions.

The results shown in Figure 6.5 raise an important issue regarding flow-through tests. Tests are often conducted by changing the flow rate during a test to drive the system to new steady state conditions. Tests are also conducted by changing the leachant composition, as discussed in Section 6.4. While this is experimentally convenient and seemingly an efficient use of sometimes limited amounts of material, there are potentially important consequences. In the case of changing

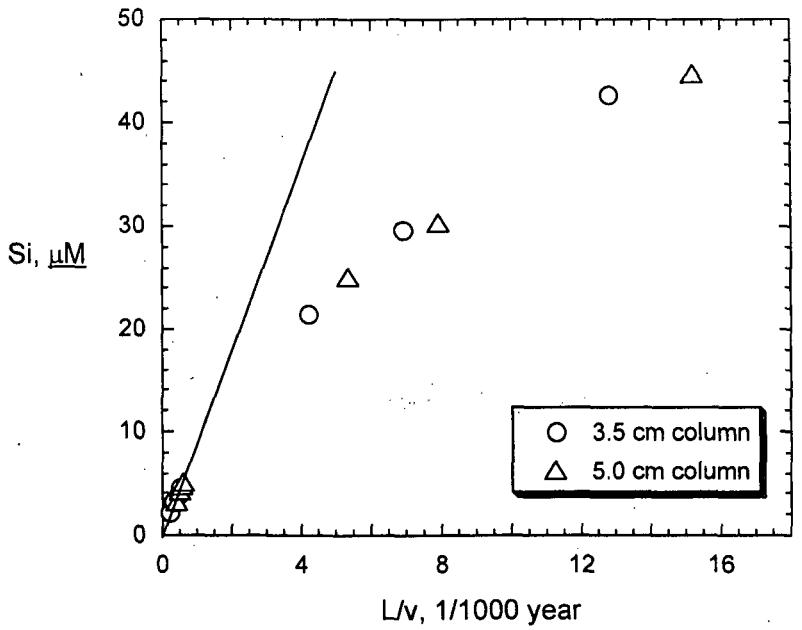

Figure 6.6. Results from Taylor et al. (2000b): Measured Si concentrations vs. *L/v* for tests conducted with $L = 3.5$ cm and $L = 5.0$ cm columns. The diagonal line is fit to the low *L/v* data to show the far-from-equilibrium limit where the steady-state concentration is linear with the inverse flow rate (at very high flow rates) and the dissolution rate is constant.

pH values, non-stoichiometric dissolution will alter the surface composition of the specimen and could affect the steady-state conditions in succeeding intervals. Another complication is the loss of reactive surface area as the test proceeds and the material dissolves. As discussed earlier, the mass of material that dissolves during the test can be calculated from the measured rate and initial surface area. After 3000 hours at the far-from-equilibrium rate, the available surface area is estimated to decrease by only 0.15%. The loss of surface area is insignificant under these conditions, but can become significant under more aggressive test conditions. The ASTM C1662 method for conducting SPFT tests calls for separate tests to be conducted at each flow/area ratio and uses the initial surface area to calculate the rate.

The point of this brief review is to show that the results of a column test conducted under a particular set of conditions are not sufficient to characterize material dissolution behavior. The leachant flow rate, particle size, column porosity, and column length all affect the output solution chemistry in addition to material dissolution, and must be taken into account to determine the material dissolution rate. This test method provides a means to study near-equilibrium conditions at very high *L/v*, but diffusion/dispersion will become the dominant transport processes under those conditions and the mathematics used to quantify test responses will be different that that discussed in this report. Despite the added difficulties of interpreting the results of packed column tests, they provide a valuable link between other laboratory tests and field behavior. This relationship will be examined further in the subsequent report: *Relationship between Laboratory Tests and Field Leaching*.

6.2 Dynamic Tests and Affinity-Controlled Dissolution

The dissolution rates of aluminosilicate minerals and silicate glasses are known to be influenced by temperature, pH, and the common ion effect, wherein the concentrations of key components in the solution affect the rates of reactions through which the material dissolves. The common ion effect is referred to generically as solution feedback. Dynamic tests have been designed to measure the dissolution rates of minerals under conditions in which solution feedback effects are held constant by continuously replacing the solution contacting the test specimen with fresh solution. Both the composition of the leachant solution and the flow rate used in the test influence the dissolution rate of the specimen to establish a unique steady-state solution composition. By measuring (1) the concentrations of soluble components (particularly silicon) in the solution that is flushed from the reaction cell and (2) the solution flow rate, the dissolution rate can be calculated at the particular level of solution feedback that is established by the test conditions that are used. The general rate expression commonly used to model the dissolution of silicate minerals is based on the affinity model discussed in Section 2.3. The form of the rate law used for glass dissolution is given as (e.g., McGrail et al. 1997a; Pierce et al. 2008):

$$rate = k_0 \bullet \Pi\, a_j^{\nu_j} \bullet 10^{\eta\, pH} \bullet \exp\left(\frac{-E_a}{RT}\right) \bullet \left(1 - \frac{Q}{K}\right) \tag{6.15}$$

where

$rate$ = specific dissolution rate, g m^{-2} d^{-1}
k_0 = intrinsic rate constant, g m^{-2} d^{-1}
$\Pi a_j^{\nu_j}$ = general term for dependence on activities of solutes j of order ν_j
η = pH dependence, unitless
E_a = activation energy, kJ mol^{-1}
R = gas constant, kJ mol^{-1} K^{-1}
Q = ion activity product of the solution, mol L^{-1}
K = pseudo-equilibrium constant for the glass, mol L^{-1}.

The term $\Pi a_j^{\nu_j}$ represents additional terms that may be needed to model some materials to take into account other chemical effects, such as solutes that catalyze (or inhibit) the reaction. The kinetic effects of species on the rate through that product term are independent of the thermodynamic effect they may have through the equilibrium constant, K. The effect of the hydronium ion is common enough to be shown explicitly in the general expression as $a_{H^+}^{\eta} = 10^{\eta\, pH}$. The term $\left(1 - \frac{Q}{K}\right)$ accounts for solution feedback, where Q/K gives the ratio of the solution concentration to that of a saturated solution. Since glass is thermodynamically unstable, the solution can never become saturated and a true equilibrium constant does not exist. Instead, the conditions under which the dissolution rates are immeasurably low are used as a surrogate for saturation conditions in the model, and the solution concentrations are represented by K. Note that the value of the Temkin coefficient discussed in Appendix A is presumed to be $\sigma = 1$ in this expression. This represents the simplest transition state theory formulation of the rate law. Other values of the Temkin coefficient and other nonlinearities with respect to the reaction free energy as discussed in Section 2.3 may be required to model the dissolution rates of some materials.

The SPFT test method can provide a measure of the dissolution rates at different values of pH, temperature, and solution compositions that are controlled during the test. The test conditions can be selected to maintain dilute solutions in which $Q<<K$ so that the measured rate is proportional to the intrinsic rate constant at particular pH and temperature values. Other test conditions can be used to measure dissolution rates at various steady-state compositions at fixed pH and temperature values to determine how the rate depends on the value of Q/K (that is, on the chemical affinity) and then calculate the value of K.

The dissolution rate when the value of the affinity term is one is referred to as the forward dissolution rate (or simply the forward rate). The forward rate includes all the terms preceding the affinity term and depends on the composition of the glass, temperature and solution pH, and may depend on other solute concentrations. It is important to note that the dissolution rate cannot be measured in the *total* absence of feedback effects because a minimum concentration is required for the analytical measurements that are used to determine the dissolution rate. That is, the analytical limit of quantization establishes the minimum solution feedback effect that must be attained to measure the dissolution rate. As discussed in the ASTM C1662 test method, the rate in the absence of feedback effects can be estimated by extrapolating the rates measured under various levels of solution feedback to zero concentration. Although this is the preferred approach, many researchers simply assign the rate measured at the highest affinity condition that is achieved to be the forward rate.

6.2.1 Determining the Dissolution Rate from Experimental Results

An experimental dissolution rate can be calculated from the amount of any soluble component i released into solution from a known exposed surface area over a known duration, if the material dissolves stoichiometrically and the mass fraction of component i in the material are known. The expression used to calculate the rate is

$$rate = \frac{m(i)}{S^{\circ} \bullet f(i) \bullet t} \tag{6.16}$$

where

$m(i)$ = mass of element i released from the test specimen, g
S° = initial surface area of the test specimen, m^2
$f(i)$ = mass fraction of element i in the original test specimen, unitless
t = test duration, s.

The term $f(i)$ is included to relate the mass of element i that is measured to have been released to the total mass of the test specimen that has dissolved. For dissolution of a mineral phase having a homogeneous composition, $f(i)$ gives the relationship between the element that is tracked and the mineral, and may be replaced by the stoichiometric coefficient. The solution concentrations of species with high solubility limits are usually tracked to represent the extent of reaction. Fractions of some components will become sequestered in alteration phases or remain as insoluble residue on the specimen surface such that their solution concentrations do not accurately represent the extent of specimen dissolution. Expressing the amount of the released component i as a concentration gives

$$rate = \frac{C(i) \bullet V}{S^{\circ} \bullet f(i) \bullet t} \tag{6.17}$$

where

$C(i)$ = concentration of element i released from the specimen, g m^{-3}
V = volume of solution, m^3.

Under flowing conditions and at steady state, the concentration of i due to dissolution is the measured steady-state concentration $C^{ss}(i)$ minus the background concentration of i present in the leachant used in the test $C^{\circ}(i)$

$$C(i) = C^{ss}(i) - C^{\circ}(i). \tag{6.18}$$

Defining the ratio V/t as the volumetric flow rate F and substituting Equation 6.18 into Equation 6.17 gives

$$rate = \frac{[C^{ss}(i) - C^{\circ}(i)] \bullet F}{S^{\circ} \bullet f(i)} \tag{6.19}$$

and

$$C^{ss}(i) - C^{\circ}(i) = \frac{rate \bullet F}{S^{\circ} \bullet f(i)} \tag{6.20}$$

where

$C^{ss}(i)$ = steady-state concentration of element i in the effluent, mg L^{-1}
$C^{\circ}(i)$ = concentration of element i in the leachant, mg L^{-1}
F = leachant volumetric flow rate, m^3 s^{-1}
S° = initial surface area of the test specimen, m^2
$f(i)$ = mass fraction of element i in the test specimen.

Note that the rate and steady-state concentration are both proportional to the ratio of test parameters F/S°, so that high flow rates and low specimen surface areas have the same effect on the steady-state concentration and on the rate.

The dissolution rates in the SPFT tests (at constant pH and temperature) are calculated using Equation 6.19. The dissolution rate is often referred to as the normalized dissolution rate, $NR(i)$, to emphasize that the rate is based on the release of element i and that it is normalized to the surface area of the test specimen. Note that the value of $NR(i)$ is in terms of the mass of the test specimen dissolved due to the $f(i)$ term in the denominator, not the mass of element i that is released.. Note also that Equations 6.19 and 6.20 are written in terms of the initial surface area, which can be measured directly for sufficiently large specimens and estimated based on the mass and the size fraction (specific surface area) of the crushed material used in the test. A commonly used method

to take the change of surface area of crushed samples during the test into account is to model the particles as shrinking spheres (e.g., McGrail et al. 1997a). This relates the decrease in surface area to the amount of material that has dissolved by calculating the final surface area of the reacted glass, S_f, from the mass of the sample at the end of the test interval as calculated from the dissolution rate and reaction time as

$$S_f = \left\{\frac{6}{\rho \bullet d_o}\right\} \bullet m_o^{1/3} \bullet m_f^{2/3}, \tag{6.21}$$

where ρ is the density of the glass, d_o is the initial diameter of the glass particle, M is the initial mass of the sample, and m is the final mass of the sample. The final mass of the sample is calculated from the mass that has dissolved as

$$m_f = m_o - rate \times S_o \times t. \tag{6.22}$$

The fractional change in the surface area is

$$\frac{S_f}{S_o} = \frac{\left\{\frac{6}{\rho \bullet d_o}\right\} \bullet M^{1/3} \bullet m^{2/3}}{\left\{\frac{6}{\rho \bullet d_o}\right\} \bullet M} = \left(\frac{m}{M}\right)^{2/3}. \tag{6.23}$$

The pH and temperature dependencies of the rates can be determined by equating Equation 6.19 and Equation 6.15 at steady state as

$$rate\ at\ steady\ state = \frac{[C^{ss}(i) - C^{\circ}(i)] \bullet F}{S^{\circ} \bullet f(i)} = k_0 \bullet \prod a_j^{\nu_j} \bullet 10^{\eta pH} \bullet \exp\left(\frac{-E_a}{RT}\right) \bullet \left(1 - \frac{Q}{K}\right). \tag{6.24}$$

Equation 6.24 provides the relationship between the experimental results at steady state and the theoretical rate law for affinity-controlled dissolution. Application of Equation 6.24 requires definition of the surface area as the initial, final, average, or weighted surface area. For tests in which the flow rate or leachant composition is varied to attain several steady-state conditions during the reaction of the same specimen, a different value of the surface area may be appropriate for different intervals. It may also be possible to relate the test results to diffusion-controlled release over a sampling increment, as quantified in Equation 4.7:

$$rate = \frac{[C(i) - C^{\circ}(i)] \bullet F}{S^{\circ} \bullet f(i)} = \frac{A_o}{V_{wf}} \left(\frac{D_e}{\pi}\right)^{1/2} T^{-1/2}. \tag{6.25}$$

It is of interest to predict the response of a material that releases contaminants by a diffusion-controlled process in a flow test. Steady-state conditions are not achieved in a diffusion-controlled process and the rate is expected to depend on the reaction time. This will provide evidence of a diffusion-controlled process for a material reacted in a flow-through test.

6.2.2 Significance of the Measured Rate

Although a dissolution rate can be calculated from the release over any test period, the meaningfulness of that rate depends on the test conditions. The objective of most tests with waste forms is to determine a material property or parameter value for a mechanistic model to calculate long-term behavior, where the release is controlled by diffusion, dissolution, or another process. Historically, the various test methods have been referred to as leach tests or dissolution tests according to the presumed release mechanism of the contaminant from the host material being tested. Unfortunately, these are often misnomers and a particular test method can be successfully applied to various materials that degrade by leaching, dissolution, oxidative-dissolution, or other mechanism. An important issue considered in this report is how to properly interpret a test response for a particular degradation mechanism. The relationship of the rate measured in a flow-through test and the material dissolution rate is discussed below.

Consider the reaction of a specimen with surface area S contained in a cell volume V that occurs when contacted by a solution with flow rate F. As an example, consider the release of Si as a silicate mineral dissolves with the affinity term dependent on the dissolved silica concentration. The variation in the concentration of Si in the reaction cell over time is the difference between the amounts of Si added by dissolution of the specimen and removed from the cell due to flow

$$\frac{dC(Si)}{dt} = \frac{S}{V} k_f \left(1 - \frac{C(Si)}{K}\right) - \frac{F\,C(Si)}{V} . \tag{6.26}$$

The first term on the right-hand side of Equation 6.26 gives the rate at which Si is added to the solution in the cell (where the rate coefficient k_f represents the product of the intrinsic rate constant, pH dependence, and temperature dependence terms) and the second term give the rate at which dissolved Si is removed from the cell. Under constant flow conditions, steady state will occur when the rate at which Si is added to the cell by specimen dissolution is the same as the rate Si is removed from the cell by flow. The rate at which Si must be added by specimen dissolution to maintain steady-state conditions at a particular flow rate is determined by setting $dC(\mathrm{Si})dt = 0$ and solving for $C(\mathrm{Si})^{ss}$. The dissolution rate necessary to maintain steady-state conditions can be expressed in terms of the number of moles of Si released under steady-state conditions $n(\mathrm{Si})^{ss}$, which is simply the product of the cell volume and steady-state Si concentration

$$n(Si)^{ss} = VC(Si)^{ss} . \tag{6.27}$$

Expressing Equation 6.26 in terms of the number of moles of silicon (or dissolved silica)

$$\frac{dn(Si)^{ss}}{dt} = V\left\{\frac{S}{V} k_f \left(1 - \frac{C(Si)}{K}\right) - \frac{F\,C(Si)}{V}\right\} \equiv 0 . \tag{6.28}$$

Solving Equation 6.28 for $C(\mathrm{Si})$ gives

$$C(Si) = \frac{Sk_f}{F + {Sk_f}/{K}} , \tag{6.29}$$

and so

$$\frac{dn(Si)^{ss}}{dt} = \left(\frac{S k_f}{F + {}^{Sk_f}/_{K}} \right) \bullet F \,. \tag{6.30}$$

In the limit of high flow rates, when the value of F dominates the value of the denominator, the dissolution rate is independent of the flow rate:

$$\frac{dn(Si)^{ss}}{dt} = S k_f \,. \tag{6.31}$$

A threshold flow rate exists at which the material dissolves at the highest possible rate and further increases in the flow rate will not affect the reaction rate, although they will lower the steady-state Si concentration. Lower flow rates establish a unique steady-state condition for each value of F/S and a material dissolution rate corresponding to C_{Si}^{ss}. In the limit of low (but non-zero) flow rates, the release rate will become proportional to the flow rate (and the equilibrium constant) as

$$\frac{dn(Si)^{ss}}{dt} = KF \,. \tag{6.32}$$

These limiting rates are shown schematically in Figure 6.7. This result is very important for interpreting any dynamic test method: the dissolution rates under moderate and slow flow conditions relevant to Equation 6.30 and Equation 6.32, respectively, will depend on the flow rate that is used in the test. Only those dissolution rates measured in tests conducted at flow rates high

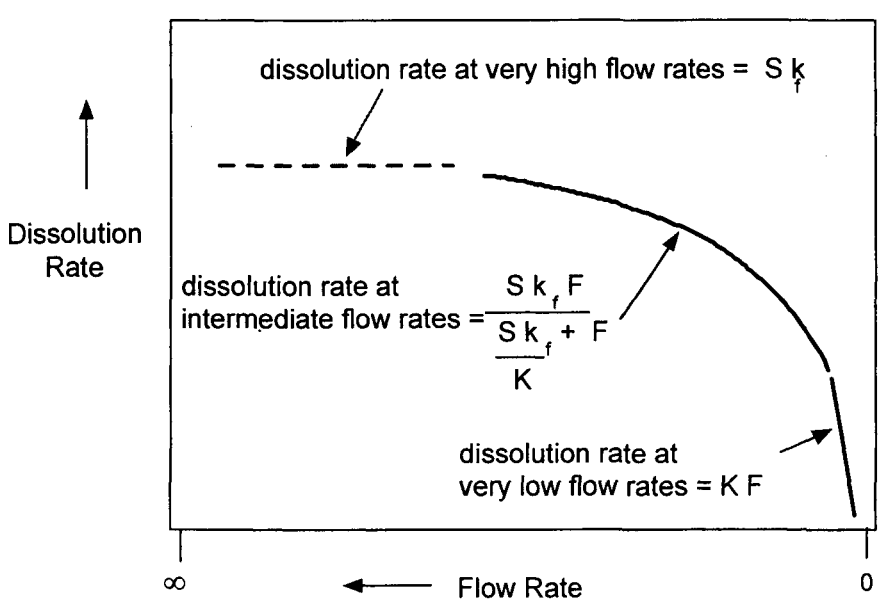

Figure 6.7. Schematic plot of dissolution rate dependence on flow rate and limiting values. The dashed horizontal line represents the forward dissolution rate.

enough that the steady-state concentration of the rate-controlling component (e.g., Si for the dissolution of most silicate minerals and glasses) is negligible with respect to the solubility product of the dissolving material are expected to be independent of the flow rate. This corresponds to the dissolution plateau in Figure 2.3 when ΔG_r has a large negative corresponding to Q/K having a value very near zero. For most materials, it will be very difficult to measure the very low steady-state concentrations generated under these test conditions and k_f can only be estimated as a limiting value constrained by the analytical uncertainty. Note that the form of Equation 6.17 assumes a linear dependence of the rate on the affinity term (ΔG_r) (that is, the parenthetical term within the braces is of first order). Nonlinearity will affect the form of Equation 6.30 but not the limiting cases in Equations 6.31 and 6.32.

Steady state cannot be attained when the flow rate is zero. In the absence of flow, dissolution will occur at a decreasing rate until the solution becomes saturated, at which time dissolution will cease. This corresponds to values of Q/K near 1 (which is equivalent to values of ΔG_r near 0). As discussed in Section 2.3, the rate-controlling process may change as equilibrium is approached, resulting in nonlinear behavior. In the case of glass, which is thermodynamically unstable, a pseudo-saturation concentration is reached and dissolution continues at a very low rate that is probably controlled by other processes involved in the dissolution mechanism, such as water diffusion into the glass, ion exchange, or the hydrolysis of bonds other than Si-O. Similar to the nonlinear dependence on ΔG_r discussed in Section 2.3, another term may be required to describe glass dissolution as ΔG_r approaches zero.

Note that Figure 6.7 was drawn to stress the similarity with Figure 2.3. The flow rate (actually F/S) that is used in a test will establish the steady-state solution composition and the value of the affinity term ($1-Q/K$), which is equivalent to $-\Delta G_r$. In fact, SPFT and column tests are used to study the relation between the dissolution rate and the free energy. Saturated solutions can be used as leachants in SPFT tests and saturated solutions can occur near the exit in packed column tests conducted at low flow rates.

Finally, the release of Si was used in this discussion to measure the extent of dissolution, but other components can be used. The component (or components) used to track material dissolution should be selected based on the material of interest and the dissolution reaction. The component must be uniformly distributed in the phase to reliably represent the volume (or mass) that has dissolved and should have a high solubility limit in the leachant so that the measured solution concentration reflects the amount that has dissolved. The release of a contaminant from a material will usually not represent the extent of material dissolution well. Instead, the measurement is intended to quantify the dissolution rate of the material hosting the contaminant.

6.3 Single-Pass Flow-Through Test Method

The single-pass flow-through (SPFT) test is a dynamic test method in which leachant is pumped through a reaction cell containing the test specimen (which is usually a crushed material) at a constant rate and the effluent solution is collected and analyzed for dissolved constituents (see Appendix E Section E.5). Tests are conducted to attain steady-state conditions within the reaction cell as determined by the leachant composition and flow rate and the material dissolution rate. Tests can be conducted to maintain particular solution conditions (and temperature) to measure the effects of specific variables on the dissolution (or precipitation) rate of the specimen. As discussed in Section 6.1.3 for column tests, the flow rate used in an SPFT test will also influence the measured rate and must be deconvoluted to characterize the dissolution rate of the specimen.

The high flow rates necessary to remove the flow dependence of the dissolution rate will almost certainly result in test solutions that are too dilute to measure solution concentrations reliably. The effect of the flow rate on the material dissolution rate occurs through the steady-state concentrations of dissolved components and how that concentration affects the affinity term. That is, the dependence of the dissolution rate on the flow rate reflects the effect of the affinity term on the dissolution rate. Therefore, the magnitude of the equilibrium constant K in the affinity term determines the sensitivity of the rate to the steady-state solution composition (which provides the value of Q in the affinity term). The dissolution rates of materials with small K values (i.e., sparingly soluble materials) will be more sensitive to the solution concentration than those of materials with large K values (i.e., highly soluble materials) because the affinity term is sensitive to the ratio of Q/K, which is the saturation index. That is, the amount of material that must dissolve to slow the dissolution of a material having a large K value is greater than the amount of a material having a small K value that must dissolve to have a similar impact.

It is important to note that the effect of a component on the affinity term is independent of the effect that component may have on k_f for the material: the effect on k_f is a kinetic effect that is quantified by the term $\prod a_j^{\nu_j}$ in Equation 6.5, whereas the effect on the affinity term is a thermodynamic effect that is quantified by the term Q/K in Equation 6.5. The kinetic effect of a component is usually measured under test conditions in which the affinity effect is negligible (i.e., under conditions in which the value of Q/K is near zero). The thermodynamic effect is measured under test conditions close to equilibrium.

6.3.1 Forward Dissolution Rates

In practice, dissolution rates are measured under several test conditions that yield a range of quantifiable solution concentrations approaching the analytical detection limit for the component that is being used to track the extent of dissolution. The observed relationship between the measured rates and concentrations is then extrapolated to estimate the forward rate when the concentration is zero (infinitely dilute solution). With reference to Figure 6.7, the experiments are used to measure the highest rates of the curve for intermediate flow rates to estimate the rate represented by the dashed horizontal line for very high flow rates. An example is provided by the results of an inter-laboratory study using the ASTM C1662 SPFT test method (Ebert 2005b). The dissolution rate of the borosilicate glass LRM was measured based on the Si concentration in tests conducted with various amounts of crushed glass reacted in flowing solution that imposed a pH of about 10 at 70°C. The combination of the surface area of glass (based on the mass of glass) and solution flow rates resulted in various steady-state Si concentrations being generated in the tests. A particular steady-state Si concentration fixes the glass dissolution rate at a particular temperature and pH through the value of Q according to Equation 6.5. The objective of the test series was to measure the dissolution rates in separate tests as the steady-state Si concentration approached the analytical detection limit. Since the steady-state concentration is sensitive to the ratio of the leachant flow rate-to-glass surface area (F/S), the variance in F/S in the set of samplings used to determine the steady-state Si concentration was limited to 10%. (The surface area was assumed to remain constant during a test and the variance was attributed solely to the flow rate.) Two examples are shown in Figure 6.8, where the ratios of the leachant flow rate to the glass surface area and the measured Si concentrations are plotted for consecutive samplings. For the experiment shown in Figure 6.8a, the flow rates were acceptably constant except for the first sampling (the results of which are shown with open symbols), so the Si concentrations measured in sample numbers 2, 3, 4, and 5 were averaged to obtain the steady-state Si concentration of 28.63 mg L^{-1} for the average F/S value of 1.75×10^{-8} m s^{-1}. These values were used in Equation 6.9 (the Si

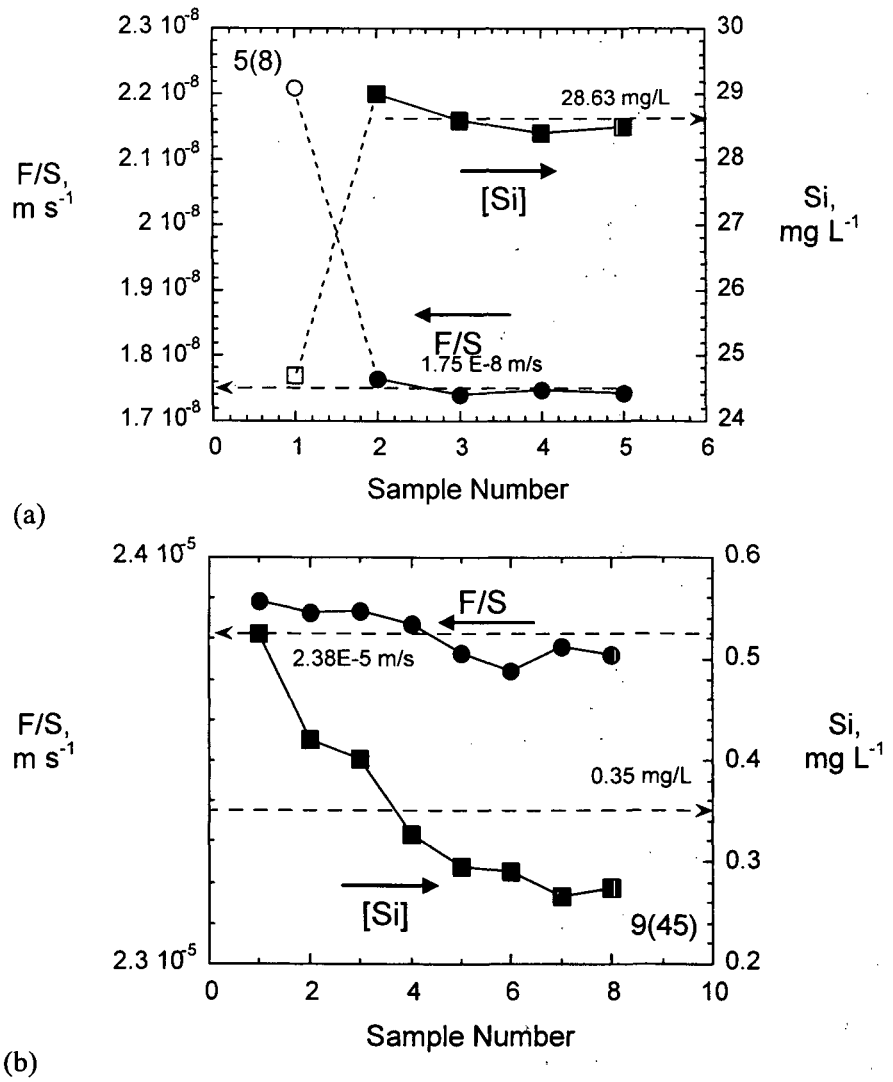

Figure 6.8. Results from Ebert (2005): SPFT tests with LRM-1 glass (a) test 5(8) conducted at an intermediate flow rate ($F/S = 1.75 \times 10^{-8}$ m s^{-1}) and (b) test 9(45) conducted at a very high flow rate ($F/S = 2.38 \times 10^{-5}$ m s^{-1}). The results shown by filled symbols were used to determine steady-state *F/S* (filled circles) and Si concentrations (filled squares) whereas results shown by open symbols were excluded.

background concentration was 0.42 mg L^{-1} and the mass fraction of Si in the glass was 0.2533) to calculate a dissolution rate of 0.168 g m^{-2} d^{-1}. For the experiment in Figure 6.8b, the flow rate was acceptably constant in all eight samplings at 2.38×10^{-5} m s^{-1} and all of the measured values were averaged to determine the steady-state Si concentration of 0.35 mg L^{-1}. The Si concentration is decreasing significantly in successive samplings due to the loss of surface area at the high dissolution rate under these high flow rate conditions. Those values were used in Equation 6.9 (the Si background concentration was 0.08 mg L^{-1} for that test) to calculate a dissolution rate of 2.20 g m^{-2} d^{-1}. Note that this steady-state Si concentration is only 4 times the background concentration. Generally, an analyte is reliable if it is more than 3 times the limit of detection. Only a slightly higher *F/S* value could have been used to measure the rate.

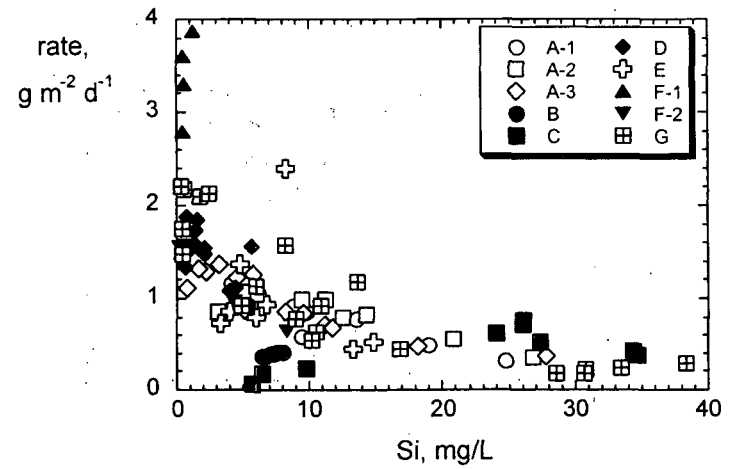

(a)

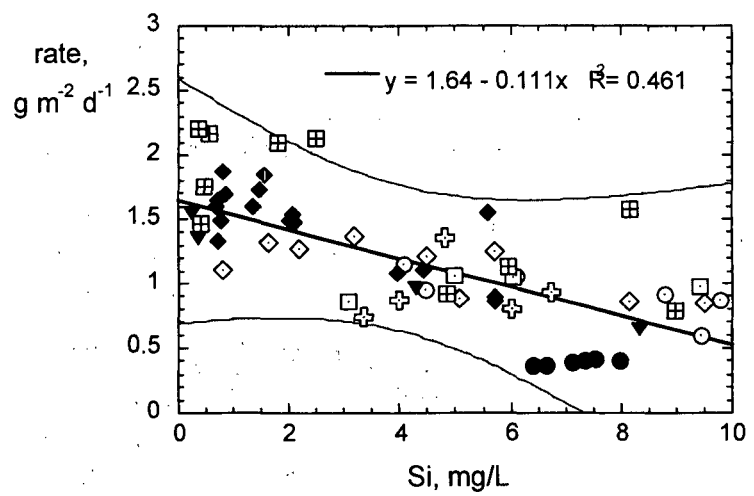

(b)

Figure 6.9. Results from Ebert (2005b): SPFT tests with LRM glass (a) combined results from all participants and (b) subset of results with rates <2.3 g m^{-2} d^{-1} and steady-state Si concentrations <10 mg L^{-1}. All of the results plotted in (b) are included in the regression fit.

The rates measured by several participants are plotted against the steady-state Si concentrations in Figure 6.9a. The pooled results with Si concentrations below 10 mg/L were used to determine the rate when the silica concentration was zero and the value of the affinity term was one by linear regression. The results provided by Participant F-1 were excluded because they represent the initial dissolution rate of the fractured surfaces rather than that of the bulk glass (see Section 6.3.2). Figure 6.9b shows a linear regression fit to data to determine the rate at Si = 0. The y-intercept of the linear regression line approximates the value of the affinity term at $Q \rightarrow 0$. For the system in Figure 6.9b, the y-intercept gives a dissolution rate of 1.64 g m^{-2} d^{-1}.

Flow-through tests are conducted to achieve steady-state conditions to measure model parameter values. Otherwise, the measured rates are limited to qualitative comparisons with the same or other materials reacted under the same or other test conditions. As mentioned previously, the initial dissolution of crushed material should be neglected in measuring the dissolution rate with the SPFT test method or any method that is sensitive to the initial stages of dissolution. This is

because crushing results in fines and particles having fractured surfaces with sharp points and edges that dissolve faster than the flat surface. Fine particulates can be removed by repeatedly rinsing the crushed material and ultrasonication, but the sharp edges must be dissolved. This could be done in a separate dissolution step in the specimen preparation procedure or allowed to occur during the test. A decrease in amount of material dissolved as the sharp edges are removed can be seen in the test response as the solution approaches a steady-state Si concentration. The initial dissolution of fracture edges of a crushed glass was measured to occur about three times as fast as dissolution of the flatter surfaces; the high rates shown for Participant F-1 in Figure 6.9a are due to dissolution of the fractured glass during the first several hours of the test. These results are discussed in the following section.

6.3.2 Surface Area of Crushed Material

A significant loss of surface area occurs in SPFT tests over time as the high-energy sites that are generated when a material is crushed for testing are dissolved faster early in the test than the smoother surfaces that predominate later in the test. Material in the sharp edges generated during fracturing will dissolve faster than the material on smooth faces and will dominate the initial test response. The higher dissolution rates of these features may be due in part to the high curvatures of the fracture edges, the residual stress from the forces that caused the fracture, the generation of excess kink, step, and edge sites relative to the reacted surfaces, etc. (e.g., Petrovich 1981, Knauss and Wolery 1986, Eggleston et al. 1989). Regardless, the majority of sites that dissolve preferentially are artifacts of specimen preparation and do not represent the dissolution behavior of the bulk material. That is, the preferential dissolution of these defect sites will lead to smoother surfaces over time. In SPFT tests, the effect of fracture artifacts on the dissolution of material at the beginning of the test can simply be ignored by excluding the initial solutions from analysis of the dissolution rate. Fracture edges also affect the results of static tests with crushed materials, such as ASTM C1285. Although the contribution of fracture sites is included in the accumulated solutes at all test durations, it provides a nearly constant contribution to all solutions that has a negligible effect on the rate, which is determined from the differences in concentrations. The contributions of the fracture surfaces to the final solution compositions become insignificant as greater amounts of bulk material dissolve during the test. The results of static tests are often used to characterize the approach to solution saturation, in which case the faster dissolution of the fracture surfaces is irrelevant.

The time required to dissolve the fracture surfaces will depend on the reaction conditions (primarily pH and temperature). The results of SPFT tests usually reveal when this occurs. An example is shown in Figure 6.10a for the dissolution of a borosilicate glass at pH 11 (measured at room temperature) and 70°C (Ebert 2005b, Figure 11b). Figure 6.10a shows the silica concentrations and flow rates (normalized to the specimen surface area, *F/S*) in successive samples to increase from about 0.2 mg L^{-1} in the initial sample to greater than 0.6 mg L^{-1} within the first 30 minutes (the Si concentration is plotted as squares corresponding to the left-hand axis). The Si concentration increases during the first few samplings because those solutions include the leachant that is present in the reaction cell and effluent line when the test is started; that solution dilutes the Si released from the glass prior to attaining steady-state conditions within the reaction cell. Steady state is also delayed due to the variance in flow during the first 286 minutes. The concentration decreases rapidly after about 290 minutes to an average value of 0.400 mg L^{-1} for samples taken between 344 and 4440 minutes (shown by the filled squares) under nearly constant flows (shown by the filled circles). The average value was used as the steady-state concentration. The test results for the steady-state Si concentration of 0.4 mg L^{-1} Si and F/S of 2.38×10^{-5} m s^{-1} give the rate of 2.8 g m^{-2} d^{-1} that is plotted in Figure 6.9a at for the test conducted by Participant F-1 as part of the interlaboratory study.

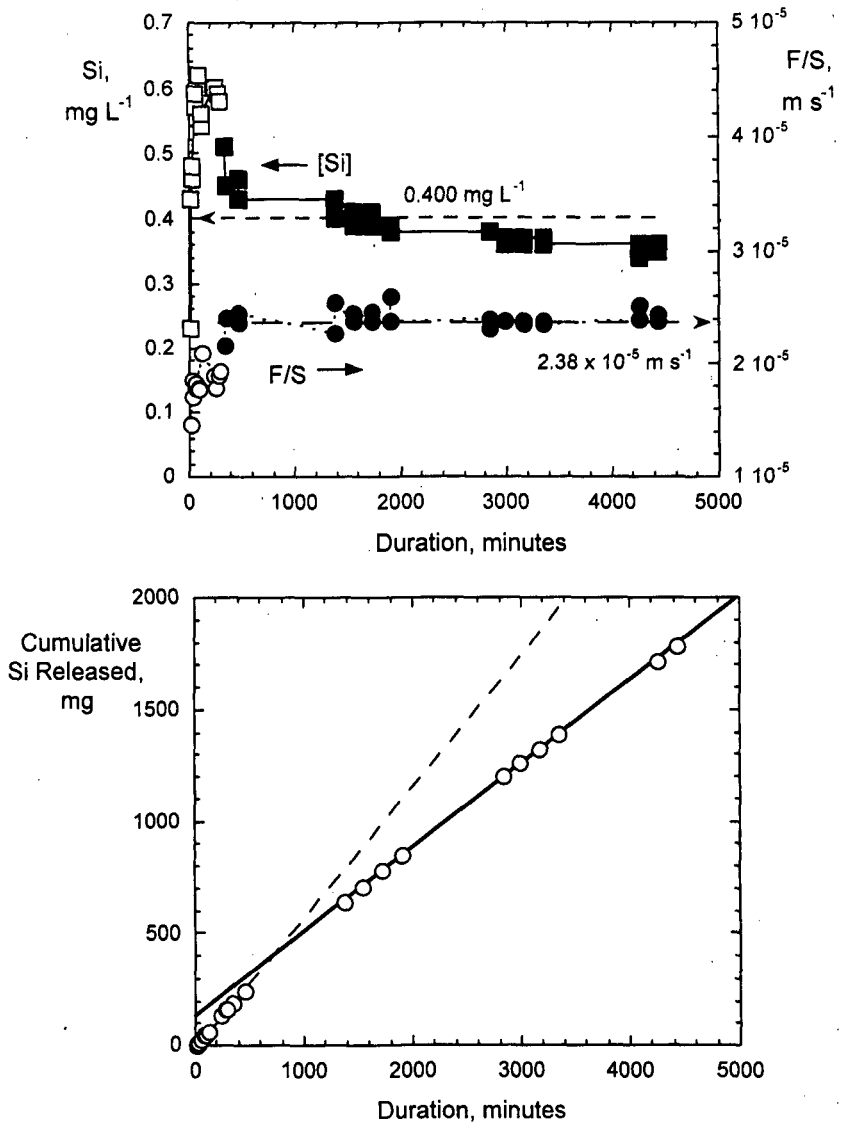

Figure 6.10. Results from Ebert (2005b): SPFT tests showing (a) leachant flow rate normalized to specimen surface area *F/S* (circles) and Si concentration (squares) for each sampling and (b) cumulative release vs. cumulative reaction time. Filled symbols in (a) were used to determine steady-state values. Results through 600 minutes show variance due to unstable flow and faster dissolution of fractured edges.

The continuing slow decrease in the Si concentration is due to the loss of surface area as the material dissolves under the aggressive conditions that were used in these tests, although the slightly higher flow rate beyond 360 minutes also contributes to the lower Si concentrations. The Si releases plotted in Figure 6.10b for samplings up to 286 minutes and beyond 1300 minutes show linear increases. The initial samplings are dominated by dissolution of the fractured edges and the later samplings indicate when all glass surfaces are dissolving at the same rate under these test conditions of temperature, pH, and leachant flow rate. This same behavior was seen in tests

with albite (Knauss and Wolery 1986). Knauss and Wolery (1986) referred to the constant rate that was attained at longer reaction times as the "limiting rate" and the mass contributed by the "disturbed" surfaces of the prepared test material as "excess mass". The y-intercept of the line in Figure 6.10b indicates that the dissolution of fracture edges contributed an excess of 135 mg Si relative to bulk dissolution. The limiting rate indicates that the results of samplings at 344, 345.5, 464, and 465.5 minutes should have been excluded from the steady state average shown in Figure 6.10a, even though the flow rate had stabilized. It is difficult to distinguish the decrease in surface area due to the dissolution of fracture edges from the decrease in surface area due to the uniform dissolution of the particles. This could be facilitated by fitting the decreasing Si concentration with the equation for the surface area of a shrinking sphere.

A much longer duration would be required for the transient effects of fracture surfaces to diminish in a packed column test than in a fluidized bed due to the lower flow rates and less aggressive conditions. Note that significant changes in the cumulative fractions of most elements occur after about 16 days in the column tests with the three slags. Considering the more aggressive conditions used in the SPFT tests (pH 11 and 70°C at very high flow rates), 16 days is not an unreasonable reaction time to dissolve the sharp fracture surfaces in the material used in the column tests. Subsequent dissolution behavior in column tests can also be affected by the formation of surface layers on the test particles due to diffusive release of some components, non-stoichiometric dissolution, and the formation of Si-bearing alteration phases from the concentrated test solutions that could form in pores and dead-end channels.

It is interesting to note that the release rate of Si is *greater* at longer cumulative durations (and for longer sampling intervals) in the column tests with all three slags (see Figure 6.2). This behavior is contrary to expectations for either diffusion-controlled or affinity-controlled release due to mass transport. Another experimental variable that must be taken into account is the solution pH. It is possible that longer residence times (due to lower flow rates) will result in higher solution pH values that increase the dissolution rates of some phases (e.g., glass). However, the pH values of the effluent solutions exceeded pH 11 in the earliest samplings. The accelerating effect of pH can overwhelm the slowing effect of the chemical affinity, as discussed in the next section. Another aspect of column reactors that must be considered is the effect of mass transport within the column. Components released near the entrance to the column may interact with solids contacted as they are transported through the column to retard their release.

6.3.3 Model Parameter Values

By using pH buffer solutions as leachants; spiking the leachant with components of interest, dissolved gases, etc.; and conducting tests at different temperatures, various dependencies can be measured to parameterize the rate model expression. In most cases, the leachant composition and test conditions are selected to maintain the value of the affinity term near one (e.g., McGrail et al. 1997a; Hanson et al. 2004; Pierce et al. 2008). For example, Figure 6.11 shows the results of SPFT tests with the borosilicate glass LD6-5412 conducted at different fixed pH values and temperatures (McGrail et al. 1997a). Regression to the pH-dependence modeled in Equation 3.3 gives $\eta = 0.40$ and then fitting the rates at a particular pH value to the Arrhenius term in Equation 3.3 gives the activation energy $E_a = 74.8$ kJ mol^{-1}. The intrinsic rate constant was then calculated to be $k_o = 112$ g m^{-2} d^{-1}). (where $\log k_o = 2.05$). If the value of K is known (e.g., from the results of ASTM C1285 Method B tests), the dissolution rate of LD6-5412 glass can be calculated with Equation 3.3 at any temperature, pH, and Si solution concentration.

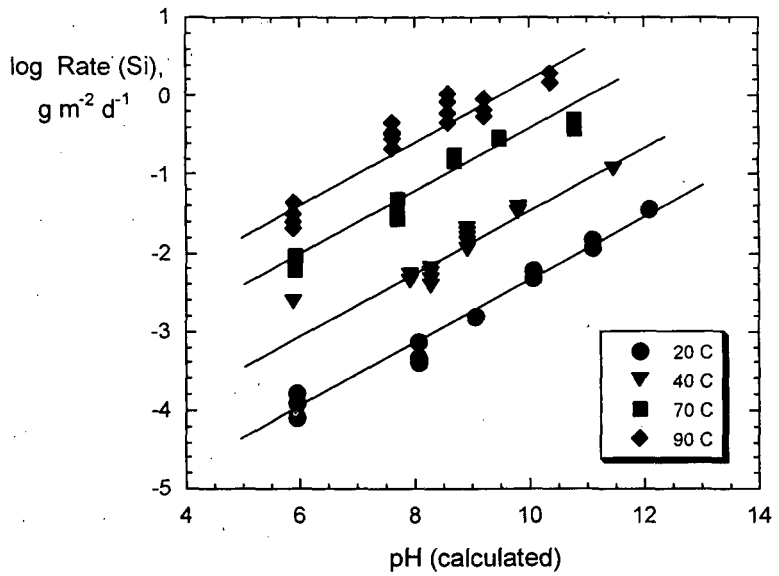

Figure 6.11. Results from McGrail et al. (1997a): SPFT tests with LD6-5412 glass at various temperatures and pH values.

6.3.4 Dependence on Chemical Affinity

The SPFT test method can be used to maintain a steady-state solution composition by spiking the leachant with the components of interest. For example, Yang and Steefel (2008) conducted tests to study the dissolution and precipitation of kaolinite at 22°C and pH 4 in solutions with various amounts of dissolved Si and Al in the leachant. The rates were calculated based on the measured Al concentration in the effluent solution after steady state was attained. The effluent composition was used to calculate the saturation index and Gibbs free energy of reaction

$$\Delta G_r = RT \ln\left[\frac{Q}{K}\right]. \tag{6.33}$$

The solubility constant was measured to be $K = 10^{7.57}$ close to equilibrium. Yang and Steefel (2008) expressed the relationship between the dissolution rates and the reaction affinity as

$$rate = -1.15\times10^{-13}\left[1-\exp\left(\frac{\Delta G}{2RT}\right)\right], \tag{6.34}$$

where the rate is in units of mol m^{-2} s^{-1} and the Gibbs free energy of reaction is in units of kJ mol^{-1}. (Note that Equation 6.34, which is plotted in Figure 6.12, differs from the equations given in the abstract and discussion sections of Yang and Steefel (2008), both of which contain typographical errors: both equations omit the negative sign in front of the constant and the equation in the abstract includes an incorrect negative sign in the argument of the exponent.) The value of 2 in the denominator of the argument of the exponential term gives the Temkin coefficient ($\sigma = 2$). The value of the constant term before the affinity term is particular to the test conditions of 22°C and pH 4 and to the composition of the kaolinite specimen, probably with functional dependencies similar to those given in Equation 6.5.

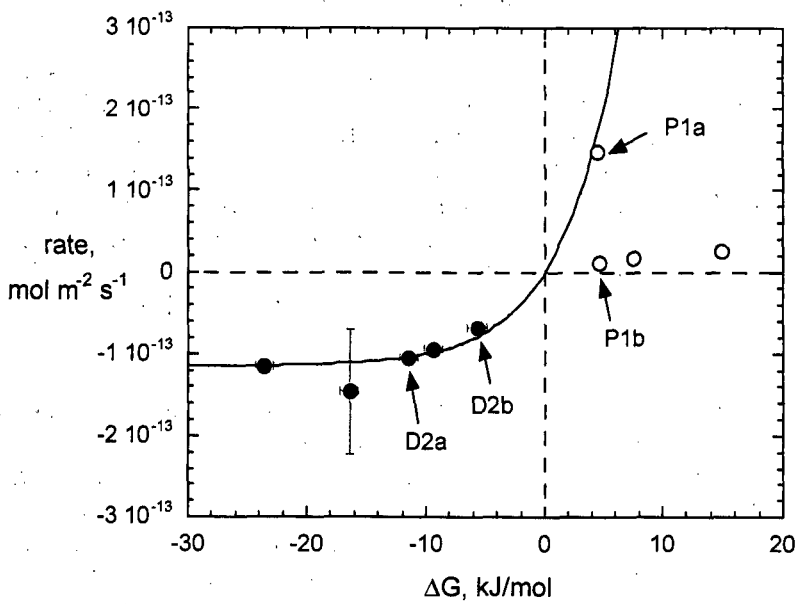

Figure 6.12. Results from Yang and Steefel (2008): SPFT tests with kaolinite at 22°C and pH 4. Measured dissolution and precipitation rates with dissolution rates fitted using Equation 6.34.

Increasing the flow rate used in the test resulted in lower steady-state concentrations, lower values of ΔG_r due to the greater diluting effect, and higher dissolution and higher precipitation rates. The data points labeled D2a and D2b in Figure 6.11 are from tests conducted with about 0.3 m<u>M</u> Si and no added Al at flow rates of 0.041 and 0.012 mL minute^{-1}, respectively. The solution is undersaturated with respect to kaolinite in both tests, but the higher flow rate resulted in lower steady-state solution concentrations, a lower value of ΔG_r and a high dissolution rate. The data points labeled P1a and P1b in Figure 6.9 are from tests conducted with about 0.5 m<u>M</u> Si and 0.1 m<u>M</u> Al at flow rates of 0.05 and 0.005 mL minute^{-1}. The leachant solution is equally supersaturated with respect to kaolinite solubility in both tests ($\Delta G_r = 5\ kJ\ mol^{-1}$), but precipitation occurred about 1.5 times faster in test P1a conducted at the higher flow rate than in test P1b, and (only) that data point is consistent with the model of the precipitation rates shown by the curve. Yang and Steefel (2008) suggested that this may have been a result of prior use of that particular test specimen in long-term dissolution experiments under conditions far from equilibrium. This may have resulted in a greater density of reactive sites on that specimen than on other specimens. The other tests did not show the same degree of reversibility (i.e., precipitation) that is seen in test P1a and display a linear dependence on ΔG_r.

We make note of these experiments for comparison to the discussion regarding near-equilibrium behavior in Section 2.3 and Figs. 2.2a and 2.2b. Most of the test methods and results evaluated in this report address conditions that are far from equilibrium. In general, the theory and experimental methodology is much further advanced for addressing the kinetic terms of the rate law equations (e.g., the description of the $rate_{forward}$ term in Equation 2.22) than the thermodynamic terms (e.g., the $1\text{-}Q/K$ term in Equation 2.22). A better understanding of near-equilibrium behavior is needed to accurately model degradation behavior in saturated microsystems, such as in pore volumes within contaminated concretes or alteration layers formed on glassy wastes.

6.4 Fluidized Bed Recirculating Reactor

A test apparatus in which the solution flows through the reaction cell only once is readily modeled using the rate equations provided above. Test apparatuses that recirculate the leachate through the reaction cell to fluidize the crushed test specimen have been used to measure mineral dissolution rates. The bed of particles is fluidized to provide a homogenized suspension of particles to intensively mix the solid and fluid. One concern with fluidized bed systems is that fracturing of the particles may occur due to particle-particle collisions (e.g., Amrhein and Suarez 1992). Fluidization prevents concentration gradients at low flow rates. The flow used to fluidize the bed is typically 10 to 20 times higher than the flow used to introduce fresh leachant and extract leachate for analysis.

Chou and Wollast (1984) described a fluidized bed reactor with a feedback loop that was used to measure mineral dissolution rates and differs from the SPFT design that was considered in previous sections. The apparatus is represented schematically in Figure 6.13. The fresh leachant solution is pumped into the bottom of the fluidized bed at a rate P2 using Pump 2. The solution in the bed is recirculated at a rate P1 using Pump 1, so solution passes through the bed at a rate P1 + P2. Leachate solution is continuously removed from the fluidized bed at a rate P2 (using Pump 2) to maintain a constant flow. Tests are conducted with a pumping rate P2 that is significantly less than pumping rate P1 to maintain a fluidized bed without generating excessive amounts of eluted solution.

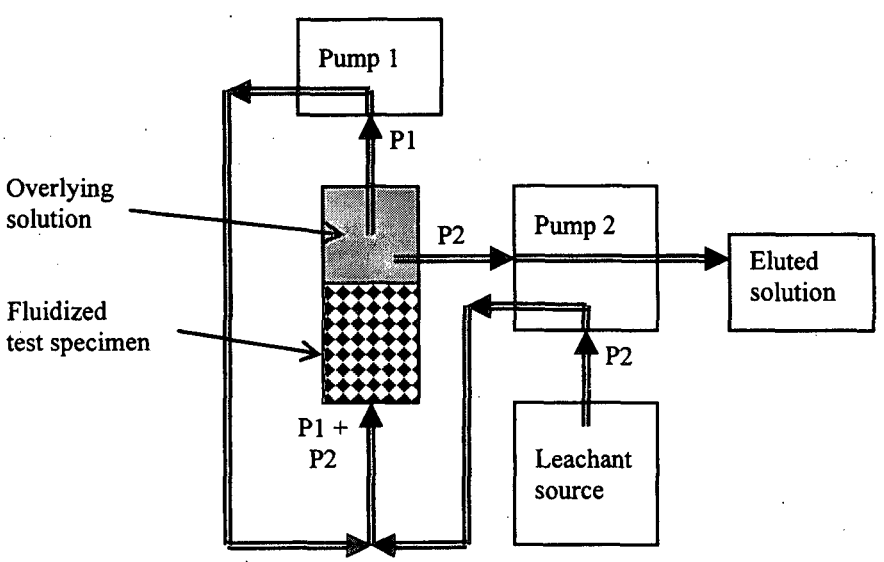

Figure 6.13. Schematic diagram of recirculating flow-through reactor.

Figure 6.14 shows the results for dissolution of albite ($NaAlSi_3O_8$) at pH 5.1 and pH 3.5 in a flow-through test conducted at P1 = 2.60 mL minute^{-1} and P2 = 0.15 mL minute^{-1}. The concentrations in the pH 5.1 leachant approach steady-state after about 100 hours of reaction. The last four measured Si concentrations give a slope of 3.3×10^{-4} μM h^{-1} and the average concentrations are 0.178 μM Al, 0.408 μM Si, and 0.390 μM Na. The flow rate *at which fresh leachant is added to* the reactor is 0.15 mL minute^{-1} and the surface area of the albite particles is about 0.3 m^2. The

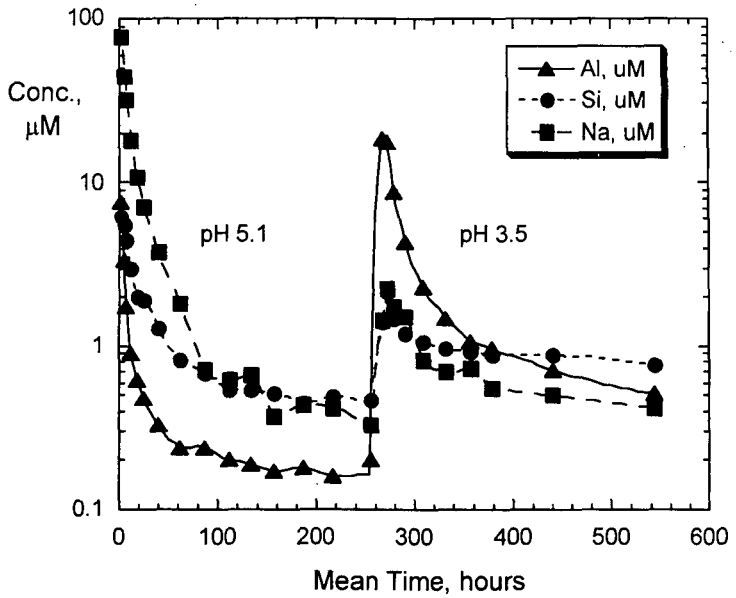

Figure 6.14. Results from Chou and Wollast (1984): Dissolution of albite at pH 5.1 and pH 3.5.

flow rate P2 is used in the calculation because the albite dissolution rate is reacting to changes in the Si concentration, not to the total flow rate *per se*; the flow provided by P1 serves only to fluidize the crushed albite and does not remove dissolved components from the solution. Assuming steady state has been attained and using Equation 6.2 (or Equation 6.9), the dissolution rates based on Na and Si are 3.25×10^{-12} and 3.42×10^{-12} mol m^{-2} s^{-1}), respectively, under these test conditions. This is the albite dissolution rate at pH 5.1 in the presence of 0.408 µM Si. From the discussion in Section 6.2.2, both the steady-state Si concentration and the albite dissolution rate will be different at different flow rates and is proportional to the flow rate at low flows.

After 263 hours, a pH 3.5 HCl solution was used as the leachant and the test continued. As seen in Figure 6.10, transient increases in the releases of Al, Na, and Si occurred that resulted in new steady-state concentrations being approached over the next 250 hours. Similar increases occurred when the leachant was changed to any pH value at which the dissolution rate increased. The few changes to lower rates did not show the transient spikes. The authors speculated that the initial increases reflected dissolution of a surface layer having a stoichiometery different from the underlying bulk. This is reasonable based on the observed non-stoichiometry of the leachates. The test results shown in Figure 6.10 may not have reached steady-state concentrations even after about 240 hours (10 days). The benefits of fluidizing the sample are debatable, considering the risk of abrasion. The response of the solution chemistry to the change in leachant composition is expected to be sluggish compared with the SPFT method due to the higher effective volume of solution in the reaction cell. The SPFT design has been used almost exclusively in waste form degradation studies.

6.5 Pressurized Unsaturated Flow Reactor

The pressurized unsaturated flow (PUF) reactor was developed recently at Pacific Northwest National Laboratory to simulate waste form degradation under hydrologically unsaturated conditions such as those expected in the Yucca Mountain disposal system (McGrail et al. 1997b).

The test apparatus utilizes a porous titanium plate at the exit of the reaction column to conduct fluid but not air when the inlet is slightly pressurized. By establishing the appropriate pressure differential, a steady flow of fluid through a bed of crushed material can be maintained under unsaturated conditions. The fluid flows downward through the column (Pierce et al. 2006). The bed may be comprised of various materials to simulate a disposal system, for example the column may be packed with regions of crushed rock that sandwich a region of crushed waste form material. The conditions within the column may be monitored during the test (temperature, solution pH, etc.) and the effluent solution can be collected for analysis. The dissolution rate of a material can be calculated from the measured effluent concentrations of components. For a component i, the normalized dissolution rate $NR(i)$ can be calculated

$$NR(i) = \frac{\left(C_{i,l} - C_{i,b}\right)\frac{\varepsilon}{\theta}F}{S\rho\left\{(1-\varepsilon)\pi\left(\frac{d}{2}\right)^2 L\right\}f_i}. \tag{6.35}$$

where:

$C_{i,l}$ = effluent concentration of i
$C_{i,b}$ = concentration of i in the leachant
d = column diameter
L = column length containing specimen
F = volumetric flow rate
S = specific surface area
ε = porosity of the packed column
ρ = density of the specimen
f_i = mass fraction of i in the specimen
θ = fractional water content in the column

Equation 6.24 is rearranged from that given by Pierce et al. (2006) to show that it is equivalent to Equation 6.13; the net dissolution rate based on the release of component i is given by $NR(i)$. The term in braces in the denominator gives the volume of crushed solid in the column. This value multiplied by the specific surface area and density gives the exposed surface area $S°$. The ratio of the porosity to the fractional water content in the numerator relates the effluent flow rate to flow in the reactor.

Figure 6.15 shows the results of a PUF test conducted at 90°C with demineralized water and an alkali borosilicate glass referred to as LAWAN102 that contains Tc and U (Pierce et al. 2006). The results are presented as the normalized mass-loss values calculated from the effluent concentrations of various glass matrix components, Tc, and U; data for samplings less than about 50 days could not be discerned from the published plots and are excluded from the analysis. Those rates were higher than those shown in Figure 6.12, and the results in Figure 6.12 likely represent steady-state conditions. Differences in the rates determined with different elements are due to the partial retention of some elements in alteration phases, including those formed on the glass surface. The release of U from the system is most affected by its sequestration in alteration phases. The dashed lines show the linear decrease in the rate based on B, which is not sequestered, and the linear increase in the rate based on U (these linear dependences on time appear as curved lines on the logarithmic y-axis scale). Pierce et al. (2006) interpreted the decreases in the releases of B, Na, Si, and Tc to indicate the approach to equilibrium with a rate-limiting alteration phase despite the increasing rate shown by U. They cite a 10-fold decrease in the rate based on the release of B over the 1.5 year experiment. The flow rate was set at 2 mL d^{-1} and the column was vented hourly to maintain its pressure and nearly constant partial pressures of O_2 and CO_2. The volumetric water content increased from about 10% to 30% over the course of the experiment. The effluent pH remained between pH 8 and pH 9.

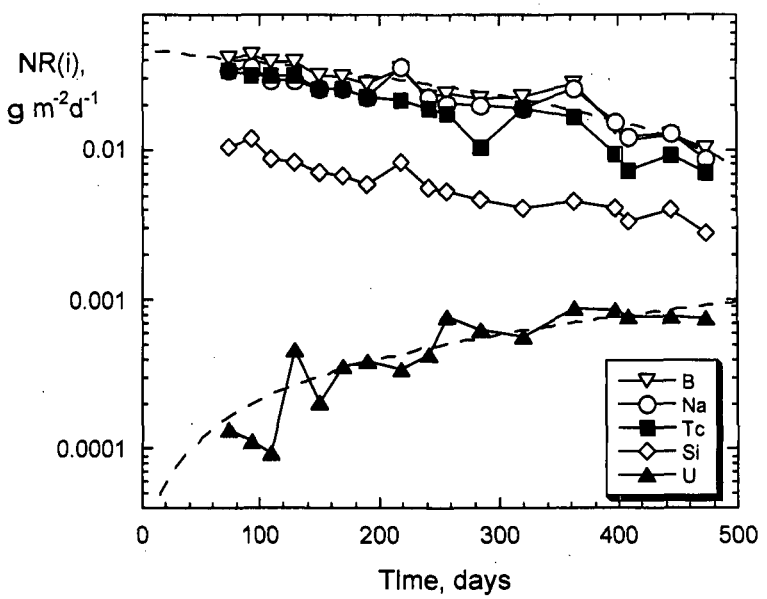

Figure 6.15. Results from Pierce et al. (2006): PUF test with LAWAN102 glass in demineralized water at 90°C.

Similar to other column test methods, the results of a PUF test are affected by solution flow, the waste degradation rate, species transport, sorption, secondary phase formation, and decrease of waste form surface area. The combined impacts of several simultaneous processes result in the contrary behavior of U compared with other elements released from the glass in Figure 6.12. The decreases in *NL(B)*, *NL(Na)*, and *NL(Tc)* are probably due, in part, to the decrease in surface area of the glass particles, since the release of these elements is not expected to be retarded by sorption or incorporation into secondary phases. The decrease in *NL(Si)* suggests Si is being incorporated into secondary phases; glass dissolution commonly results in lower values of *NL(Si)* than *NL(B)* and *NL(Na)*. The increase in *NL(U)* may indicate dissolution of a U-bearing phase that had formed early in the reaction or reflect the slower transport of U through the column. Rather than approaching equilibrium, as suggested by Pierce et al. (2006), the results may instead reveal steady-state behavior affected by the loss of reactive surface area as discussed previously for column tests. The measured rates would then be a function of the flow rate and not a characteristic of the glass.

The PUF test is a very useful method for characterizing waste form degradation under simulated service conditions of unsaturated groundwater flow. Regions of crushed geological materials can be included in the column upstream and downstream of the waste to simulate interactions of meteoric water and ground water with naturally occurring phases before and after interaction with the waste. However, the effects of several processes occurring simultaneously complicate the interpretation of the results. In most cases, other tests are needed to characterize the individual processes (waste form dissolution, sorption, secondary phase formation) to facilitate the interpretation of PUF test results. The dependence of the steady-state rates on the flow rate and other test parameters must be determined, as in hydrologically saturated column tests, to properly interpret the test results. With regard to the dependence of the measured rate on the Gibbs free energy (through the flow rate) illustrated in Figure 2.3, the measured rate represents some value of ΔG_r on the steep portion of the curve that depends on rate law dependence on the reaction affinity.

6.6 Forced-Through Reactor

In what is referred to as the forced-through reactor, leachant solution is forced to flow through the pore structure of a porous test specimen rather than around the specimen. While this simulates a disposal system in which the waste form (e.g., concrete) is more permeable than its surroundings (e.g., clay), a more important use is to accelerate the leaching of sparingly soluble components. The methodology has been discussed by Butcher et al. (1996). The reaction conditions are different than other leach test due to the much higher *S/V* ratios within the pore structure, although relatively high leachant flow rates can be maintained using high pressure gradients to avoid saturation and promote dissolution. While the release kinetics under these test conditions are probably not representative of degradation in a disposal site, this test method provides insight into chemical reaction behavior within pore structures that may not otherwise be available using typical laboratory test methods.

6.6.1 Butcher et al.

Test specimens were prepared with ordinary portland cement, pulverized fuel ash, dried synthetic waste, and water (Butcher et al. 1996). The synthetic waste was prepared from the hydroxides formed by adding NaOH to a solution of heavy metal nitrates. These were separated by vacuum filtration and dried, then ground to about 0.5 mm. Test specimens were cast as cylinders 49 mm in diameter and 5 mm high. The test specimen was placed in a triaxial cell and leachant forced upwards at pressures up to 400 kPa, which was the pressure exerted on the circumference of the specimen. (A triaxial cell is commonly used to measure permeability under a confined pressure.) Tests were conducted at room temperature with purified water and with an acetic acid solution (TCLP leachant No. 2; see Appendix E Section E.10). The results of tests conducted with the acetic acid leachant at 300 kPa are summarized in Figure 6.16. The concentrations measured in

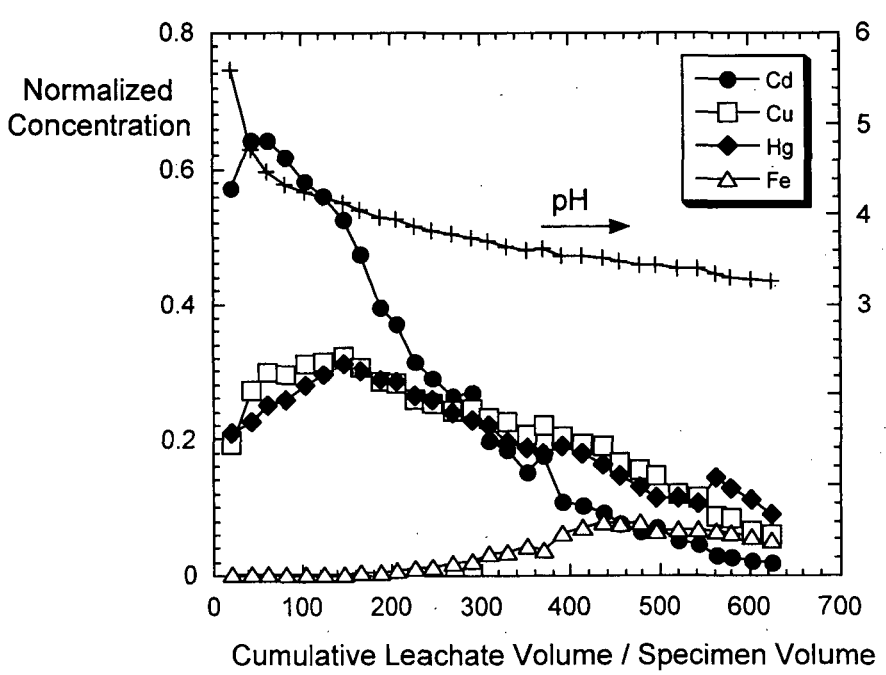

Figure 6.16. Results from Butcher et al. (1996): Force-through tests with ordinary portland cement and acetic acid.

the effluent solution have been normalized to the amounts of each metal in specimen. The effluent pH is initially high but decreases steadily to approach the leachant pH of 2.88 as the buffering capacity of the cement due to reactions with $Ca(OH)_2$ and then with Ca_3SiO_5 and Ca_3SiO_4. The leaching of Ca follows the same trend as the pH and essentially all available Ca is leached midway through the test. The Cd is readily leached, but the releases of Cu and Hg do not peak until about 150 specimen volumes have been passed; thereafter they are released congruently with Cd. The delay may be an effect of the pH. The release of Fe is negligible until after about 300 specimen volumes and does not peak until after about 450 specimen volumes of leachant have been passed. The release behavior of Zn is similar to that of Cd, the release behaviors of Ni and Pb are similar to that of Cu and Hg, and the release behavior of Cr is similar to that of Fe.

6.6.2 Poon et al.

Poon et al. (2001) studied the leaching of heavy metals from a cement-based waste form by demineralized water using a forced-through reactor. One material that was tested was made with type I portland cement, pulverized fuel ash, and a potassium dichromate solution. A test specimen was cast as a cylinder 7 cm in diameter and 3 cm deep. The cured specimen was clamped in a tube and demineralized water forced through at a pressure of about 50 kPa; the pressure was adjusted to maintain a nearly constant flow rate. The eluate was analyzed periodically after 500 mL had been collected. The results for leaching Ca and Cr are shown in Figure 6.17 as the percent of the Ca or Cr that has been leached against the ratio of the accumulated leachate volume normalized to the specimen volume. That ratio is analogous to the number of column volumes and proportional to time for a constant leachant velocity. The results for Ca have been multiplied by 30 to show the results on the same plot as the Cr. The results show that about 25% of the Cr was essentially flushed from the specimen (probably as $Cr_2O_7^{2-}$) with little retardation by the cement and that Ca was released at a constant rate (probably controlled by the dissolution of $Ca(OH)_2$ in the cement). The delayed release of Ca may indicate that a small extent of degradation of the cement pore structure is required prior to free release.

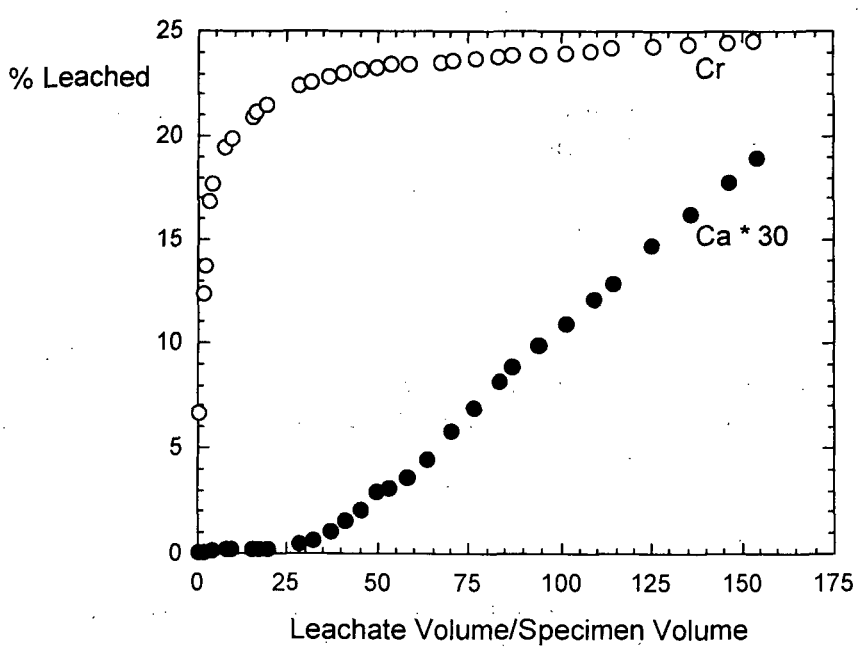

Figure 6.17. Results from Poon et al. (2001): Force-through test with portland cement and water.

The authors interpreted the results by applying the diffusion equation in a moving coordinate system that had been proposed earlier by Poon et al. (1999). In the derivation of that model, the volume-to-surface area ratio of the test specimen is used to define a characteristic length L in the direction of solution flow. If the fluid velocity is F, it will penetrate a depth Ft into the specimenover time t. This transform allows advection to be included within the diffusion equation. The conservation of mass for component C is written

$$\frac{\partial C}{\partial t} = -F\frac{\partial C}{\partial x} + D_e\frac{\partial^2 C}{\partial x^2} - K_1\frac{\partial C}{\partial t} - k_f\frac{\partial C}{\partial t}, \tag{6.36}$$

where the first term accounts for advection with velocity F, the second term for diffusion with an effective diffusion coefficient D_e, the third term for sorption with a linear isotherm constant K_1, and the fourth term for chemical reaction at constant rate k_f. Collecting terms gives

$$\left(1 + K_1 + k_f\right)\frac{\partial C}{\partial t} = -F\frac{\partial C}{\partial x} + D_e\frac{\partial^2 C}{\partial x^2}, \tag{6.37}$$

which can be simplified as

$$\frac{\partial C}{\partial t} = \frac{-F}{\left(1 + K_1 + k_f\right)}\frac{\partial C}{\partial x} + \frac{D_e}{\left(1 + K_1 + k_f\right)}\frac{\partial^2 C}{\partial x^2} \equiv -F'\frac{\partial C}{\partial x} + D_e'\frac{\partial^2 C}{\partial x^2}. \tag{6.38}$$

The modified values F' and D_e' include the effects of sorption and chemical reaction and cast the equation in standard form having the standard solution:

$$C(x,t) = \frac{A_0}{2\left(\pi D_e' t\right)^{1/2}}\exp\left(\frac{-\left(x - F't\right)^2}{4 D_e' t}\right), \tag{6.39}$$

where A_0 is the initial mass of the contaminant in the specimen. Poon et al. (1999) give the concentration at the back surface of the specimen

$$C(t) = \frac{A_0}{2\left(\pi D_e' t\right)^{1/2}}\exp\left(\frac{-\left(l - F't\right)^2}{4 D_e' t}\right), \tag{6.40}$$

where l is the specimen thickness. Using Equation 6.40 to calculate D_e' from the measured concentrations, the value for Cr increases nearly linearly with the leaching period and the value for Ca is $D_e' = 0$ throughout the experiment (Poon et al. 1999). The increase in D_e' probably reflects degradation of the cement pore structure.

6.7 Soxhlet Reactor

In a Soxhlet reactor, water in a reservoir is boiled and the steam recondensed and channeled into a reaction cup containing the test specimen, which can be a monolith or crushed material. A schematic diagram of a typical Soxhlet reactor is shown in Figure 6.18 (adapted from ISO 2008;

Figure 1). The volume of the sample cup is usually small enough that solution overflows the cup and drips back into the reservoir. The solution in the reservoir is periodically sampled and analyzed for components released from the test specimen. The reactor can be operated so that condensed water flows into the reaction cup at a known and controlled rate to determine the specimen dissolution rate (e.g., as if is were a SPFT test). The leachant is restricted to distilled water (or an azeotrope solution) that can be evaporated and recondensed, but tests can be conducted over a range of temperatures by adjusting the pressure to attain different boiling points. The low temperatures of interest to surface waste sites require very low pressures.

6.7.1 Delage and Dussossoy

Soxhlet tests have been utilized (primarily in Europe) to measure the dissolution rates of waste glasses. The results of a Soxhlet test conducted with a borosilicate glass referred to as R7T7 (at 90 °C in demineralized water) are shown in Figure 6.19 (Delage and Dussossoy 1991). The test was conducted at a solution flow rate of about 500 mL h^{-1}. The solution in the reservoir was sampled intermittently but not replaced. The releases of B, Na, and Si are linear with time and nearly congruent at about 1 g m^{-2} d^{-1}; the release of Li is slightly faster at about 1.2 g m^{-2} d^{-1}. These tests are conducted at high solution flow rates and short durations to avoid concentrated solutions in the reaction cup and any effects of glass surface alteration.

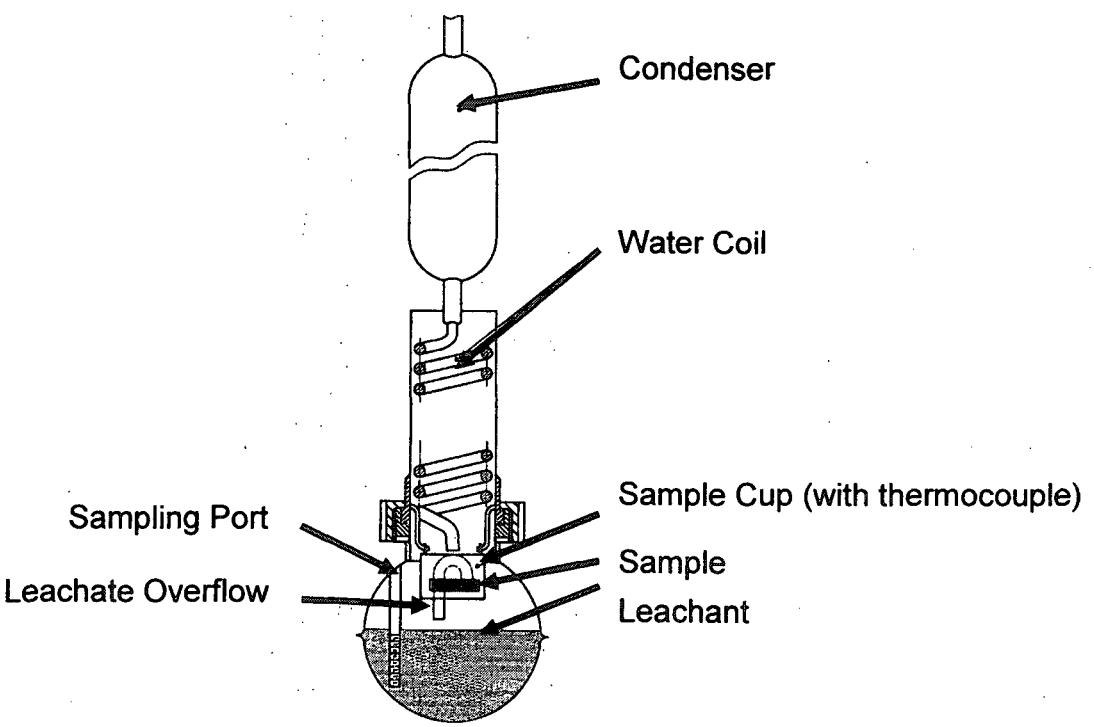

Figure 6.18. Schematic diagram of a Soxhlet reactor.

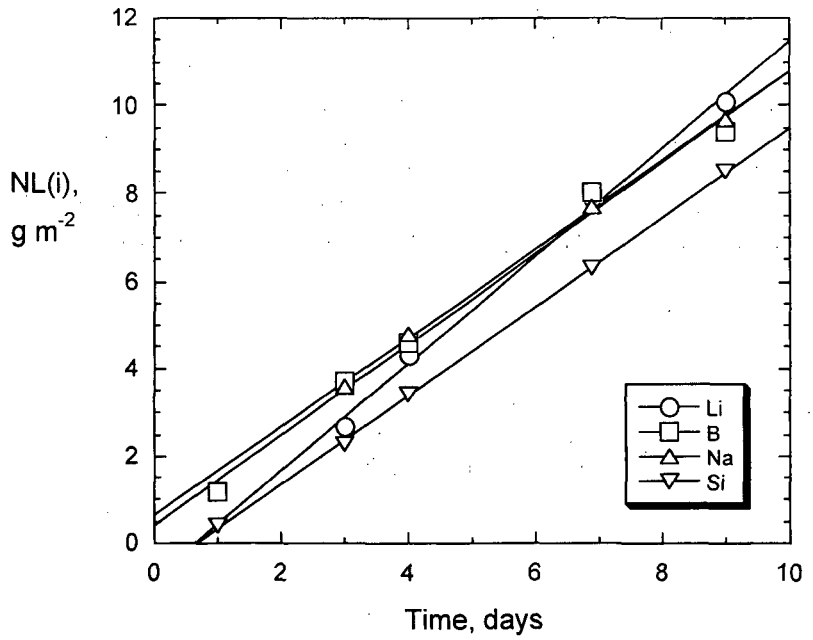

Figure 6.19. Results from Delage and Dussossoy (1991): Soxhlet tests with R7T7 glass.

6.7.2 Atkinson et al.

Waste forms made with ordinary portland cement and clinoptilolite and doped with CsCl and $SrCl_2$ solutions were prepared and tested using a Soxhlet reactor (Atkinson et al. 1984). Both Cs and Sr are known to sorb onto clinoptilolite. A test specimen was subjected to a Soxhlet test in which the sample chamber and recondensed water were maintained at 30°C. The test was conducted with 500 mL of water in the boiler that was heated so as to maintain an effective flow rate of 3 mL/minute in the sample chamber. The distillation was interrupted intermittently to analyze and change the water. The results were presented in terms of the calculated depletion depth based on the measured solution concentrations of Cs and Sr plotted against the sampling times and reproduced in Figure 6.20; it is assumed that the calculated depletion depth is proportional to the cumulative mass loss. In Figure 6.20a, the results for the first 5 samplings (collected at about 1-day intervals), samplings 7 through 15 (about 1-day intervals), and for the last samplings (2.7-day to 5.9-day intervals) are shown regressed separately. The sixth sampling was after 2.1-day interval and the sixteenth sampling was after a 5.4-day interval; both were excluded from the regressions because of the different sampling intervals. The results are plotted against the square root of the time in Figure 6.17b with the short-term, intermediate, and longer-term results fit separately. The slopes of the root-time fits increase with the cumulative reaction time, whereas the slopes to the linear fits decrease. Both the time and root-time fits to the first and second sets of 1-day samplings give different slopes. Atkinson et al. (1984) regressed each (entire) data set with the diffusion equation and found that "for neither isotope does the kinetics conform rigorously to this [root-time] relationship, but the relationship is reasonable for Cs after approximately 4 days." Figures 6.20a and 6.20b show the results to be consistent with both linear and root-time dependencies for subsets collected after similar intervals. However, the increasing slopes with increased sampling intervals are not consistent with a diffusion-controlled release mechanism; the slope should decrease. The phenomenon responsible for the apparent effect

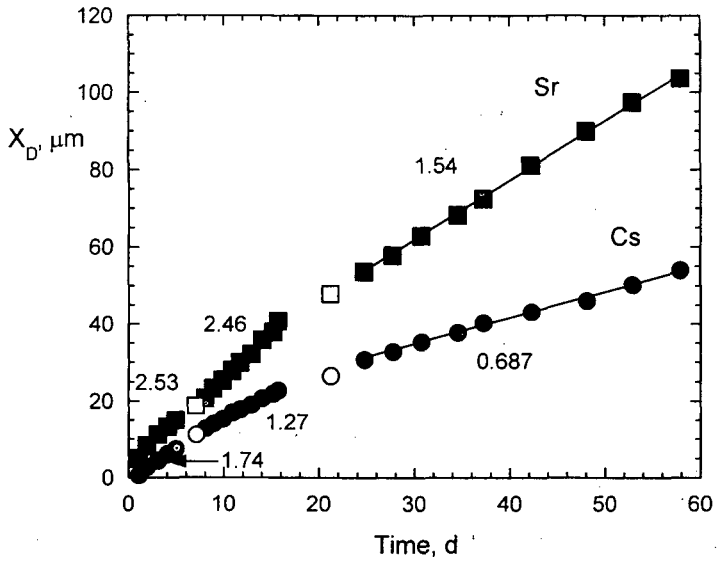

(a)

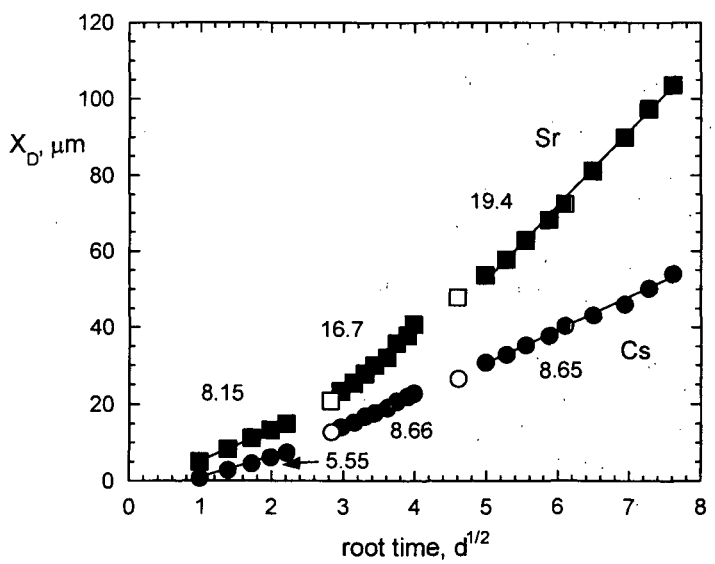

(b)

Figure 6.20. Results from Atkinson et al. (1984): Soxhlet tests with cement (a) depletion depth vs. time and (b) depletion depth vs. root time. The values give the slopes of the regression lines.

of the sampling interval is not known. In the Soxhlet test, the increase in solution concentrations (which was used to calculate the depletion depth in the test specimen) occurs in a water reservoir that does not contact the waste form. The dependence on sampling interval appears to be the same as that seen in solution exchange tests. It is speculated that depletion of Cs and Sr at the specimen surface occurs at a rate having a root-time dependence that results in the observed sensitivity to the sampling interval. The flow rate (which is determined by the boiling and recondensation rates) may also complicate the observed time dependence.

7 Discussion

Insights gained from the reviews and analyses presented in the preceding sections are discussed with regard to the suitability of current test methods to characterize the processes controlling the release of contaminants consistent with a mechanistic understanding and the suitability of current materials models to represent the behavior as a source term sub-model in dose assessment calculations. Application of testing and modeling results to future analyses of site assessments are briefly addressed, then the evaluation of test methods and process models are discussed.

7.1 Modeling Waste Site Releases

Preliminary analyses of contaminant dispersion models suggest that a layered approach may be appropriate for modeling surface waste sites wherein the pile of slag or concrete waste (or other waste material) can be treated as a layer with characteristic transport properties. A similar "cellular" approach is being used in RESRAD (Yu 1987, Yu et al. 2001) and in performance assessment calculations for the Hanford disposal system (e.g., Bacon and McGrail 2005; Bacon et al. 2004). It is anticipated that the methodologies in these simulation models can be applied to the near-surface piles of rubblized concrete and slag wastes subject to NRC assessment and licensing. Possible approaches will be evaluated in Part IV of this project: *Application of Leaching Model to Dose Assessment Codes*. For example, separate source term models could be assigned for the release of each radionuclide of interest from various waste materials that comprise the pile. Depending on the distribution of the wastes and contaminants, the pile could be treated as a homogeneous slab or discrete cells with characteristic properties. That is, separate surface areas, $Q_{\text{dissolution}}$ terms, etc., could be defined to apply the release and transport equations to these slabs or individual cells. Existing laboratory tests could be used to identify and parameterize the appropriate models to represent $Q_{\text{dissolution}}$ for the wastes and individual contaminants in the transport models, as discussed in this report. Estimates of the effective surface area of each waste material and the porosity of the layer of waste materials will be required for deterministic analyses based on inspection of the site. Alternatively, the sensitivity of the release to a range of configurations and properties of the waste materials could be considered in a stochastic approach analogous to the approach taken for the Yucca Mountain disposal system.

Laboratory tests are used to measure intrinsic properties of the waste material and characteristic responses to environmental conditions that can be used to predict degradation behavior under a range of disposal conditions. The specific test parameters used in a laboratory test will differ from the environmental conditions in a disposal system or waste site, but the dependence of the material property on the variable will be the same and can be related to the disposal system through the waste degradation model. The physical dimensions of the laboratory test specimen do not need to represent those of the actual waste material. For example, a test specimen in the shape of a right cylinder is often used to facilitate the use of an analytical solution to the diffusion equation to measure the effective diffusion coefficient of a contaminant in a host material matrix. The diffusion coefficient does not depend on the geometry of the test specimen (if the release is truly diffusion controlled). The measured diffusion coefficient can then be used to calculate the release of that contaminant from a piece of that material with any size or shape, from fine-grained particles to particles aggregated with other phases to boulder-size masses within the disposal system or waste site. That calculation would take into account the dimensions of the solids and the accessible surface areas of the materials of interest. Likewise, series of tests can be conducted at various temperatures to model the diffusion coefficient as a function of temperature, and that

dependence is used to predict the release at a particular temperature in the disposal system, where the functionality of the temperature dependence determined in the laboratory tests is incorporated into the degradation model for the waste site.

7.2 Relating Models and Laboratory Tests to Waste Sites

The key parameters for relating the kinetics measured in laboratory tests to behavior in a natural system are the waste material S/V ratio (where V is the solution volume), water infiltration and flow rates, range of solution pH values and temperature, and the phase compositions of the waste materials. The surface area can be estimated based on the geometry of the system. Simple geometries are given as an example. (More detailed models, such as those that take surface roughness into account, will be considered in future reports.) For flow through a fracture of width w, the S/V ratio is simply

$$\frac{S}{V} = \frac{2}{w} . \tag{7.1}$$

For simple cubic packing of spheres having a diameter d, the area and volume of each spherical particle are πd^2 and $(\pi d^3)/6$ centered in an occupied volume of d^3, so the S/V ratio is

$$\frac{S}{V} = \frac{\pi d^2}{d^3 - \frac{\pi d^3}{6}} = \frac{6.6}{d} . \tag{7.2}$$

For a close-packed arrangement of uniform spheres,

$$\frac{S}{V} = \frac{17}{d} . \tag{7.3}$$

In many cases, the contaminant-bearing phases of interest will be dispersed as inclusions within other materials and exposed surface areas of the wastes must be adjusted for the concentrations of the phase of interest in the solid. For example, if the mean grain size of a phase of interest P is d_P and the phase occupies a volume fraction x_P of the solid, then the number of grains per volume of rock N_P is

$$N_P = \frac{6 x_P}{\pi d_P{}^3} . \tag{7.4}$$

For porous phases such as rubblized concrete, a unit volume of waste material, the volume of fluid within the material, V_s, is equal to the porosity ϕ, so

$$\frac{A_P}{V_L} = \frac{\pi d_P{}^2 N_P}{\phi} = \frac{6 x_P}{d_P \phi} \tag{7.5}$$

The surface area fraction is usually assumed to equal the bulk volume fraction for uniformly distributed phases. For any given dissolution rate, Equation 7.5 indicates the speed at which the solution approaches a steady-state concentration as it percolates through the waste: small particles, low porosity, and high volumetric contents of contaminant-bearing phases will all contribute to rapid saturation of the solution.

The release of a radionuclide i includes release from all phases P in the waste form that contain that radionuclide,

$$R_i = \sum_P \upsilon_{iP} \frac{A_P}{V_L} R_P \ , \tag{7.6}$$

where υ_{iP} is the mole fraction (or mass fraction, matching the units of R_P) of radionuclide i in a phase P and R_P is the degradation rate of phase P. Each phase P can be an isolated single phase, such as a mineral or homogeneous waste glass, or part of a composite waste form. The time dependencies of the particle sizes, reactive surface area, and material porosity can be estimated from the geometry. As discussed above, the solution concentration of a radionuclide may be affected by the presence of more than one phase containing that radionuclide (see Equation 3.2). The actual concentration may be less than the solubility limit due to the slow dissolution kinetics of the less-stable phase or exceed the solubility limit due to the slow precipitation of the more-stable phase (see discussion in Section 3.1). Laboratory tests are available to measure these concentrations and relate them to the dissolution kinetics of the host phases, as detailed in the preceding sections. The precipitation kinetics of the alteration phases can be studied using some of the same test methods developed to measure dissolution kinetics and modeled using similar approaches, but in the opposite direction. For example, the SPFT tests conducted by Yang and Steefel (2008) with super-saturated leachants included precipitation reactions (see Section 6.3.3).

The coupled dissolution of multiple phases is a particularly important concept for the slag wastes being addressed in this report. As detailed elsewhere (e.g., Veblen et al. 2004), these slags are composed of many phases including glass, mineral, silicate, oxide, and metal phases with a complicated distribution of radionuclides and other contaminants. The compositions reflect the ores or feed materials that were processed and the added chemicals, and the physical nature of the slag is sensitive to the process that was used, when the slags were separated from the alloy, and how they cooled. Some slags contain an abundant glassy phase from silica added to remove contaminants from the metals; some are quenched and some are allowed to cool slowly. The phase distribution is usually not the thermodynamically stable distribution and the materials may be weathered to various extents. Any sample collected for characterization or use in testing carries uncertainty regarding how well it represents the whole. The comparisons of any test results must take into account the likely variability in the phase compositions of different test specimens. Tests with crushed materials have the advantage of a high specific surface area that is expected to provide a more representative sampling of the component phases than a monolithic specimen. Both monolithic and crushed test specimens offer the opportunity to track the degradation of specific components (albeit difficult) by microscopic analyses.

7.3 Testing Objectives and Test Method Selection

Test methods have been developed for several different purposes, but can be grouped as either "benchmark performance test methods" or "characterization test methods." Benchmark performance test methods are designed to be compared with a response that has been deemed to be

compliant with a regulation or specification. That is, the test response is interpreted as a "pass/fail" indicator. These are used to objectively evaluate material response under specific test conditions that may represent a particular service condition or may be generic. Several benchmark performance test methods have been developed by specifying the test parameters of a characterization test based on measured sensitivities. For example, the test parameters used in the Product Consistency Test (ASTM C1285 method A) were selected to provide acceptable precision and composition discrimination for crushed glass prepared in a hot cell.

Performance in a benchmark test is often touted as providing a standardized performance criterion for comparing various waste form materials and treatment options. The Materials Characterization Center test method number 1, which was the forerunner of ASTM C1220, was used to compare the durabilities of a wide variety of materials considered for use as waste forms, including glass, cement, cermet, and ceramics. However, without considering the release modes for contaminants and the degradation mechanism of the host matrix, there is no technical basis for using the comparison of single data points to evaluate the relative performance of those materials. Series of tests may provide insight into the degradation mechanism, but a single test method is usually not sufficient to project the long-term durability of a waste form under disposal conditions and can be misleading. For example, material A may dissolve at a higher rate than material B but have a lower solubility limit. A benchmark test that generates solution conditions that are more dilute than those expected to occur in a disposal system would rank candidate waste forms in reverse order with respect to durability under disposal conditions: material A would dissolve faster than material B in the dilute test conditions, but dissolution of material A in the disposal system would essentially cease when the groundwater became saturated while material B would continue to dissolve.

Characterization test methods are designed to provide information regarding material behavior; for example, to support development of a mechanistic model that can be used to predict the long-term degradation behavior. The ASTM standard practice C1174 outlines the various purposes of testing to develop material degradation models (ASTM 2009a). These include *attribute tests* to measure intrinsic materials properties such as density, thermal conductivity, and hardness; *characterization tests* to identify alteration modes and environmental effects; *accelerated tests* to increase the reaction rates and aging of the material; *service condition tests* to measure alteration under anticipated service conditions; and *validation* and *confirmation tests* to validate the process model and confirm its applicability in the disposal system. The standard does not identify specific test methods for use as attribute tests, characterization tests, etc., since these will depend on the material being evaluated and the disposal system. A particular test method can serve more than one purpose depending on the test conditions.

Too often, waste form materials are subjected to test methods without forethought about whether the method is appropriate for the material or represents the service condition, or about the significance of the test response. A good example of this is application of ASTM C1285 Product Consistency Test (PCT) Method A (ASTM 2009a); because the PCT has been shown to be appropriate for tracking the consistency in the dissolution rate of glass waste forms as a function of their composition, it is commonly applied to measure the dissolution rates of a wide variety of materials, many of which do not degrade by an affinity-controlled mechanism. Even the direct comparison of PCT responses for various glasses is sometimes invalid. This is because the PCT calls for a particular mass ratio of glass and water, because glasses with different densities will have different specific surface areas the reactive surface areas that are available in the tests can differ significantly. (Failure to address the specific surface area of glass used in the test is a shortcoming of the current ASTM C1285 method that should be addressed.)

In most of the examples provided in this report, a material was subjected to a particular test method, the results were fit with equations based on hypothetical models, and then model coefficient values were extracted, with the degree of uncertainty being indicated by the goodness of fit. Sometimes a modification of the equation to reflect an adjustment in the mechanism was necessary to fit the trend in the test results, and sometimes the abilities of different models to fit the results were compared empirically. It was shown for several examples that deviations from the model used to interpret the data could be attributed to experimental artifacts, such as the effect of the sampling interval or preferential dissolution of fracture edges generated by crushing. In other examples, the wrong model had been applied to the test results. When predicting long-term behavior, using the wrong process model can lead to significant errors in the projected performance of a waste material or waste form. Therefore, it is prudent to evaluate test methods and test results with regard to optional process models to gain confidence in how the data are interpreted and used in predictive models.

Most of the test methods used to generate the literature results discussed in this report have been summarized in the text. Appendix E provides summaries of other laboratory test methods that can be used to assess waste material degradation and contaminant release. Several test methods have been developed to measure the extent of contaminant extraction into particular solutions, including demineralized water, acetic acid, and mixtures of inorganic acids, that are intended to mimic natural conditions. The U.S. Environmental Protection Agency (EPA) has mandated the use of specific methods for quantitative comparison of material responses with regulatory limits for EPA-regulated hazardous contaminants in municipal and industrial wastes. The most commonly used methods are the EPA Toxicity Characteristic Leaching Procedure (TCLP) and Synthetic Precipitation Leaching Procedure (SPLP), the ASTM test method of shake Extraction of Solid Waste with Water (ASTM D3987), and the State of California Waste Extraction Test. Other agencies and organizations use common test methods to establish compliance to particular specification and to assess environmental impacts. The U.S. Geological Survey (USGS) uses various field extraction methods such as the Field Leach Test (USGS 2005) and Net Acid Production test (e.g., Fey et al. 2000; Hageman 2004) for assessing environmental impacts of mine wastes and predicting surface runoff, etc. These have been referred to as "reconnaissance" tests. Although these test methods fulfill the purposes of assessing regulatory compliance or gross characterization, they are not useful for the purpose of modeling waste material behavior for the purpose of performance assessment. For example, most methods do not provide a test response that can be quantified on the per-area basis needed to extrapolate to specific field systems.

7.4 Interpreting Test Results

Several aspects of how test results are evaluated and the potential uncertainties of the conclusions that are drawn are discussed. Probably the most important information that can be garnered from the test results is the process that controls the observed test response. This will be influenced to a significant degree by the test method that is used because the test conditions can highlight one process over others and could lead to misinterpretations by force-fitting a process model to the data. The model may fit the short-term test data adequately, but could deviate significantly from the long-term behavior. Therefore, it is important that the mechanistic basis for the laboratory test response be understood and that the test method highlight the process that will control the long-term behavior. In addition, possible artifacts of the test method must be understood and taken into account when interpreting the results and applying them to the model. Several test methods were developed to parameterize a particular process model. The best example is probably the ANS 16.1 method developed for diffusion-controlled release, where solution exchange is performed to maintain dilute conditions to represent a mathematical model that presumes an infinitely dilute

solution phase. As a part of this discussion, the responses are considered for materials governed by a process other than the process for which the test method was developed. Such an understanding can avoid misinterpreting the relationship between the measured test response and behavior represented in the source term model.

7.4.1 Affinity vs. Diffusion

The initial accumulation of released soluble components may be similar regardless of whether the release is controlled by diffusion or by reaction affinity, and the mechanism controlling the release may not be discernable from the trend alone. For example, each test result plotted in Figure 7.1 is from a separate ASTM C1220-type batch test conducted with a simple borosilicate glass in which the released Si accumulated during that test duration to the measured concentration (Bourcier 1991). These are not the cumulative releases from several test intervals with the same test specimen that are typically plotted for diffusion tests. Rather, each data point represents the result of a separate batch test. In the series of ASTM C1220 tests shown in Figure 7.1, the cumulative release from six separate test specimens was measured after a different duration and the results combined to show the release as a function of time. The results were evaluated by Bourcier (1991) using both the affinity model and the diffusion model, as shown by the solid and dotted curves in Figure 7.1.

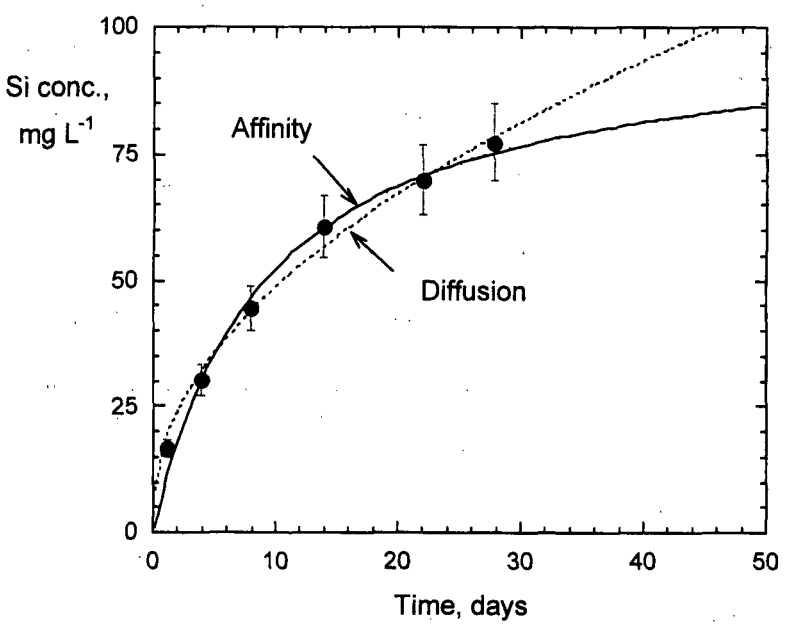

Figure 7.1. Results from Bourcier et al. (1991): Static tests fit to diffusion and affinity models.

The equations used for diffusion-controlled release and for affinity-controlled release both fit the data well within the presumed test uncertainty, which is plotted at 10% of the measured value. The equations that were fit, regressed coefficient values, and residuals are

$$\sum[Si] = A + B\,t^{0.5} \quad with\ A = 4.2\ and\ B = 14.1 \quad \sum residual^2 = 26.3 \tag{7.7}$$

for diffusion-controlled release and

$$\sum[Si] = \frac{k_f}{\frac{1}{t} + \frac{k_f}{K}} \quad with\ k_f = 11.0\ and\ K = 100 \quad \sum residual^2 = 142 \tag{7.8}$$

for affinity-controlled release. (Note: Equation 7.8 was derived from Equation 2.22 by defining the rate as [Si]/t, both cumulative values, setting Q = [Si], and then solving for [Si].) The diffusion equation gives a better fit based on the residuals. An effective diffusion coefficient can be calculated from the slope and the dimensions of the test specimen.

Whereas the short-term predictions of the models are nearly identical, the model predictions diverge at longer times. Assuming 10% analytical uncertainty, tests run 50 days and longer would be required to distinguish the Si concentrations predicted by the two models. This shows how simple regression of short-term test data without consideration of the mechanism can be misleading. First, the simple diffusion equation is not valid for test conditions resulting in such high concentrations of the diffusing species. Derivation of that equation assumed infinite dilution of released components. Second, glass is known to dissolve by an affinity control mechanism rather than dissolution (Bourcier 1991). Although the release of Si is certainly not diffusion controlled, this example shows that an effective Si diffusion coefficient could be determined from this short-term data with confidence. The release of waste components can be misjudged just as easily. Therefore, it is important to understand the responses of different release mechanisms in various laboratory tests and how test conditions can be used to distinguish those mechanisms.

7.4.2 Comparing Responses from Static and Semi-Static Tests

The ASTM C1220 test method uses separate test specimens and solutions to measure the accumulated release of a species over several test durations. The test specimens used in a series of tests are assumed to be equivalent such that the releases measured in different tests can be scaled to the specimen surface area. That is, the data are assembled to represent the release from a single test specimen. For each successive interval, the solution concentration at the beginning of the interval is the same as the solution concentration at the end of the previous test interval. The surfaces of the test specimens also evolve during the test.

In a common modification of the ASTM C1220 test method, the release of a species is monitored using a single test by periodically sampling the solution. The series of solution results represents the reaction of a single test specimen. The removed leachate may or may not be replaced with fresh leachant. Either way, interpretation of the test results based on the solution concentrations is complicated. If the leachate is not replaced, then the solution concentration at the beginning of the interval is the same as the solution concentration at the end of the previous test interval, but the effective S/V ratio of the test will increase after each sampling. This effect may or may not be negligible, depending on the volume of the aliquant taken and the reaction rate. If the leachate is replaced, the solution will be diluted and the reaction affinity will increase slightly between intervals. The solution concentration will be lower at the beginning of the interval than at the end of the previous test interval. Both the solution chemistry and the condition of the test specimen surface will evolve as the test proceeds.

In the ANS 16.1 and ASTM C1308 methods, the cumulative release is assembled from the releases measured over all intervals. The same sample is used throughout the test and the diffusion path length increases with every successive test interval. In the sequence of test intervals, the solution concentration is re-zeroed at the beginning of each test interval but the condition of the test specimen surface evolves. The surface region becomes depleted of leached components and may become more or less porous as the matrix responds to the chemical changes. Further evolution of the leached layer may include ion exchange with other components in the solution, condensation reactions within the layer, precipitation of alteration phases, etc. The model for diffusion from a semi-infinite solid is based on the surface concentration of contaminant species remaining at zero and no modification of the leached layer.

The dissolution of a material could be misidentified as being diffusion-controlled just as easily with each of the three test methods. The ANS 16.1 and ALT tests mimic a SPFT test conducted at a low effective flow rate. If the reaction intervals are of constant duration and about the same amount of material dissolves during each interval, the measured rate will *appear* to be constant even though the actual rate is not constant. Diffusion-controlled release rates will decrease during the test interval due to the increasing diffusion path length in the specimen, whereas affinity-controlled release will decrease during the test interval due to the increasing solution concentration and decreasing reaction affinity. Replacing the leachate with fresh leachant will reset the affinity term in a dissolution-controlled reaction mechanism to one (thereby maintaining a high gradient to promote diffusion), but it does not affect the diffusion path length that also affects the release rate in a diffusion-controlled release mechanism.

7.4.3 Effect of Sampling Interval

The effect of the sampling interval on the incremental release rate when the release slows with time is shown schematically in Figure 7.2. If the release follows the solid curve, the average rate over the test interval from t_{j-1} to t_j (Rate A shown by the dashed line) is higher than the average rate over the test interval from t_{j-1} to t_{j+1} (Rate B shown by the dotted line). The roll-over could be due to either affinity control or diffusion control of the release. In either case, the true rate can only be measured using a sampling interval over which the curvature is negligible. In practice, the shortest meaningful sampling interval will be determined by the analytical capacity to measure the concentration of the contaminant in the test solution and the measurement uncertainty. This will depend on the species to be analyzed and its release rate. The effect of the sampling interval will also depend on the specimen surface area/solution volume ratio used in the test: higher ratios will generate more concentrated solutions faster than lower ratios.

The approach recommended in ASTM C1662 (SPFT test) to overcome analytical limits can be applied to solution exchange tests such as ASTM C1308. In that approach, several series of tests are conducted to measure the dissolution rates at different solution flow rate/specimen surface area ratios to measure the rates over a range of steady-state solution concentrations. The rates are plotted against the steady-state concentrations and the correlation extrapolated to zero concentration. Solution exchange tests can be conducted using different (constant) exchange intervals and the measured rates (or the diffusion coefficients that are extracted from the rates) extrapolated to represent the rate (diffusion coefficient) for an infinitesimally short exchange period.

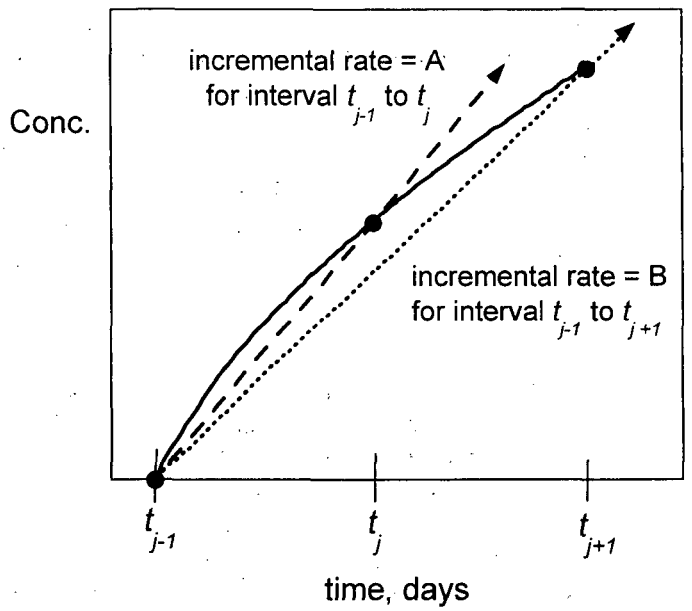

Figure 7.2. Schematic illustration of effect of sampling interval on incremental rate.

7.4.4 Effect of Solution Exchange on Affinity-Controlled Release

The effect of the leachate exchange frequency on the release from a material that dissolves following an affinity-controlled mechanism is illustrated schematically in Figure 7.3a. The figure shows the cumulative releases when the leachate is exchanged at 1-day, 2-day, and 3-day intervals. Shorter exchange intervals minimize the influence of solution feedback on the dissolution rate. In other words, the average value of the affinity term over the interval remains higher (nearer to 1) in shorter intervals. The rate observed for the over-all test duration is highest for 1-day exchanges and lowest for 3-day exchanges. The effect of the exchange frequency in replacement tests such as ANS 16.1 and the ASTM C1308 test is analogous to the effect of flow rate in dynamic flow-through tests. Compared with the simple system described in Figure 7.3a, changing the interval times in a series of exchanges will result in complex release behavior that will be difficult to attribute to either mechanism. Analyzing each leachate sample would generate a linear plot for each series, but the release rates (slopes) determined by the tests would decrease with increasing time between samplings. Figure 7.3b compares the expected responses of materials with affinity-controlled and diffusion-controlled releases to leachate replacement. The replacement has little effect on the diffusion-controlled release because the release is controlled by diffusion through the test specimen; the solution composition has only a small effect on the release rate except perhaps at long replacement intervals. The replacement has a significant effect on the affinity-controlled release because the dissolution rate is controlled by the solution concentrations of dissolved components. When those dissolved components are removed (after 1, 2, and 3 days in Figure 7.3b), the value of the reaction affinity is reset to 1 and dissolution resumes at the forward rate. The periodic analysis of recovered solution from an affinity-controlled reaction (filled circles at 2 and 3 days) results in a reaction rate that appears to be linear (shown by the dashed line) whereas the solutions from a diffusion-controlled reaction (open circles at 2 and 3 days) will describe the root- time diffusion behavior (bold curve). This is because the time dependence derives from the generation of a depleted region on the test specimen that is not affected by the solution concentration.

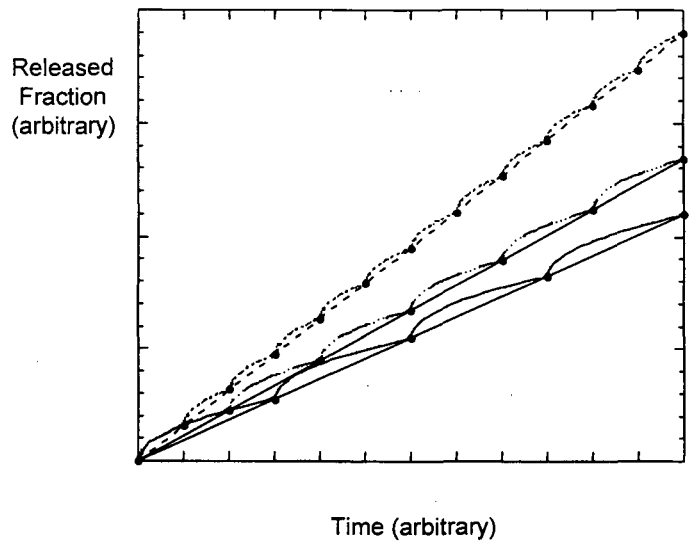

(a)

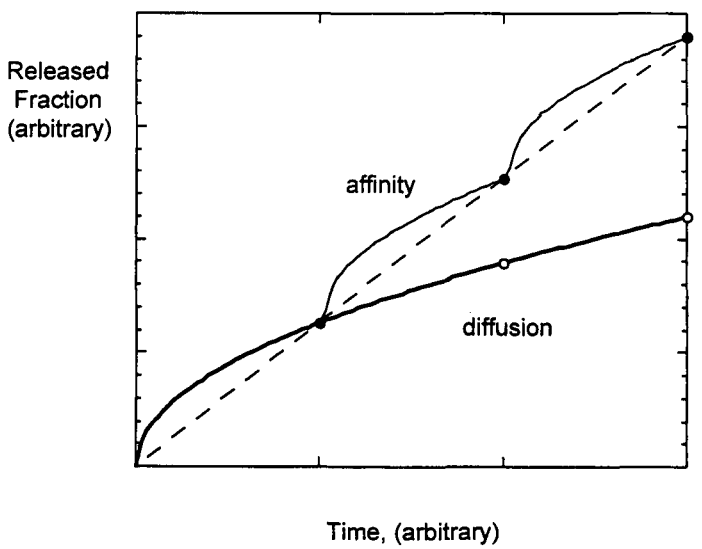

(b)

Figure 7.3. Schematic illustrations of (a) the effect of leachant exchange frequency on measured release rate and (b) the expected responses for diffusion-controlled and affinity-controlled release mechanisms.

The illustrations in Figure 7.3 are idealized to emphasize the difference between affinity-controlled release and diffusion-controlled release. In reality, the response of a material with affinity-controlled release will have a minor diffusion-controlled component due to changes in the surface during reaction and the response of a material with diffusion-controlled release will have a minor affinity-controlled component due to solution feedback effects. These complicating effects can be minimized by using short test intervals.

7.4.5 Effect of Flow on Diffusion-Controlled Release

The effect of leachant flow is to remove dissolved components from the surface of the dissolving material. In the case of affinity-controlled dissolution, flow maintains a constant solution composition near the specimen surface that depends on the material dissolution rate and the

solution flow rate. Flow is less important for diffusion-controlled release. The driving force for diffusive release is the activity gradient between the interface of the specimen with the solution and a point in the bulk. This is expected to become less sensitive to the flow rate as the near surface region is depleted of the contaminant being leached. The difference is shown schematically in Figure 7.4a. The curve shows a sigma-shaped decrease in contaminant activity from the high bulk value to the lower surface value due to earlier leaching. The depletion thickness is usually identified by the inflection point in the curve. Continued diffusion is expected to be less sensitive to the activity in solution than is dissolution at the surface because the low activity in the depletion zone drives diffusion almost as effectively as low activity at the surface/solution interface. That is, changes in the solution concentration will affect the activity in the depletion zone very near the specimen surface, but the activity gradients for species within the depletion zone will not change significantly. For example, a sudden increase in the solution activity could change the profile within the depletion zone to a U-shaped profile, as shown in Figure 7.4b. Diffusion on the bulk side of the zone would continue to be driven by the gradient to the bottom of the U, whereas surface dissolution would slow or even cease.

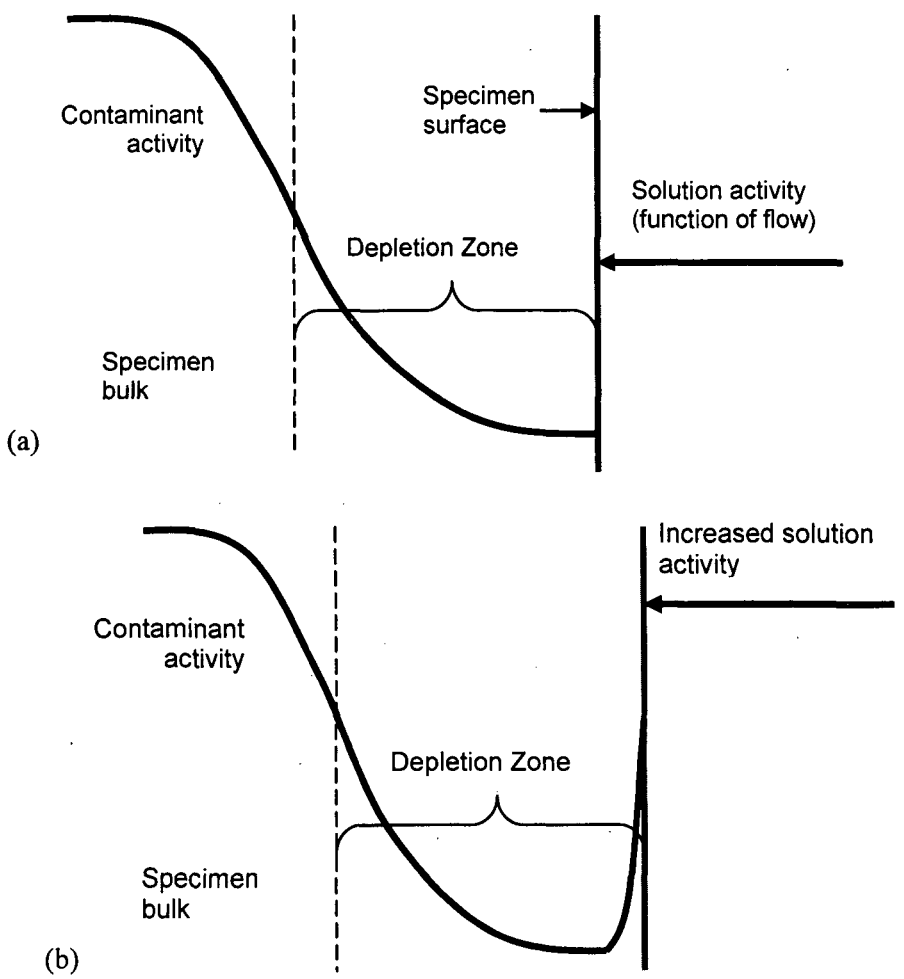

Figure 7.4. Schematic illustration of depleted surface region of diffusion-controlled release (a) before and (b) after increase in solution concentration of contaminant due to an external source.

7.5 Conclusions and Comments

The following conclusions are based on the initial analyses of literature data summarized in this report. These conclusions should be viewed as preliminary and may be modified as work proceeds in the evaluation of field testing, characterization of concrete and slag materials, and integration of release mechanisms with reactive transport computer simulations.

The objective of this series of reports is to relate laboratory tests with measured and modeled field behavior of contaminated materials. Computer codes developed to predict contaminant migration through engineered and natural systems use the same governing equations for chemical reactions coupled with transport. Contaminant source terms due to the weathering of waste materials can be incorporated as time-dependent functions and combined with terms representing advective and dispersive transport, precipitation, sorption, colloid formation, radioactive decay, etc. Factors affecting contaminant transport may lessen the impact of waste material and waste form durability on the system performance, including solubility controls (precipitation of sparingly soluble phases) and irreversible sorption to immobile materials. The same mathematical models used to describe the release of contaminants from specimens in laboratory (and field) tests and can be used to predict the long-time releases of contaminants from full-sized wastes and waste forms at the disposal site. However, modeling field behavior requires the coupling of various process models whereas most laboratory tests are controlled by a single process. How well a particular laboratory test or series of tests provides an understanding that is relevant to an actual disposal system will depend on how well the test specimen represents the actual waste (e.g., the phase assemblage and distribution of contaminants) and the extent to which the test response represents the processes controlling the behavior of the waste in the disposal system.

7.5.1 Contaminant Source Term Models

Three processes are of primary importance to modeling contaminant release from waste materials and waste forms: diffusion, oxidation, and dissolution. The relative importance of each will depend on the contaminant, the encapsulating phase (if any), and the reaction conditions.

Diffusion-controlled release from waste materials and waste forms is modeled using the same equations that govern diffusive transport in hydrologically saturated and unsaturated media. Analytical solutions to the governing differential equations have been derived for various sample geometry and boundary conditions appropriate for the specimens used in laboratory tests. These include mechanistically based equations for diffusion from a semi-infinite solid and from a finite cylinder, and for diffusion coupled with a first-order reaction to produce or consume mobile constituents. These equations can be used to model systems in which the slow diffusion of reactants (water and oxygen) is coupled with reactions to release contaminants by rapid diffusion from waste materials as well as systems in which slow reactions to mobilize contaminants are coupled with the diffusion-controlled release of the contaminants.

Oxidation is important for multi-valent contaminants due to the different solubilities of the metallic and various oxide phases. Conceptual electrochemical models have been developed but are incomplete. Despite all of the research that has been conducted worldwide to model the dissolution of spent UO_2 fuel, empirical models are currently being used in repository assessments. The approach commonly used to empirically model reaction kinetics can be applied to model redox-sensitive reactions: the free energy term describes the difference between the potential at the surface of the waste and the redox potential of the groundwater. The effects of solutes and temperature are modeled empirically.

Dissolution models have been developed to quantify the effect of chemical affinity on the dissolution kinetics using non-equilibrium thermodynamics. The rate coefficient and environmental effects on the dissolution kinetics, including waste composition, temperature, pH, and various solute species, are represented by empirical models. For example, the dissolution rates of most silicate minerals can be represented using an intrinsic rate constant, empirical terms quantifying the dependence on pH and temperature, and a simple affinity term (e.g., where only silica need be taken into account). Simplified models that neglect solution feedback can be used for systems that will remain far from equilibrium and usually provide overly conservative estimates. The adequacy of that approach will depend on the waste material, disposal system, and required precision. More realistic models address the system's approach to equilibrium and accompanying decrease in weathering rate.

In most cases, diffusion, dissolution, and sometimes redox reactions will all contribute to the release kinetics of a contaminant. Which process is dominant will usually depend on the waste material and the reaction conditions. The conditions used (or attained) in a laboratory test will highlight a particular process, which may or may not be important in the disposal system. It is crucial that the process(es) responsible for a test response be understood before using laboratory test results to predict long-term behavior. *A particular process model is sometimes imposed on a particular test response when that test response is more a consequence of the test procedure, testing artifacts, or how the results are compiled and presented than the material degradation behavior or radionuclide release mechanism.* This is clearly the case for the ANS 16.1 test method, which uses a diffusional release mechanism for all materials. This is acceptable for the expressed purpose of that test "to measure the ability of the solid to impede the release of radioisotopes when water comes into contact with them" (ANS 2009), but it must be recognized that those test results are not appropriate for projecting long-term behavior. In many cases, more than one test method must be used to determine the degradation mechanism or demonstrate the hypothesized mechanism. Comments regarding testing approaches, test methods, and interpretations of test results are provided in the following sections.

7.5.2 Testing

Tests are conducted for a variety of purposes and to address behavior at a range of scales. Of particular interest in this report are tests conducted to understand and model the release of contaminants from a waste material or waste form. The models used to interpret test results are based on scientific understanding at a nearly atomistic (microscopic) scale that can be quantified using explicit algebraic expressions. The laboratory tests measure the environmental effects on the kinetics of material degradation and contaminant release on a moderate (mesoscopic) scale that averages minor inhomogeneities present in the specimen and differences in the reactivities that may occur at the atomic scale. The models are then used to predict the long-term release behaviors of radioactive contaminants into an environment of macroscopic scale over century-long durations. Mechanistic models are the key to reliable long-term predictions, although some aspects of the degradation/release processes can only be modeled empirically or phenomenologically. For example, the temperature dependencies of activated processes are described by the well-established Arrhenius form, which is an empirical expression that has not been improved upon 120 years after it was first proposed.

Many laboratory tests provide information regarding the interactions of pure phases with well-characterized solutions and provide material-specific values. However, details such as identifying the reactive sites (surface steps, pits, defects, etc.) that are important at the atomic scale are usually invisible to testing. For example, particular reactive sites on mineral surfaces are identified as reactants in atomistic models, but these cannot currently be quantified for testing or analysis, and

experimentally measured rates are instead normalized to the entire surface area. The disposal systems and waste sites of interest cannot be characterized or evaluated to the same accuracy as laboratory systems due to the much more complex combinations of materials, ground water chemistries, chemical and physical interactions, flow paths, etc. occurring in natural systems. Modeling these systems requires the use of "effective" values that may represent the combined responses of several materials and several processes rather than the material-specific or process-specific values that are usually measured in well-controlled laboratory tests and used to parameterize the models. The effective values can be estimated by mathematical combinations of values measured for various materials and conditions, or by conducting laboratory tests with complex mixtures of solids or groundwaters that represent the waste site. Comparisons of laboratory tests and field measurements will be considered in greater detail in a subsequent report.

7.5.3 Laboratory Test Methods

For convenience, test methods are grouped as dynamic, semi-dynamic, and static depending on whether the solution phase is refreshed continuously, intermittently, or not refreshed during the test. Specific test methods are differentiated by the state of the test specimen (crushed or monolithic) and the dynamics of the solution contacting the specimen (continuously or intermittently pumped, recondensed, physically decanted and replaced, or static).

The responses measured in dynamic tests such as column tests, SPFT tests, stirred reactor tests, recycling flow-through tests, and Soxhlet tests are sensitive to the leachant flow rate. *The effect of the flow rate on the measured test response must be taken into account to determine the intrinsic material property to parameterize a model.* This usually requires that tests be conducted at several flow rates to quantify the effect. *The system must also come to steady state to determine the material dissolution rate under the particular conditions used in the test.* In many instances, tests have been conducted under conditions that are expected to minimize the effect of flow or simulate natural conditions, but this is often neither justified (i.e., demonstrated experimentally) nor realistic. The testing conditions required to avoid experimental artifacts often do not represent the natural system. For example, the very high flow rates required to minimize solution feedback effects do not represent flows in a disposal system and the finely crushed materials used to provide the high surface areas needed to generate measurable solution concentrations do not represent waste materials. The use of experimental techniques to highlight a particular material response presumes that the response can be extrapolated to relevant service conditions. In the examples just cited, the effect of flow rate on the dissolution rate occurs due to the influence of the solution concentrations of key solutes on the value of the affinity term, which reflects the deviation of the system from equilibrium. The dissolution rate varies with the deviation from equilibrium, and so will vary with the steady-state solution composition that is determined, in part, by the flow rate used in the test.

Laboratory rates are measured on a per area basis and directly scaled to field dimensions in performance calculations. Crushing materials to provide large surface areas in laboratory tests introduces fracture surfaces and defects that dissolve faster than the bulk materials. The effects of fractured surfaces on the laboratory-measured rate must be either taken into account with a separate transient rate term or avoided by ignoring the initial test response in the test. Because the reactive surface areas cannot be measured directly, laboratory rates are normalized to the physical surface area, which itself can be defined either as the area measured by gas adsorption or the area approximated geometrically. Although the measured surface area is physically well-defined, most experiments scale better using the geometric surface area rather than the measured area (e.g., Oversby 1982). The geometric surface area is also expected to be more appropriate for scaling to

macroscopic systems that are characterized geometrically; this will be evaluated in the subsequent report on the relationship between laboratory testing and field leaching.

The responses measured in semi-static solution exchange test methods such as ANS 16.1 and ASTM C1308 (ALT) are sensitive to the sampling interval regardless of whether the release of contaminants is controlled by diffusion or by dissolution. This is because while the release kinetics is not linear over the sampling interval, only a linear average release rate over the test interval can be determined from the test data. Model parameter values derived from these tests will depend on the sampling interval and may not represent the intrinsic material property well in performance calculations. This is because the analytical equations used to calculate diffusive release provide an instantaneous release rate whereas the experiments provide the integrated rate for each interval. Data sets with short and constant exchange frequencies should be used to quantify the release rate. Test conditions (e.g., the solution volume/specimen surface area ratio) should be adjusted to attain measureable solution concentrations within a few days sampling interval. Test series with variable exchange intervals demonstrate the effect of the interval duration on the test response and are useful for determining the release mechanism, but they do not provide dissolution rates appropriate for modeling long-term behavior. Based on the analyses summarized in Section 7.4.3, the variance in sampling intervals in the ANS 16.1 method and the use of the average value from different intervals are not consistent with the diffusion-controlled mechanism that is used to calculate the leach index. Because of this, the leachability index does not provide a reliable measure of the effective diffusion coefficient that is needed for performance modeling or any other characteristic of the material that is used in the test.

Diffusion-controlled and dissolution-controlled release mechanisms cannot be distinguished in static tests such as ASTM C1220 and ASTM C1285 because the effects of the buildup of released constituents in solution and the formation of a diffusion barrier on the test specimen lead to similar short-term release trends. Solution feedback effects can affect contaminant release rates regardless of whether the release is controlled by diffusion or by dissolution. The effect is usually (but not always) more significant for dissolution-controlled release than for diffusion-controlled release because matrix components such as silica often have lower solubility limits than the contaminants of interest. The chemical affinity for the reaction controlling mineral dissolution is expected to be more sensitive to the solution concentration than the concentration gradient between a species in the bulk and a site near the surface that promotes diffusion.

Short-term solution exchange tests can distinguish between diffusion-controlled and dissolution-controlled release mechanisms based on the time dependence. Diffusion-controlled release increases as the square root of time and dissolution-controlled release increases linearly in time if the value of the affinity term remains near one (assuming the pH and temperature remain constant). A 1-day exchange interval should maintain sufficiently dilute solutions to avoid solution feedback effects for most materials and significant pH excursions, so the response of a dissolution-controlled mechanism is expected to provide a measure of the forward dissolution rate.

The response of a dynamic test is affected by the effective solution flow rate except when the flow rate is high enough that the specimen is reacting at the highest possible rate. This typically requires fluidization of crushed material to maintain highly dilute conditions, such as the ASTM C1662 SPFT test method. Column tests in which leachant is allowed to percolate through a bed of crushed material or is pumped through the bed at a moderate rate (or at a rate thought to simulate a natural environment) may also provide data useful for determining dissolution model parameter values, although the test response will be affected by the flow rate, flow paths, and interactions that may retard the transport of some species. The effect of the flow rate must be deconvoluted from the measured release rate to determine the dissolution rate, and this can only be

done after the system has attained steady state. The system may be complicated by a range of flow paths, nearly static cells related to porosity, and, for tests conducted with crushed materials, the uncertain effects of fracture surfaces. This test method is better suited for use as a service condition test, for example, to calibrate a model with respect to groundwater flow under representative conditions, rather than quantifying a material response.

7.5.4 Laboratory Test Interpretations

The predominant approach taken in the literature that was reviewed as a part of this evaluation was to regress test data to a model to determine a model parameter, usually an effective diffusion coefficient, with too little concern regarding the appropriateness of the model. As stated in the ANS 16.1 procedure and discussed in Section 4.2.1, the early stages of material reaction usually *appear to be* controlled by diffusion whether diffusion is the controlling process or not. The data sets are, therefore, usually fitted with a form of the diffusion equation appropriate for the shape of the test specimen and an effective diffusion coefficient value is extracted. In the majority of the literature results that were analyzed in this report, the value of the diffusion coefficient that was extracted depended on the subset of data that was used. Sometimes the subset was determined based on the exchange interval, but it was usually selected based on which data were better fit with the diffusion equation. In many cases, the selected data were measured after long cumulative reaction times and over long sampling intervals. Considerations of the reaction behavior and test methodology as described throughout this report provide a technical basis for generating and selecting data sets to extract model parameter values. These include diffusion coefficients, reaction rate constants, pH and temperature dependencies, and saturation concentrations.

Geochemists have found that the in-the-field dissolution rates of many minerals are significantly lower than the rates measured in laboratory tests, in some cases five orders of magnitude lower. Several reasons for the discrepancies have been discussed in the literature: sorption of organic and inorganic materials masking reaction sites, uncertainties in the true reactive surface areas of the reacting materials in laboratory tests and in nature, increase in density of reactive sites due to crushing, different surface finishes in field materials and laboratory test specimens, different fluid chemistries in microclimes within the pore structure and surface regions of materials in the field, restricted fluid flow through fractures, bacteria, experimental measurement uncertainties, and other factors. While the cause of such discrepancies and the relevance to waste material and waste form degradation and contaminant release rates will be addressed in greater detail in a future report, it is important to add to that list a conclusion from this review: the use of an inappropriate laboratory test method and misapplication of test results. The release rates measured under particular test conditions should not be interpreted as being a characteristic rate of the waste or waste form without consideration of the process controlling the release, artifacts of the test method, or the effects of testing parameters. Several examples were found in the literature reviewed for this report where the release rate measured in a subset of the test data that looked right, such as showing the expected root-time dependence or being linear, was used to extract an effective diffusion coefficient or release rate for use in calculating long-term behavior. Beyond being scientifically indefensible for modeling data and for predicting long-term behavior, the apparent behavior of the subset may have been contrary to the rest of the data set and taken out of context. In some cases, interpretations were biased by the way the data were presented, for example, by plotting incremental or cumulative fractional release values rather than measured concentrations, plotting against linear or square root cumulative time, or not verifying that steady state was achieved. In many cases, data must be exercised using different models with several presentations to determine the relationship to a test variable, and often also compared with the results of other tests to discriminate between different possible interpretations.

For complex systems, it is usually necessary to study contributing processes separately and develop separate process models that are later combined to represent the system. *When modeling waste form performance, it is important to both verify that the analytical model represents the physical or chemical process being modeled and to confirm the role of the modeled process affecting waste performance in the disposal system.* Historically, standardized laboratory test methods have been used to characterize waste form materials with little regard to the relevance of the test method (or test response) to the disposal system. These tests include the PCT (ASTM C1285 Method A), ANS 16.1, and various EPA methods. Although these methods provide comparisons of the responses of different materials, those responses are usually not related to the degradation mechanisms that are operative in a disposal system and so the comparisons are usually anecdotal. For example, most laboratory tests are conducted with a great excess of water relative to the amount of water in a disposal system in order to facilitate analyses. Material behavior may be quite different under these test conditions and under the actual hydrologically unsaturated site conditions (for example), and material degradation in the field could even be controlled by a different process than the process responsible for the response measured in the laboratory test.

7.5.5 Recommended Test Methods

For most waste sites, the amount of testing and modeling necessary to determine and parameterize a mechanistic model to reliably predict long term behavior will not be feasible with regard to cost or the time required. In addition, the level of complexity and variations of the waste itself (phase composition, inhomogeneity of contaminant distribution, range of physical dimensions, etc.) will greatly increase the effort required to develop, validate, confirm, and apply mechanistically based models for predicting long-term performance. For example, homogeneous borosilicate waste glasses have been studied for many years, and that research has drawn on a long and rich history of research addressing commercial and archaeological glass. Nevertheless, several aspects of glass degradation important to its long-term performance as a waste form are still poorly understood, such as identifying the process that controls continued glass degradation in concentrated solutions. Modeling the degradation of slag wastes that may contain several dozen oxide, silicate, and metallic inclusion phases bound within a glassy matrix is much more complicated than modeling waste glass. This is because interactions between the various phases and a common solution will impact the dissolution behavior of all phases, the dissolution of less-durable phases will slow the dissolution of more-durable phases, the assemblage of alteration phases will establish solubility limits different than those controlling the dissolution of isolated phases, etc. Representations of the waste (or waste form) and disposal site (or system) must be simplified for long-term performance assessments using reasonable models that capture the time dependencies of the processes controlling the degradation, contaminant release, and transport behaviors, but are compatible with limited characterizations of the complex waste solids and limited computation capacity.

The critical review that was conducted as part of this report was intended to identify aspects of laboratory tests that are important for understanding the underlying mechanism and providing defensible measures of parameter values used in a simplified model. One objective was to identify a small number of tests that could be used to characterize the waste degradation behavior to support performance assessments when detailed studies were not practical. Some nuances of the degradation behavior may not be detected in short-term tests, such as reactions to provide transportable components that are subsequently released by a diffusion-controlled process or the complex relation between the solution chemistry and release rate in an affinity-controlled process. To the extent possible, the limited data base of short-term tests should utilize insights regarding the waste material to select the test method, test conditions, and process model that will best inform the performance assessment. Probably the most important aspect of long-term predictions is the

time dependence of the process controlling contaminant release, and whether that is a diffusion-controlled or affinity-controlled process. The long-term effects of environmental variables such as temperature, pH, Eh, and groundwater chemistry will likely be less than the transport-related variables such as groundwater flow and geochemical effects that retard contaminant dispersal.

If the likely degradation and release mechanisms of a waste material are known based on the nature of the material (e.g., concrete, glassy, or crystalline composite), then the relevant test method can be selected to characterize the material for modeling (and verify the process) and extract a model parameter. It is important to recognize how a material that degrades by a mechanism that is different than the one highlighted by the test method will respond in order to add confidence that the correct process model is being used. The first two methods are minor modifications of existing standardized test methods ASTM C1308 and ASTM C1220 based on analyses of test results discussed in this report. The third method is a hydrid of the two that is proposed based on a technical understanding of the two methods but has not been implemented.

- For materials that react by a diffusion-controlled release mechanism (e.g., relevant to cement-based wastes), a modification of ASTM C1308 is recommended with two series of sampling frequencies (for example, six 1-day intervals followed by six 7-day intervals). Contaminants released by a diffusion-controlled mechanism are expected to show CFL values that are linear with root-time for both intervals, but with different slopes. The results for the 7-day exchange intervals are expected to have a smaller slope due to the longer sampling interval. The releases in the 1-day interval samplings can be used to extract an effective diffusion coefficient. This presumes that (1) a 1-day interval is sufficient to generate measurable solution concentrations of the contaminant of interest, and (1) the effect of the 1-day sampling interval on the extracted value of D_e is within the test uncertainty. If this test method is applied to a material having an affinity-controlled dissolution mechanism, the six 1-day intervals and the six 7-day intervals are both expected to show linear behavior with time (instead of with root-time), but the rate from the 1-day intervals will be higher and approximate the forward reaction rate. The lower rate from the 7-day intervals will reflect the decreasing reaction affinity as the test solution becomes more concentrated over the longer test duration. Using two sampling intervals will help distinguish between diffusion-controlled and affinity-controlled release and provided insight into the model parameter values that are extracted: in the case of D_e extracted for diffusion-controlled release, the difference in slopes in the CFL vs. root-time plot provides confidence that the release is controlled by diffusion and that the value of D_e from the short sampling intervals represents the contaminant and material. In the case of k_f, the difference in slopes will provide some insight into the value of K. The difference in rates will be greater for materials having smaller values of K, although the difference will not be sufficient to determine a value of K that can be used in modeling.

- For an affinity-controlled dissolution release mechanism (e.g., relevant to slag wastes), a modification of ASTM C1220 is recommended with small sample aliquants (the minimum volume required for reliable analysis) taken at increasing intervals (without replacement). When normalized mass-loss values (which can be used to adjust the solution concentrations to the S/V ratio at each sampling; see Equation 3.5) are plotted against time, the early samplings are expected to show linear release and the later sampling are expected to deviate negatively. The data set can be regressed with the affinity model to determine the forward rate (k_f) and an effective saturation concentration (K). This is the saturation concentration responsible for the decrease in the rate from the forward rate (i.e., at the dissolution plateau at very negative values of ΔG_r). As discussed in Section 2.3, a different functional dependence on the saturation index (and K) could control the dissolution rate under near-equilibrium conditions. The value of K relevant to near-equilibrium conditions should be measured by conducting

ASTM C1285 Method B tests with periodic samplings to track the solution composition as equilibrium is approached. (The slight change in the S/V ratio of the test will not affect the solution composition or approach to equilibrium; *fresh solution should not be added to the test.*) Both k_f and K will represent average values for all phases bearing the contaminant of interest weighted by the fraction each phase contributes to the surface area and the intrinsic dissolution rate of the phase. Application of the modified ASTM C1220 test method to a material for which the release is diffusion-controlled is expected to show root-time behavior, but may deviate negatively over time if high solution concentrations are generated.

- If the release mechanism is not known, a hybrid test method that combines aspects of the ASTM C1308 and ASTM C1220 methods in sequence is proposed to (1) measure the diffusion coefficient or intrinsic dissolution rate (at particular temperature and pH), (2) distinguish between diffusion-controlled and dissolution-controlled release mechanisms, and (3) estimate the saturation concentration for dissolution-controlled reactions. The initial samplings are conducted following the ASTM C1308 methodology by replacing the entire solution at constant 1-day exchange intervals. These samplings are expected to indicate whether the contaminant release is linear with the square-root of time (characteristic of diffusion-control) or linear with time (characteristic of affinity-controlled dissolution), or has an intermediate time-dependence, which could indicate that both diffusion and reaction processes are important. The subsequent samplings are conducted weekly following the ASTM C1220 method without adding fresh leachant. A diffusion-controlled mechanism is expected to show root-time release (at a lower rate) and an affinity-controlled mechanism is expected to deviate negatively from linear release due to the decreasing reaction affinity as the solution becomes more concentrated. The combined evidence from the initial ASTM C1308 test and subsequent ASTM C1220 test with the same specimen and solution is expected to reveal the release mechanism and provide model parameters. The ASTM C1308 samplings would provide a value of either D_e or k_f, and the ASTM C1220 samplings would provide an estimate of K and confirmation of the controlling process.

7.5.6 Concluding Remarks

Relatively simple laboratory tests are used to evaluate the release of contaminants from concrete and, more recently, slag waste materials. The theoretical models used to interpret these test results range from simply fitting (or force-fitting) the data with an analytical equation for diffusion (e.g., from a finite or semi-infinite solid) to using the test results to extract parameters for affinity-controlled or combined diffusion/reaction processes. The evaluations discussed in this report point out the relationships between how test data are collected and interpreted in the laboratory and how they are applied in a particular process model. As shown with several examples taken from the literature, the trends in some data sets that indicate a problem in the way a model was being applied can be explained as testing artifacts that can be easily eliminated or taken into account. The first examples address the effect of the sampling interval used in a solution exchange test such as ANS 16.1 and ASTM C1308 (and the earlier methods that evolved into these standardized methods) on the extracted value of the diffusion coefficient. Other trends may indicate an unavoidable limitation of the test method or test conditions. The second examples address the effect of the flow rates used in column tests, SPFT tests, and PUF tests. The flow rate is known to affect the dissolution and contaminant release rates that are measured, but the effect is often not taken into account when relating the measured rates to material behavior. In some studies, particular test conditions were used to simulate a system and provide a direct measurement of the reaction rate in the field. Such condition-specific rates are generally not useful for parameterizing a rate law and may lead to erroneous predictions due to difficulties in replicating the field conditions, including flow path and contacted surface area, and flow rate. This will be discussed

in more detail in the following report on the relationship between laboratory tests and field. How the laboratory test data are compiled can also contribute also to misinterpretations and errant predictions. For example, focusing on the cumulative release of a contaminant of interest is not relevant for a dynamic test system approaching steady state, but will nevertheless provide a misleading time dependence. Additional insights are summarized below:

- Analytical expressions are available for quantifying material degradation processes that occur during laboratory tests, including dissolution, mass transport (bulk diffusion), oxidation, and simply coupled processes based on a molecular-scale understanding of the major processes. The models provide relationships between contaminant release and process variables, environmental variables, and transport-related variables. Laboratory tests can be used to determine the values of model parameters for specific waste materials that can then be used for predicting their long-term behaviors under a wide range of environmental conditions.

- Theoretical frameworks are available for improved modeling and better utilization of test results in performance calculations. The relationship between material, rate-controlling process, test method, and modeled results should be understood before predicting long-term behavior in a disposal system. Different test methods or test conditions are often required to describe behavior under different environmental conditions and after various extents of reaction. For example, in the treatment of coupled reaction and diffusion processes by Godbee and Joy (1974) discussed in Section 4.3.1 and Appendix C, the reaction component was modeled using a constant dissolution rate. Although this is probably sufficient in the dilute conditions that exist in a solution exchange test, taking the affinity term into account may provide a useful means to model the release under more relevant conditions that are closer to equilibrium in highly concentrated solutions.

- The sampling interval used in solution replacement tests such as ANS 16.1 and ASTM C1308 will affect the value of the effective diffusion coefficient that is extracted from the data. Tests should be conducted with a short and constant sampling interval so the test results are consistent with the model. Specifically, the model equation for diffusion-controlled release is derived using an infinitesimal time interval that should be approximated with a short sampling interval. The interval must be long enough for a measurable extent of reaction to occur.

- The effective diffusion coefficient of a contaminant is determined from test data based on the geometry of the test specimen, but the value itself is independent of that geometry. The extent of diffusion from that material in the field will depend on its geometry.

- Short-term static and semi-dynamic tests may not be sufficient to discriminate between diffusion-controlled and affinity-controlled releases, and long-term predictions of the two mechanisms will differ significantly. The time dependence of the initial stages of affinity-controlled release in a static solution is often well fit using a root-time dependence, even though the process is not a function of $t^{1/2}$. For example, effect of the affinity term on the dissolution rate could lead to an apparent root-time dependence. Different test conditions, longer duration tests, or a different test method may be necessary to determine the release mechanism and time dependence.

- The leachant flow rate affects the dissolution rate of materials in dynamic tests including SPFT tests, stirred reactor tests, and column tests (both hydrologically saturated and unsaturated systems) except at very high flow rates that maintain far-from-equilibrium conditions. The effect of flow rate occurs because the steady-state solution composition that is established depends on the material dissolution rate, surface area, and flow rate. This should not be

confused with erosion of the material, which is a physical effect of flow. Erosion may be an artifact of very high flow rates due to the abrasion of particles due to turbulence within the reaction cell.

- The transport of released components through packed columns (in column and PUF tests) may be retarded relative to the transport of water and soluble components due to the interactions of solutes with other solids. Longer test durations may be required for some components to attain steady-state concentrations at the column outlet.

- Crushing materials to increase the accessible surface area in a test generates artifacts, including fine materials, fracture edges, defect sites, and strained and roughened surfaces. Material at these sites dissolves at a higher rate than the bulk material. This leads to initial transient rates that are anomalously high but decrease to the bulk rate as the artifact sites are dissolved. The influence of these fast-dissolving sites on the test response should be avoided, e.g., by discarding the initial test solutions, or taken into account when evaluating the data.

- Steady state may not be attained in flow tests due to the loss of surface area during the test, particularly under far-from-equilibrium conditions. Because the steady-state concentrations depend on both the dissolution rate and the surface area, it may be difficult to discriminate between the loss of surface area due to the dissolution of high-energy surfaces early in the test from the loss of surface area after the high-energy sites have been dissolved.

- Crushed test material should be sized according to maximum and minimum sieve mesh sizes to better constrain the particles size and surface area used in the test. This is important for relating the measured rate to the surface area available during the test. Small particles and fines may completely dissolve during a test and result in misleading results due to a significant decrease in the surface area during the test.

- The specific surface area of particulate samples used in dissolution tests are usually measured by gas adsorption (the BET method) or estimated geometrically based on sieve fraction size. Although the BET surface area is often measured both before and after the test, the actual mass of material remaining after the test is seldom (if ever) reported, probably due to the difficulty of recovering all of the sample from the reactor. Knowledge of the after-testing specific surface area is by itself of little or no value. Tests consistently show the preferential dissolution of fracture sites during the initial stages, so the particles are becoming smoother as they become smaller. The smaller size increases the specific surface area of each particle, whereas the loss of fracture sites decreases the specific surface area. The formation of alteration phases on the sample surface will also increase the specific surface area that is measured, although this does not increase the reactive surface area of the test material, and may decrease the reactive surface area by blocking access to the material surface.

- Conducting dissolution tests for long durations complicates the determination of the reaction rate due to increased uncertainties in the reactive surface area. The surface area remaining at any time during the test can be estimated from the measured dissolution rate, test duration, and initial specimen mass. Whereas the specimen surface area is used to scale the rate measured in the laboratory to the field, it is the reacted volume that is related to the measured solution concentrations. The relevance of details regarding laboratory tests and modeling to performance calculations will be examined further in the subsequent report: *Relationship between Laboratory Tests and Field Leaching.*

8 References

Amarantos, S.G. (1976). Leaching Kinetics of Ions from Solidified Radioactive Wastes. International Atomic Energy Agency report IAEA-R-1383-F.

Amarantos, S.G. and Petropoulos, J.H. (1972). *A Study of Leaching Kinetics of Ions from Wastes Incorporated in Bitumen.* GREEK A.E.C. DEMO 72/11.

Amrhein, C., and Suarez, D.L. 1992. "Some Factors Affecting the Dissolution Kinetics of Anorthite at 25°C." *Geochimica et Cosmochimica Acta, 56*, 1815-1826.

ANS (2009) Measurement of the Leachability of Solidified Low-Level Radioactive Wastes by a Short-Term Test Procedure, ANS/ANSI 16.1, American Nuclear Society, La Grange Park, Illinois.

ASTM (2009a) Annual Book of ASTM Standards, Vol. 12.01, West Conshohocken, Pennsylvania: ASTM-International.

ASTM (2009b). Annual Book of ASTM Standards, Vol. 11.04, West Conshohocken, Pennsylvania: ASTM-International.

Atkinson, A., Nickerson, A.K., and Valentine, T.M. (1984). "The Mechanism of Leaching from Some Cement-Based Nuclear Wasteforms." *Radioactive Waste Management and the Nuclear Fuel Cycle, 4(4),* 357-378.

Bacon, D.H. and McGrail, B.P. (2005). *Waste Form Release Calculations for the 2005 Integrated Disposal Facility Performance.* Pacific Northwest National Laboratory report PNNL-15198.

Bacon, D.H., White, M.D., and McGrail, B.P. (2004). *Subsurface Transport Over Reactive Multiphases (STORM): A Parallel, Coupled, Nonisothermal Multiphase Flow, Reactive Transport, and Porous Medium Alteration Simulator, Version 3.0. User's Guide.* Pacific Northwest National Laboratory report PNNL-14783.

Bethke, C.M. (1996) *Geochemical Reaction Modeling.* New York, New York: Oxford University Press.

Bourcier, W.L. (1991). "Overview of Chemical Modeling of Nuclear Waste Glass Dissolution." *Scientific Basis for Nuclear Waste Management,* ed. T. Abrajano, Jr. and L.H. Johnson. Vol. 212, 3-18.

Bourcier, W.L., Carroll, S.A., and Phillips, B.L. (1994), "Constraints on the Affinity Term for Modeling Long-term Glass Dissolution Rates," in *Scientific Basis for Nuclear Waste Management XVIII,* ed. Aa. Barkatt and R.A. Van Konynenburg, pp. 507-512.

BSC 2004. *CSNF Waste Form Degradation: Summary Abstraction.* Bechtel SAIC Company report ANL-EBS-MD-000015, Rev. 02, issued 2004, ACN 002 issued August 2005.

Burch, T.E., Nagy, K.L., and Lasaga, A.C. (1993). "Free Energy Dependence of Albite Dissolution Kinetics at 80 °C and pH 8.8." *Chemical Geology, 105*, 137-162.

Butcher, E.J., Cheesemen, C.R., Sollars, C.J., and Perry, R. (1996). "Flow-Through Leach Testing Applied to Stabilized/Solidified Wastes" in *Stabilization and Solidification of Hazardous, Radioactive, and Mixed Wastes: 3rd Volume*, ed. T.M. Gilliam and C.C. Wiles, ASTM STP 1240.

CA WET (2005) *Waste Extraction Test (WET) Procedures,* California Code of Regulations Title 22 Division 4.5, Chapter II, Article 5, Section 66261.126 Appendix II.

Chou, L. and Wollast, R. (1984). "Study of the Weathering of Albite at Room Temperature and Pressure with a Fluidized Bed Reactor," *Geochimica et Cosmochimica Acta, 48*, 2205-2217.

Christensen, H. (1982). "Leaching of Cesium from Cement Solidified BWR and PWR Bead Resins." *Nuclear and Chemical Waste Management, 3*, 105-110.

Christensen, H., and Sunder, S. (2000). "Current State of Knowledge of Water Radiolysis Effects on Spent Nuclear Fuel Corrosion." *Nuclear Technology 131,* 102-123.

Colombo, P., Doty, R., Dougherty, D., Fuhrmann, M., and Heiser, J. (1985). *Accelerated Leach Test(s) Program Annual Report.* BNL-51955. Brookhaven National Laboratory: Upton, NY.

Côté, P.L, Constable, T.W., and Moreira, A. (1987). "An Evaluation of Cement-Based Waste Forms Using the Results of Approximately Two Years of Dynamic Leaching." *Nuclear and Chemical Waste Management 7*, 129-139.

Crawford, R.W., Glasser, F.P. Rahman, A.A., Angus, M.J, and McCulloch, C.E. (1984). "Diffusion Mechanisms and Factors Affecting Leaching of Caesium-134 from Cement-Based Waste Matrices." *Radioactive Waste Management and the Nuclear Fuel Cycle, 6,* 177-196.

Danckwerts, P.V. (1950). "Absorption by Simultaneous Diffusion and Chemical Reaction," *Transactions of the Faraday Society, 46*, 300-304.

Delage, F. and Dussossoy, J.L. (1991) "R7T7 Glass Initial Dissolution Rate Measurements Using a High-Temperature Soxhlet Devise," in *Scientific Basis for Nuclear Waste Management XIV: Proceedings of the Material Research Society Symposium Proceedings 212*, 41-47.

DOE (2008) License Application for a High-Level Waste Geologic Repository at Yucca Mountain, U.S. Department of Energy, http://www.ocrwm.doe.gov/license_application/index.shtml

Ebert, W.L. and Bates, J.K. (1993). "A Comparison of Glass Reaction at High and Low Surface Area to Volume," Nuclear Technology 104(3) 372-384.

Ebert, W.L. (1995). *The Effects of the Glass Surface Area/Solution Volume Ratio on Glass Corrosion: A Critical Review*, Argonne National Laboratory Report ANL-94/34 (1995).

Ebert, W.L., Zyranov, V.N., and Cunnane, J.C. (2000). "Estimating Model Parameter Values for Total System Performance Assessment," *Material Research Society Symposium Proceedings, 608*, 751-758.

Ebert, W.L. (2005a). *Testing to Evaluate the Suitability of Waste Forms Developed for Electrometallurgically Treated Spent Sodium-Bonded Nuclear Fuel for Disposal in the Yucca Mountain Repository.* Argonne National Laboratory report ANL-05/43.

Ebert, W.L. (2005b). *Interlaboratory Study of the Reproducibility of the Single-Pass Flow-Through Test Method: Measuring the Dissolution Rate of LRM Glass at 70 °C and pH 10.* Argonne National Laboratory report ANL-05/33.

Ebert, W.L. (2006). *Comparison of the Results of Short-Term Static Tests and Single-Pass Flow-Through Tests with LRM Glass.* Argonne National Laboratory report ANL-06/51.

Eggleston, C.M., Hochella, M.F. Jr., and Parks, G.A. (1989). "Sample Preparation and Aging Effects on the Dissolution Rate and Surface Composition of Diopsite." *Geochimica et Cosmochimica Acta, 53*, 797-804.

EPA (2009). *Test Methods for Evaluating Solid Wastes—Physical/Chemical Methods*, SW-846, 3rd edition, as amended by Updates I (July 1992), II, IIA (August 1993), IIB, III and IIIA, Washington, D.C.: U. S. Environmental Protection Agency.

Fey, D.L., Desborough, G.A., and Finney, C.J. (2000). *Analytical Results for Total-Digestions, EPA-1312 Leach, and Net Acid Production for Twenty-Three Abandoned Metal-Mining Related Wastes in the Boulder River Watershed, Northern Jefferson County, Montana,* U.S. Geological Survey Open-File Report 00-114.

Frugier, P., Gin, S., Minet, Y., Chave, T., Bonin, B., Godon, N., Lartigue, J.-E., Jollivet, P., Ayral, A., DeWindt, L. and Santarini, G. (2008) "SON68 Nuclear Glass Dissolution Kinetics: Current State of Knowledge and Basis of the New GRAAL Model," *Journal of Nuclear Materials 380, 8*-21.

Fuhrmann, M, Heiser, J.H., Pietrzak, R., Franz, E.-M., and Colombo, P. (1990). *User's Guide for the Accelerated Leach Test Computer Program.* BNL-52267. Brookhaven National Laboratory, Upton, NY.

Fuhrmann, M. and Schoonen, M. (1997). *Leaching of Slag from Steel Recycling: Radionuclides and Stable Elements.* BNL-71445-2003. Brookhaven National Laboratory, Upton, NY.

Godbee, H.W., Compere, E.L., Joy, D.S., Kibbey, A.H., Moore, J.G., Nestor, C.W., Anders, O.U., and Neilson, R.M. (1980) Application of Mass Transport Theory to the Leaching of Radionuclides from Waste Solids." *Nuclear and Chemical Waste Management 1*, 29-35.

Godbee, H.W., and Joy, D.S. (1974). *Assessment of the Loss of Radioactive Isotopes from Waste Solids to the Environment. Part I: Background and Theory*, Oak Ridge National Laboratory report ORNL-TM-4333.

Habayeb, M.A. (1985) "Leaching Performance of Cemented Decontamination Wastes." *Nuclear and Chemical Waste Management*, 5, 305-314.

Hageman, P.L. (2004). *Use of Short-Term (5-minute) and Long-Term (18-hour) Leaching Tests to Characterize, Fingerprint, and Rank Mine-Waste Material from Historical Mines in the Deer Creek, Snake River, and Clear Creed Watersheds in and around the Montezuma Mining District, Colorado,* U.S. Geological Survey Scientific Investigations Report 2004-5104.

Hanson, B.D., Friese, J.I., and Soderquist, C.Z. (2004). "Initial Results from Dissolution Testing of Spent Fuel Under Acidic Conditions," in *Scientific Basis for Nuclear Waste Management XXVIII, ed. J.M. Hanchar, S. Stroes-Gascoyne, and L. Browing.* pp. 113-118. Materials Research Society, Warrendale, PA.

Hellmann, R., and Tisserand, D. (2006). "Dissolution Kinetics as a Function of the Gibbs Free Energy of Reaction: An experimental Study Based on Albite Feldspar." *Geochimica et Cosmochimica Acta, 70*, 364-383.

Hillel, D. (1980) *Fundamentals of Soil Physics*, Academic Press Inc., Orlando, Florida

ISO (1982) *Long-Term Leach Testing of Solidified Radioactive Waste Forms*, International Standard ISO 6961:1982, Geneva, Switzerland: International Standards Organization.

ISO (2008) *Nuclear energy—Soxhlet-mode chemical durability test—Application to vitrified matrixes for high-level radioactive waste*, International Standard ISO 16797:2004, Geneva, Switzerland: International Standards Organization.

Johnson, S.G., Noy, M., DiSanto, T., and Keiser, D.D., Jr. (2002). "Long-Term Immersion Test Results of the Metallic Waste Form from the EMT Process of EBR-II Spent Metallic Fuel." In *Proceedings of the DOE Spent Nuclear Fuel and Fissile Materials Management Meeting held September 17-20, 2002. Charleston, South Carolina. Waste Form Testing session.* American Nuclear Society.

Knauss, K.G., and Wolery, T.J. (1986). "Dependence of Albite Dissolution Kinetics on pH and Time at 25°C and 70°C." *Geochimica et Cosmochimica Acta, 50*, 2481-2497.

Lasaga, A.C. (1981). "Rate Laws of Chemical Reactions," in *Reviews in Mineralogy, Vol. 8: Kinetics of Geochemical Processes,* ed. A.C. Lasaga and R.J. Kirkpatrick, pp. 1-68. Mineralogical Society of America.

Lasaga, A.C. (1984). "Chemical Kinetics of Water-Rock Interactions." *Journal of Geophysical Research 89(B6),* 4009-4025.

Lasaga, A.C. (1995). "Approaches to Describing Dissolution/Precipitation Rates," in *Reviews in Mineralogy, Volume 31 Chemical Weathering Rates in Silicate Minerals,* ed. A.F. White and S.L. Brantley, pp. 23-86, Mineralogical Society of America.

Lasaga, A.C., and Luttge, A. (2001) "Variation of Crystal Dissolution Rate Based on a Dissolution Stepwave Model," *Science 291,* 2400-2404.

Mattigod, S.V., Whyatt, G.A., Serne, R.J., Martin, P.F., Schwab, K.E., and Wood, M.I. (2001). *Diffusion and Leaching of Selected Radionuclides (Iodine-129, Technetium-99, and Uranium) Through Category 3 Waste Encasement Concrete and Soil Fill Material.* Pacific Northwest National Laboratory report PNNL-13639.

McDeavitt, S.M., Abraham, D.P., and Park, J.Y. (1998). "Evaluation of Stainless Steel-Zirconium Alloys as High-Level Nuclear Waste Forms." *Journal of Nuclear Materials, 257,* 21–34.

McGrail, B.P., Ebert, W.L., Bakel, A.J., and Peeler, D.K. (1997a). "Measurement of Kinetic Rate Law Parameters on a Na-Ca-Al Borosilicate Glass for Low-Activity Waste," *Journal of Nuclear Materials, 249*, 175-189.

McGrail, B.P, Martin, P.F., and Lindenmeier, C.W. (1997b). "Accelerated Testing of Waste Forms Using a Novel Pressurized Unsaturated Flow (PUF) Method," *Material Research Society Symposium Proceedings, 465*, 253-260.

Mogollon, J.L., Ganor, J., Soler, J.M., and Lasaga, A.C. (1996). "Column Experiments and the Full Dissolution Rate Law of Gibbsite." *American Journal of Science, 296*, 729-765.

Neilson, R.M. Jr, Kalb, P.D., and Colombo, P. (1982). *Lysimeter Study of Commercial Reactor Waste Forms: Waste Form Acquisition, Characterization and Full-Scale Leaching.* Brookhaven National Laboratory report BNL-51613.

Ogard, A.E. and Bryant, E.A. (1982). "The Misused and Misleading IAEA Leach Test.: *Nuclear and Chemical Waste Management, 3*, 79-81.

OND (1991). Caractérisation des colis de déchets radioactifs FA/MA. Caractéristiques liées au confinement. Résistance à la lixiviation OND-03, FT 04.001.

Oversby, V.M. (1982). *Leach Testing of Waste Forms: Interrelationship of ISO- and MCC- Type Tests*, Lawrence Livermore National Laboratory report UCRL 87621.

Pescatore, C. (1990). "Improved Expressions of Modeling Diffusive, Fractional Cumulative Leaching from Finite Size Waste Forms," *Waste Management 10*, 155–159.

Petrovich, R. (1981). "Kinetics of Dissolution of Mechanically Comminuted Rock-Forming Oxides and Silicates-II. Deformation and Dissolution of Oxides and Silicates in the Laboratory and at the Earth's Surface." *Geochimica et Cosmochimica Acta, 45*, 1675-1686.

Pickett, D.A., Prikryl, J.D., Turner, D.R., and Russel, J.L. (1998). *Evaluation of Leach Tests for Estimating Release from Slag Sites Subject to Decommissioning: Final Report.* Prepared for Nuclear Regulatory Commission Contract NRC-02-97-009, Center for Nuclear Waste Regulatory Analyses, San Antonio, Texas.

Pierce, E.M., McGrail, B.P., Valenta, M.M. and Strachan, D.M. (2006) "The Accelerated Weathering of a Radioactive Low-Activity Waste Glass Under Hydraulically Unsaturated Conditions: Experimental Results from a Pressurized Unsaturated Flow Test." *Nuclear Technology, 155*, 149-165.

Pierce, E.M., Rodriquez, E.A., Calligan, L.J., Shaw, W.J., and McGrail, B.P. (2008) "An Experimental Study of the Dissolution Rates of Simulated Aluminoborosilicate Waste Glasses as a Function of pH and Temperature under Dilute Conditions." *Applied Geochemistry, 23*, 2559-2573.

Poon, C.S., Chen, Z.Q., and Wai, O.W.H. (2001). "The Effect of Flow-Through Leaching on the Diffusivity of Heavy Metals in Stabilized/Solidified Wastes" *Journal of Hazardous Materials, B81*, 179-192.

Poon, C.S. and Wai, O.W.H. (1999). "A Flow-Through Leaching Model for Monolithic Chemically Stabilized/Solidified Hazardous Waste." *Journal of the Air Waste Management Association 49*, 569-575.

Relyea, J.F. (1982). "Theoretical and Experimental Considerations for the use of the Column Method for Determining Retardation Factors." *Radioactive Waste Management and the Nuclear Fuel Cycle, 3*, 151-166.

Rorif, F., Van Iseghem, P., and Fays, J. (2005) "An Accelerated Procedure for Testing the Quality of Cemented Waste Forms in Nuclear Power Plants." Presented by P. Van Iseghem at ASTM Symposium on Accelerated Test Methods, Tampa, Florida, January 31, 2005.

Shoesmith, D.W., and Sunder, S. (1991). *An Electrochemistry-Based Model for the Dissolution of UO_2.* Atomic Energy of Canada Limited report AECL-10488.

Shoesmith, D.W., and Sunder, S. (1992). "The Prediction of Nuclear Fuel (UO_2) Dissolution Rates Under Waste Disposal Conditions." *Journal of Nuclear Materials, 190*, 20-35.

Shoesmith, D.W. (2000). "Fuel Corrosion Processes Under Waste Disposal Conditions." *Journal of Nuclear Materials 282,* 1-31.

Smith, A.J. (1969) *Leaching of Radioactive Sludges Incorporated in Cement and Bitumen,* AERE M. 2223.

Spence, R.D. and Cox, R.L. (1990). "A Theoretical Study of the Effect of the Leach Interval on a Semidynamic Leach Test." *Scientific Basis for Nuclear Waste Management,* Vol. 176, 101-107.

Sullivan, T.M. (1993) "DUST - Disposal Unit Source Term: Data Input Guide." NUREG/CR-6041, BNL-NUREG-52375.

Taylor, Aa.S., Blum, J.D., and Lasage, A.C. (2000a). "The Dependence of Labradorite Dissolution and Sr Isotope Release Rates on Solution Saturation State." *Geochimica et Cosmochimica Acta, 64,* 2389-2400.

Taylor, Aa.S., Blum, J.D., Lasage, A.C., and MacInnis, I.N. (2000b). "Kinetics of Dissolution and Sr Release during Biotite and Phlogopite Weathering." *Geochimica et Cosmochimica Acta, 64,* 1191-1208.

USGS (2005). A Simple Field Leach Test to Assess Potential Leaching of Soluble Constituents from Mine Wastes, Soils, and Other Geologic Materials, Fact Sheet 2005-3100 version 1.0. http://pubs.usgs.gov/fs/2005/3100.

Van Iseghem, P. (2005). "An Accelerated Procedure for Testing the Quality of Cemented Waste Forms in Nuclear Power Plants," presentation at ASTM-International Symposium on Accelerated Test Methods held in Atlanta, Georgia, January 30, 31, 2005.

Veblen, L.A., Farthingt, D., O'Donnell, E., and Randall, J.D. 2004). *Characterization of Radioactive Slags.* NUREG-1703, Washington, D.C.: U.S. Nuclear Regulatory Commission.

White A.F. and Brantley, S.L. (2003). "The Effect of Time on the Weathering of Silicate Minerals: Why do Weathering Rates Differ in the Laboratory and Field?" *Chemical Geology 202,* 479-506.

Yang, L. and Steefel, C.I. 2008. *Kaolinite Dissolution and Precipitation Kinetics at 22 °C and pH 4. Geochimica et Cosmochimica Acta, 72,* 99-116..

Yu, C. (1987). "Modeling of Low-Level-Waste Disposal for Environmental Impact Analysis." *Waste Management '87,* 385-390.

Yu, C., Zielen, A.J., Cheng, J.-J., LePoire, D.J., Gnanapragasam, E., Kamboj, S., Arnish, J., Wallo, A. III, Williams, W.A., and Peterson, H. (2001) *Users's Manual for RESRAD Version 6, RESRAD 6 manual (August 30, 2001)* Argonne National Laboratory. http://web.ead.anl.gov/resrad/documents.

Appendix A

Affinity-Controlled Dissolution

Dissolution reactions are usually modeled as competing forward and reverse reactions, where the forward reaction results in the release of a component into solution and the reverse reaction results in the consumption of a dissolved species in a condensation reaction. The net rate of a reaction step is simply the difference between the forward and reverse rates:

$$rate_{net} = rate_{forward} - rate_{reverse}. \tag{A.1}$$

which can be rearranged as

$$rate_{net} = rate_{forward} \bullet \left(1 - \frac{rate_{reverse}}{rate_{forward}}\right). \tag{A.2}$$

For a system at equilibrium

$$\left(\frac{rate_{reverse}}{rate_{forward}}\right) = 1, \tag{A.3}$$

and the net rate is zero. For a system that is not at equilibrium

$$\left(\frac{rate_{reverse}}{rate_{forward}}\right) = \exp\left(\frac{-A}{RT}\right), \tag{A.4}$$

where A is the reaction affinity, R is the ideal gas constant, and T is absolute temperature. The reaction affinity is defined as the negative partial derivative of the Gibbs free energy $\boldsymbol{G}$ with respect to the reaction progress variable ξ.

$$A = -\left(\frac{\partial G}{\partial \xi}\right)_{T,P}. \tag{A.5}$$

The Gibbs free energy is a function of temperature, pressure, and the number of moles of each species, and its derivative can be written as

$$dG = \left(\frac{\partial G}{\partial T}\right)_{P,N} dT + \left(\frac{\partial G}{\partial P}\right)_{T,N} dP + \sum_i \left(\frac{\partial G}{\partial N_i}\right)_{T,P,Nj\neq i} dN_i. \tag{A.6}$$

At constant temperature and pressure, this reduces to

$$dG = \sum_i \left(\frac{\partial G}{\partial N_i}\right)_{T,P,Nj\neq i} dN_i \,. \tag{A.7}$$

The partial derivative of the Gibbs free energy with respect to the extent of reaction is

$$\left(\frac{\partial G}{\partial \xi}\right)_{T,P} = \sum_i \mu_i \upsilon_i \,, \tag{A.8}$$

where μ_i is the chemical potential and v_i is the stoichiometric coefficient of species i in the reaction. Substituting for the chemical potential as

$$\mu_i = \mu_i{}^\circ + RT \ln a_i \tag{A.9}$$

in Equation A.8 gives

$$\left(\frac{\partial G}{\partial \xi}\right)_{T,P} = \sum_i \left(\mu_i{}^\circ + RT \ln a_i\right)\upsilon_i \,, \tag{A.10}$$

which can be rewritten

$$\left(\frac{\partial G}{\partial \xi}\right)_{T,P} = \sum_i \mu_i{}^\circ \upsilon_i + \sum_i RT \ln a_i^{\upsilon_i} \,. \tag{A.11}$$

The summation of a_i^{υ} in the second term in Equation A.11 is the ion activity product, Q. By definition,

$$\sum_i \mu_i{}^\circ \upsilon_i = \Delta G^\circ = -RT \ln K \,, \tag{A.12}$$

where K is the equilibrium constant. Therefore, Equation A.11 can be written as

$$\left(\frac{\partial G}{\partial \xi}\right)_{T,P} = -RT \ln K + RT \ln Q = RT \ln\left(\frac{Q}{K}\right) = -A \,. \tag{A.13}$$

The last equality is written based on Equation A.5. Substituting this expression for the affinity, A, in Equation A.4 results in

$$\left(\frac{rate_{reverse}}{rate_{forward}}\right) = \exp\left(\frac{RT\ln\left(\frac{Q}{K}\right)}{RT}\right) = \left(\frac{Q}{K}\right), \tag{A.14}$$

and then Equation A.4 into Equation A.2 produces

$$rate_{net} = rate_{forward} \bullet \left(1 - \frac{Q}{K}\right). \tag{A.15}$$

The parameters A, Q, and K represent a particular intermediate reaction step in the overall dissolution of the material, namely, the decomposition of the activated complex that results in dissolution. The progress of the overall reaction is related to the progress of each reaction step in a sequence

$$A = \sum_j \sigma_j A_j , \tag{A.16}$$

where σ_j is the rate of the intermediate reaction step relative to the overall reaction rate (sometimes called the Temkin constant or Temkin's average stoichiometric number) and A and A_j are the chemical affinities for the overall reaction and intermediate step. Substituting A/σ for A in the above derivation for the decomposition of the activated complex (where σ is the Temkin constant for that step) produces

$$rate_{net} = rate_{forward} \bullet \left[1 - \left(\frac{Q}{K}\right)^{1/\sigma}\right]. \tag{A.17}$$

This is the general rate expression for affinity-controlled dissolution where the measured rate, Q, and K for the overall reaction are related to the decomposition rate of the activated complex. Following transition state theory, the reaction rate depends primarily on a particular intermediate step referred to as the rate limiting step. The value of σ can be determined from experimental data, but is often assumed to be $\sigma = 1$ for the rate limiting step. Lasaga (1995) has argued that the formulation may be invalid when $\sigma \neq 1$. As discussed in Section 6.3.3, Li and Steefel (2007) fit test data for the dissolution of kaolinite at 22°C and pH 4 to Equation A.17 with $\sigma = 2$. Equation A.17 is commonly applied to silicate minerals and glass using $\sigma = 1$ for the hydrolysis reaction breaking the Si-O bond of the activated complex of a terminal $Si(OH)_4$ group bonded to the silicate lattice as the rate-limiting step. In the case of glasses, which are thermodynamically unstable, the value of K is approximated by that of a fictitious SiO_2 phase having a solubility equal to the apparent solubility established by the kinetic limits on the dissolution rate. Of course, the values of Q and K determined from experiments relate to the overall reaction. Approaches for determining the value of σ from dissolution tests are discussed by Bourcier et al. (1994) and McGrail et al. (1997).

Appendix B

Method Used to Reproduce Data Plots from Literature

Test data were extracted from plots in literature publications when tabulated data were not provided to facilitate the analyses and evaluations of the data sets conducted as part of this Task. Measurements were made using enlarged photocopies of the plots to increase the accuracy. An architect scale with 50 divisions per inch was used to measure the distance between the center of a plotted point and both the x-axis and y-axis. The scale was also used to measure the distance from the origin (or convenient point of reference) to the furthest unit on each axis. For example, consider an x-axis representing time in days with the furthest tick mark being 12 days. The distance on the axis from the origin (0 days) to the tick mark at 12 days is measured to be 430/50 inches. A data point measured to be 248/50 inches from the origin corresponds to a test duration of (the denominators of 50 cancel and are excluded)

$$x - \text{value of data} = 248 \text{ inches} \times \left(\frac{12 \text{ days}}{430 \text{ inches}} \right) = 6.92 \text{ days} \tag{B.1}$$

Each measured value is estimated to have an uncertainty of 2/50 inch (1/50 at each end of the measured range). For the above example, the range of values for the time is 6.83 days (if the data point was at 246/50 inches and the tick mark for 12 days was at 432 days) to 7.01 days (if the data point was at 250/50 inches and the tick mark for 12 days was at 428 days). The relative uncertainty is highest for data points near the origin.

The reproduced plots were compared with the original plots to verify qualitative agreement. When possible, fits to the reproduced plots were compared with the equations provided with the original. Reproducing plotted data in this way permitted alternative fits to the data, analyses of subsets of the data, and estimation of the goodness of fits.

Appendix C

Diffusion-Controlled Release with Concentration-Dependent Reactions

Following Danckwerts (1950), consider a semi-infinite medium having a uniform initial concentration of the mobile species $C = 0$ that increases with time and a saturation concentration C_s. Additional mobile species are provided at the surface at a rate = $k_f (C_s - C)$ per unit time and volume (e.g., by sorption from a contacting gas or liquid phase). The surface concentration is maintained at C_s and no additional species are provided (sorb) when $C = C_s$. The diffusion equation must satisfy mass balance across the surface of a layer having thickness dx over time dt including the following terms

Diffusing in: flux = $-D\dfrac{\partial C}{\partial x}dt$. (C.1)

Diffusing out: flux = $-\left[-D\,dt\left(\dfrac{\partial C}{\partial x}+\dfrac{\partial^2 C}{\partial x^2}dx\right)\right]$. (C.2)

Reacting: $-k_f\,C\,dt \bullet dx$. (C.3)

Combining these terms produces

$$-D\frac{\partial C}{\partial x}dt-\left[-D\,dt\left(\frac{\partial C}{\partial x}+\frac{\partial^2 C}{\partial x^2}dx\right)\right]-k_f\,C\,dt\bullet dx\,. \tag{C.4}$$

The net increase in C within volume defined by dx is

$$\left(D\frac{\partial^2 C}{\partial x^2}-k_f\,C\right)dt\bullet dx\equiv dC\bullet dx, \tag{C.5}$$

where the increase in C within the volume of interest is expressed as dC. Rearranging Equation C.5 by eliminating dx and dividing by dt produces

$$\frac{\partial C}{\partial t}=D\frac{\partial^2 C}{\partial x^2}-k_f C\,. \tag{C.6}$$

This has been solved by Danckwerts (1950) for the condition where the concentration at the surface is maintained at saturation by using the following boundary conditions:

$C = 0 \quad x > 0 \quad t = 0$
$C = C_s \quad x = 0 \quad t > 0$
$C = 0 \quad x = \infty \quad t > 0$

The solution is

$$\frac{C}{C_s} = \frac{1}{2}\left\{\exp\left[-x\left(\frac{k}{D}\right)^{1/2}\right] erfc\left[\frac{x}{2(Dt)^{1/2}} - (kt)^{1/2}\right] + \exp\left[x\left(\frac{k}{D}\right)^{1/2}\right] erfc\left[\frac{x}{2(Dt)^{1/2}} + (kt)^{1/2}\right]\right\}. \quad \text{(C.7)}$$

To apply Danckwerts' solution to the condition where the concentration of C at the surface is maintained at 0, Godbee and Joy (1974) introduced the variable $f(x,t)$ and saturation concentration C_s, where

$$f(x,t) = C_s - C(x,t) \quad \text{(C.8)}$$

Comparison of the boundary conditions is provided in Table C.1.

Table C.1. Boundary conditions in Danckwerts (1950) and in Godbee and Joy (1974).

Boundary Conditions		In Danckwerts	In Godbee and Joy	
for $x > 0$	$t = 0$	$C = 0$	$f = 0$	$C = C_s$
for $x = 0$	$t > 0$	$C = C_s$	$f = C_s$	$C = 0$
for $x = \infty$	$t > 0$	$C = 0$	$f = 0$	$C = C_s$

Relating $f(x,t)$ to $C(x,t)$ produces

$$\frac{\partial f}{\partial t} = \frac{-\partial C}{\partial t} \quad \text{and} \quad \frac{\partial^2 f}{\partial x^2} = \frac{-\partial^2 C}{\partial x^2} \quad \text{(C.9)}$$

Substituting these expressions into Equation C.6 produces

$$-\frac{\partial f}{\partial t} = -D\frac{\partial^2 f}{\partial x^2} + k_f\, f(x,t) \quad \text{(C.10)}$$

which can be rearranged as

$$\frac{\partial f}{\partial t} = D\frac{\partial^2 f}{\partial x^2} - k_f\, f(x,t). \quad \text{(C.11)}$$

The solution to Equation C.11 for the condition that the surface concentration of C is maintained at zero is

$$\frac{f(x,t)}{C_s} = \frac{1}{2}\left\{\exp\left[-x\left(\frac{k}{D}\right)^{1/2}\right] erfc\left[\frac{x}{2(Dt)^{1/2}} - (k_f\, t)^{1/2}\right] + \exp\left[x\left(\frac{k_f}{D}\right)^{1/2}\right] erfc\left[\frac{x}{2(Dt)^{1/2}} + (kt)^{1/2}\right]\right\}. \tag{C.12}$$

Rearranging the expression in Equation C.8 as $C = C_s - f(x,t)$ and then substituting for the variable $f(x,t)$ in Equation C.12 produces

$$C = C_s - \frac{C_s}{2}\exp\left[-x\left(\frac{k_f}{D}\right)^{1/2}\right] erfc\left[\frac{x}{2(Dt)^{1/2}} - (k_f\, t)^{1/2}\right] - \frac{C_s}{2}\exp\left[x\left(\frac{k_f}{D}\right)^{1/2}\right] erfc\left[\frac{x}{2(D\, t)^{1/2}} + (kt)^{1/2}\right]. \tag{C.13}$$

This expression provides the concentration of the mobile species in the medium as a function of position x and time t. As in Danckwerts (1950) and Godbee and Joy (1974), Equation C.13 is first differentiated with respect to position and then the concentration gradient at $x = 0$ is evaluated to calculate the flux at the surface:

$$\left(\frac{\partial C}{\partial x}\right)_{x=0} = -C_s \bullet \left(\frac{k_f}{D}\right)^{1/2} \bullet \left[erf(k_f\, t)^{1/2} + \frac{e^{-k_f t}}{(\pi\, k_f\, t)^{1/2}}\right]. \tag{C.14}$$

Fick's first law is used to calculate the flux at the surface

$$\left(\frac{\partial q}{\partial t}\right) = -D\left(\frac{\partial C}{\partial x}\right)_{x=0} = C_s \bullet (D\, k_f)^{1/2} \bullet \left[erf(k_f t)^{1/2} + \frac{e^{-k_f t}}{(\pi\, k_f\, t)^{1/2}}\right]. \tag{C.15}$$

The variables in Equation C.15 are related to experimental variables as:

$$q = \frac{a}{S};\ Q = \frac{\sum a_n}{S};\ C_s = \gamma \frac{A_o}{V_{wf}} \tag{C.16}$$

and

$$\frac{dq}{dt} \approx \frac{a_n}{S\, t_n}, \tag{C.17}$$

where γ is a constant relating the saturation concentration to the initial concentration of the contaminant C in the test specimen and, by definition, $D_e = \gamma^2 D$. Making the substitutions given in Equation C.17 (and using the average mean root cumulative time T for the interval) produces

$$\left(\frac{a_n}{A_o}\right)\left(\frac{V_{wf}}{S}\right)\left(\frac{1}{t_n}\right)=\left(D_e\,k_f\right)^{1/2}\bullet\left[erf\left(k_f\,T\right)^{1/2}+\frac{e^{-k_f T}}{\left(\pi\,k_f\,T\right)^{1/2}}\right] \tag{C.18}$$

for the incremental leach rate at the surface. At large $k_f T$, the incremental rate in Equation C.18 reduces to

$$\left(\frac{a_n}{A_o}\right)\left(\frac{V_{wf}}{S}\right)\left(\frac{1}{t_n}\right)\approx\left(D_e\,k_f\right)^{1/2} \quad . \tag{C.19}$$

At small $k_f T$ (e.g, $k_f T$ <0.5) due to a low dissolution rate and/or short durations, the value of $erf(x)$ approaches $\frac{2x}{\pi^{1/2}}$ and the exponential term can be approximated as $1- k_f t$. Equation C.18 can therefore be simplified to

$$\left(\frac{a_n}{A_o}\right)\left(\frac{V_{wf}}{S}\right)\left(\frac{1}{t_n}\right)\approx\left(\frac{D_e}{\pi}\right)^{1/2}\left(1+k_f\,T\right)\bullet T^{-1/2}\,. \tag{C.20}$$

At the limit $k_f = 0$, Equation C.20 reduces to Equation 4.7. Integrating Equation C.18 over time, with Q being the total amount of mobile species that has left the medium in time t per unit surface area, and substituting the values from Equation C.17 produces

$$Q=C_s\bullet\left(D_e\,k_f\right)^{1/2}\bullet\left[\left(t+\frac{1}{2\,k_f}\right)erf\left(k_f\,t\right)^{1/2}+\left(\frac{t}{\pi\,k_f}\right)^{1/2}e^{-k_f t}\right]. \tag{C.21}$$

Using the relationships given in Equation C.16, the total amount leached is related to test parameters as

$$\frac{Q}{C_s}=\frac{\sum a_n/S}{\gamma\,A_o/V_{wf}}=\left(\frac{\sum a_n}{A_o}\right)\left(\frac{V_{wf}}{\gamma\,S}\right) \tag{C.22}$$

and

$$\left(\frac{\sum a_n}{A_o}\right)\left(\frac{V_{wf}}{S}\right)=\left(D_e\,k_f\right)^{1/2}\bullet\left[\left(t+\frac{1}{2\,k_f}\right)erf\left(\left(k_f\,t\right)^{1/2}\right)+\left(\frac{t}{\pi\,k_f}\right)^{1/2}e^{-k_f t}\right]. \tag{C.23}$$

Note that time in Equation C.23 is the cumulative time, not the root mean time T. Since the limiting conditions of large and small $k_f t$ are of interest, it is convenient to express Equation C.23 in an equivalent form by multiplying the right-hand side by $\frac{k_f}{k_f}$:

$$\left(\frac{\sum a_n}{A_o}\right)\left(\frac{V_{wf}}{S}\right)=\frac{(D_e\,k_f)^{1/2}}{k_f}\bullet\left[\left(k_f t+\frac{k_f}{2\,k_f}\right)erf((k_f\,t)^{1/2})+\left(\frac{k_f{}^2 t}{\pi\,k_f}\right)^{1/2}e^{-k_f t}\right] \tag{C.24}$$

which reduces to

$$\left(\frac{\sum a_n}{A_o}\right)\left(\frac{V_{wf}}{S}\right)=\left(\frac{D_e}{k_f}\right)^{1/2}\bullet\left[\left(k_f\,t+\frac{1}{2}\right)erf((k_f\,t)^{1/2})+\left(\frac{k_f\,t}{\pi}\right)^{1/2}e^{-k_f t}\right]. \tag{C.25}$$

When $k_f t$ is large due to a high dissolution rate and/or long durations, the second term in braces becomes negligible, the value of the error function approaches 1, and Equation C.25 reduces to

$$\left(\frac{\sum a_n}{A_o}\right)\left(\frac{V_{wf}}{S}\right)\approx\left(\frac{D_e}{k_f}\right)^{1/2}\bullet\left(k_f\,t+\frac{1}{2}\right), \tag{C.26}$$

which gives a linear time dependence and a nonzero intercept

$$\left(\frac{\sum a_n}{A_o}\right)\left(\frac{V_{wf}}{S}\right)\approx(D_e k_f)^{1/2}\,t+\left(\frac{D_e}{4k_f}\right)^{1/2}. \tag{C.27}$$

When the product $k_f t$ is small (e.g, <0.5) due to a low reaction rate and/or short durations, the value of $erf(x)$ approaches $\frac{2x}{\pi^{1/2}}$ and the exponential term can be approximated as $(1 - k_f t)$. With these substitutions, Equation C.25 reduces to

$$\left(\frac{\sum a_n}{A_o}\right)\left(\frac{V_{wf}}{S}\right)=\left(\frac{D_e}{k_f}\right)^{1/2}\bullet\left[\left(k_f\,t+\frac{1}{2}\right)2\left(\frac{k_f\,t}{\pi}\right)^{1/2}+\left(\frac{k_f\,t}{\pi}\right)^{1/2}(1-k_f\,t)\right], \tag{C.28}$$

which reduces further to

$$\left(\frac{\sum a_n}{A_o}\right)\left(\frac{V_{wf}}{S}\right)=\left(\frac{D_e}{k_f}\right)^{1/2}\bullet\left(\frac{k_f\,t}{\pi}\right)^{1/2}\left[(2k_f\,t+1)+(1-k_f\,t)\right]. \tag{C.29}$$

This can be simplified as

$$\left(\frac{\sum a_n}{A_o}\right)\left(\frac{V_{wf}}{S}\right)=k_f\,t\bullet\left(\frac{D_e\,t}{\pi}\right)^{1/2}+2\left(\frac{D_e\,t}{\pi}\right)^{1/2}. \tag{C.30}$$

For a given value of k_f, short leaching times are predicted by Equation C.30 to show an approximately root-time dependence and long leaching times are predicted to show a linear time dependence according to Equation C.25. In the limit $k_f t << 2$, Equation C.30 reduces to

$$\left(\frac{\sum a_n}{A_o}\right)\left(\frac{V_{wf}}{S}\right) = 2\left(\frac{D_e t}{\pi}\right)^{1/2} . \tag{C.31}$$

Very long leaching intervals are needed to quantify small values of k_f. Values are needed for both D_e and k_f to apply Equation C.25. These can be determined by regression analysis of the appropriate experimental results.

Appendix D

Diffusive Release from a Finite Cylinder

The release of components by mass transport through a solid is modeled based on the diffusion rate being proportional to the concentration gradient, as formulated in Fick's second law:

$$\frac{\partial C}{\partial t} = -D_e \nabla^2 C , \tag{D.1}$$

where C is the concentration of the species of interest, t is time, D_e is the effective diffusion coefficient, and $\nabla^2 C$ is the spatial rate of change in the direction of the concentration gradient.

The model for diffusion through a semi-infinite medium is usually appropriate for porous materials that give low CFL values in the ALT (e.g., CFL < 0.2). It is the simplest model and provides an initial value of D_e for use in other models. The CFL is calculated in the semi-infinite solid model as

$$CFL = \frac{\sum a_n}{A_o} = 2\frac{S}{V}\left[\frac{D_e t}{\pi}\right]^{1/2} , \tag{D.2}$$

where a_n is the total amount of the species of interest released in all leaching intervals through time t, A_o is the initial amount of the species of interest in the specimen (i.e., the source term), S is the surface area of the specimen, V is the specimen volume, and D_e is the effective diffusion coefficient.

The model for diffusion through a finite cylinder takes into account depletion of the solid due to leaching and is usually appropriate for materials that give high CFL values in the ALT (e.g., CFL > 0.2). The mathematical solution is based on diffusion from a cylindrical solid of height H and radius R. In the finite cylinder model, the diffusive fractional cumulative release is calculated as a double series expression:

$$\text{CFL} = \frac{\sum a_n}{A_o} = \left(1 - \frac{32}{\pi^2} S_p(t)\, S_c(t)\right) \tag{D.3}$$

with the series

$$S_p(t) = \sum_{n=1}^{\infty} \frac{1}{(2n-1)^2} \exp\left[\frac{-(2n-1)^2 \pi^2 D t}{H^2}\right] \tag{D.4}$$

and the series

$$S_c(t) = \sum_{m=1}^{\infty} \frac{1}{\beta_m^{\,2}} \exp\left[\frac{-\beta_m^{\,2} Dt}{R^2}\right], \tag{D.5}$$

where the parameter β_m represents the mth zero of the zeroth order cylindrical Bessel function. Values of the β_m for m=1 to 20 are provided in Table D.1. In the ALT program provided with ASTM C1308, an *ad hoc* term is added to Equation D.3 to account for the nonzero y-intercept typical in experimental results. The numerical convergence for these open series is extremely slow, and analytical closed forms expressions have been developed (Pecsatore 1990). The closed forms include separate terms to represent the closed series and the maximum absolute error introduced by truncating the open series. The equations developed by Pescatore (1990) are given here for completeness. For the $S_p(t)$ series

$$S_p(t) = S_{p,N}(t) + E_{p,N}(t), \tag{D.6}$$

$$S_{p,N}(t) = \sum_{n=1}^{N-1} \frac{\exp\left(-(2n-1)^2 \gamma^2(t)\right)}{(2n-1)^2} + \frac{N}{(2N-1)^2} \exp\left[-(2N-1)^2\, \gamma^2(t)\right] - \left(\frac{\pi^{1/2}}{2}\right) \gamma(t)\, erfc[(2N-1)\gamma(t)], \tag{D.7}$$

with

$$\gamma(t) = \frac{\pi (D_e t)^{1/2}}{H} \tag{D.8}$$

and the error term

$$0 < E_{p,N}(t) < \frac{1}{6(2N-1)} \left[\gamma^2(t) + \frac{2}{(2N-1)^2}\right] \exp\left[-(2N-1)^2\, \gamma^2(t)\right]. \tag{D.9}$$

The values n and N represent the series term and the number of terms included in the sum. For the $S_c(t)$ series

$$S_c(t) = S_{c,M}(t) + E_{c,M}(t), \tag{D.10}$$

$$S_{c,M}(t) = \sum_{m=1}^{M-1} \frac{\exp\left(-\beta_m^{\,2} \theta^2(t)\right)}{\beta_m^{\,2}} + \left[\frac{1}{\beta_M f_M} + \frac{1}{2\beta_M^{\,2}}\right] \exp\left[-\beta_M^{\,2}\, \theta^2(t)\right] - \frac{\pi^{1/2} \theta(t)}{f_M}\, erfc[\beta_M\, \theta(t)] \tag{D.11}$$

with $f_M = \pi - \dfrac{1}{8\pi M^2}, \quad M >> 1$

$$\theta(t) = \frac{(D_e t)^{1/2}}{R} \tag{D.12}$$

and the error term

$$E_{c,M}(t) < \frac{f_M}{6\beta_M}\left[\theta^2(t) + \frac{1}{\beta_M^{\,2}}\right]\exp\left[-\beta_M^{\,2}\,\theta^2(t)\right]. \tag{D.13}$$

The values m and M represent the series term and the number of terms included in the sum.

Table D.1. Values of the parameters β_m for $m = 1$ to 20[a].

m	β_m	m	β_m	m	β_m	m	β_m
1	2.4048255577	6	18.0710639679	11	33.7758202136	16	49.4826098974
2	5.5200781103	7	21.2116366299	12	36.9170983537	17	52.6240518411
3	8.6537279129	8	24.3524715308	13	40.0584257646	18	55.7655107550
4	11.7915344391	9	27.4934791320	14	43.1997917132	19	58.9069839261
5	14.9309177086	10	30.6346064684	15	46.3411883717	20	62.0484691902

[a]These parameters satisfy the equation $J_0(\beta_m) = 0$, with $J_0(x)$ the zeroth order cylindrical Bessel function.

Appendix E

Summary of Laboratory Test Methods

Two approaches commonly used to study the weathering rates of materials are laboratory tests and experiments under controlled test conditions and field studies under uncontrolled and natural conditions. In most cases, the objective of laboratory tests is to measure alteration behavior from a materials perspective on a small scale (on a scale of centimeters) to develop a mechanistically based model. The models and simulations that are developed based on laboratory tests are on an atomistic scale (nanometers), and the use of empirical model components is minimized. Field studies are focused on the impact of specific environmental conditions on material behavior on a large scale (on a scale of meters); this information is needed to first identify the range of service conditions that must be addressed by the model and then calibrate or confirm the model. Each increase in scale in going from the model to laboratory studies and then to field studies adds uncertainty due to decreasing homogeneity of the material and conditions on each scale.

In the context of this report, the terms *test* and *experiment* are distinguished with regard to the level of mechanistic understanding and expectation regarding the test response. In general, experiments are conducted to identify and understand important processes, whereas tests are conducted to measure parameter and coefficient values for characterizing known processes. The same methodology can serve as an experiment or a test, depending on the level of expectation of the response. For example, the same test method can serve as an experiment to determine whether mass diffusion is an important process in the degradation mechanism or as a test to measure the effective diffusion coefficient at a particular temperature.

Laboratory tests used to study the dissolution of a material can be categorized into a small number of test types according to how the solution contacts the material. There are a limited number of ways a test specimen can be contacted by water

- it can be immersed in a fixed volume of water,
- it can be immersed in a volume of water that is partially or completely replaced with fresh water on a prescribed schedule,
- it can be immersed in a stream of flowing water,
- it can be contacted by dripping water that is added to or recondensed within the system, or
- it can be contacted by water vapor that condenses directly on the sample (due to thermal and deliquescence effects).

The test specimen can be a monolith (defined to have measureable macroscopic dimensions), to provide a low specific surface area, or an amount of crushed material to provide a high specific surface area. Because most test responses are due to surface reactions, specimen preparation can have a significant effect on the test response such that the response of a specimen in a short-term test may not represent the behavior of the bulk material. The effect of the specimen surface must usually be determined experimentally or inferred from changes in the response as the surface is dissolved during the test. Depending on the material, the surface finish of monoliths can be made consistent by polishing, heating, etc. A surface film may form on a cast material that behaves differently than the bulk. Crushed materials provide a range of fracture surfaces, edges, points, and stresses that affect the dissolution behavior. These usually react faster than bulk material due to the additional strain energies. These effects must be taken into account when conducting tests and interpreting results. It may be necessary to pre-react some materials to eliminate anomalous surface effects and measure behavior representing the bulk material.

The solution prior to contact with the specimen is commonly referred to as the *leachant* and the solution after contact with the specimen is referred to as the *leachate*, even though the degradation mechanism may not include leaching.

Particular standardized test methods specify the leachant solution composition, specimen preparation, and various test parameters including temperature, solution-to-specimen surface area ratio, duration, and sampling schedule. The advantage of standardized test methods is that test parameters are well defined and the test responses of different materials can be compared directly within and between laboratories. However, the meaning of the comparison depends on whether or not the materials degrade by the same mechanism. If not, then the comparison is empirical and only applies to the particular test conditions. Many laboratory tests and experiments can be considered modifications of standardized methods. For example, tests to measure a distribution coefficient can be considered a modification of ASTM C1285 (PCT). This is because the sized fraction of particulates are immersed in a fixed volume of solution at a known ratio at a controlled temperature and the solution is sampled and analyzed for the change in concentration of elements of interest at particular durations.

Table E.1 summarizes the test parameters for several standardized test methods and useful modifications of those tests. These test methods are usually used to study the degradation behavior of a material and are not intended to simulate a particular environment, although aspects of the tests are sometimes intended to represent important aspects of the anticipated service environment, such as the ranges of temperature and the solution chemistry. In general, the tests are conducted to understand the dependence of material degradation on key environmental factors to model a range of conditions rather than directly measure the response under a specific set of conditions. Of course, verification tests can be conducted under specific conditions to evaluate the fidelity of the model to the service environment.

Various test methods are used to impose extreme conditions (relative to the service environment) and highlight particular aspects of the material degradation mechanism. Different test methods can be used to maintain dilute solutions with low concentrations of dissolved components, generate concentrated solutions with high concentration of dissolved components, or provide some control of the evolving solution chemistry. Test methods can maintain dilute solutions by immersing specimens with low specific surface areas (monolithic specimens) in large solution volumes so that dissolution has only a small effect on the solution chemistry (e.g., ASTM C1220), by occasionally replacing some or all of the leachate with fresh leachant (e.g., ASTM C1308), or by continuously replacing the leachate with fresh leachant (e.g., ASTM C1662). Other test methods can quickly lead to high concentrations of dissolved material components by reacting specimens having large specific surface areas (crushed specimens) in small solution volumes (e.g., ASTM C1285) or restricting the leachant to very small volumes (e.g., vapor hydration test).

The advantage of field studies is that the system of interest is characterized directly. This provides important environmental information needed to guide laboratory studies, such as the water contact parameters (volume, flow rate, chemistry, etc.) and temperature. The disadvantage is that measurements reflect the combined and often convoluted effects of many processes under the particular conditions when the measurements were made. These do not provide information regarding the weathering mechanism that can be used to calculate long-term performance or evaluate the impact of other potential conditions. Probably the best use of field studies (for the purpose of performance assessment) is to calibrate the mechanistic model developed by laboratory studies and provide a measure of the fidelity of the model to the system.

Table E.1. Summary of test methods.

Test Method	Specimen	Leachant			Analytes
		Contact Method	Leachate Replacement Schedule	Composition	
ANS/ANSI 16.1	Monolith, cylindrical	Immersion, pseudo-dynamic	Total replacement after specified intervals	Demineralized water	Soluble components
ASTM C1220	Monolith	Immersion, static	Leachate not replaced	Demineralized water; silicate solution, brine solution; pH buffers; groundwater (actual or synthetic); etc.	Soluble components; specimen surface
Modified C1220	Monolith	Immersion, pseudo-dynamic	Small fraction removed for analysis; may be replaced or not replaced	Demineralized water; silicate solution, brine solution; pH buffers; groundwater (actual or synthetic); etc.	Soluble components; specimen surface
ASTM C1285	Crushed	Immersion, static	Leachate not replaced	Demineralized water	Soluble components
Modified C1285	Crushed	Immersion, pseudo-dynamic	Small fraction replaced	Demineralized water; silicate solution, brine solution; pH buffers; groundwater (actual or synthetic); etc.	Soluble components; specimen surface
ASTM C1308	Monolith, cylindrical	Immersion, static	Total replacement after specified intervals	Demineralized water	Soluble components
ASTM C1662	Crushed	Immersion, dynamic	Continuous replacement by flowing leachant	Demineralized water; silicate solution, brine solution; pH buffers; groundwater (actual or synthetic); etc.	Soluble components
ISO 16797 Soxhlet	Monolith or crushed	Immersion, pseudo-dynamic	Slow replacement by condensed water	Condensed water	Soluble components
Vapor hydration test	Monolith	Condensed water, static	Leachate not replaced	Condensed water	Specimen surface
Modified vapor hydration test	Monolith	Condensed water	Periodic replacement by condensed water	Condensed water	Soluble components, Specimen surface

Table E.1. (cont.).

Test Method	Specimen	Leachant			Analytes
		Contact Method	Leachate Replacement Schedule	Composition	
EPA 1310B Extraction procedure (EP) toxicity test	<9.5 mm	Immersion, agitated	Leachate not replaced	Acetic acid solution pH 5	Regulated metals
EPA 1311 Toxic characteristic leach procedure (TCLP)	<3/8 inch particulates	Immersion, agitated	Leachate not replaced	Acetic acid solution	RCRA-regulated components
EPA 1312 Synthetic precipitation leach procedure (SPLP)	<2mm particulates	Immersion, agitated	Leachate not replaced	Adjust to pH 4.2 with H_2SO_4/HNO_3	Soluble components
Net acid production	-200 mesh (<0.075 mm)	Immersion, static	Leachate not replaced	30% H_2O_2	Acidity by titration
CA WET	<2mm particulates	Immersion, agitated	Leachate not replaced	0.2 M sodium citrate	Soluble metals

Brief descriptions of several standardized test methods are provided below with comments regarding the benefits and uncertainties associated with each method. Whenever appropriate, approaches found to be successful with similar waste forms should be considered first. The recommendations are based on experience in testing homogeneous glass, glass-bonded ceramic, cement, and alloyed metallic waste forms. It is possible that an approach used previously will not be successful for a particular waste form and a modified or alternative approach must be developed. If that is the case, then the methods used should be documented in detail and provided when reporting the results. New or modified test methods used to address waste acceptance issues, such as product consistency, should be formalized and evaluated as consensus standards. Thorough technical review of the procedure and the use of the results will add credence to the method and support waste acceptance.

E.1 ANS 16.1 Leach Test (ANS 2009)

The ANS 16.1 test method provides "a uniform procedure to measure and index the release of radionuclides from waste forms as a result of leaching in demineralized water for 5 days. The results of this procedure do not apply to any specific environmental situation except through correlative studies of actual disposal site conditions." The method is not intended to address long-term leaching behavior. A test specimen with a simple geometric shape (cylinder or parallelepiped) and known dimensions is immersed in a volume of demineralized water at room temperature for specified interval and then removed and immersed in the volume of fresh demineralized water for a specified interval. The volume of water, in cm^3, is 10 times the surface area, in cm^2. The water is analyzed for components released from the specimen after the specimen is removed. The leachate solution is to be replaced with fresh demineralized water at intervals of 2, 5, 17, 24, 24, 24, and 24 hours, which is a cumulative duration of 5 days. The extended test includes additional exchanges at intervals of 14, 28, and 43 days for a cumulative test duration of 90 days.

The test results are interpreted using a diffusive release model for a semi-infinite solid. A diffusion coefficient value is calculated with the results for each test interval. If more than 20% of the leached species is removed during an increment, then a geometry-specific model must be used to determine the diffusion coefficient. Solutions for diffusion from cylinders are provided in the test method, and it is recommended that tests be conducted with cylindrical test specimens.

E.2 ASTM C1220 Monolith Immersion Test (ASTM 2009a)

The ASTM C1220 test method is a static test in which a monolithic specimen of known geometric surface area is immersed in the appropriate volume of leachant to provide a low specimen surface area–to–solution volume (*S/V*) ratio (between 0.5 and 10.0 m^{-1}). The test vessel is sealed and placed in a constant-temperature oven for a prescribed duration. The solution concentrations of components of interest are measured at the end of the test. Tests can be conducted with demineralized water, synthetic or actual groundwaters, pH buffer solutions, etc. The test has been used to compare the relative reactivities of various waste form materials (usually in 28-day tests at 90°C and 10.0 m^{-1}). ASTM C1220 is more sensitive to the waste form composition than most other test methods because the test response is dominated by waste form dissolution. Short-term tests at low *S/V* ratios (e.g., 1 m^{-1}) can be used to measure specimen dissolution rates at chemical affinity values near 1 and are convenient for measuring the effects of temperature and pH. Modified long-term tests at high *S/V* ratios (e.g., 100 m^{-1}) can be used to promote corrosion for examining corroded surfaces.

The geometric surface area of a specimen can be measured to allow accurate calculation of the specific dissolution rate. The surface finish of the test specimen can be controlled by polishing. The test is easy to run, can be conducted under a wide range of conditions, provides sufficient solution volumes for analysis, and is economical. Only small volumes of waste solution are generated. Short-term tests can be used to measure the effects of temperature, pH, and components in the leachant on the dissolution rate of materials that degrade by dissolution. Responses in longer-term tests become affected by the chemical affinity of the solution and can be used to estimate the solubility of the waste form by regressing data with the rate expression. For metallic specimens, aspects of ASTM G31 regarding specimen preparation and cleaning should be followed when conducting ASTM C1220 tests.

The solution chemistry evolves over the test interval as the specimen dissolves and only the cumulative changes are measured. The effect of the chemical affinity can be taken into account if the solubility is known. Initial dissolution is affected by artifacts from sample preparation (e.g., surface finish). The production of monolithic samples is usually the most difficult aspect of the test when conducted with radioactive materials.

E.3 ASTM C1285 Product Consistency Test (ASTM 2009a)

The ASTM C1285 test method is a static test in which a crushed material is immersed in a volume of leachant at a known mass/volume ratio. The mass and size fraction of the crushed material in the test is known and can be used to estimate the surface area for nonporous materials (e.g., glass). The test vessel is sealed and placed in a constant-temperature oven for a prescribed duration. The solution concentrations of components of interest are measured at the end of the test. The ASTM C1285 method A (PCT-A) is conducted under specific test conditions:–100+200 mesh size fraction material; demineralized water; solid/solution mass ratio of 1/10; 90 °C; 7 days; Type 304L stainless steel vessel. ASTM C1285 method B (PCT-B) permits the use of different test parameter values and can be conducted with actual or synthetic groundwaters. PCT-B tests are useful for generating concentrated solutions to study chemical affinity effects on the dissolution rate and can be used to measure solubility limits (for thermodynamically stable phases such as minerals) or apparent solubility limits (for kinetically stable phases such as glass). PCT-B tests at high temperatures and high glass/solution mass ratios can be used to promote the formation of alteration phases to (1) identify the kinetically favored alteration phases (2) determine their propensity to sequester radionuclides, and (3) evaluate the effect of their formation on the continued waste form dissolution rate.

The test response is sensitive to solution feedback after very short test duration and concentrated solutions are generated after little material has dissolved. It is easy to run and economical. Only small volumes of waste solution are generated. The test method is best suited for studying dissolution in concentrated solutions and the effects of solution feedback; it is less sensitive to variations in the waste form composition than other tests (e.g., ASTM C1220). Method B provides well-controlled test parameters representing a wide variety of static tests with crushed material at a constant temperature. This includes test methods commonly used to measure solubility limits of thermodynamically stable phase, such as mineral phases formed to sequester radionuclides. Method B can also be used to measure apparent solubility limits that are due to kinetic constraints as in the case of borosilicate glasses.

The surface area of the crushed material must be estimated; the surface is affected by artifacts due to crushing (e.g., high-energy sites such as edges and points). The test results in very rapid changes in the solution composition even after short reaction times (i.e., within minutes) that

occur too fast to be tracked. Since the sample mass is used as a test parameter, the density of the material will affect the surface area that is exposed during the test. This must be taken into account when comparing the test responses of materials having significantly different densities and presenting the results on a per unit area basis. Alternatively, the masses of materials used in the tests can be adjusted to achieve a common *S/V* ratio.

E.4 ASTM C1308 Accelerated Leach Test (ASTM 2009a)

The ASTM C1308 ALT is a modification of the ANS/ANSI 16.1 test method that can be used to (1) determine whether the release of a component is controlled by diffusion and (2) determine the effective diffusion coefficient based on a model for diffusion from a finite cylinder. It is a semi-dynamic test in which a monolithic specimen of prescribed dimensions is immersed in a large volume of leachant in a sealed vessel for a relatively short interval. The leachate solution is removed for analysis at prescribed time intervals and replaced with fresh leachant to continue the test. The cumulative amounts of species of interest released from the specimen in successive test intervals are fitted with the diffusion equation for a finite cylinder. The test results can be used to qualitatively determine whether the release of a component is controlled by diffusion alone, partitioned into leachable and non-leachable fractions, or affected by solution saturation effects. Although evaluation of the diffusion coefficient requires the use of a monolithic specimen having right cylinder geometry, the test method can be modified for use with crushed materials to determine (qualitatively) whether release is being controlled by diffusion. Very large volumes of waste solution can result from testing, and waste disposal constraints should be considered when designing the test. To the extent possible, small specimens and small solution volume-to-specimen area ratios should be used to minimize the volume waste solution that is generated during the test.

The ASTM C1308 test method provides for the determination of an effective diffusion coefficient using a mechanistic model. The procedure can be used to determine whether release from small or irregular specimens is controlled by diffusion or matrix dissolution, even though the specimens cannot be modeled to determine a diffusion coefficient from the test data. Use of ASTM C1308 is recommended instead of ANS/ANSI 16.1 because the modeling aspects of ASTM C1308 provide a calculated diffusion coefficient value rather than the leaching index provided by ANS/ANSI 16.1.

Test results can be affected by retention of species of interest in non-leachable fractions (in the waste form or precipitation after release) and the effects of surface films on test specimens formed by casting.

E.5 ASTM C1662 Single-Pass Flow-Through Test (ASTM 2009a)

The ASTM C1662 test method is a consolidation of various SPFT test methods that have been used in different laboratories; the ASTM method was specifically developed to measure glass dissolution rates, usually under controlled temperature and pH conditions, using specific procedures for specimen preparation, test execution, and data analysis to facilitate inter-laboratory comparisons. It is a dynamic test method in which leachant is flowed through a reaction cell containing crushed glass that is held at a constant temperature. The mass and size fraction of the crushed glass is known and used to estimate the surface area (or the specific surface area can be measured directly). The effluent solution is sampled periodically to measure the flow rate and concentrations of dissolved components. When steady-state concentrations are attained, the dissolution rate can be calculated from the steady-state concentration, flow rate, and

material surface area. Tests with a range of flow rates and specimen surface areas can provide a measure of the dissolution rate when the chemical affinity value is near 1. Tests conducted at various temperatures and with controlled leachant compositions can be used to measure the effects of temperature and solution composition on the dissolution rate. Note that SPFT tests have been conducted at several laboratories for many years, but researchers followed different procedures that affected the test results. The ASTM C1662 test method was developed to provide a single procedure to allow direct comparison of the results from different laboratories. The test is moderately complicated to conduct (compared with ASTM C1220) and several tests are needed for each set of conditions to take the effects of solution flow rate into account. Large volumes of waste solution are generated under most test conditions.

The composition of the leachant solution can be controlled precisely and dissolution rates can be measured fairly precisely to determine the effects of temperature and pH. The effects of the solution flow rate and sample surface area are taken into account when determining the dissolution rate using the rate equation for borosilicate glass dissolution. The test method should be appropriate for other materials that dissolve by a surface dissolution mechanism sensitive to solution feedback effects, such as aluminosilicate minerals. The SPFT test is best suited for use with crushed materials to provide a large surface area, but can be conducted with monolithic specimens if analyzable solutions are generated. The method can be used to measure the effects of various leachant components when waste solution volume is not a limitation (e.g., with non-radioactive materials).

Use of crushed material results adds uncertainty to the surface area of the sample, artifacts due to crushing (e.g., high-energy edges and points that dissolve faster than the bulk material), and non-negligible decreases in sample surface area as the material dissolves in the test. Dissolved components can precipitate or plate out onto the tubing exiting the reaction cell. These effects must be taken into account when calculating the dissolution rate.

E.6 Pressurized Unsaturated Flow Test (McGrail et al. 1997a)

The pressurized unsaturated flow (PUF) test was developed to simulate the flow of water/air mixtures in a hydrologically unsaturated environment. The test method is similar to the SPFT and column test methods in that the water/air mixture flow through a crushed sample and the effluent is collected periodically for analysis, although some *in situ* measurements can be conducted continuously. The leachant can be preconditioned by placing other materials upstream of the sample, for example to measure interactions with geologic or engineering materials, and interactions of released species can be simulated by placing other materials downstream of the sample. Reacted sample materials can be extracted and analyzed at the end of the test.

The PUF test method can be used to directly incorporate materials interactions in the test and simulate integrated hydrologically unsaturated systems. Leachant composition is controlled and can be preconditioned prior to contacting the specimen. Altered specimen and alteration phases can be collected for analysis after testing. It is appropriate for confirmation testing of waste form corrosion mechanisms under integrated environmental conditions, whether hydrologically saturated or unsaturated.

The surface area of crushed samples, including fracture edges, preferential solution flow paths through sample, and interactions between the effluent and downstream surfaces prior to collection will all affect the results. The data resulting from several processes occurring in parallel or series

can be difficult to relate to each specific process. The PUF test apparatus is complex, relative to the other methods that have been discussed, and the test method has not been standardized.

E.7 ISO 16797 Soxhlet-Mode Chemical Durability Test (ISO 1982)

The Soxhlet test is used to measure the chemical durability of waste glasses and other materials at temperatures up to near the boiling point of water (or an azeotrope). Fresh leachant is generated as recondensed water vapor periodically drips into a sample cup holding the sample. The drip rate depends on the refluxing conditions. A range of boiling temperatures can be attained by varying the pressure in the system, and the condensate can be cooled prior to dripping into the sample cup. The volume of the sample cup determines the effective *S/V* ratio conditions during the test and the flow rate of condensate into the cup can be held constant (typically within 10%) by controlled heating. Both affect how quickly dissolved glass components are removed from the sample cup by overflow into the reservoir. The dissolution rate of the test specimen is determined from the mass loss of the specimen and the concentrations of soluble components in the reservoir at the end of the test duration as if it were a static dissolution test. Tests are typically conducted for between 1 and 28 days, but can be run for longer durations. The solution pH in the sample cup is not controlled and the composition of the solution in the cup is not monitored during the test. Both will vary as the specimen dissolves, with the volume of the sample cup, and with the effective water flow rate through the cup. The solution is sampled as it accumulates in the reservoir separate from the specimen.

Although it has been used to measure initial glass dissolution rates and temperature dependencies, the Soxhlet test method is not recommended for determining release or degradation mechanisms or measuring model parameter values because of limited range of test parameter values that can be studied and lack of control. The possible impact of the effective flow rate through the reaction cell is usually not taken into account, other than qualitatively being deemed fast enough. Use of other test methods providing greater control of test solution volume and flow rate and simpler sampling is recommended.

E.8 Solution Replacement Tests (Johnson et al. 2002)

Several researchers have used test methods in which a small portion of the leachate solution in a static test is periodically removed for analysis and replaced with fresh leachant. Such replacement tests are intended to simulate very low flow rates that are difficult to attain using mechanical pumps, and are sometimes referred to as pulsed flow tests. The tests are characterized by the fraction of solution that is replaced and the replacement interval. Either monolithic or crushed specimens can be used, and various leachant compositions can be used. The ANS 16.1 and ASTM C1308 test methods are complete solution replacement tests conducted under specified conditions and intended for materials that degrade by diffusion-controlled releases. The results of tests with materials that degrade by other mechanisms can be interpreted using other models, including affinity-control, constant dissolution, and surface rinse models.

Solution replacement tests provide a convenient means for comparing the relative releases of different components from a waste form and from different waste forms. The dissolution behavior can be monitored for long durations in a single test with the same test specimen. The method can be used to assess the qualitative effects of solution composition on the waste form dissolution rate. This test method is recommended for use in scoping tests to assess the significance of variations in the waste form composition and environmental conditions, but is not recommended for quantifying the effects of either. Tests may be used as part of model validation

to distinguish between competing processes, such as diffusion and saturation effects. The test may also represent wet/dry cycling in confirmation tests.

The test responses of materials that are sensitive to the solution composition (e.g., borosilicate glasses) will be affected by the replacement interval and the solution fraction. If the volume of leachate removed for analysis is replaced by an equal volume of fresh leachant, the test solution will be diluted and will cause the dissolution rate to increase slightly. If the aliquant is not replaced, the effective surface-to-volume ratio of the test increases slightly for subsequent test intervals and the dissolution rate will decrease slightly. Due to uncertainties in quantifying the effect of solution replacement, the test responses provide only qualitative insights to dissolution behavior.

E.9 Lysimeter Tests

Lysimeters can be used in field and laboratory tests to determine coupled leaching and transport characteristics due to percolation of groundwater through soil and waste material degradation. Tests with lysimeters provide an intermediary between small-scale laboratory tests and full-scale field tests, and can be conducted in a laboratory or in the field. In the laboratory, the lysimeter can be used as a column test in which a leachant percolates through a bed of crushed solids, which can be layered to represent the host geology, waste form, and backfill of a disposal system, at a controlled rate and is then collected for analysis upon exiting the column. In the field, the lysimeter can be buried such that groundwater enters and flows through the bed(s) of materials within the column, which may include buried waste forms, and is collected as it exits the column for periodic recovery analysis. Lysimeter test methods *per se* do not exist; instead, lysimeters are usually designed to include materials representing the disposal system and probes for real-time monitoring and analyses. Fluids can be sampled during the test, and core samples can be taken at the end of the test for detailed analyses in the laboratory.

Lysimeters can be utilized in both laboratory and field applications as model validation and confirmation tests. In field tests, they can be used to measure environmental parameters such as groundwater composition and complex interactions such as sorption on minerals in the host geology and engineering materials coupled with waste form degradation. Lysimeter field studies require long-term commitments (e.g., >10 years). The fidelity of the experimental design to the system being modeled and the evaluation of the model must be demonstrated. For example, variations in ambient rainfall may not represent the groundwater flow rate over long times. Additional water may be required to generate sufficient solution for analyses in field tests. Test responses are usually dominated by transport behavior and variances in groundwater volume and flow, both of which obfuscate waste material corrosion behavior. Lysimeter test results are better suited to confirming release/transport models than measuring model parameter values. Due to the variability in the geometries of the lysimeter, collection cups, etc., test methods utilizing lysimeters should be fully documented.

E.10 EPA Methods

Several test methods have been promulgated by the US Environmental Protection Agency for use in regulating hazardous wastes. For the most part, these methods provide a measured response under particular imposed conditions that is directly compared with benchmark value. These responses are not directly related to a waste material property that can be integrated into a performance calculation. However, data from these tests may be available for waste materials being analyzed and may provide insight useful in interpreting other test results.

EPA Method 1310B: Extraction Procedure (EP) Toxicity Test Method and Structural Integrity Test (EPA 2009)

The extraction procedure is used to determine whether a waste is characteristically toxic with regard to the procedure. The waste may be crushed to pass through a 9.5 mm sieve (3/8 inch) or formed into a cylinder for measuring the structural integrity. The specimen is leached in demineralized water under agitation for 24 hours. Then 100 g of material is leached with a mass of leachant that is 16 times the mass of solids. The leachate solution is acidified to below pH 5 using acetic acid, if necessary. This procedure or procedure 1311 can be used to measure toxicity with respect to As and Pb.

EPA Method 1311: Toxicity Characteristic Leach Procedure (EPA 2009)

The EPA Method 1311, commonly referred to as the Toxicity Characteristic Leach Procedure (TCLP) was developed to determine whether material containing a regulated component is characteristically hazardous. In the test, the solid material is reduced in size, if necessary, to <9.5 mm (3/8 inch) and immersed in one of two leachant solutions: if leaching in demineralized water results in a leachate with pH <5, TCLP is conducted with fluid #1; if the pH >5, TCLP is conducted with fluid #2 (fluid #1 has a pH near 4.93 and fluid #2 has a pH near 2.88). The sized material is immersed in the appropriate TCLP fluid (50 g solid/1000 g fluid) in a sealed polyethylene bottle and agitated for 18 hours at room temperature. The leachate solution is filtered and analyzed for the species of interest. The measured concentration is compared with the regulatory level and universal treatment limit, which are listed in Table E.2 for regulated inorganic constituents.

Table E.2. Regulatory levels for RCRA-regulated inorganic elements.

Element	Regulatory level, mg L^{-1}	Universal treatment standard limit, mg L^{-1}	Element	Regulatory level, mg L^{-1}	Universal treatment standard limit, mg L^{-1}
Ag	5.0	0.14	Hg	0.2	0.025
As	5.0	5.0	Ni	—	11
Ba	100	21	Pb	5.0	0.75
Cd	1.0	0.11	Se	1.0	5.7
Cr (total)	5.0	0.60			

Use of the TCLP is required to determine whether a waste form is hazardous if it contains RCRA-regulated metals, whether a hazardous material has been treated sufficiently to be declared non-hazardous, or to meet land disposal requirements. The test is only recommended to show compliance with RCRA requirements. The method may be useful for screening materials for compliance during waste form development. The test response is expected to vary with the size range of the crushed material due to differences in the exposed surface area, so similar size fractions should be used when comparing different materials. For example, the EPA method does not allow for sieving the ≥ 3/8 inch fraction to reduce the particle size range. The leaching solution cannot be modified to evaluate pH effects caused by the waste.

EPA Method 1312: Synthetic Precipitation Leaching Procedure (EPA 2009)

EPA Method 1312, commonly referred to as the Synthetic Precipitation Leaching Procedure (SPLP) was developed to provide a measure of the mobility of species in wastes, soils, and liquids. In the test, the solid material is size-reduced, if necessary, and immersed in one of two leachant solutions for 18 ± 2 hours. If the material is a waste, a pH 4.20 ± 0.05 extractant solution (fluid #1) is used. If the material is a soil, fluid #1 is used for soils east of the Mississippi River and a pH 5.00 ± 0.05 extractant solution (fluid #2) is used for soils west of the Mississippi River. Fluids #1 and #2 are prepared by adding appropriate amounts of a 60/40 mass percent mixture of sulfuric and nitric acids to reagent demineralized water. Reagent water (referred to as extratant fluid #3) is used to leach cyanide-containing materials to avoid forming hydrogen cyanide gas. Liquids are analyzed without extraction. Method 1312 includes provisions for analyzing samples containing volatiles and pore water. At the end of the extraction period, solids are removed by filtration and the leachate solution is analyzed.

EPA Method 1320: Multiple Extraction Procedure (EPA 2009)

The EPA Method 1320, commonly referred to as the Multiple Extraction Procedure (MEP) was developed to provide a measure of the leachability of a waste by acid rain. In the test, the solid material is size-reduced, if necessary, and leached following the Extraction Procedure Toxicity Test (EPA Method 1310). If the material is a waste, a pH 4.20 ± 0.05 extractant solution (fluid #1) is used. If the material is a soil, fluid #1 is used for soils east of the Mississippi River and a pH 5.00 ± 0.05 extractant solution (fluid #2) is used for soils west of the Mississippi River. Fluids #1 and #2 are prepared by adding appropriate amounts of a 60/40 mass percent mixture of sulfuric and nitric acids to reagent demineralized water. Reagent water (referred to as extratant fluid #3) is used to leach cyanide-containing materials to avoid forming hydrogen cyanide gas. Liquids are analyzed without extraction. Method 1320 includes provisions for analyzing samples containing volatiles and pore water. At the end of the extraction period, solids are removed by filtration and the leachate solution is analyzed.

E.11 Other Test Methods

ASTM D3987 Shake Extraction of Solid Waste with Water (ASTM 2009b)

This method is intended to rapidly extract leachable constituents from a solid waste into reagent water. The test is conducted with 70 a solid and an amount of water that is 20 times the mass of solid. The mixture is continuously agitated for 18 hours, then passed through a 0.45-μm or 0.8-μm pore size filter. The leachate is analyzed for pH and dissolved constituents.

ASTM D4793 Sequential Batch Extraction of Waste with Water (ASTM 2009b)

Particulate solids are leached in reagent water under agitation. The test is conducted with 100 g solid and an amount of water that is 20 times the mass of solid. The mixture is continuously agitated for 18 hours, then passed through a 0.45-μm or 0.8-μm pore size filter under pressure. The leachate is analyzed for pH and dissolved constituents. The filtrate is analyzed and the solids are recovered and placed back into the extraction vessel to repeat the test.

ASTM D5284 Sequential Batch Extraction of Waste with Acidic Extraction Fluid (ASTM 2009b)

Particulate solids are leached in a 60/40 sulfuric acid/nitric acid solution under agitation. The leachant is diluted to achieve the desired pH value. The test is conducted with 100 g solid and an amount of leachant that is 20 times the mass of solid. The mixture is continuously agitated for 18 hours, then passed through a 0.45-μm or 0.8-μm pore size filter under pressure. The leachate is analyzed for pH and dissolved constituents. The solids are recovered and placed back into the extraction vessel to repeat the test.

ASTM D4874 Leaching Solid Material in a Column Apparatus (ASTM 2009b)

This method addresses the use of gravity-flow and pressurized column apparatuses. Particle size is restricted to less than 10% of the column diameter and particle size reduction is not recommended. The column is filled by compacting or vibrating, then saturated with reagent water. The pressure or hydraulic head is adjusted to achieve a flow rate of 1 column volume in 24 hours. Column effluents are to be collected continuously in discrete void volume increments. At a minimum, effluents from volumes 1, 2, 4, and 8 are analyzed.

California Wet Extraction Test (WET) Procedure (CA WET 2005)

This method is used to measure extraction into a 0.2 M sodium citrate solution (except Cr is extracted into demineralized water). Fifty grams of crushed and sized solid is extracted with 0.5 L leachant under agitation for 48 hours between 20°C and 40°C. The resulting leachate is passed through a 0.45-μm pore size filter and analyzed for the metals of interest for comparison with regulatory limits.

NRC FORM 335
(9-2004)
NRCMD 3.7

U.S. NUCLEAR REGULATORY COMMISSION

BIBLIOGRAPHIC DATA SHEET

(See instructions on the reverse)

1. REPORT NUMBER
(Assigned by NRC, Add Vol., Supp., Rev., and Addendum Numbers, if any.)
NUREG/CR-7025

2. TITLE AND SUBTITLE
Radionuclide Release from Slag and Concrete Waste Materials
Part I: Conceptual Models of Leaching from Complex Materials and Laboratory Test Methods

3. DATE REPORT PUBLISHED

MONTH	YEAR
December	2010

4. FIN OR GRANT NUMBER
N6669

5. AUTHOR(S)
William L. Ebert

6. TYPE OF REPORT
Technical

7. PERIOD COVERED *(Inclusive Dates)*
2008-2010

8. PERFORMING ORGANIZATION - NAME AND ADDRESS *(If NRC, provide Division, Office or Region, U.S. Nuclear Regulatory Commission, and mailing address; if contractor, provide name and mailing address.)*
Argonne National Laboratory
9700 South Cass Ave.
Argonne, IL 60439

9. SPONSORING ORGANIZATION - NAME AND ADDRESS *(If NRC, type "Same as above"; if contractor, provide NRC Division, Office or Region, U.S. Nuclear Regulatory Commission, and mailing address.)*
Division of Risk Analysis
Office of Nuclear Regulatory Research
U.S. Nuclear Regulatory Commission
Washington, DC 20555-0001

10. SUPPLEMENTARY NOTES
M. Fuhrmann, NRC Project Manager

11. ABSTRACT *(200 words or less)*
The technical literature was surveyed to evaluate test methods and modeling approaches used to characterize the release of contaminants during the weathering of portland cement-based materials and slag wastes from metal processing and recycling operations. Data sets were selected to represent various approaches used to study contaminant leaching, mineral dissolution, and waste material corrosion, and both the testing methods and data interpretations were evaluated. Models were evaluated with regard to both interpreting the test results and predicting long-term behavior. This study concludes that test results can be misinterpreted if testing artifacts are not taken into account, such as the interval used in solution replacement tests, the flow rate used in dynamic tests, and failure to reach steady-state, or if an inappropriate process is modeled. Contaminant release may be controlled by a diffusion process (mass transport) or by the chemical reaction affinity, and oxidation reactions can affect the releases of multivalent contaminants, such as Tc. The mechanism controlling the release might not be identifiable by a single test method. While well-established models for each of these processes and standardized test methods are available, the challenge is to identify which process controls contaminant release under the conditions of interest and how the laboratory test results relate to the model and long-term material behavior.

12. KEY WORDS/DESCRIPTORS *(List words or phrases that will assist researchers in locating the report.)*
Radionuclide, leaching, leach tests, leaching models, contaminant release, leaching mechanisms, radionuclide release, models of leaching

13. AVAILABILITY STATEMENT
unlimited

14. SECURITY CLASSIFICATION
(This Page)
unclassified
(This Report)
unclassified

15. NUMBER OF PAGES

16. PRICE

PRINTED ON RECYCLED PAPER

Printed
on recycled
paper

Federal Recycling Program

UNITED STATES
NUCLEAR REGULATORY COMMISSION
WASHINGTON, DC 20555-0001

OFFICIAL BUSINESS